Sulfite Reductase and Thioredoxin in Oxidative Stress Responses of Methanogenic Archaea

Dwi Susanti

Dissertation submitted to the faculty of the Virginia Polytechnic Institute and State University in partial fulfillment of the requirements for the degree of

Doctor of Philosophy
In
Genetics, Bioinformatics and Computational Biology

Biswarup Mukhopadhyay, committee chair
David R. Bevan
Dennis R. Dean
David L. Popham
Robert H. White
T.M. Murali

July 2nd, 2013
Blacksburg, Virginia

Keywords: sulfite reductase, thioredoxin, *Methanocaldococcus jannaschii*, methanogens, oxidative stress, redox, regulation

Sulfite Reductase and Thioredoxin in Oxidative Stress Responses of Methanogenic Archaea

Dwi Susanti

(ABSTRACT)

Methanogens are a group of microorganisms that utilize simple compounds such as H_2 + CO_2, acetate and methanol for the production of methane, an end-product of their metabolism. These obligate anaerobes belonging to the archaeal domain inhabit diverse anoxic environments such as rice paddy fields, human guts, rumen of ruminants, and hydrothermal vents. In these habitats, methanogens are often exposed to O_2 and previous studies have shown that many methanogens are able to tolerate O_2 exposure. Hence, methanogens must have developed survival strategies to be able to live under oxidative stress conditions. The anaerobic species that lived on Earth during the early oxygenation event were first to face oxidative stress. Presumably some of the strategies employed by extant methanogens for combating oxidative stress were developed on early Earth.

Our laboratory is interested in studying the mechanism underlying the oxygen tolerance and oxidative stress responses in methanogenic archaea, which are obligate anaerobe. Our research concerns two aspects of oxidative stress. (i) Responses toward extracellular toxic species such as SO_3^{2-}, that forms as a result of reactions of O_2 with reduced compounds in the environment. These species are mostly seen in anaerobic environments upon O_2 exposure due to the abundance of reduced components therein. (ii) Responses toward intracellular toxic species such as superoxide and hydrogen peroxide that are generated upon entry of O_2 and subsequent reaction of O_2 with reduced component inside the cell. Aerobic microorganisms experience the second problem. Since a large number of microorganisms of Earth are anaerobes and the oxidative defense mechanisms of anaerobes are relatively less studied, the research in our laboratory has

focused on this area. My thesis research covers two studies that fall in the above-mentioned two focus areas.

In 2005-2007 our laboratory discovered that certain methanogens use an unusual sulfite reductase, named F_{420}-dependent sulfite reductase (Fsr), for the detoxification of SO_3^{2-} that is produced outside the cell from a reaction between oxygen and sulfide. This reaction occurred during early oxygenation of Earth and continues to occur in deep-sea hydrothermal vents. Fsr, a flavoprotein, carries out a 6-electron reduction of SO_3^{2-} to S^{2-}. It is a chimeric protein where N- and C-terminal halves (Fsr-N and Fsr-C) are homologs of $F_{420}H_2$ dehydrogenase and dissimilatory sulfite reductase (Dsr), respectively. We hypothesized that Fsr was developed in a methanogen from pre-existing parts. To begin testing this hypothesis we have carried out bioinformatics analyses of methanogen genomes and found that both Fsr-N homologs and Fsr-C homologs are abundant in methanogens. We called the Fsr-C homolog dissimilatory sulfite reductase-like protein (Dsr-LP). Thus, Fsr was likely assembled from freestanding Fsr-N homologs and Dsr-like proteins (Dsr-LP) in methanogens. During the course of this study, we also identified two new putative $F_{420}H_2$-dependent enzymes, namely $F_{420}H_2$-dependent glutamate synthase and assimilatory sulfite reductase.

Another aspect of my research concerns the reactivation of proteins that are deactivated by the entry of oxygen inside the cell. Here I focused specifically on the role of thioredoxin (Trx) in methanogens. Trx, a small redox regulatory protein, is ubiquitous in all living cells. In bacteria and eukarya, Trx regulates a wide variety of cellular processes including cell divison, biosynthesis and oxidative stress response. Though some Trxs of methanogens have been structurally and biochemically characterized, their physiological roles in these organisms are unknown. Our bioinformatics analysis suggested that Trx is ubiquitous in methanogens and the pattern of its distribution in various phylogenetic classes paralleled the respective evolutionary histories and metabolic versatilities. Using a proteomics approach, we have identified 155 Trx targets in a hyperthermophilic phylogenetically deeply-rooted methanogen, *Methanocaldococcus jannaschii*. Our analysis of two of these targets employing biochemical assays suggested that Trx is needed for reactivation of oxidatively deactivated enzymes in *M. jannaschii*. To our knowledge, this is the first report on the role of Trx in an organism from the archaeal domain.

During the course of our work on methanogen Trxs, we investigated the evolutionary histories of different Trx systems that are composed of Trxs and cognate Trx reductases. In collaboration

with other laboratories, we conducted bioinformatics analysis for the distribution of one of such systems, ferredoxin-dependent thioredoxin reductase (FTR), in all organisms. We found that FTR was most likely originated in the phylogenetically deeply-rooted microaerophilic bacteria where it regulates CO_2 fixation via the reverse citric acid cycle.

To my parents Endang Prasetyaning Utami and Susarwadi, my husband Bennu Guntoro and my little sunshine Adelia Fathiya Putri Guntoro

ACKNOWLEDGMENTS

I would like to thank Dr. Biswarup Mukhopadhyay for providing me opportunities to carry out graduate research in his laboratory. I thank him for his input and guidance in both scientific and personal matters. I respect him for his passion in science, his knowledge as well as his research- and work-ethics. Most importantly, I would like to thank him for the supports, encouragements and advice. I could not ask for a better adviser.

I also would like to thank Dr. Endang Purwantini. I would have not been here at Virginia Tech if it was not because of her. She trained me how to perform research during my undergraduate studies. She introduced me to the opportunity of studying abroad for pursuing my Ph.D. I would never have thought that I would be able to continue my education in this country or even in any other country than Indonesia. I enjoyed our discussion about scientific issues and about how we, as a scientist, could contribute to solving problems in Indonesia.

I would like to thank my committee members, Drs. David R. Bevan, David L. Popham, Dennis R. Dean, Robert H. White and T.M. Murali for their time, advice and scientific input throughout my Ph.D. training. My thanks to Dennie Munson for all her help from the beginning of the admission process to the final exam. I am really grateful to be part of the Genetics, Bioinformatics and Computational Biology program.

Many thanks to my labmates Dr. Lakshmi Dharmarajan, Jason R. Rodriguez, Eric F. Johnson and Usha Loganathan for encouragements, discussions and fun that we had in the lab. My thanks to all my colleagues in the GBCB program and many thanks to the members of Indonesian student association (PERMIAS) and Indonesian community in Blacksburg for all the supports and awesome time that we had.

I would like to express my deepest love, gratitude and appreciations to my family, my parents (Endang Prasetyaning Utami, Susarwadi, Maryam and Sumardjo), my husband Bennu, my little angel Adelia, my sister and brothers and their families for their unconditional love and endless support. My special thanks are to the love of my life, Bennu and Adelia.

ATTRIBUTIONS

Results presented in chapter 3 have been published in PLOS ONE (1). This study is supported by NASA Astrobiology: Exobiology and Evolutionary Biology grants NNG05GP24G and NNX09AV28G to Dr. Biswarup Mukhopadhyay. I thank Dr. William B. Whitman of University of Georgia, for the genomic data on *Methanothermococcus thermolithotrophicus* reported in this work.

Chapter 4 will soon be submitted for publication in a peer-reviewed journal. I would like to thank the following collaborators who have contributed to the research presented here: Drs. Joshua Wong of University of California Berkeley and William H. Vensel of United States Department of Agriculture for their contributions in 2D-gel electrophoresis and mass spectrometric analysis; Usha Loganathan for her assistance in the generation of Trx and Mtd proteins; Drs. Bob B. Buchanan of University of California Berkeley, Ruth A. Schmitz of Institut Für Allgemeine Mikrobiologie Germany and Monica Balsera of Instituto de Recursos Naturales y Agrobiología de Salamanca Spain for contributing their expertise. The research on thioredoxins of methanogens in our laboratory is supported by the NSF grant MCB # 1020458 to Drs. Biswarup Mukhopadhyay and Bob B. Buchanan.

The finding presented in chapter 5 has been published in PLANTA (2). My primary contributions in this paper are shown in Figure 5.2 and Table 5.1.

My collaborative work that is outside the main focus of this dissertation has been presented in the Appendices. Appendix A contains results that have been published in the Journal of Bacteriology (3). Our laboratory was the lead for this project. I generated genomic materials for the genome sequencing of *Desulfurococcus fermentans* and was the major contributor for the data analysis. This work was supported by the Community Sequencing Program (CSP) of the

U.S. Department of Energy's Joint Genome Institute (DOE-JGI). Appendix B presents results from a project led by Dr. Venkat Gopalan of Ohio State University that have been published in the Proceedings of the National Academy of Sciences (4). I constructed a *Methanococcus maripaludis* strain that generates RPP30, a subunit of RNase P complex, tagged with $(His)_6$-HA at its N-terminus as well as provided cell mass for both wildtype and engineered strain for the purification of RNase P.

Publications:

1. Susanti D & Mukhopadhyay B (2012) An intertwined evolutionary history of methanogenic archaea and sulfate reduction. *PLoS One* 7(9):e45313.
2. Balsera M, *et al.* (2013) Ferredoxin:thioredoxin reductase (FTR) links the regulation of oxygenic photosynthesis to deeply rooted bacteria. *Planta* 237(2):619-635.
3. Susanti D, *et al.* (2012) Complete genome sequence of *Desulfurococcus fermentans*, a hyperthermophilic cellulolytic crenarchaeon isolated from a freshwater hot spring in Kamchatka, Russia. *Journal of bacteriology* 194(20):5703-5704.
4. Cho I-M, Lai LB, Susanti D, Mukhopadhyay B, & Gopalan V (2010) Ribosomal protein L7Ae is a subunit of archaeal RNase P. *Proceedings of the National Academy of Sciences* 107(33):14573-14578.

Contents

LIST OF FIGURES

LIST OF TABLES

1 Introduction

The broader focus of research presented in this thesis is on responses of methanogens towards two types of oxidative stresses, one towards extracellular and the other for intracellular toxic species resulting in reactions of reduced compounds with molecular O_2.

Methanogens are a group of strictly anaerobic microorganisms belonging to the kingdom of Archaea that use simple compounds such as $H_2 + CO_2$, acetate, and methanol to produce methane and the process is called methanogenesis. Methanogens inhabit diverse anoxic environments, from rice paddy fields to deep-sea hydrothermal vents. The habitats of methanogens are sometimes not fully anoxic. However, previous studies have shown that methanogens can tolerate O_2. Oxidative stress in anaerobic environments can be caused by at least two factors, namely exposure to O_2 and increase in the reduction potential. Both of these could bring external and internal effects mentioned above.

Below are short descriptions of the research materials presented in this thesis:

Chapter 2: Literature review. This chapter will provide background information on methanogens, methanogenesis, current knowledge on responses of methanogens towards oxidative stress and also respective defense strategies in a broad range of organisms.

Chapter 3: Research on response of methanogens towards toxic extracellular species. Toxic extracellular species are produced from reactions of O_2 with reduced components in the environment. An example is SO_3^{2-}, a product of incomplete oxidation of S^{2-}.

SO_3^2 is toxic for methanogens since it inhibits methanogenesis pathway. Certain methanogens generate F_{420}-dependent sulfite reductase for sulfite detoxification, an enzyme that was discovered in our laboratory in 2005. Fsr is a chimeric of two enzymes, N-terminal and C-terminal halves of Fsr are similar to $F_{420}H_2$ dehydrogenase and dissimilatory sulfite reductase (Dsr), respectively. In my research on Fsr, I focused in the evolutionary origin of the enzyme and the results from this work have been presented in this chapter.

Chapter 4: Work on response of methanogens towards intracellular reactive oxygen species. Toxic intracellular O_2 species such as superoxide, hydroperoxide and hydroxyl radicals, also called reactive oxygen species (ROS), are generated when O_2 enters in the cell and reacts with reduced compounds in the cell. ROS have deleterious effects on DNA, protein and lipids. For example, cysteine residues in proteins can be oxidized through formation of disulfide bonds leading to enzyme inactivation. One of the protein disulfide oxidoreductases that are responsible for reactivating oxidatively deactivated enzymes is thioredoxin (Trx). Results presented in this chapter elucidate the role of Trx in methanogens.

Chapter 5: In this chapter, I focused on the origin of ferredoxin-dependent thioredoxin reductase (FTR). This study was performed in collaboration with other laboratories.

Appendices: Exerpts from two publications have been presented here. These include my analysis of the genome sequence of the first known cellulolytic crenarchaeon *Desulfurococcus fermentans* and my contributions in the discovery of archaeal ribosomal protein L7Ae as a component of *M. maripaludis* RNase P.

2 Literature review:
Oxidative stress responses in methanogenic archaea

2.1 METHANOGENIC ARCHAEA

Methanogens are a group of strictly-anaerobic microorganisms that are specialized in their energy metabolism. This group of phylogenetically diverse organisms produces methane from simple compounds such as $H_2 + CO_2$, formate, methanol, methylamine as well as acetate (1-3). Methanogens can be found in various anoxic environments such as rice paddy fields, freshwater and marine sediments, landfills, anaerobic digesters, rumen of ruminants, human digestive tract and several extreme environments, for example, hot springs, deep-sea hydrothermal vents and salt lake (reviewed in (2)). Based on their 16S-ribosomal RNA sequences, these methane producers belong to the domain of Archaea more specifically to the phylum of *Euryarchaea* (4). Archaea, similar to bacteria, can be easily distinguished from eukarya based on their unicellular morphology and the absence of nuclear membrane. From their bacterial counterpart, archaea can be differentiated by their unique membrane lipid components and the absence of peptidoglycans containing muramic acid in their cell wall (reviewed in (1)). Unlike bacteria, the methanogens membrane lipids are composed of isoprenoid ether-linked to glycerol (5-7) rather than ester of glycerol and fatty acids and their peptidoglycans are built with pseudomurein in place of murein that is in the bacterial peptidoglycans (8). These cell wall properties contribute to methanogens' resistance towards antibiotics such as penicillin, cycloserin and valinomycin that inhibit cell wall synthesis (9).

Despite their common specialized metabolic properties, methanogens are very diverse. These diversities are seen in their morphologies, growth temperatures, habitats, energy sources and

genomes, as can be seen in Table 2.1. Based on the substrates used for methanogenesis, the signature energy generation pathway, methanogens can be divided into three groups, namely hydrogenotrophic, methylothropic and aceticlastic. Hydrogenotrophic and methylotrophic methanogens use H_2 + CO_2 and methyl-group containing compounds such as methanol, methylamine, dimethylsulfide, respectively. Some of the hydrogenotrophic methanogens can also utilize formate (10, 11). Aceticlastic methanogens generate methane via acetate fermentation (12). Among all methanogenesis substrates, H_2+CO_2 is the most energetically favorable and acetate is the least preferred (2). Therefore, there are more hydrogenotrophic than aceticlastic methanogens (2).

Nutritional requirement is not the only means to classify methanogens. In 1979, Balch, et. al classified methanogens based solely on the 16S-ribosomal RNA sequences (13). Later, Boone and Whitman added additional criteria, also known as "minimal standards" (14), for describing new methanogen taxa. These parameters include morphology, Gram staining, electron microscopy, susceptibility to lysis, colony morphology, motility and antigenic fingerprint. Based on these criteria, methanogens are classified into five orders, namely *Methanococcales*, *Methanobacteriales*, *Methanomicrobiales*, *Methanosarcinales* and *Methanopyrales* (1).

Methanogens are important both ecologically and economically. In their habitats, methanogens utilize CO_2, H_2 and acetate –the end products of anaerobic biomass degradation in anaerobic environements- to produce methane. Their activities help to maintain the low level of H_2, thus relieving a thermodynamic block for various biomass degradation pathways and pulling the reactions forward (15).

As a result of methanogen's activities, methane is released to the atmosphere. Methanogenesis is responsible for the production of 1 billion tons of CH_4 per year (3, 16). Noteworthy, like CO_2 methane is a greenhouse gas. Although methane is less abundant than CO_2 in the atmosphere, it's effect on the climate changes is more detrimental (17). On a volume basis, methane is a 33 times more potent greenhouse gas than CO_2 (17). Thus, mitigation of methane emission from sources such as rumen of ruminants and rice paddy fields has been of research interest (18). Methanogens also have economical values. Methane can be burned as fuel and used in industry as feedstock.

TABLE 2.1 Diversity of Methanogens

Class **Family** **Organism name**	**Morphology**	**Thermophilicity**	**Natural habitat**	**Substrate utilized for methanogenesis**	**Genome size (Mb)**	**GC content (%)**	**Refs.**
Methanopyri ***Methanopyraceae* fam. nov.**							
Methanopyrus kandleri AV19	Rod	Hyperthermophile	Hydrothermal vent	hydrogen + CO_2	1.69	61.2	(19, 20)
Methanococci ***Methanocaldococcaceae***							
Methanocaldococcus infernus ME	Coccus	Hyperthermophile	Hydrothermal vent	hydrogen + CO_2	1.33	33.6	(21, 22)
Methanocaldococcus.sp. FS406-22	Coccus	Hyperthermophile	Hydrothermal vent	hydrogen + CO_2	1.77	32	(22, 23)
Methanocaldococcus fervens AG86	Coccus	Hyperthermophile	Hydrothermal vent	hydrogen + CO_2	1.51	32.2	(22, 24)
Methanocaldococcus vulcanius M7	Coccus	Hyperthermophile	Hydrothermal vent	hydrogen + CO_2	1.76	31.6	(22, 24)
Methanocaldococcus jannaschii DSM 2661	Coccus	Hyperthermophile	Hydrothermal vent	hydrogen + CO_2, some species use formate	1.66	31.3	(25, 26)
Methanotorris igneus Kol 5	Coccus	Thermophile	Shallow submarine vent	hydrogen + CO_2	1.85	32.3	(22, 27)
Methanocaldococcaceae							
Methanothermococcus okinawensis IH1	Irregular coccus	Thermophile	Hydrothermal vent	hydrogen + CO_2, formate	1.68	29.3	(28, 29)
Methanococcus aeolicus Nankai-3	Coccus	Mesophile	Marine sediment	hydrogen + CO_2, formate	1.57	30	(22, 30)
Methanococcus maripaludis S2	Coccus	Mesophile	Salt marsh sediment	hydrogen + CO_2, formate	1.66	33.1	(31, 32)
Methanococcus voltae A3	Coccus	Mesophile	Sediment	hydrogen + CO_2, formate	1.94	28.6	(22, 33, 34)
Methanococcus vannielii SB	Coccus	Mesophile	Mud flat	hydrogen + CO_2, formate	1.72	31.3	(22, 35)

Methanothermaceae							
Methanothermus fervidus DSM 2088	Rod	Thermophile	Sewage digester	hydrogen + CO_2	1.24	31.6	(36, 37)
Methanobacteriaceae							
Methanothermobacter marburgensis str. Marburg	Rod	Thermophile	Sewage digester	hydrogen + CO_2, formate	1.64	48.6	(38, 39)
Methanothermobacter thermautotrophicus str. delta H	Rod	Thermophile	Sewage digester	hydrogen + CO_2, formate	1.75	49.5	(39, 40)
Methanobrevibacter ruminantium M1	Short rod	Mesophile	Rumen	hydrogen + CO_2, formate	2.94	32.6	(41, 42)
Methanobrevibacter smithii ATCC 35061	Short rod	Mesophile	Rumen	hydrogen + CO_2, formate	1.85	31	(43, 44)
Methanosphaera stadtmanae DSM 3091	Coccus	Mesophile	Human intestine	hydrogen , methanol	1.77	27.6	(45, 46)
Methanomicrobia **Family : *NA***							
Methanosphaerula palustris E1-9c	Coccus	Mesophile	Peatlands	hydrogen + CO_2, formate	2.92	55.4	(22, 47)
Methanospirillaceae							
Methanospirillum hungatei JF-1	Spirillum	Mesophile	Sewage sludge	hydrogen + CO_2, formate, some species use isopropanol and isobutanol	3.54	45.1	(48, 49)
Family : *NA*							
Methanoregula boonei 6A8	Dimorphic of thin rod and irregular coccus	Mesophile	Acidic bog	hydrogen + CO_2	2.54	54.5	(22, 50)

Methanomicrobiaceae							
Methanoplanus petrolearius DSM 11571	Irregular disc-shape	Mesophile	Offshore oil field	hydrogen + CO_2, formate, propanol	2.84	47.4	(51, 52)
Methanocorpuscullaeae							
Methanocorpuscullum labreanum Z	Irregular coccus	Mesophile	Sediment of Tar Pits lake	hydrogen + CO_2, formate	1.8	50	(48, 53)
Methanomicrobiaceae							
Methanoculleus marisnigri JR1	Irregular coccus	Thermophile	Sediment of Black sea	hydrogen + CO_2, formate, isopropanol and isobutanol	2.48	62.1	(48, 54, 55)
Methanoculleus bourgensis MS2	Irregular coccus	Mesophile	Sewage sludge digester	hydrogen + CO_2, formate	2.79	60.6	(56, 57)
Methanocellaceae							
Methanocella arvoryzae MRE50	Rod	Mesophile	Rice paddy soil	hydrogen + CO_2, formate	3.18	54.6	(58, 59)
Methanocella conradii HZ254	Rod	Thermophile	Rice field soil	hydrogen + CO_2	2.38	52.7	(60, 61)
Methanocella paludicola SANAE	Rod	Mesophile	Rice paddy soil	hydrogen + CO_2, formate	2.96	54.9	(62-64)
Family : *Methanosaetaceae fam. nov.*							
Methanosaeta harundinacea 6Ac	Rod	Mesophile	Anaerobic sludge reactor	Acetate	2.57	60.6	(65, 66)
Methanosaeta concilii GP6	Rod	Mesophile	Anaerobic sludge reactor	Acetate	3.03	53.5	(67, 68)
Methanosaeta thermophila PT	Rod	Thermophile	Anaerobic digester	Acetate	1.88	51	(22, 67)
Family : *Methanosarcinaceae*							
Methanohalobium evestigatum Z-7303	Flat polygons	Thermophile	Geothermally heated sea sediment	Methanol, methylamine, dimethylamine, trimethylamine	2.41	36.4	(22, 69)

Methanosalsum zhilinae DSM 4017	Irregular coccus	Thermophile	Bosa lake	Methanol, methylamine, dimethylamine, trimethylamine, dimethylsulfide and methanethiol	2.14	39.2	(22, 70)
Methanococcoides burtonii DSM 6242	Coccus	Psycrophile	Ace lake	Methanol, methylamine, dimethylamine, trimethylamine	2.58	40.8	(71, 72)
Methanohalophilus mahii DSM 5219	Irregular coccus	Mesophile	Great salt lake	Methanol, methylamine, dimethylamine, trimethylamine	2.01	42.6	(73, 74)
Methanolobus psychrophilus R15	Oval	Psycrophile	Wet sand soil	Methanol	3.07	44.6	(75, 76)
Methanosarcina barkeri str. Fusaro	Large and small aggregates	Mesophile	Freshwater lake	hydrogen + CO_2, methanol, methylamine, dimethylamine, trimethylamine, acetate	4.87	39.3	(8, 77)
Methanosarcina mazei Go1	Coccus, macrocyst	Mesophile	Sewage plant, animal rumen, human large intestine	Methanol, methylamine, dimethylamine, trimethylamine, acetate and some species use hydrogen + CO_2	4.1	41.5	(78, 79)
Methanosarcina acetivorans C2A	Coccus, macrocyst	Mesophile	Marine sediment	Methanol, methylamine, dimethylamine, trimethylamine, acetate	5.75	42.7	(80, 81)

2.2 METHANOGENESIS PATHWAY

The pathways for biological methane production from simple compounds such as H_2+CO_2, formate, methyl group-containing molecules and acetate have been studied extensively. Here, the methane production from H_2+CO_2, or so-called hydrogenotrophic methanogenesis, will be the focus of discussion. Methanogenesis from other substrates such as methyl group-containing compounds as well as from acetate will be discussed briefly.

Hydrogenotrophic methanogenesis

As shown in Table 2.1, all methanogens belonging to the class *Methanococci* and *Methanobacteria*, such as *Methanocaldococcus jannaschii* and *Methanothermobacter thermoautotrophicus*, and few members of *Methanomicrobia*, for example *Methanosphaerula palustris*, *Methanoculleus marisnigri* and *Methanosarcina barkeri* employ electrons from H_2 for the reduction of CO_2 to methane (CH_4) in the reaction shown below (82).

$$CO_2 + 4H_2 \rightarrow CH_4 + 2H_2O$$

Five unusual cofactors are required in the pathway. They are methanofuran (83), tetrahydromethanopterin (84, 85), coenzyme F_{420} (86, 87), coenzyme M (88) and coenzyme B (89). Overall reactions of the methanogenesis pathway are illustrated in Figure 2.1. The first reaction in the hydrogenotrophic pathway is the reduction of CO_2 to formyl group which then binds to a furan cofactor called methanofuran forming formyl-methanofuran (83). This endergonic reaction is catalyzed by a membrane-bound protein complex, formyl-methanofuran dehydrogenase (Fmd) (90). Two isoforms of formyl-methanofuran dehydrogenase, one tungsten-dependent (Fwd) and the other molybdenum-dependent (Fmd), are employed depending on the level of required metal ions in the environment (82). It has been shown that this endergonic reaction is coupled with an exergonic reaction catalyzed by a cytoplasmic hydrogenase (MvhADG)/heterodisulfide reductase (HdrABC) complex, the last step of methanogenesis (91).

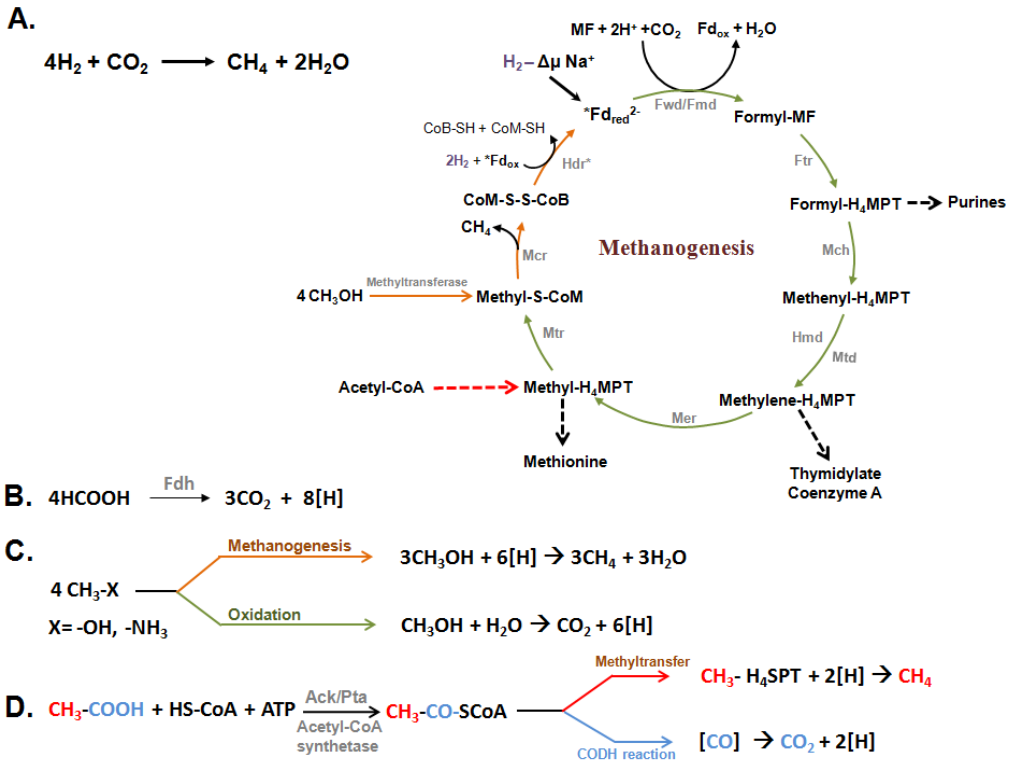

Figure 2.1 Methanogenesis from various substrates. **A.** H_2 + CO_2: hydrogenotrophic methanogenesis. The pathway has been redrawn from (92). Arrow color: Olive, reactions that operate in reverse direction while methyl-containing compounds are oxidized, as shown in the reaction C; orange, reactions used for methane production from methyl groups of methylated compounds as shown in C; and red, methyl-transfer from acetate as shown in D. Dashed black arrows show the extended biosynthetic routes for which details are not shown. **B.** Conversion of formate by formate dehydrogenase (Fdh) generating CO_2 and reducing equivalents that are used for CO_2-reduction pathway. **C.** Methanogenesis from methylated compounds. **D.** Acetate fermentation. Reactions B, C, D were adapted from (82, 93, 94). **Abbreviations:** Fwd, tungsten-dependent formylmethanofuran dehydrogenase; Fmd, molybdenum-dependent formylmethanofuran dehydrogenase; Ftr, formylmethanofuran/H_4MPT formyltransferase; Mch, methenyl-H_4MPT cyclohydrolase; Mtd, F_{420}-dependent methylene-H_4MPT dehydrogenase; Hmd, H_2-dependent methylene-H_4MPT dehydrogenase; Mer, methylene-H_4MPT reductase; Mtr, methyl-H_4MPT/coenzyme M methyltransferase; Mcr, methyl-coenzyme M reductase; Hdr, electron-bifurcating hydrogenase-heterodisulfidereductase complex; Fru, F_{420}-reducing hydrogenase with selenocysteine residues; Fdh, formate dehydrogenase; Ack/Pta, Acetate kinase/phosphotransacetylase; CODH, carbon monoxide dehydrogenase; F_{420}, coenzyme F_{420}; *Fd, specific ferredoxin; H_4MPT, tetrahydromethanopterin; H_4SPT, thetrahydrosarcinapterine; MF, methanofuran; CoB, coenzyme B; CoM, coenzyme M; [CO], enzyme-bound carbon monoxide (CO); ATP, adenosine triphosphate; $\Delta\mu Na^+$, electrochemical sodium ion potential.

The formyl group on the methanofuran is then transferred onto another cofactor called tetrahydromethanopterin (H_4MPT). The product of this reaction is N^5-formyl-H_4MPT (82). This transfer reaction is catalyzed by a cytoplasmic air-stable enzyme formyl-methanofuran:tetrahydromethanopterin formyltransferase (Ftr) (95). The next step is the conversion of N^5-formyl-H_4MPT to N^5,N^{10}-methenyl-H_4MPT which is catalyzed by N^5,N^{10}-methenyl-H_4MPT cyclohydrolase (Mch), a soluble air-stable enzyme (96). N^5,N^{10}-Methenyl-H_4MPT is then reduced to N^5,N^{10}-methylene-H_4MPT using two electrons either from H_2 or $F_{420}H_2$ (97). Enzymes catalyzing this reaction are H_2-dependent methylene-tetrahydromethanopterin dehydrogenase (Hmd) and F_{420}-dependent methylene-tetrahydromethanopterin dehydrogenase (Mtd) for H_2- and $F_{420}H_2$-dependent reductions, respectively (98-100). Hmd exhibits low affinity toward H_2 and catalyzes the reduction reaction under high supply of hydrogen, whereas Mtd is the primary reductase under hydrogen-limited growth (101-104). $F_{420}H_2$ used in the Mtd reaction is generated by F_{420}-reducing hydrogenase (97).

N^5,N^{10}-Methylene-H_4MPT is further reduced to N^5-methyl-H_4MPT by O_2-stable coenzyme F_{420}–dependent methylene-H_4MPT reductase (Mer), a homotetramer or homohexamer (82). The Methyl-moiety is then transfered to another coenzyme, coenzyme M, by a corrinoid-containing transmembrane enzyme complex, called methyltetrahydromethanopterin-coenzyme M methyltransferase (Mtr) (82). In this reaction, the methyl group is first transferred to the reduced form of corrinoid (Co^{1+}) from where it is transferred to the coenzyme M. This methyl transfer is coupled to energy conservation by generating Na^+ gradient across cell membrane.

The last step of methanogenesis pathways is the reduction of methyl group of methyl-coenzyme M to methane (82). This reaction involves methyl-coenzyme M reductase, coenzyme F_{420}-non-reducing hydrogenase and heterodisulfide reductase (Hdr). Coenzyme F_{420}-non reducing hydrogenase or also called methylviologen-reducing hydrogenase (Mvh), facilitates electron transfer from hydrogen to the methyl coenzyme M reductase via Hdr. Methyl coenzyme M reductase, a coenzyme F_{430}-containing enzyme, catalyzes reduction of coenzyme M-bound methyl group to methane and coenzyme M (105) with coenzyme B generating CoM-S-S-CoB. To regenerate free coenzyme M and coenzyme B, the disulfide bond in CoM-S-S-CoB is reduced by the heterodisulfide reductase (Hdr). As mentioned earlier, flavin-containing

Hdr/Mvh complex is coupled with the first reaction, formylmethanofuran dehydrogenase reaction, through an electron bifurcations mechanism (91).

Methanogenesis from methylated carbon compounds (methylotrophic methanogenesis)

Methylated compounds such as methanol, methylamine and methylsulfide are used for methanogenesis by methanogens that belong to the class of *Methanomicrobia* (see Table 2.1). As shown in Figure 2.1, methanogenesis from methanol can be summarized in the following reaction.

$$4CH_3OH \rightarrow 3CH_4 + CO_2 + 2H_2O$$

1 mol of methanol is oxidized to CO_2 generating 6 electrons. These electrons are used for the reduction of three mols of methanol to methane (93). Oxidation of methanol to carbon dioxide involves transfer of methyl moiety from methanol to H_4MPT, one carbon carrier, catalyzed by methyltransferases (93). Methyl-H_4MPT is then oxidized employing the enzymes similar to those in the hydrogenotrophic methanogenesis (shown as olive arrows in Fig. 2.1, but in the opposite direction). Similarly, reduction of methyl moiety from methanol to methane begins via methyl transfer to Coenzyme M, shown as orange arrows in Fig. 2.1. Methyl-coenzyme M is then reduced to methane following the same path as in the hydrogenotrophic methanogenesis (93).

Acetate fermentation (acetoclastic methanogenesis)

Only a few methanogens ferment acetate. They belong to the genera of *Methanosarcina* and *Methanosaeta* (106). As shown in Fig. 2.1(D), the first step of methanogenesis from acetate involves activation of acetate to acetyl-CoA by acetate kinase/phosphotransacetylase or by acetyl-CoA synthetase (107-109). Then, the carbon-carbon and carbon-sulfur bonds of acetyl CoA are cleaved by a multienzyme complex, acetyl CoA decarbonylase/synthase (110), the central enzyme in acetoclastic methanogenesis (111). The methyl group is transferred to Co^{1+} of a corrinoid-iron-sulfur protein from where it is transferred to H_4MPT forming methyl-H_4MPT, entering the main methanogeneis pathway. The carbonyl group is oxidized to CO_2 generating 2 electrons.

2.3 DEEP-SEA HYDROTHERMAL VENTS

As described earlier, methanogens inhabit environments that might not be always anoxic (112-116). One such environment is deep-sea hydrothermal vent. Below is a description of a deep-sea hydrothermal vent and natural processes by which O_2 is introduced to this environment. Also, a description of hyperthermophilic methanogen *Methanocaldococcus jannaschii*, has been included.

Biogeochemistry of hydrothermal vents

Two different types of hydrothermal vents have been studied (117-119). One is warm-vent such as the ones at the Galapagos rift (117), the place where the first hydrothermal vent was discovered in 1970 (117, 120) and the other one is hot-vent such as those found at the East Pacific Rise (119). A warm-vent emits cold to ambient temperature seawater from the seafloor (water temperature of 5-23^{o}C and flow rate of 0.5-2 cm/sec) whereas a hot-vent puts out hot hydrothermal liquid forcefully (exit temperature and flow rate, 270-380^{o}C and 2 m/sec, respectively) (121).

The water that emerges from the vents is a mixture of seawater and rising hydrothermal fluid. Hydrothermal fluid is composed of highly reduced compounds that come from the basalt of the Earth crust. Examples of these reduced compounds are S^{2-}, S^{0}, $S_2O_3^{2-}$, Fe^{2+}, NH_4^{+}, NO_2^{-} and H_2 (121). On the other hand, seawater contains more oxidized compounds including oxygen. Oxygen reacts with the reduced components from hydrothermal fluid eventually generating $CaSO_4$ precipitate and NO_3^{2-}, compounds that do not exist in the original hydrothermal liquid (121).

Depending on the exit temperature and types of minerals it generates, a hot vent can be classified into two types. The first one is “white smoker” which has exit-water temperatures of $\leq 300^{o}$C and is white due to precipitates of $CaSO_4$. The other one is “black smoker” that emits water with temperatures around $350^{o}C \pm 2^{o}$C and containing black FeS particles (121). The precipitates are produced from a mixing between seawater and hydrothermal fluid that occurs in the shallow mixing regions, 20-100 m below the ocean floor.

The mixing of permeated cold oxygen-containing seawater with very hot anoxic hydrothermal liquid generates a region that is more habitable for microorganisms. Fruitful bacterial growth has been observed in these regions (122, 123).

In the deep-sea hydrothermal vent environments, most of microorganisms have been found in the warm vents and all of these are mesophiles (121). However, several organisms have been observed and isolated from the hot-vent environments such as reported by Baross et.al. (124, 125). Many of vent organisms are chemolithotrophs and considered primary producers in the vent environment as they use inorganic compounds available in the vent fluids to generate their cellular components such as proteins, lipids and sugars. This conversion of the chemical energy of inorganic compounds into bioproducts is known as 'chemosynthesis' (121, 126).

Methanocaldococcus jannaschii, a primary producer in the deep-sea hydrothermal vent

One of the microorganisms that live in the deep-sea hydrothermal vents is *Methanocaldococcus jannaschii*. It uses H_2 and CO_2 for its energy generation and produces methane. This hyperthermophilic hydrogenotrophic methanogen grows at the optimum temperature of 85^{o}C (127). It was isolated by J.A. Leigh from a sample that was taken from the base of a "white smoker chimney" in the deep-sea hydrothermal vent field on the East Pacific Rise at 2600 m below the ocean surface (127). The samples were collected by a group of researchers from Woods Hole Oceanographic Institution using a manned submergence vehicle known as ALVIN (127).

M. jannaschii cells are irregular cocci with the average width of 1.5 µm. Electron microscopic observations of the *M. jannaschii* cells show a complex flagella structures. The expression of *M. jannaschii* flagellins, major structural protein components of flagella, is controlled by the H_2 partial pressure in the environment (103). Under a low hydrogen partial pressure such as 0.650 kPa, most *M. jannaschii* cells are flagellated whereas under high hydrogen partial pressure, 178 kPa, they lack flagella (103).

The study on the swimming behavior of *M. jannaschii* has revealed an interesting finding (128). It has been shown that *M. jannaschii* and another hydrothermal vent organism, *Methanocaldococcus villosus*, are two of the fastest organisms reported as for today. *M. jannaschii* and *M. villosus* swim at the average speed of 400 to 500 bps whereas *E. coli* and Cheetah, the fastest animal, move only at 20 bps, (bps, bodies per second) (128). This ability enables *M. jannaschii* to move quickly toward an area with high H_2 partial pressure.

In a mineral-salts medium with H_2 and CO_2 as substrates for methanogenesis, *M. jannaschii* exhibits a doubling time of 26 min at 85^{o}C. Because *M. jannaschii* inhabits submarine

hydrothermal vents, it shows a requirement for rather high salt concentration for growth, the optimum concentration of NaCl in the media being 0.5 M.

In 1996, the *M. jannaschii* genome was sequenced (129). *M. jannaschii* genetic material is composed of three distinct components, namely one circular chromosomal DNA and one large and one small circular extra-chromosomal elements with the size of 1,665-, 58- and 16-kbp, respectively. The chromosomal DNA encodes 1682 predicted proteins whereas the large and small plasmids encode 44 and 12 predicted proteins, respectively (129).

Sulfite exposure in the vents

As mentioned above, a mixing between oxic-cold seawater with the hot-mineral rich anoxic hydrothermal fluid permits microbial growth in the hydrothermal vent by providing inhabitable temperatures. However, the mixing process might also produce sulfite, a product of incomplete oxidation of sulfide. The sulfide from rising vent fluid reacts with oxygen from seawater below the ocean floor. Due to its reactivity towards proteins, this oxyanion is highly toxic for all living cell (130).

For methanogens, sulfite has a specific detrimental effect on the energy metabolism (131, 132). It is due to the inhibition of methyl-coenzyme M reductase, an essential enzyme in the methanogenesis pathway, by sulfite (133, 134). However, some methanogens have been shown to not only detoxify sulfite but also use sulfite as sole sulfur source (135-137). This observation led to the discovery of a novel type of sulfite reductase in *Methanocaldococcus jannaschii* which uses $F_{420}H_2$ for reduction sulfite to sulfide (137, 138). The enzyme is known as F_{420}-dependent sulfite reductase (137, 138).

2.4 F_{420}-DEPENDENT SULFITE REDUCTASE (FSR)

To begin a discussion on the structure-function relationships of Fsr, I provide general information about sulfite reductases. Sulfite reductase catalyzes six electrons reduction of sulfite to sulfide. This enzyme plays an essential role in the sulfate reduction pathway, one of the most ancient metabolic pathways on earth (139). Depending on the fate of sulfide produced, sulfate reduction pathway can be classified into two distinct processes, namely assimilatory and dissimilatory sulfate reduction. In the assimilatory pathway, sulfide is used for biosynthesis of cysteine (140, 141) whereas in the dissimilatory pathway, most of the sulfide is excreted outside

the cells. Organisms that operate dissimilatory sulfate reduction use sulfate as an electron acceptor in their anaerobic respiration processes (142).

Structurally, assimilatory sulfite reductases (aSir) are distinguishable from the dissimilatory counterpart (Dsr). Based on the structures of two assimilatory sulfite reductase, *Escherichia coli* sulfite reductase hemoprotein subunit (Ec-SirHP) (143) and assimilatory sulfite reductase of *Mycobacterium tuberculosis* (NirA) (144), and of two dissimilatory sulfite reductases of *Desulfovibrio vulgaris* (145) and *Archaeoglobus fulgidus* (146), the characteristics of the sulfite reductases can be summarized as follows. Assimilatory sulfite reductases exhibit pseudo-two folds symmetry fused by an extended strand (143), whereas dissimilatory sulfite reductases are composed of two subunits, DsrA and DsrB, that tightly associate forming a tetramer or an $\alpha_2\beta_2$ structure (147, 148). The symmetry represented by the arrangement of α and β subunits in a heterodimer αβ of Dsr is similar to that found in the assimilatory sulfite reductases. ASir and Dsr share a similar motif for the siroheme-[Fe_4-S_4] center at which six electron reduction of sulfite to sulfide occurs. However, the pseudo-two fold symmetry of aSir is composed of only one siroheme-[Fe_4-S_4] center whereas Dsr heterodimer contains two siroheme-[Fe_4-S_4] moieties. The second siroheme-[Fe_4-S_4] center in one of the Dsr subunits is non-functional (147). Another difference found between aSir and Dsr is the ferredoxin domain which is only found in the latter but not in the former (148). This ferredoxin domain is called peripheral iron sulfur cluster (147) and it has been proposed to be an intermediate electron transfer unit connecting an yet-unknown electron donor to the siroheme-[Fe_4-S_4]. In aSir, for example Ec-SirHP, the electron donor is NADPH (149).

Structure-functions relationship of Fsr

Unlike other sulfite reductases that use NADPH or ferredoxin as electron donors, Fsr uses $F_{420}H_2$ as electron donor (137). Thus, it is called $F_{420}H_2$-dependent sulfite reductase (Fsr). F_{420} contains the deazaflavin derivative, 7,8-didemethyl-8-hydroxy-5-deazariboflavin, that functions as two-electron carrier in many organisms including methanogens and actinobacteria (150). Fsr is a chimera of two enzymes (Figs. 2.2). The primary structure of N-terminal half of Fsr (Fsr-N) is similar to an $F_{420}H_2$-quinone oxidoreductase of *Archaeoglobus fulgidus*, FqoF, (151, 152) or $F_{420}H_2$-phenazine oxidoreductase of *Methanosarcina mazei* (153), FpoF, Fig. 2.2. Fsr-N retrieves electrons from $F_{420}H_2$ and transfers those to a one-electron carrying iron sulfur cluster through a 1-electron/2-electron switch, protein bound flavin. The C-terminal half of Fsr (Fsr-C)

is a homolog of a dissimilatory sulfite reductase (147, 148). Thus, Fsr has a unique characteristic since it functions as assimilatory enzyme that converts sulfite to sulfide. The sulfide is used as sulfur source for *M. jannaschii* but the primary structure of its sulfite reductase unit is similar to dissimilatory sulfite reductase.

Electrons from Fsr-N are transferred to Fsr-C which represents a dissimilatory sulfite reductase. A comparison with Dsr shows that Fsr-C has an additional [Fe_4-S_4] signature sequence at its C-terminus (154). This additional [Fe_4-S_4] cluster might act as a connecting unit between Fsr-N and Fsr-C (154). This [Fe_4-S_4] center is a possible homolog of similar components that connect FqoF subunit of $F_{420}H_2$ dehydrogenase and NuoF of NADH dehydrogenase complex (a complex I) to the respective immediate acceptors in the membrane (Fig. 2.2).

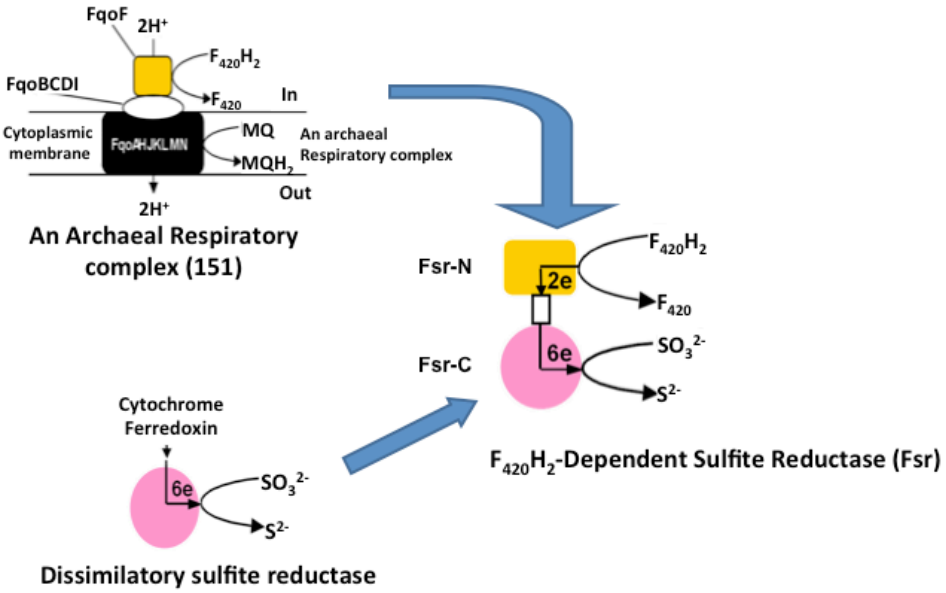

Figure 2.2. Chimeric structure of $F_{420}H_2$ dependent sulfite reductase (Fsr). Fsr is composed of two distinct parts; Fsr-N, yellow box, is similar to F_{420}:quinone oxidoreductase F subunit of $F_{420}H_2$ dehydrogenase complex of *A. fulgidus* (151) whereas Fsr-C, pink circle, is a homolog of dissimilatory sulfite reductase (Dsr). Fqo, $F_{420}H_2$-quinone oxidoreductase.

Fsr homologs are found in the hyperthermophilic/thermophilic methanogens from hydrothermal vents and in certain halophilic methanogens (154). Searches of Fsr-N and Fsr-C homologs in methanogens, as a part of efforts to study their evolutionary histories, revealed two putative new F_{420}-dependent enzymes and wide distribution of Fsr-C homologs in methanogens (154). The details of this work will be discussed in Chapter 3.

2.5 OXIDATIVE STRESS

Methanogens are often exposed to O_2 in their habitats (112-116). Several studies have been shown that methanogens are able to tolerate air exposure for several hours and resume their growth once anaerobic conditions are restored (155, 156). Here, I will discuss oxidative stress in aerobic and anaerobic microorganisms and their responses toward this stress.

Chemical properties of molecular oxygen

O_2 is a potent oxidant. The mid-potential of O_2 reduction at pH 7 is +800 mV (157). In the ground state, molecular O_2 contains two high spin unpaired electrons. This species, also called triplet O_2, is prohibited to accept two electrons at one time from a donor molecule. This characteristic is responsible for the non-reactivity of the dioxygen molecule towards organic compounds which generally participate in 2-electrons-transfer redox reactions (158).

In the cell, flavins through the formation of stable flavosemiquinone are reactive towards O_2, reducing it to a reactive oxygen molecule called superoxide. Other than flavins, cytochrome bc1 is also able to generate superoxide (reviewed in (157)). Univalent electron reduction of superoxide results in the formation of another reactive oxygen species (ROS) called hydrogen peroxide which could further react with transition metals such as Fe^{2+} generating the most reactive oxygen species named hydroxyl radical. The reaction of transition metal with hydrogen peroxide is also known as “Fenton reaction” (159).

These ROS react with different components of a living cell causing growth inhibition and cell death (160). The main cellular targets of ROS are lipids, DNA and RNA, and proteins.

The oxidation of lipids by ROS also called lipid peroxidations causes disruption of the membrane integrity which could lead to cell death (161). Mutations and strand breaks occur in DNA/RNA when ROS react with the sugar phosphate backbone or the nucleotides of DNA/RNA molecules (162). ROS are reactive toward proteins as well (162) where the oxidation targets are thiol groups of cysteine residue and also other amino acid residues such as methionine, lysine, arginine, proline and threonine (163).

Oxidative stress responses in aerobes

In aerobic organisms, ROS are generated as by-products from the electron-transport reactions in the respiration process (164). Bacterial responses toward ROS can be categorized into two ways

(159). The first is primary response which includes expression of several enzymes that scavenge ROS in the cells. The next is secondary response that helps cells to recuperate from the oxidative damages caused by ROS which includes DNA strand break repair, degradation of damaged proteins and lipids, and reduction of oxidized proteins by glutaredoxin/thioredoxin (Grx/Trx) systems. The last item will be discussed in more detail later. Below is the summary of primary responses.

(i) Response to superoxide

Superoxide in the cell is sensed by an [Fe_2-S_2]-containing transcriptional activator, SoxR (165). SoxR activates the expression of Mn-superoxide dismutase (SOD) and other enzymes such as endonuclease IV, glucose-6-phosphate dehydrogenase and ferredoxin reductase (reviewed in (159)). SOD scavenges superoxide and converts it to hydrogen peroxide and molecular oxygen (166, 167). Five types of SODs are known, namely Zn-SOD, Mn-SOD and Cu/Zn-SOD (159), Fe-SOD (168) and Ni-SOD (169).

(ii) Response to hydrogen peroxide

OxyR, a transcriptional regulator that is induced upon H_2O_2 exposure, regulates the expression of about two dozen genes including those for removing H_2O_2 such as catalase and alkylhydroperoxide reductase (157). Catalase converts H_2O_2 yielding water and molecular oxygen (170). During exponential-aerobic growth, hydroperoxide I (HPI) catalase is expressed (171) whereas during stationary state, hydroperoxide II (HPII) catalase is the primary H_2O_2 removing enzyme (172).

Oxidative stress responses in obligate anaerobes

Obligate anaerobes are groups of organisms that require anoxic conditions for growth. Two characteristics of the anaerobes that explain the need of anoxic environments for their growth are described (157, 173). First, unlike aerobic organisms, anaerobes need relatively lower environmental reduction potential for their metabolic processes. Methanogenic archaea, for example, grow only in the medium with low redox potential (lower than -300 mV) (42). The presence of O_2 in the medium increases the reduction potential preventing methanogens from growing. Anaerobic organisms also carry oxygen-sensitive proteins. Four types of such proteins are [Fe-S]-dehydratases, ferredoxin-dependent dehydrogenase, flavin-dependent

enzyme catalyzing dehydration of refractory substrates and enzymes with solvent-exposed [Fe_4-S_4] clusters (reviewed in (157)).

The damaging effect of oxygen species on exposed iron-sulfur clusters in the cell can be explained as follows. Irons in the iron sulfur cluster of proteins of anaerobes exist mostly in the form of [Fe_4-S_4]. Reactive oxygen species oxidize this cluster into the unstable [Fe_3-S_3] form which then is degraded forming unknown degradation products. During this process, Fe^{2+} is released into the cytoplasm. This transition metal further reacts with H_2O_2 yielding hydroxyl radicals through the Fenton reaction, which causes more damages to the cellular components (173).

In addition to iron-sulfur containing proteins, obligate anaerobes also harbor cofactors that are unstable under oxidizing environment. An example is tetrahydromethanopterin of methanogens (174, 175). It is oxidized upon O_2 exposure and degraded into biologically inactive compounds such as 7-methylpterin and 6-acetyl-methyl-7,8-dihydromethanopterin (175).

Although strict anaerobes are generally sensitive to oxygen, the habitats in which these organisms live are periodically exposed to oxygen (114, 176). Moreover, it is known that some obligate anaerobes tolerate oxygen and scavenge the oxidative compounds that form in the cell upon oxygen exposure (114, 155, 177). The mechanisms underlying these processes are however more complex than those in the aerobic organisms (178).

The degree of oxygen tolerance of an anaerobe is determined by several factors, as reviewed in (178). Those include levels of antioxidant proteins, sensitivity of cellular components toward ROS, the ability of the organism to move away from the oxygen source ("negative aerotaxis"), the ability to produce transmembrane chemoreceptor and the capacity, rate and mechanisms of O_2 removal by the cellular reductants (178).

Below I summarize cellular responses adopted by the strict anaerobes, especially methanogenic archaea, to survive under oxygen exposure.

(i) Aerotolerance in methanogens

The first study on oxygen tolerance of methanogens was reported by Keiner, A. and Leisinger, T. in 1983 (155). In this study, Keiner and Leisiner exposed washed starved-methanogen cells to air for several hours. The survival of those cells was then examined by plating the air-exposed cells onto solid media and

incubated them under anaerobic condition. They found that three out of five methanogens studied tolerated air exposure for 10-30 hours without any significant decrease in colony forming units. Those methanogens were *Methanothermobacter thermoautotrophicum*, *Methanobrevibacter arboriphilus* and *Methanosarcina barkeri.* The other two methanogens, *Methanococcus vannielii* and *Methanococcus voltae,* were relatively sensitive to oxygen as shown by the 100-fold decrease in colony forming units after 10 hours of air exposure (155).

Noteworthy in this study is that before the air exposure, cells were washed with medium without reducing agent, rezasurin, to remove reductants from the buffer. Therefore, there was no reaction between the reductant and dioxygen which could lead to the generation of superoxide and hydrogen peroxide. Cells were also starved for about an hour prior to air exposure to reduce metabolic activity of the cells thus preventing ROS generation in the presence of oxygen. Mukhopadhyay and Wolfe (unpublished data, as reported by J. Imlay (157)) performed similar experiments with *M. thermoautotrophicus* strain ΔH. They observed that this hydrogenotrophic methanogen tolerated substantial amount of oxygen. They flushed the culture with air for 6 hours and the growth of *M. thermoautotrophicus* resumed after anaerobic condition was restored. They also found that the recovery from transient aerobiosis was relatively faster when the cells were washed with non-reducing medium following the air exposure.

(ii) Morphological adaptation

Some methanogens have been shown to form aggregates in order to protect themselves from oxygen exposure. Keiner, A. and Leisinger observed that the number of *Methanosarcina barkeri* colonies on a plate after 30 hours air exposure did not change significantly compared to that before the air exposure (155). However they found that the colonies of the former were much smaller compared to that from the culture that was not exposed to air. This might be due to the fact that *M. barkeri* forms aggregates (155, 179). Thus, the cells on the outer surface of the aggregate were exposed to oxygen protecting the inner cells from oxygen exposure.

(iii) Negative aerotaxis

Several sulfate reducing such as *Desulfovibrio oxycliane* that grows on cyanobacterial mats and *Desulfovibrio vulgaris* are able to move toward anaerobic area in response to changes in their environments (180-182). In a capillary tube experiment with anaerobic suspension of *D. oxycliane*, the cells migrated away from O_2 bubble that was introduced to the capillary tube and formed a sharp band creating the oxic-anoxic interface (181).

Changes in the levels of reductants in the environment could also create conditions that mimic those under air exposure. A study with *Methanocaldococcus jannaschii*, a hyperthermophilic hydrogenotrophic methanogen, showed that under low hydrogen concentration, where reductants are scarce, *M. jannaschii* expresses flagella. Presumably, a redox sensor and flagella facilitate mobility of *M. jannaschii* toward a zone with high level of reductant source, in this case H_2 (103).

(iv) Formation of consortia with facultative anaerobes

Methanogenic bacteria are known to associate with facultative anaerobes in their environments. An example of such a case is found in granular sludge that forms during waste water treatment (114). Facultative anaerobes consume O_2 thus providing anoxic conditions for methanogens (114).

(v) Expression of antioxidant proteins

SOD and catalase are two common antioxidant proteins used by aerobic bacteria to detoxify superoxide and hydroxyl peroxide, respectively. In some anaerobic bacteria such as *Methanosarcina barkeri*, SOD and catalase are also employed for protecting cells from ROS toxicity (183). SOD scavenges superoxide producing oxygen as one of the end products thereby incompatible with many anaerobic systems. Therefore, some of the anaerobes have developed strategies to scavenge reactive O_2 species in the cell via superoxide reductase and different types of peroxidases such as peroxiredoxin, rubrerythrin and rubredoxin as discussed below.

Superoxide reductase—Superoxide reductase (SOR) activity was first observed in *Pyrococcus furiosus* (184), an anaerobic archaeon that lacks SOD. Unlike SOD,

SOR reduces superoxide to hydrogen peroxide using low potential electrons delivered by rubredoxin (184). Oxidized rubredoxin is replenished by the action of NAD(P)H-rubredoxin oxidoreductase with NAD(P)H as electron donor (184). Hydrogen peroxide produced as the end product of SOR reaction is then oxidized into water by virtue of peroxiredoxin using electrons from NADH through NADH peroxidase (185). In *Pyrococcus furiosus*, a hyperthermophilic archaeon, rubredoxin can be replaced with other unknown redox proteins (186).

Flavodiiron protein A – A study with *P. furiosus* showed that flavodiiron protein A was the primary avenue to detoxify O_2 into water. The electrons for this reaction comes from NAD(P)H through a rubredoxin (186).

Methanoferrodoxin – A variant of superoxide reductase was found in an aerotolerant methanogen, *Methanosarcina mazei* (187). Unlike other superoxide reductase, *M. mazei* enzyme carries an iron-sulfur cluster [Fe_4-S_4] as a second prosthetic group in addition to its [$Fe(NHis)_4(SCys)$] catalytic site. It has been proposed that methanoferrodoxin contributes to the aerotolerance nature of *M. mazei*.

$F_{420}H_2$ oxidase (FprA) – It has been shown that a cell suspension of *Methanobrevibacter arboriphilus*, a methanogen that was isolated from anaerobic sewage sludge (188), is able to reduce O_2 in the presence of H_2. The O_2 reduction activity is catalyzed by $F_{420}H_2$ oxidase (FprA) (189, 190). FprA reduces O_2 with H_2 via the oxidation of F_{420}. Since FprA is a cytoplasmic protein, it has been proposed that this protein provides an avenue to reduce intracellular O_2 (190).

NADH oxidase (Nox) –Nox generally reduces molecular O_2 into hydrogen peroxide or water via 2 or 4-electron reduction with NADH. Anaerobic archaea *P. furiosus* and *A. fulgidus* are known to use NADH oxidase for defense against oxidative stress (191, 192). Other than O_2, Nox is known to reduce a variety of substrates such as the disulfide of coenzyme A, sulfur and cytochrome c (193-195). *M. jannaschii* Nox homolog exhibits O_2 reduction activity with high apparent K_m for O_2 suggesting that O_2 might not be the true biological substrate for this enzyme (196).

(vi) Post-translational protein modifications by thioredoxin system

Pyruvate:ferredoxin oxidoreductase (PFOR), an iron-sulfur containing protein, is known to be highly sensitive to O_2 due to its solvent exposed [Fe_4-S_4] center (197). However, PFOR of *Desulfovibrio africanus* (Da-PFOR) was found to be oxygen tolerant (198). Primary sequence comparison with other PFORs revealed an additional domain containing two regulatory cysteine residues forming C-X-X-C motif in Da-PFOR that confers O_2 stability to this enzyme (199). It was shown that during O_2 exposure, two specific cysteine residues in the regulatory domain form disulfide bond. When anaerobiosis is restored, reduced-thioredoxin (Trx-2SH) reduces the disulfide bond of the regulatory cysteines of PFOR, thereby reactivating PFOR (200). Thioredoxin-based metabolic regulation will be discussed in a following section.

(vii) Formation of O_2 sensor molecule, a study of F_{390} in methanogenic archaea

Upon O_2 exposure, *Methanothermobacter thermoautotrophicus*, a thermophilic methanogen, generates two redox inactive chromophores that exhibit absorbance maxima at 390 nm (201). The compounds, F_{390}-A and F_{390}-G, are phosphodiesters of coenzyme F_{420} with adenosine monophosphate (AMP) and guanosine monophosphate (GMP), respectively (201). Cellular levels of F_{390}-A and F_{390}-G are maintained by the actions of two enzymes, coenzyme F_{390} synthetase and F_{390} hydrolase, that catalyze F_{390} production and degradation, respectively (202). F_{390} is considered a reporter of oxidative stress that is caused by either O_2 exposure or reductant limitations (203).

Physiological implications of F_{390} generation during oxidative stress is that the level of coenzyme F_{420}, a precursor of F_{390} and also an obligate two-electron carrier, decreases during this time. This is one of the reasons as to why methanogenesis, an energy generation pathway that is highly dependent on $F_{420}H_2$, shuts down during O_2 exposure. Another major implication is that F_{390}, acting as a sensor/regulator molecule, might control the expression of proteins that are responsible for O_2 removal (201).

2.6 THIOREDOXIN SYSTEMS

Under normal physiological conditions, cytoplasm in all living cells provides a reduced environment (204), which is optimal for the function of a variety of proteins particularly in a wide range of biological processes. Thiol-containing proteins are generally found in their reduced-forms, having free thiol groups. However, cells are sometimes subjected to oxidative stresses such as UV radiation and exposure to strong oxidants or toxic reactive oxygen species (ROS) that are by-product of aerobic respiration processes (205). To protect itself from this detrimental effect of oxidation, a cell produces anti-oxidant proteins that remove ROS and reduce the oxidized proteins to their functional reduced-forms. One of the latter type proteins is thioredoxin (Trx). Here, I will describe the Trx systems that are composed of Trxs and Trx reductases (TR) and their roles in oxidative stress response and other important biological systems.

Trxs are ubiquitous redox active disulfide proteins containing two active cysteine residues separated by two variable amino acids forming the C-X-X-C motif (206). These relatively small proteins with average molecular weight of 12 kDa are responsible for redox-based regulation of many important cellular processes ranging from classical 'light-dark' regulation in higher plants (207) to regulation of oxidative-stress induced apoptosis in mammalian cells (208), maintaining redox homeostasis (209), providing reducing equivalents to peroxiredoxin for H_2O_2 removal (210, 211), and serving as a reductant for essential enzymes such as ribonucleotide reductase, phosphoadenosinephosphosulfate (PAPS) reductase and methionine sulfoxide reductase (212-214).

Trxs have been studied extensively (215). This acidic and heat stable protein is found in almost all organisms in the three domains of life—Archaea, Bacteria and Eukarya (216). Trx was first described in yeast by Asahi et.al and Black et.al (212, 213) in 1960 in two separate unrelated experiments and was assigned different names.

Asahi et al. studied phosphoadenosinephosphosulfate (PAPS) reductase, an enzyme in sulfate reduction pathway converting PAPS to sulfite (212, 217). They found that three different protein fractions were required for the reduction of PAPS to sulfite, namely enzyme A, enzyme B and

fraction C. Enzyme B is responsible for the reduction of PAPS to sulfite with NADPH as electron donor. Enzyme A channels electrons from NADPH to fraction C from where the electrons are ultimately transferred to enzyme B.

A similar phenomenon was observed by Black and colleagues (213). A mixture of three enzymes (enzyme I, II and III) was required for the reduction of methionine sulfoxide to form methionine and water. Methionine sulfoxide forms non-enzymatically inside a cell by the action of reactive oxygen species on methionine. In a methionine sulfoxide reductase reaction, enzyme III reduces methionine sulfoxide to methionine whereas the other two, enzymes I and II, exhibit properties similar to that of enzyme A and fraction C as observed by Asahi, et.al.

The name 'thioredoxin' was later introduced by Reichard, et. al in 1964 (214). This group studied the mechanism of ribonucleotide reductase, an essential enzyme that generates building blocks for DNA molecules. They showed that Trx plays an important role in the formation of deoxyribonucleotides from ribonucleotides that is catalyzed by ribonucleotide reductase. Trx provides reducing equivalents for the enzyme. Later they also discovered another protein, called thioredoxin reductase, that reduces Trx using the two electrons from NADPH (218).

Depending on the electron donor used for Trx reductions, Trx systems can be divided into two types, namely NADPH-dependent thioredoxin systems (NTS), using NADPH as an electron donor, and ferredoxin-dependent thioredoxin system (FTS), employing electrons from reduced-ferredoxin (see Fig. 2.3). Below, I describe in more detail the physical properties and mechanisms of action of Trx and Trx reductase (TR), the two components of a thioredoxin system.

Thioredoxin (Trx)

As the genome sequences of many organisms have become available, it is now relatively easier to study the distribution and evolutionary relationships among Trxs. Generally, almost all living organisms possess Trx. The size of Trx ranges from 105-110 amino acid residues (219). They share 27-69% sequence identity carrying a classical C-G-P-C active site (220). This suggests that Trxs in extant organisms developed from a common ancestor.

Structure-functions relationship

The first crystal structure of Trx to be elucidated was for the oxidized form of *E. coli* Trx. This structure was determined in 1975 to 2.8 resolution (221) and later was refined to 1.68 Å in 1990 (222). *E. coli* Trx is composed of 108 amino acid residues with the classical redox active motif of C-G-P-C (223). The three dimensional structure of Trx is characterized by 5 stranded β-sheets separated by 4 α-helices. A similar fold is also owned by other proteins that belong to the thioredoxin superfamily which share a fold composed of 4 stranded β-sheets flanked by 3 α-helices, known as the "Trx fold".

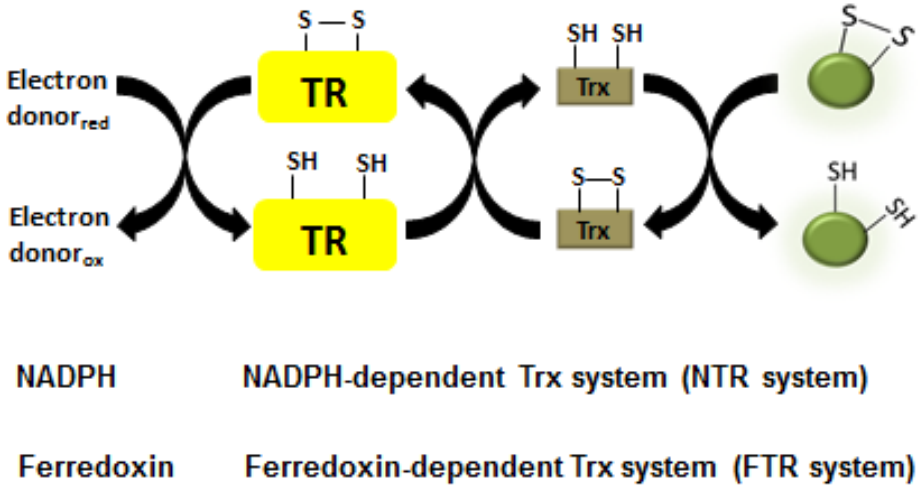

Figure 2.3 Thioredoxin systems. NADPH-dependent thioredoxin systems (NTS) and ferredoxin-dependent thioredoxin system (FTR). Thioredoxin system is composed of thioredoxin (Trx, olive boxes), thioredoxin reductase (TR, yellow boxes), target proteins (green circle; reduced, –SH; oxidized, S-S) and electron donor. Trx is reduced by NADPH- or Ferredoxin-dependent thioredoxin reductase using electrons from either NADPH or Ferredoxin, respectively. The reduced Trx regulates the activity of target proteins by reducing disulfide bonds on their regulatory cysteine residues.

Based on the studies on the crystal structures of oxidized and reduced forms of *E. coli* Trx, the mechanism of thiol-disulphide exchange by Trx can be described as follows (224, 225). First, an oxidized-target protein binds to the flat hydrophobic surface of the reduced Trx surrounding the redox active residues of the protein (226). Then the thiol-disulfide exchange reaction is initiated by a nucleophilic attack by the thiolate of Cys32, the N-terminal active

cysteine residue, to one of the sulfur in the disulphide bond of the target, forming mixed disulphide transition state. Then, the thiolate of Cys35 is deprotonated and it attacks the sulfur of Cys32 forming a disulfide bond while the target protein is reduced to 2 free thiol groups as shown in Fig. 2.4. The reaction follows the ping-pong mechanism of enzyme action (227).

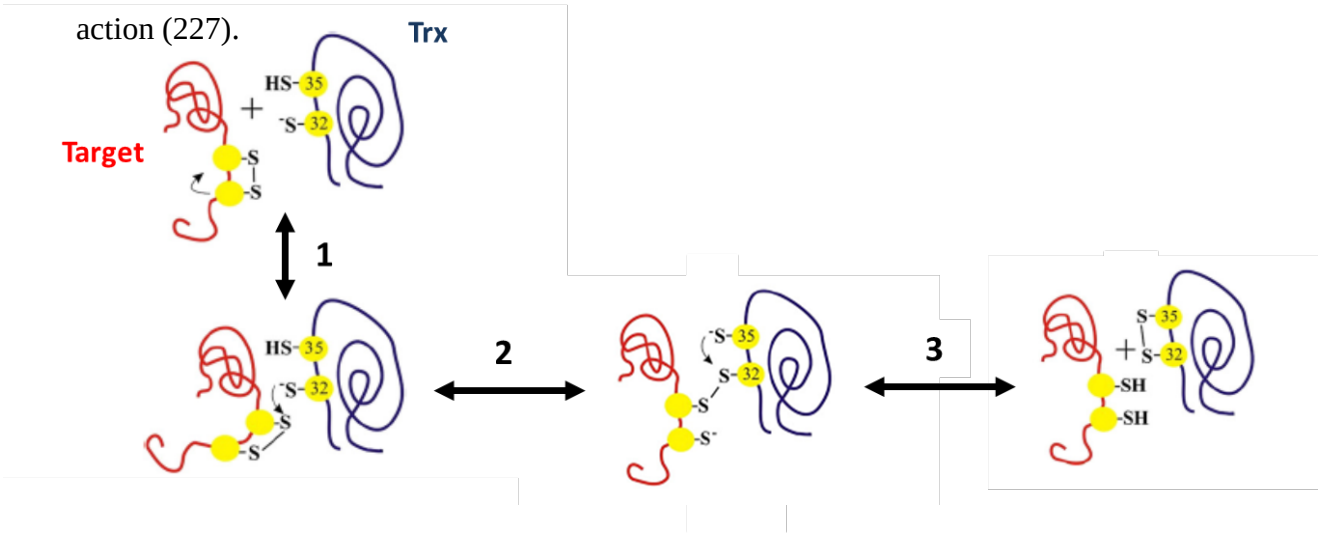

Figure 2.4 Thiol-disulfide exchange mechanism of Trx. The reduction of a Trx target protein, shown in red, by Trx, shown in blue, follows a two-electron transfer reaction involving two redox active cysteine residues, shown in yellow. *E. coli* Trx is used as a model. Cys-32 is the solvent-accessible residue that acts as a nucleophile attacking one of the sulfur in the disulfide bridge of the target protein (reaction 2) yielding a mixed-disulfide. The buried cysteine of Trx, Cys35, then attacks the sulfur of Cys32. Subsequent electron transfer to one of the sulfur moiety of the target protein generates free sulfuhydryl groups at this site and disulfide bond between Cys32 and 35 (reaction 3). These reactions occur in either direction depending on the redox status of the environment. This figure has been adapted from (228).

A comparison between the structures of oxidized and reduced forms of *E. coli* Trx shows that there is only a slight difference between the two structures. This includes local conformational shifts at and around the redox active site –C-G-P-C-. The distance between C^{α} of C32 and C^{α} of C35 is shortened upon disulfide bond formation (224). The major difference between the two forms of Trx is in the stability of the protein, with reduced-Trx being structurally less stable than the oxidized counterpart (224).

Trx superfamily

As mentioned earlier, proteins that contain one or more Trx fold are categorized into the Trx superfamily. Seven distinct protein families belong to the Trx superfamily (229, 230). They are (1) Trx, (2) Glutaredoxin/Grx, (3) DsbA, (4) Protein disulfide isomerase (PDI), (5)

glutathione-S-transferase, (6) Glutathione peroxidase and (7) Protein kinase-C-interacting cousin of thioredoxin (PICOT) (230, 231). Here, I will describe the members of the Trx superfamily that share the -C-X-X-C- cysteine redox motif, namely Trx, Grx, DsbA and PDI.

Although they belong to the same superfamily, these proteins have limited primary sequence homology and exhibit different functions (232). The closest relatives among all are Trx and Grx. Trx and Grx also have similar conserved residues and the examples are Arg73, Gly-74, Ile-75, Pro-76 (numbering based on *E. coli* Trx) (226). It has been suggested that Grx evolved from Trx (233).

(i) Trx

Thioredoxin (Trx) is the most potent reductant of all members of Trx superfamily (234) with the standard redox potential of about -270 mV. Three-dimensional structure of Trx shows that it carries additional one β-sheet and one α-helix at the N-terminus and the classical active site motif of -C-G-P-C- is positioned within a loop connecting β1 and α1 (221, 222).

(ii) Grx

Grx carries -C-P-Y-C- motif and the structure of this protein is characterized by 4 stranded β-sheet surrounded by 3 α-helices, the minimal Trx-fold (235). Glutaredoxin reduces specific disulfide bonds in a variety of protein targets. Unlike Trx, Grx depends on a tripeptide molecule, glutathione (GSH), for catalyzing the thiol-disulfide exchange reaction. The oxidized Grx resulting from the reduction of a target is reduced by GSH and oxidized glutathione is regenerated by the enzyme known as glutathione reductase (236).

(iii) DsbA

DsbA is a bacterial periplasmic protein that catalyzes the formation of disulfide bond in target proteins (237-240). It has a standard reduction potential of -90 to -125 mV (241-243) and carries the –C-P-H-C- motif at the redox active center (243). DsbA plays important roles in protein folding by introducing disulfide bonds in unfolded/partially folded protein targets (244). In target proteins with more than two cysteine residues, DsbA could introduce non-native disulfide bonds (245-247). To solve this problem, a protein called DsbC, also a periplasmic protein, rearranges the non-optimal disulfide bonds in the target

proteins into their correct forms (239, 248-250). To allow these functions, both oxidized DsbA and reduced DsbC need to be regenerated. DsbB, a membrane-bound protein, re-oxidizes DsbA and transfers electrons to menaquinone and in the other case, DsbD, an inner membrane protein, reduces DsbC using electrons from thioredoxin in the cytoplasm (246, 251-256).

(iv) PDI

Protein disulfide isomerase (PDI) is an enzyme with similar function as DsbA that operates in endoplastic reticulum of eukaryotic cells (257-260). Unlike DsbA, PDI has more negative standard reduction potential ($\Delta E'^{o}$ = -180 mV) and it employs a –C-G-H-C- redox active motif in catalysis (261).

Redox properties of Trx

The N-terminal cysteine residue (Cys32 in *E. coli* Trx) that initiates the redox reaction is solvent accessible and at a physiological pH it is deprotonated (224). This is because the pKa of a nucleophilic Cys is unsually low, 6.3 – 7.5 (224, 262-267). The general pKa for a cysteine residue is 8.5 (268).

One of the factors determining the pKa of a nucleophilic cysteine residue is the nature of the variable residues (Xs) in the active site motif, -C-X-X-C-. The replacement of the variable residues of Trx, -G-P-, with that of the PDI, -G-H-, lowers the pKa of nuclophilic cysteine and increases the overall redox potential to -235 mV (269, 270). This increase in reduction potential is accompanied by the acquirement of an isomerase activity in the variant Trx (270, 271). When the -G-H- sites of DsbA is converted to -G-P- of Trx, the standard reduction potential of DsbA decreases by 92 mV (242). Therefore, the variable residues in the –C-X-X-C- motif act as 'rheostat' that determines the redox properties and functions of Trx superfamily members (272, 273).

Measuring the thiol-disulphide reductase activity using insulin

In 1979, Holmgren (227) showed that with DTT or dihydrolipoamide as an electron donor, Trx is able to reduce disulfide bridges in insulin molecules releasing chain A and chain B. Freed chain B of insulin is not stable in solution and forms aggregate (274). This reaction can be observed as the formation of white precipitates and the rate can be quantitatively followed spectrophotometrically at 650 nm. Since Trx reduces insulin with a second order

rate constant 10^4 times higher than DTT alone, the insulin reduction assay is routinely used for determining the oxidoreductase activity of Trx, replacing more laborious, ribonucleotide reductase assay (275).

Roles of Trx

Followings are the cellular roles of Trx: maintaining redox balance (209), responding to oxidative stress (208), regulating protein function via redox active cysteine residue (207) and providing electrons for enzymes (212-214). All these roles could be summarized in two general actions. First, Trx provides reductant for several enzymes such as ribonucleotide reductase (276), an essential enzyme for generating building blocks for DNA synthesis, PAPS reductase, an enzyme in the assimiltory sulfate reduction pathway generating sulfite from PAPS, methionine sulfoxide reductase, an enzyme that reduces the oxidized product of methionine (212-214), and peroxiredoxin which catalyzes the reduction of H_2O_2 (210, 211). The second function of Trx is to reduce specific disulfide bonds in oxidized target proteins (277).

Trx also acts as essential component of virus assembly and replication machineries (278-281). Trx increases the processivity of T7 DNA polymerase and enhances the assembly of filamentous f1 and M13 phages. However, the fundamental mechanisms of these processes remain unknown (278-281).

Trx targets identification

Described below are descriptions of several common approaches to identify the protein targets of Trx.

(i) *In-vitro* approach

Two major in-vitro approaches are employed in Trx target identification, namely affinity chromatography with immobilized Trx variants (282) and two-dimensional gel electrophoresis with proteins labeled with sulfhydryl-based fluorescence compound, followed by mass spectrometric analysis (283). These two methods involve incubation of cell lysate with Trx in-vitro. In the affinity chromatography method, the C-terminal cys residue of a Trx has been replaced with serine. This variant is immobilized onto a resin and a cell lysate of interest is

loaded onto a column containing the resin. Protein targets bind to the immobilized Trx variant through mixed disulfide with the N-terminal cys and cannot leave due to the absence of C-terminal cys that prevents the next step in catalysis (284). The bound Trx target proteins are then eluted with DTT, an artificial electron donor. Eluted proteins are identified by mass spectrometric analysis.

In the two-dimensional gel electrophoresis based analysis (283), a cell lysate preparation is incubated with Trx and an electron donor which is generally DTT (285). In some cases, a physiologically-relevant electron donor such as NADPH and a Trx reductase, an enzyme that transfer electron from NADPH to Trx are added in place of DTT (285, 286). At the end of the incubation period, monobromobimane, a sulfhydryl-specific fluorescent probe, is added. The resulting protein mixture is resolved on a two-dimensional electrophoresis gel, followed by the identification of fluorescence protein spots under UV light (365 nm). Both of them are in use in our laboratory. In order to enhance fluorescence detection of the Trx target proteins on the gel, Maeda et.al. employed a cyanine dye maleimide, cy5m, in place of monobromobimane (287).

(ii) *In-vivo* method

In addition to the *in vitro* approaches, *in vivo* assays have also been developed to identify proteins that are linked to Trx. Yeast two hybrid system (Y2H) has been employed by some researchers (288, 289)). In this method, wildtype or variant Trx (with the C-terminal cys replaced with serine) is used as a bait. Vignols, et.al. used yeast strain CY306 for their studies (288, 289). CY306 is a yeast strain lacking Trxs. The Trx bait and a target protein were cloned into two different plasmids and then transformed to the CY306. Strains containing these two plasmids are selected and complex formation between these two proteins is analyzed.

Trx target proteins

Plant Trx targets have been studied extensively (207). The process in which these proteins participate range from DNA replication, transcription and translation, biosynthesis of amino

acid, lipid and glycogen/glucose cell biosynthesis, oxidative stress response to cell division (207).

Trx in methanogenic archaea

Unlike Trxs from the Bacterial and Eukaryal domains, Trxs from the Archaea, the third domain of life, have not been studied extensively. Studies on archaeal Trxs are limited to their biochemical and structural properties (127, 290-299). Only three methanogen Trxs have been studied, they are MTH895 and MTH807 of *Methanothermobacter thermoautotrophicum* strain ΔH, a thermophilic methanogen (296, 297), and MJ0307 of *Methanocaldococcus jannaschii*, a hyperthermophilic methanogen (299, 300).

Methanogen Trxs are unique in the sequences of their redox active motifs and three-dimensional structures. MJ0307, MTH895 and MTH807 carry non-canonical Trx motifs, -C-P-H-C-, -C-A-N-C- and –C-P-Y-C-, respectively (Table 2.2). As described previously, the amino acid residues located in between two active cysteine residues determine the reduction potential as well as functional properties of these proteins (272, 273). However, this is only one of the many factors that could influence the redox properties of a Trx (273). MJ0307 serves as a good example in this regard. C-P-H-C, the redox active motif of MJ0307, is similar to the canonical motif of DsbA, a potent oxidant. We might think that MJ0307 would behave like a DsbA (241-243). However, Lee, et.at (299) showed that the standard mid-point redox potential of MJ0307 is actually lower than that of *E. coli* Trx, -277 mV for MJ0307 and -270 mV for *E. coli* Trx. Also, MJ0307 reduced insulin with 1.5 fold higher rate than *E. coli* Trx.

Methanogen Trxs are structurally more similar to Grx than to Trx (297, 300). However, an analysis of thiol content in washed cell extract of *Methanothermobacter thermoautotrophicus* revealed the absence of glutathione or related peptides in this archaeon (296). Therefore, the possibilities of methanogens Trxs actually being Grx are small. However, it is possible that these Grx-like proteins use a novel system, independent of glutathione and glutathione reductase, for regenerating their reduced forms.

TABLE 2.2 Characteristics of Methanogen Trxs in comparison with *E. coli* Trx and Grx

Organism	Locus tag number	Number of amino acids	Redox active center	pKa value[a]	Standard redox potential ($\Delta E^{o'}$, mV)	Secondary structures N→C terminal (pdb id)	Biochemical properties: Grx activity	Biochemical properties: Act as a component in T7 DNA polymerase complex	Biochemical properties: Insulin reductase activity	Refs.
Methanocaldococcus jannaschii	MJ_0307	85	CPHC	6.3	-277	βαβαββα (1FO5)	None	Yes	Yes	(299, 300)
Methanothermobacter thermoautotrophicum strain ΔH	MTH807	85	CPYC	6.2	NA	βαβαββα (1NHO)	Weak	NA	Yes	(296, 297)
	MTH895	77	CANC	6.7	NA	βαβαββα (1ILO)	Weak	Yes[b]	Yes	(298)
Escherichia coli	Trx1	109	CGPC	6.3-10	-270	βαβαβαββα (2TRX)	Weak	Yes	Yes	(222, 297, 298, 301, 302)
	Grx1	85	CPYC	3.8	-233	βαβαββα (1EGR)	Yes	No	No	(297, 298, 303-305)

[a] pKa values are for the N-terminal Cysteine residues
[b] observation was based on modeling studies

The sizes of methanogen's Trxs are comparable to that of Grx. Average size of a Grx is 82 amino acid residues whereas that of a Trx is 100-125 amino acid residues (219). Thus, this regard smaller Trxs of methanogens are more related to Grxs than to Trx. A methanogen Trx is composed of a canonical Trx fold, β-α-β-α-β-β-α, but it misses one β-sheet and α-helix in its N-terminal. Interestingly, MTH807 not only has the Grx fold but it also carries the active site motif of –C-P-Y-C- that is typical for the Grx family (297). However, it has been shown that MTH807 exhibits weak Grx activity (297).

From the above description, it is not clear as to why methanogen Trxs have their distinct characteristics. Is it possible that the unique characteristics of Trx are required for functioning in an anaerobe? Are these proteins the ancestors of Trxs found in the Bacteria and Eukarya? Moreover, nothing is known about the physiological roles and the mechanism underlying disulfide reduction by methanogen Trxs.

Thioredoxin reductase (TR)

To date, there are two known types of thioredoxin reductases, namely NADPH-dependent thioredoxin reductase (NTR) and ferredoxin-dependent thioredoxin reductase (FTR). These two reductases are structurally unrelated to each other and also use different mechanisms in Trx reduction.

NTR is a flavoprotein of the pyridine nucleotide oxidoreductase family that uses NAPDH as an electron donor whereas FTR is an iron-sulfur cluster-containing protein that uses ferredoxin as its source of reductant. NTRs are found in most eukaryotes, bacteria and archaea (277). In contrast, the distribution of FTR has been thought to be limited to the oxygenic photosynthetic bacteria and eukaryotic photosynthetic organelles (306). However, genome-based searches have revealed the presence of FTR-like proteins in various photosynthetic and non-photosynthetic bacteria and archaea (307-309). Here, I review the distribution, evolutionary history, structure-functions relationships and mechanisms of action of each type of thioredoxin reductase.

NADPH-dependent thioredoxin reductase (NTR)

NTR was first purified in *E. coli* in 1964 as a flavoprotein that reduces Trx for supplying reductants for ribonucleotide reductase reaction (218). This thioredoxin reductase is widely

distributed in the bacteria, archaea and eukarya. In addition to flavin, NTR possesses two redox active cysteine residues that are responsible for the Trx reduction activity.

Protein Structure comparison between NTR of bacteria and that of human suggested that NTR can be divided into two types. The first one is a low-molecular weight NTR (small NTR), with the average size of 35 kDa, that is found in bacteria, archaea and some eukarya (277). The other is a high-molecular weight selenocysteine-containing NTR (large NTR), with the average size of 55 kDa, that is found only in some eukaryotic organisms including human (310, 311).

(i) *Low-molecular weight NTR*

The low molecular weight NTR is found in organisms from all three domains of life-Archaea, Bacteria and Eukarya, including fungi, plants, protozoa and intestinal parasite. The protein is a homodimer with the average subunit molecular weight of 35 kDa. Each subunit contains bound FAD and possesses two redox active cysteine residues in C-A-T-C motif (312).

The electrons from NADPH are channeled to FAD and then reduced-FAD transfers the electrons to the disulfide bond in the redox active center (313). Similar to the redox active Cys in Trx, the solvent accessible Cys residue, Cys138, in the redox center acts as a nucleophile attacking the disulfide of Trx, releasing reduced Trx (314). The redox center of small NTR is located near the NADPH binding site. However, NADPH binding site is not in the vicinity of the FAD binding site (315). Therefore, during catalysis a major conformational change in the protein is needed to facilitate the electron transfer from NADPH to FAD (315, 316).

(ii) *High molecular weight NTR*

In mammalian systems, NADPH-dependent Trx reduction is carried out by a selenocysteine-containing NTR (310, 311). Selenocysteine is known to be more reactive than the cysteine counterpart due to its lower pKa (5.3) (317). In mammalian NTR, the -G-C-SeC-G- motif, where SeC is a selenocysteine residue, is located away from the redox active center, -C-V-N-V-G-C-. The selenocysteine is essential for NTR catalysis (318). Also, the selenium-containing redox center in mammalian NTR is thought to be

responsible for the promiscuity of the enzyme (319). Other than Trx, the mammalian NTR also reduces a wide variety of substrates such as lipoic acid (320), lipid hydroperoxide (321), the cytotoxic peptide NK-lysin (322) and vitamin K_3 (227).

Structurally, mammalian NTR is more related to glutathione reductase than to low molecular weight NTR. The similarity concerns the site for substrate binding as well (323-325). The only clear difference between these two proteins is the additional C-terminal domain containing the selenocysteine active center in NTR that is absent in the glutathione reductase (323).

In term of disulfide oxidoreductase mechanism, a major difference between small and the mammalian NTR is that the former undergoes conformational change during catalysis as observed in the *E. coli* NTR. In the large NTR, NADPH and FAD binding domains are located in close proximity (326). Therefore, no major conformational changes occur during electron transfer from NADPH to FAD. However, conformational movement is observed in the additional C-terminal element at which the second redox center containing selenocysteine resides (326). The flow of electrons from NADPH to Trx via the mammalian NTR can be summarized as follows (326), NADPH → FAD → two cysteine redox center → selenocysteine-containing redox center → Trx.

(iii) *Homolog of NTR with an unknown electron donor in archaea, a study of NTR-like protein of* Thermoplasma acidophilum

A study on thioredoxin system in *Thermoplasma acidophilum*, an anaerobic thermoacidophilic archaeon isolated from a self-heating coal refuse pile and solfatara fields (327), revealed a unique NTR-like thioredoxin reductase with unknown electron donor (290). *T. acidophilum* genome encodes one Trx (Ta0866) and one thoredoxin reductase (Ta0984) (327).

Structurally, Ta-TR is similar to the *E. coli* NTR (290). However, the residue H175, R176, R177, R181 of *E. coli* NTR responsible for binding of NADPH was substituted with E185, M186, Y187, and M191 in Ta-TR, respectively (290). The inability of Ta-TR to accept electrons from NADPH is not due to redox potential barrier, as the mid-potential redox potentials of the redox active center of Ta-TR and *E. coli* NTR differ only by about 35 mV (290).

(iv) *Distribution of NTR in methanogenic archaea*

Based on our bioinformatics analysis on NTR homologs in the genomes of methanogens, it seems that NTR homologs are widely distributed in methanogens as shown in Figure 2.5 (Dwi Susanti and Biswarup Mukhopadhyay, manuscript in preparation).

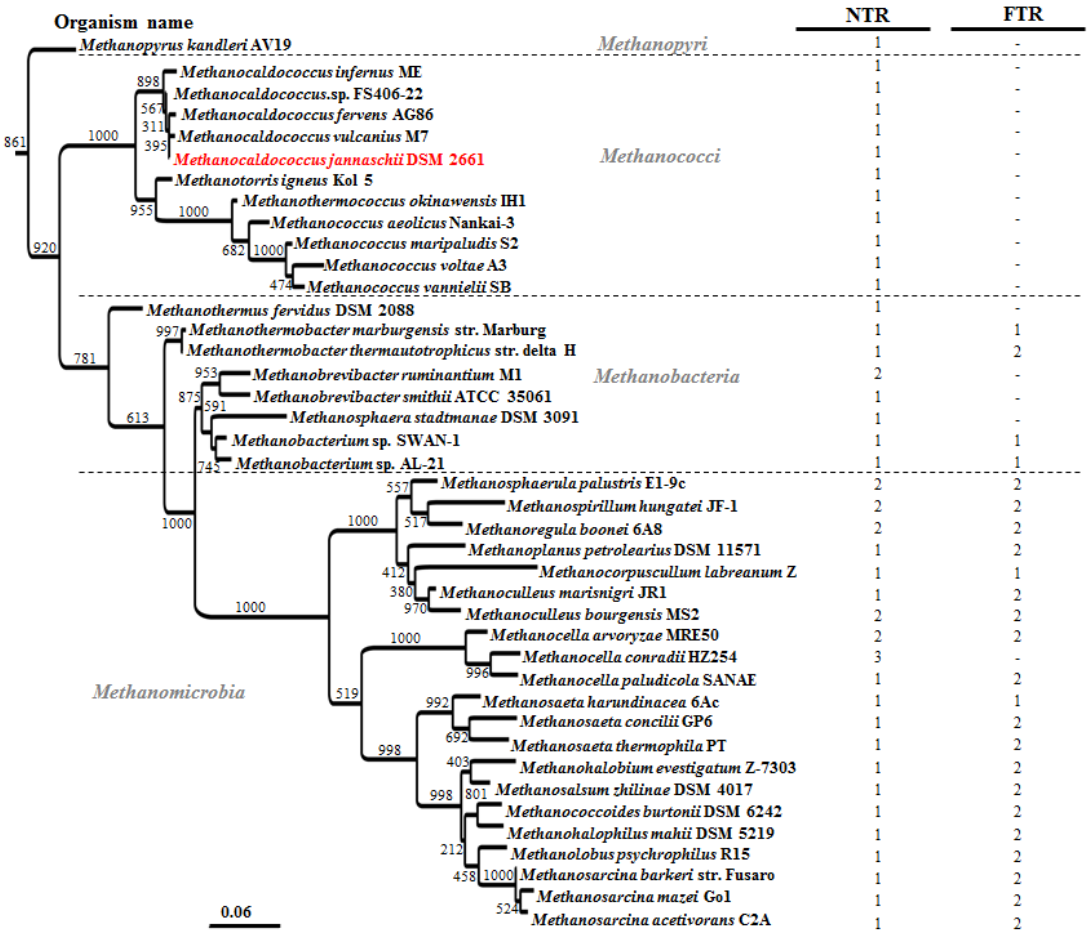

Figure 2.5. Distribution of NADPH-dependent thioredoxin reductase (NTR) and Ferredoxin-dependent thioredoxin reductase (FTR) homologs in methanogenic archaea.

NTR homologs were found in all methanogens analyzed. The typical NTR, similar to *E. coli* NTR, were found in the late evolved methanogens such as those belonging to the classes of *Methanobacteria*, *Methanomicrobia* and *Methanosarcina*. In addition to the NTR homolog, each of these methanogens also possesses at least one FTR homolog. Interestingly, the phylogenetically deeply-rooted methanogens such as those belonging to the class of *Methanopyrus* and *Methanococcus* contained only one NTR homolog that is

similar to Ta-TR, lacking the NADPH binding site. These enzymes are currently under investigation in our laboratory.

Ferredoxin-dependent thioredoxin reductase (FTR)

Unlike the NTR system that is comprised of 3 protein components, the ferredoxin/thioredoxin system (FTS) consists of four proteins, namely ferredoxin, [Fe_4-S_4]-containing ferredoxin-dependent thioredoxin reductase, thioredoxin and target proteins (306). Regulation by FTS was first identified in a Calvin-Benson Cycle enzyme, fructose-1,6-bisphosphatase by Buchanan, et.al (328). Different from the widely distribution of NTR in the three domains of life, the FTS was thought to exist exclusively in the oxygenic photosynthesis organisms (306). However, genome sequence analysis have shown that FTR-like proteins exist in various deeply-rooted bacteria and also methanogenic archaea, leading to a hypothesis on the evolutionary history of FTR that will be discussed in Chapter 5 (309). In this section, I describe the properties of each component of the FTS.

(i) *Ferredoxin (Fdx)*

Plant-Fdx is a small soluble, acidic protein (average molecular weight of 12 kDa) that contains one-electron channeling [Fe_2-S_2] cluster (329). This electron carrier protein has a low mid-point standard redox potential of -432 mV, facilitating the redox cascade from Fdx to target proteins via sequential electron transfer to FTR and Trx (330).

(ii) *Ferredoxin-dependent thioredoxin reductase (FTR)*

FTR is a heterodimer protein composed of one catalytic subunit (subunit α) and one variable subunit (subunit β) (307, 330, 331). The catalytic subunit (FTRc) with the average molecular weight of 20-25 kDa has an alpha helical structure containing an [Fe_4-S_4] center whereas the variable subunit (FTRv) is an open beta barrel structure with no recognizable motif and of an average size of 7-13 kDa (307, 331). The variable subunit is not involved in the catalysis. It is believed that the role of FTRv is mainly in the protection of the iron-sulfur cluster center of FTRc. Disruption of the gene encoding FTRv results in the absence of FTRc in the cell. This might be due to the instability of the lone FTRc subunit (332).

The redox active center of FTR situated within the catalytic subunit is built by 6 cysteine residues forming the typical $\underline{C}^{55}PC^{57}\text{-}X_{16}\text{-}\underline{C}^{74}P\underline{C}^{76}\text{-}X_8\text{-}\underline{C}^{85}HC^{87}$ motif, where X is a variable amino acid residue and numbering is based on the *Synechocystis* sp. PCC6803 FTR (333). The iron sulfur cluster of the FTR is coordinated by four cysteine residues in the motif, as underlined, and the other two cys are responsible for the thiol-disulfide exchange reaction, where C57 and C87 are solvent-accessible and buried cysteine residue, respectively (333).

The crystal structure of recombinant FTR from *Synechocystis* sp.PCC6803 generated in *E. coli* shows a unique arrangement of the catalytic subunit that is positioned on top of the heart-shaped variable subunit forming a thin, concave, disc-like structure (331, 333). The structures of FTR complexed with Fdx and Trx show that the binding sites of Fdx and Trx are located on two opposite sides of the disc-like structure (331) suggesting that the electrons flow from Fdx on one side to the FTR then to the Trx on the other site. Noteworthy that Fdx is a one-electron carrier protein. It transfers one electron at a time. Therefore, in order to reduce a disulfide bond in Trx, two Fdx molecules need to bind to the FTR. Described below is the proposed mechanism of how electrons flow from Fdx to the Trx via FTR.

In the resting stage, FTR is in its oxidized form where the thiol of Cys57 forms disulfide bond with that of Cys87. A Fdx, reduced for example by light through the photosystem I, transfers one electron to the disulfide bond resulting in the cleavage of the disulfide bridge generating free thiol on the solvent accessible Cys57 and thyil radical on the buried Cys^{87}. The radical is stabilized by covalent binding to one of irons in the $[Fe_4\text{-}S_4]$ cluster. The free thiol of the accessible Cys57 then acting as a nucleophile attacks the solvent accessible cysteine residue of Trx forming mixed disulfide between FTR and Trx. Binding of second reduced Fdx, reduces the covalent bond between Cys87 and one of the irons in the $[Fe_4\text{-}S_4]$. This event is followed by reduction of mixed disulfide between Cys57 and solvent-accessible Cys of Trx by the free thiol of Cys87 releasing reduced Trx and forming oxidized FTR. An alternative electron transfer path has also been proposed (331). This involved the binding of two consecutive Fdxs on the FTR generates free thiols of Cys57 and Cys87. Oxidized Trx binds to the FTR and the reaction proceeds via the nucleophilic attack of Cys57 to the

solvent-accessible Cys of Trx followed by the reduction of mixed disulfide by the thiolate of Cys87.

(iii) *A non-typical FTR, a Flavin-containing Fdx-dependent thioredoxin reductase from* Clostridium pasteurianum

Hammel discovered a thioredoxin reductase in *Clostridium pasteurianum* that was dependent on Fdx (334). Surprisingly, the enzyme is a flavoprotein enzyme and lacks iron sulfur cluster. Unfortunately, there was no study that followed up this finding. It is possible that there are new groups of thioredoxin reductases that are not related to either NTR or FTR.

(iv) *Distribution of FTR in methanogenic archaea*

FTR homologs were found only in the phylogenetically late-evolved methanogens (Figure 2.5). Based on our bioinformatics analysis, FTR in methanogens can be classified into two types. Both groups of FTR are similar to the typical plant-type enzyme except one has an additional bacterial element, a rubredoxin domain at its C-terminus (335). *Methanosarcina acetivorans* enzyme belonging to the latter group has been expressed in a recombinant form in *E. coli* and purified to homogeneity, and its X-ray crystallographic structure has been determined to 2.8 resolution (335).

2.7 REFERENCES

1. Boone DR, Whitman WB, & Rouviere P (1993) Diversity and taxonomy of methanogens. *Methanogenesis: ecology, physiology, biochemistry and genetics.*, ed Ferry JG (Chapman and Hall, New York, NY), pp 35-80.
2. Garcia JL, Patel BK, & Ollivier B (2000) Taxonomic, phylogenetic, and ecological diversity of methanogenic Archaea. *Anaerobe* 6(4):205-226.
3. Thauer RK, Kaster AK, Seedorf H, Buckel W, & Hedderich R (2008) Methanogenic archaea: ecologically relevant differences in energy conservation. *Nature reviews. Microbiology* 6(8):579-591.
4. Woese CR, Kandler O, & Wheelis ML (1990) Towards a natural system of organisms: proposal for the domains Archaea, Bacteria, and Eucarya. *Proceedings of the National Academy of Sciences of the United States of America* 87(12):4576-4579.
5. Grant WD, Pinch G, Harris JE, De Rosa M, & Gambacorta A (1985) Polar Lipids in Methanogen Taxonomy. *Journal of general microbiology* 131(12):3277-3286.
6. Jones WJ, Nagle DP, Jr., & Whitman WB (1987) Methanogens and the diversity of archaebacteria. *Microbiological reviews* 51(1):135-177.
7. Langworthy TA, Tornabene TG, & Holzer G (1982) Lipids of Archaebacteria. *Zentralblatt für Bakteriologie Mikrobiologie und Hygiene: I. Abt. Originale C: Allgemeine, angewandte und ökologische Mikrobiologie* 3(2):228-244.
8. Kandler O & Hippe H (1977) Lack of peptidoglycan in the cell walls of *Methanosarcina barkeri*. *Archives of microbiology* 113(1-2):57-60.
9. Hilpert R, Winter J, Hammes W, & Kandler O (1981) The sensitivity of archaebacteria to antibiotics. *Zentralblatt für Bakteriologie Mikrobiologie und Hygiene: I. Abt. Originale C: Allgemeine, angewandte und ökologische Mikrobiologie* 2(1):11-20.
10. Belay N, Sparling R, & Daniels L (1986) Relationship of formate to growth and methanogenesis by *Methanococcus thermolithotrophicus*. *Applied and environmental microbiology* 52(5):1080-1085.
11. Wood GE, Haydock AK, & Leigh JA (2003) Function and regulation of the formate dehydrogenase genes of the methanogenic archaeon *Methanococcus maripaludis*. *Journal of bacteriology* 185(8):2548-2554.
12. Li Q, *et al.* (2006) Electron Transport in the Pathway of Acetate Conversion to Methane in the Marine Archaeon *Methanosarcina acetivorans*. *Journal of bacteriology* 188(2):702-710.
13. Balch WE, Fox GE, Magrum LJ, Woese CR, & Wolfe RS (1979) Methanogens: reevaluation of a unique biological group. *Microbiological reviews* 43(2):260-296.
14. Boone DR & Whitman WB (1988) Proposal of Minimal Standards for Describing New Taxa of Methanogenic Bacteria. *International Journal of Systematic Bacteriology* 38(2):212-219.
15. Zinder SH (1993) Physiological ecology of methanogens. *Methanogenesis: ecology, physiology, biochemistry, and genetics*, ed Ferry JG (Chapman and Hall, N.Y.), pp 128-206.
16. Thauer RK (1998) Biochemistry of methanogenesis: a tribute to Marjory Stephenson. 1998 Marjory Stephenson Prize Lecture. *Microbiology* 144 (Pt 9):2377-2406.
17. Colwell FS & Ussler W, III (2010) Global Scale Consequences of Biological Methane Production. *Handbook of Hydrocarbon and Lipid Microbiology*, ed Timmis K (Springer Berlin Heidelberg), pp 3053-3065.
18. Boadi D, Benchaar C, Chiquette J, & Massé D (2004) Mitigation strategies to reduce enteric methane emissions from dairy cows: Update review. *Canadian Journal of Animal Science* 84(3):319-335.
19. Kurr M, *et al.* (1991) *Methanopyrus kandleri*, gen. and sp. nov. represents a novel group of hyperthermophilic methanogens, growing at 110°C. *Archives of microbiology* 156(4):239-247.
20. Slesarev AI, *et al.* (2002) The complete genome of hyperthermophile *Methanopyrus kandleri* AV19 and monophyly of archaeal methanogens. *Proceedings of the National Academy of Sciences* 99(7):4644-4649.
21. Jeanthon C, *et al.* (1998) *Methanococcus infernus* sp. nov., a novel hyperthermophilic lithotrophic methanogen isolated from a deep-sea hydrothermal vent. *International Journal of Systematic Bacteriology* 48(3):913-919.
22. The Joint-Genome Institute UDoE (2009) (The Joint-Genome Institute, US Department of Energy).

23. Mehta MP & Baross JA (2006) Nitrogen fixation at 92 degrees C by a hydrothermal vent archaeon. *Science* 314(5806):1783-1786.
24. Jeanthon C, *et al.* (1999) *Methanococcus vulcanius* sp. nov., a novel hyperthermophilic methanogen isolated from East Pacific Rise, and identification of *Methanococcus* sp. DSM 4213Tas *Methanococcus fervens* sp. nov. *International Journal of Systematic Bacteriology* 49(2):583-589.
25. Bult CJ, *et al.* (1996) Complete genome sequence of the methanogenic archaeon, *Methanococcus jannaschii*. *Science* 273(5278):1058-1073.
26. Jones WJ, Leigh JA, Mayer F, Woese CR, & Wolfe RS (1983) *Methanococcus jannaschii* sp. nov., an extremely thermophilic methanogen from a submarine hydrothermal vent. *Archives of microbiology* 136(4):254-261.
27. Burggraf S, *et al.* (1990) *Methanococcus igneus* sp. nov., a novel hyperthermophilic methanogen from a shallow submarine hydrothermal system. *Syst Appl Microbiol.* 13:263-269.
28. Takai K, Inoue A, & Horikoshi K (2002) *Methanothermococcus okinawensis* sp. nov., a thermophilic, methane-producing archaeon isolated from a Western Pacific deep-sea hydrothermal vent system. *International journal of systematic and evolutionary microbiology* 52(4):1089-1095.
29. Health NCfBIotNIo ((National Center for Biotechnology Information of the National Institutes of Health).
30. Kendall MM, *et al.* (2006) *Methanococcus aeolicus* sp. nov., a mesophilic, methanogenic archaeon from shallow and deep marine sediments. *International journal of systematic and evolutionary microbiology* 56(Pt 7):1525-1529.
31. Hendrickson EL, *et al.* (2004) Complete Genome Sequence of the Genetically Tractable Hydrogenotrophic Methanogen Methanococcus maripaludis. *Journal of bacteriology* 186(20):6956-6969.
32. Jones WJ, Paynter MJB, & Gupta R (1983) Characterization of *Methanococcus maripaludis* sp. nov., a new methanogen isolated from salt marsh sediment. *Archives of microbiology* 135(2):91-97.
33. Whitman WB, Shieh J, Sohn S, Caras DS, & Premachandran U (1986) Isolation and characterization of 22 mesophilic *Methanococci*. *Systematic and Applied Microbiology* 7(2–3):235-240.
34. Ward JM (1970) Master (University of Florida, Gainesville, Florida).
35. Stadtman TC & Barker HA (1951) Studies on the methane fermentation X: A New Formate-Decomposing Bacterium, *Methanococcus vannielii*. *Journal of bacteriology* 62(3):269-280.
36. Stetter KO, *et al.* (1981) *Methanothermus fervidus*, sp. nov., a novel extremely thermophilic methanogen isolated from an Icelandic hot spring. *Zentralblatt für Bakteriologie Mikrobiologie und Hygiene: I. Abt. Originale C: Allgemeine, angewandte und ökologische Mikrobiologie* 2(2):166-178.
37. Anderson I, *et al.* (2010) Complete genome sequence of *Methanothermus fervidus* type strain (V24S). *Standards in genomic sciences* 3(3):315-324.
38. Liesegang H, *et al.* (2010) Complete Genome Sequence of *Methanothermobacter marburgensis*, a Methanoarchaeon Model Organism. *Journal of bacteriology* 192(21):5850-5851.
39. Zeikus JG & Wolee RS (1972) *Methanobacterium thermoautotrophicus* sp. n., an Anaerobic, Autotrophic, Extreme Thermophile. *Journal of bacteriology* 109(2):707-713.
40. Smith DR, *et al.* (1997) Complete genome sequence of *Methanobacterium thermoautotrophicum* deltaH: functional analysis and comparative genomics. *Journal of bacteriology* 179(22):7135-7155.
41. Leahy SC, *et al.* (2010) The Genome Sequence of the Rumen Methanogen *Methanobrevibacter ruminantium* Reveals New Possibilities for Controlling Ruminant Methane Emissions. *PLoS ONE* 5(1):e8926.
42. Smith PH & Hungate RE (1958) Isolation and characterization of *Methanobacterium ruminantium* n. sp. *Journal of bacteriology* 75(6):713-718.
43. Miller TL, Wolin MJ, de Macario EC, & Macario AJ (1982) Isolation of *Methanobrevibacter smithii* from human feces. *Applied and environmental microbiology* 43(1):227-232.
44. Samuel BS, *et al.* (2007) Genomic and metabolic adaptations of Methanobrevibacter smithii to the human gut. *Proceedings of the National Academy of Sciences* 104(25):10643-10648.
45. Fricke WF, *et al.* (2006) The Genome Sequence of *Methanosphaera stadtmanae* Reveals Why This Human Intestinal Archaeon Is Restricted to Methanol and H_2 for Methane Formation and ATP Synthesis. *Journal of bacteriology* 188(2):642-658.

46. Miller TL & Wolin MJ (1985) *Methanosphaera stadtmanae* gen. nov., sp. nov.-a species that forms methane by reducing methanol with hydrogen. *Arch. Microbiol.* 141:116-122.
47. Cadillo-Quiroz H, Yavitt JB, & Zinder SH (2009) Methanosphaerula palustris gen. nov., sp. nov., a hydrogenotrophic methanogen isolated from a minerotrophic fen peatland. *International journal of systematic and evolutionary microbiology* 59(5):928-935.
48. Anderson I, *et al.* (2009) Genomic Characterization of *Methanomicrobiales* Reveals Three Classes of Methanogens. *PLoS ONE* 4(6):e5797.
49. Qian Z & Zhu J (1987) Isolation and characterization of Methanospirillum hungatei JZ1. *Acta Microbiologica Sinica* 27(3):201-205.
50. Bräuer SL, Cadillo-Quiroz H, Ward RJ, Yavitt JB, & Zinder SH (2011) Methanoregula boonei gen. nov., sp. nov., an acidiphilic methanogen isolated from an acidic peat bog. *International journal of systematic and evolutionary microbiology* 61(1):45-52.
51. Brambilla E, *et al.* (2010) Complete genome sequence of Methanoplanus petrolearius type strain (SEBR 4847). *Standards in genomic sciences* 3(2):203-211.
52. Ollivier B, *et al.* (1997) *Methanoplanus petrolearius* sp. nov., a novel methanogenic bacterium from an oil-producing well. *FEMS microbiology letters* 147(1):51-56.
53. Anderson IJ, *et al.* (2009) *Complete genome sequence of Methanocorpusculum labreanum type strain Z*
54. Anderson IJ, *et al.* (2009) Complete genome sequence of Methanoculleus marisnigri Romesser et al. 1981 type strain JR1. *Standards in genomic sciences* 1(2):189-196.
55. Romesser JA, Wolfe RS, Mayer F, Spiess E, & Walther-Mauruschat A (1979) *Methanogenium*, a new genus of marine methanogenic bacteria, and characterization of *Methanogenium cariaci* sp. nov. and *Methanogenium marisnigri* sp. nov. *Archives of microbiology* 121(2):147-153.
56. Bernard M, Ollivier, Mah RA, Garcia JL, & Boonei DR (1986) Isolation and Characterization of *Methanogenium bourgense* sp.nov. . *International Journal of Systematic Bacteriology* 36(2):297-301.
57. Maus I, *et al.* (2012) Complete Genome Sequence of the Hydrogenotrophic, Methanogenic Archaeon *Methanoculleus bourgensis* Strain MS2T, Isolated from a Sewage Sludge Digester. *Journal of bacteriology* 194(19):5487-5488.
58. Sakai S, Conrad R, Liesack W, & Imachi H (2010) *Methanocella arvoryzae* sp. nov., a hydrogenotrophic methanogen isolated from rice field soil. *International journal of systematic and evolutionary microbiology* 60(12):2918-2923.
59. Erkel C, Kube M, Reinhardt R, & Liesack W (2006) Genome of Rice Cluster I Archaea—the Key Methane Producers in the Rice Rhizosphere. *Science* 313(5785):370-372.
60. Lü Z & Lu Y (2012) *Methanocella conradii* sp. nov., a Thermophilic, Obligate Hydrogenotrophic Methanogen, Isolated from Chinese Rice Field Soil. *PLoS ONE* 7(4):e35279.
61. Lü Z & Lu Y (2012) Complete Genome Sequence of a Thermophilic Methanogen, *Methanocella conradii* HZ254, Isolated from Chinese Rice Field Soil. *Journal of bacteriology* 194(9):2398-2399.
62. Sakai S, *et al.* (2008) *Methanocella paludicola* gen. nov., sp. nov., a methane-producing archaeon, the first isolate of the lineage 'Rice Cluster I', and proposal of the new archaeal order *Methanocellales* ord. nov. *International journal of systematic and evolutionary microbiology* 58(4):929-936.
63. Sakai S, *et al.* (2007) Isolation of Key Methanogens for Global Methane Emission from Rice Paddy Fields: a Novel Isolate Affiliated with the Clone Cluster Rice Cluster I. *Applied and environmental microbiology* 73(13):4326-4331.
64. Sakai S, *et al.* (2011) Genome Sequence of a Mesophilic Hydrogenotrophic Methanogen *Methanocella paludicola*, the First Cultivated Representative of the Order *Methanocellales*. *PLoS ONE* 6(7):e22898.
65. Zhu J, *et al.* (2012) The Genome Characteristics and Predicted Function of Methyl-Group Oxidation Pathway in the Obligate Aceticlastic Methanogens, *Methanosaeta* spp. *PLoS ONE* 7(5):e36756.
66. Ma K, Liu X, & Dong X (2006) *Methanosaeta harundinacea* sp. nov., a novel acetate-scavenging methanogen isolated from a UASB reactor. *International journal of systematic and evolutionary microbiology* 56(1):127-131.

67. Patel GB & Sprott GD (1990) *Methanosaeta concilii* gen. nov., sp. nov. ("*Methanothrix concilii*") and *Methanosaeta thermoacetophila* nom. rev., comb. nov. *International Journal of Systematic Bacteriology* 40(1):79-82.
68. Barber RD, *et al.* (2011) Complete Genome Sequence of *Methanosaeta concilii*, a Specialist in Aceticlastic Methanogenesis. *Journal of bacteriology* 193(14):3668-3669.
69. T.N. Z & G.A. Z (1987) *Methanohalobium evestigatus*, n. gen., n. sp. The extremely halophilic methanogenic Archaebacterium. *Dokl. Akad. Nauk SSSR* 293:464-468.
70. Mathrani I, Boone D, Mah R, Fox G, & Lau P (1988) *Methanohalophilus zhilinae* sp. nov., an alkaliphilic, halophilic, methylotrophic methanogen. *Int J Syst Bacteriol* 38(2):139-142.
71. Allen MA, *et al.* (2009) The genome sequence of the psychrophilic archaeon, Methanococcoides burtonii: the role of genome evolution in cold adaptation. *The ISME journal* 3(9):1012-1035.
72. Franzmann PD, Springer, N., Ludwig, W., Conway De Macario, E., Rohde, M. (1992) A Methanogenic Archaeon from Ace Lake, Antarctica: *Methanococcoides burtonii* sp. nov. *Systematic and Applied Microbiology* 15(4).
73. Paterek JR, Smith, P.H. (1988) *Methanohalophilus mahii* gen. nov. sp. nov. a Methylotrophic Halophilic Methanogen. *International Journal of Systematic Bacteriology* 38(1):122-123.
74. Spring S, *et al.* (2010) The genome sequence of *Methanohalophilus mahii* SLP(T) reveals differences in the energy metabolism among members of the *Methanosarcinaceae* inhabiting freshwater and saline environments. *Archaea* 2010:690737.
75. Chen Z, Yu H, Li L, Hu S, & Dong X (2012) The genome and transcriptome of a newly described psychrophilic archaeon, *Methanolobus psychrophilus* R15, reveal its cold adaptive characteristics. *Environmental Microbiology Reports* 4(6):633-641.
76. Zhang G, Jiang N, Liu X, & Dong X (2008) Methanogenesis from Methanol at Low Temperatures by a Novel Psychrophilic Methanogen, "*Methanolobus psychrophilus*" sp. nov., Prevalent in Zoige Wetland of the Tibetan Plateau. *Applied and environmental microbiology* 74(19):6114-6120.
77. Maeder DL, *et al.* (2006) The *Methanosarcina barkeri* Genome: Comparative Analysis with *Methanosarcina acetivorans* and *Methanosarcina mazei* Reveals Extensive Rearrangement within *Methanosarcinal* Genomes. *Journal of bacteriology* 188(22):7922-7931.
78. U D, *et al.* (2002) The genome of *Methanosarcina mazei*: evidence for lateral gene transfer between bacteria and archaea. *J Mol Microbiol Biotechnol.* 4(4):453-461.
79. Deppenmeier U, Blaut M, Jussofie A, & Gottschalk G (1988) A methyl-CoM methylreductase system from methanogenic bacterium strain Go 1 not requiring ATP for activity. *FEBS letters* 241(1-2):60-64.
80. Sowers K, Baron S, & Ferry J (1984) *Methanosarcina acetivorans* sp. nov., an Acetotrophic Methane-Producing Bacterium Isolated from Marine Sediments. *Appl Environ Microbiol.* 47(5):971-978.
81. Galagan JE, *et al.* (2002) The genome of *M. acetivorans* reveals extensive metabolic and physiological diversity. *Genome research* 12(4):532-542.
82. Thauer RK, Hedderich R, & Fischer R (1993) Reactions and enzymes involved in methanogenesis from CO_2 and H_2. *Methanogenesis: Ecology, Physiology, Biochemistry and Genetics*, ed Ferry JG (Chapman & Hall, Inc., New York).
83. Leigh JA, Rinehart KL, Jr., & Wolfe RS (1985) Methanofuran (carbon dioxide reduction factor), a formyl carrier in methane production from carbon dioxide in *Methanobacterium*. *Biochemistry* 24(4):995-999.
84. Escalante-Semerena JC, Leigh JA, Rinehart KL, & Wolfe RS (1984) Formaldehyde activation factor, tetrahydromethanopterin, a coenzyme of methanogenesis. *Proceedings of the National Academy of Sciences of the United States of America* 81(7):1976-1980.
85. Escalante-Semerena JC, Rinehart KL, Jr., & Wolfe RS (1984) Tetrahydromethanopterin, a carbon carrier in methanogenesis. *The Journal of biological chemistry* 259(15):9447-9455.
86. Jacobson F & Walsh C (1984) Properties of 8-Hydroxy-7-Dimethyl-5-Deazaflavins Relevant to Redox Coenzyme Function in Methanogen Metabolism. *Biochemistry* 23:979-988.
87. Eirich LD, Vogels GD, & Wolfe RS (1978) Proposed structure for coenzyme F_{420} from *Methanobacterium*. *Biochemistry* 17(22):4583-4593.

88. Taylor CD & Wolfe RS (1974) Structure and methylation of coenzyme M($HSCH_2CH_2SO_3$). *The Journal of biological chemistry* 249(15):4879-4885.
89. Noll KM, Rinehart KL, Jr., Tanner RS, & Wolfe RS (1986) Structure of component B (7-mercaptoheptanoylthreonine phosphate) of the methylcoenzyme M methylreductase system of *Methanobacterium thermoautotrophicum*. *Proceedings of the National Academy of Sciences of the United States of America* 83(12):4238-4242.
90. Börner G, Karrasch M, & Thauer RK (1989) Formylmethanofuran dehydrogenase activity in cell extracts of *Methanobacterium thermoautotrophicum* and of *Methanosarcina barkeri*. *FEBS Letters* 244(1):21-25.
91. Kaster A-K, Moll J, Parey K, & Thauer RK (2011) Coupling of ferredoxin and heterodisulfide reduction via electron bifurcation in hydrogenotrophic methanogenic archaea. *Proceedings of the National Academy of Sciences* 108(7):2981-2986.
92. Thauer RK (2012) The Wolfe cycle comes full circle. *Proceedings of the National Academy of Sciences of the United States of America* 109(38):15084-15085.
93. Vogels G & Keltjens J (1993) Conversion of methanol and methylamine to methane and carbon dioxide. *Methanogenesis: ecology, physiology, biochemistry and genetics*, ed Ferry J (Chapman and Hall, New York).
94. Feery J (1993) Fermentation of acetate. *Methanogenesis: ecology, physiology, biochemistry and genetics*, ed Ferry JG (Chapman and Hall, New York), pp 304-334.
95. Donnelly MI & Wolfe RS (1986) The role of formylmethanofuran: tetrahydromethanopterin formyltransferase in methanogenesis from carbon dioxide. *The Journal of biological chemistry* 261(35):16653-16659.
96. Donnelly MI, Escalante-Semerena JC, Rinehart KL, Jr., & Wolfe RS (1985) Methenyl-tetrahydromethanopterin cyclohydrolase in cell extracts of *Methanobacterium*. *Arch Biochem Biophys* 242(2):430-439.
97. Jacobson FS, Daniels L, Fox JA, Walsh CT, & Orme-Johnson WH (1982) Purification and properties of an 8-hydroxy-5-deazaflavin-reducing hydrogenase from *Methanobacterium thermoautotrophicum*. *The Journal of biological chemistry* 257(7):3385-3388.
98. Mukhopadhyay B & Daniels L (1989) Aerobic purification of N5,N10-methylenetetrahydromethanopterin dehydrogenase, separated from N5,N10-methylenetetrahydromethanopterin cyclohydrolase, from *Methanobacterium thermoautotrophicum* strain Marburg. *Canadian journal of microbiology* 35(4):499-507.
99. Mukhopadhyay B, Purwantini E, Pihl TD, Reeve JN, & Daniels L (1995) Cloning, sequencing, and transcriptional analysis of the coenzyme F_{420}-dependent methylene-5,6,7,8-tetrahydromethanopterin dehydrogenase gene from *Methanobacterium thermoautotrophicum* strain Marburg and functional expression in *Escherichia coli*. *The Journal of biological chemistry* 270(6):2827-2832.
100. von Bunau R, Zirngibl C, Thauer RK, & Klein A (1991) Hydrogen-forming and coenzyme-F_{420}-reducing methylene tetrahydromethanopterin dehydrogenase are genetically distinct enzymes in *Methanobacterium thermoautotrophicum* (Marburg). *European journal of biochemistry / FEBS* 202(3):1205-1208.
101. Xia Q, *et al.* (2009) Quantitative proteomics of nutrient limitation in the hydrogenotrophic methanogen *Methanococcus maripaludis*. *BMC microbiology* 9:149.
102. Kato S, Kosaka T, & Watanabe K (2008) Comparative transcriptome analysis of responses of *Methanothermobacter thermautotrophicus* to different environmental stimuli. *Environmental Microbiology* 10(4):893-905.
103. Mukhopadhyay B, Johnson EF, & Wolfe RS (2000) A novel pH2 control on the expression of flagella in the hyperthermophilic strictly hydrogenotrophic methanarchaeaon *Methanococcus jannaschii*. *Proceedings of the National Academy of Sciences* 97(21):11522-11527.
104. Morgan RM, Pihl TD, Nolling J, & Reeve JN (1997) Hydrogen regulation of growth, growth yields, and methane gene transcription in *Methanobacterium thermoautotrophicum* deltaH. *Journal of bacteriology* 179(3):889-898.
105. Ellefson WL & Wolfe RS (1981) Component C of the methylreductase system of *Methanobacterium*. *The Journal of biological chemistry* 256(9):4259-4262.

106. Zinder SH (1993) Physiological ecology of methanogens. *Methanogenesis: ecology, physiology, biochemistry and genetics* ed Ferry JG (Chapman & Hall, New york), pp 128-206.
107. Aceti DJ & Ferry JG (1988) Purification and characterization of acetate kinase from acetate-grown *Methanosarcina thermophila*. Evidence for regulation of synthesis. *The Journal of biological chemistry* 263(30):15444-15448.
108. Lundie LL, Jr. & Ferry JG (1989) Activation of acetate by *Methanosarcina thermophila*. Purification and characterization of phosphotransacetylase. *The Journal of biological chemistry* 264(31):18392-18396.
109. Kohler H-PE & Zehnder AJB (1984) Carbon monoxide dehydrogenase and acetate thiokinase in *Methanothrix soehngenii*. *FEMS microbiology letters* 21(3):287-292.
110. Grahame DA (1991) Catalysis of acetyl-CoA cleavage and tetrahydrosarcinapterin methylation by a carbon monoxide dehydrogenase-corrinoid enzyme complex. *Journal of Biological Chemistry* 266(33):22227-22233.
111. Raybuck SA, *et al.* (1991) Demonstration of carbon-carbon bond cleavage of acetyl coenzyme A by using isotopic exchange catalyzed by the CO dehydrogenase complex from acetate-grown *Methanosarcina thermophila*. *Journal of bacteriology* 173(2):929-932.
112. Liu C-T, Miyaki T, Aono T, & Oyaizu H (2008) Evaluation of Methanogenic Strains and Their Ability to Endure Aeration and Water Stress. *Current microbiology* 56(3):214-218.
113. Morozova D & Wagner D (2007) Stress response of methanogenic archaea from Siberian permafrost compared with methanogens from nonpermafrost habitats. *FEMS Microbiol Ecol* 61(1):16-25.
114. Kato MT, Field JA, & Lettinga G (1993) High tolerance of methanogens in granular sludge to oxygen. *Biotechnology and bioengineering* 42(11):1360-1366.
115. Peters V & Conrad R (1995) Methanogenic and other strictly anaerobic bacteria in desert soil and other oxic soils. *Applied and environmental microbiology* 61(4):1673-1676.
116. Peter Mayer H & Conrad R (1990) Factors influencing the population of methanogenic bacteria and the initiation of methane production upon flooding of paddy soil. *FEMS microbiology letters* 73(2):103-111.
117. Corliss JB, *et al.* (1979) Submarine Thermal Sprirngs on the Galápagos Rift. *Science* 203(4385):1073-1083.
118. Jannasch HW & Wirsen CO (1981) Morphological survey of microbial mats near deep-sea thermal vents. *Applied and environmental microbiology* 41(2):528-538.
119. Spiess FN, *et al.* (1980) East pacific rise: hot springs and geophysical experiments. *Science* 207(4438):1421-1433.
120. WEISS RF, LONSDALE P, LUPTON JE, BAINBRIDGE AE, & CRAIG H (1977) Hydrothermal plumes in the Galapagos Rift. *Nature* 267(5612):600-603.
121. Jannasch HW & Mottl MJ (1985) Geomicrobiology of deep-sea hydrothermal vents. *Science* 229(4715):717-725.
122. Jannasch HW & Wirsen CO (1979) Chemosynthetic Primary Production at East Pacific Sea Floor Spreading Centers. *BioScience* 29(10):592-598.
123. Karl DM, Wirsen CO, & Jannasch HW (1980) Deep-Sea Primary Production at the Galapagos Hydrothermal Vents. *Science* 207(4437):1345-1347.
124. Baross JA & Deming JW (1983) Growth of `black smoker' bacteria at temperatures of at least 250 ^{o}C. *Nature* 303(5916).
125. Baross JA, Deming JW, & Becker RR (1984) Evidence for microbial growth in high-pressure, high-temperature environments. *Current perspectives in microbial ecology*, eds Klug MJ & Reddy CA (American Society for Microbiology, Washington, D.C), pp 186-195.
126. Pfeffer W (1897) *Pflanzenphysiologie* (W. Engelmann, Leipzig).
127. Jones WJ, Leigh JA, Mayer F, Woese CR, & RS W (1983) *Methanococcus jannaschii* sp. nov., an extreme thermophilic methanogen from a submarine hydrothermal vent. *Archives of microbiology* 136:254-261.
128. Herzog B & Wirth R (2012) Swimming behavior of selected species of Archaea. *Applied and environmental microbiology* 78(6):1670-1674.

129. Bult CJ, *et al.* (1996) Complete genome sequence of the methanogenic archaeon, *Methanococcus jannaschii*. *Science* 273(5278):1058-1073.
130. Massey V, *et al.* (1969) The reactivity of flavoproteins with sulfite. Possible relevance to the problem of oxygen reactivity. *The Journal of biological chemistry* 244(15):3999-4006.
131. Prins RA, Nevel CJ, & Demeyer DI (1972) Pure culture studies of inhibitors for methanogenic bacteria. *Antonie van Leeuwenhoek* 38(1):281-287.
132. Balderston WL & Payne WJ (1976) Inhibition of methanogenesis in salt marsh sediments and whole-cell suspensions of methanogenic bacteria by nitrogen oxides. *Applied and environmental microbiology* 32(2):264-269.
133. Becker DF & Ragsdale SW (1998) Activation of methyl-SCoM reductase to high specific activity after treatment of whole cells with sodium sulfide. *Biochemistry* 37(8):2639-2647.
134. Mahlert F, Bauer C, Jaun B, Thauer RK, & Duin EC (2002) The nickel enzyme methyl-coenzyme M reductase from methanogenic archaea: In vitro induction of the nickel-based MCR-ox EPR signals from MCR-red2. *Journal of biological inorganic chemistry : JBIC : a publication of the Society of Biological Inorganic Chemistry* 7(4-5):500-513.
135. Daniels L, Belay N, & Rajagopal BS (1986) Assimilatory reduction of sulfate and sulfite by methanogenic bacteria. *Applied and environmental microbiology* 51(4):703-709.
136. Rothe O & Thomm M (2000) A simplified method for the cultivation of extreme anaerobic Archaea based on the use of sodium sulfite as reducing agent. *Extremophiles : life under extreme conditions* 4(4):247-252.
137. Johnson EF & Mukhopadhyay B (2005) A new type of sulfite reductase, a novel coenzyme F_{420}-dependent enzyme, from the methanarchaeon *Methanocaldococcus jannaschii*. *The Journal of biological chemistry* 280(46):38776-38786.
138. Johnson EF & Mukhopadhyay B (2007) A novel coenzyme F_{420}-dependent sulfite reductase and a small size sulfite reductase in methanogenic archaea. *Proceedings of the International Symposium on Microbial Sulfur Metabolism*, eds Dahl C & Friedrich CG (Springer, New York, N.Y.).
139. Canfield DE & Raiswell R (1999) The evolution of the sulfur cycle. *American Journal of Science* 299:697-723.
140. Nakayama M, Akashi T, & Hase T (2000) Plant sulfite reductase: molecular structure, catalytic function and interaction with ferredoxin. *Journal of inorganic biochemistry* 82(1-4):27-32.
141. Wirtz M & Droux M (2005) Synthesis of the sulfur amino acids: cysteine and methionine. *Photosynth Res* 86(3):345-362.
142. Hansen TA (1994) Metabolism of sulfate-reducing prokaryotes. *Antonie van Leeuwenhoek* 66(1-3):165-185.
143. Crane BR, Siegel LM, & Getzoff ED (1995) Sulfite Reductase Structure at 1.6 Å: Evolution and Catalysis for Reduction of Inorganic Anions. *Science* 270(5233):59-67.
144. Schnell R, Sandalova T, Hellman U, Lindqvist Y, & Schneider G (2005) Siroheme- and [Fe4-S4]-dependent NirA from *Mycobacterium tuberculosis* is a sulfite reductase with a covalent Cys-Tyr bond in the active site. *The Journal of biological chemistry* 280(29):27319-27328.
145. Oliveira TF, *et al.* (2008) The crystal structure of *Desulfovibrio vulgaris* dissimilatory sulfite reductase bound to DsrC provides novel insights into the mechanism of sulfate respiration. *The Journal of biological chemistry* 283(49):34141-34149.
146. Dahl C & Truper HG (2001) Sulfite reductase and APS reductase from *Archaeoglobus fulgidus*. *Methods in enzymology* 331:427-441.
147. Schiffer A, *et al.* (2008) Structure of the Dissimilatory Sulfite Reductase from the Hyperthermophilic Archaeon *Archaeoglobus fulgidus*. *Journal of molecular biology* 379(5):1063-1074.
148. Oliveira TF, *et al.* (2008) The Crystal Structure of *Desulfovibrio vulgaris* Dissimilatory Sulfite Reductase Bound to DsrC Provides Novel Insights into the Mechanism of Sulfate Respiration. *Journal of Biological Chemistry* 283(49):34141-34149.
149. Siegel LM, Davis PS, & Kamin H (1974) Reduced nicotinamide adenine dinucleotide phosphate-sulfite reductase of enterobacteria. 3. The Escherichia coli hemoflavoprotein: catalytic parameters and the sequence of electron flow. *The Journal of biological chemistry* 249(5):1572-1586.

150. DiMarco AA, Bobik TA, & Wolfe RS (1990) Unusual coenzymes of methanogenesis. *Annu Rev Biochem* 59:355-394.
151. Bruggemann H, Falinski F, & Deppenmeier U (2000) Structure of the $F_{420}H_2$:quinone oxidoreductase of *Archaeoglobus fulgidus* identification and overproduction of the $F_{420}H_2$-oxidizing subunit. *European journal of biochemistry / FEBS* 267(18):5810-5814.
152. Kunow J, Linder D, Stetter KO, & Thauer RK (1994) $F_{420}H_2$: quinone oxidoreductase from *Archaeoglobus fulgidus*. Characterization of a membrane-bound multisubunit complex containing FAD and iron-sulfur clusters. *European journal of biochemistry / FEBS* 223(2):503-511.
153. Abken HJ, *et al.* (1998) Isolation and characterization of methanophenazine and function of phenazines in membrane-bound electron transport of *Methanosarcina mazei* Go1. *Journal of bacteriology* 180(8):2027-2032.
154. Susanti D & Mukhopadhyay B (2012) An intertwined evolutionary history of methanogenic archaea and sulfate reduction. *PLoS One* 7(9):e45313.
155. Kiener A & Leisinger T (1983) Oxygen sensitivity of methanogenic bacteria. *Syst Appl Microbiol* 4(3):305-312.
156. Jarrell KF (1985) Extreme Oxygen Sensitivity in Methanogenic Archaebacteria. *BioScience* 35(5):298-302.
157. Imlay JA (2002) How oxygen damages microbes: Oxygen tolerance and obligate anaerobiosis. *Advances in Microbial Physiology*, (Academic Press), Vol Volume 46, pp 111-153.
158. Naqui A, Chance B, & Cadenas E (1986) Reactive oxygen intermediates in biochemistry. *Annu Rev Biochem* 55:137-166.
159. Cabiscol E, Tamarit J, & Ros J (2000) Oxidative stress in bacteria and protein damage by reactive oxygen species. *International microbiology : the official journal of the Spanish Society for Microbiology* 3(1):3-8.
160. Imlay JA & Linn S (1988) DNA damage and oxygen radical toxicity. *Science* 240(4857):1302-1309.
161. Farr SB, Touati D, & Kogoma T (1988) Effects of oxygen stress on membrane functions in *Escherichia coli*: role of HPI catalase. *Journal of bacteriology* 170(4):1837-1842.
162. Demple B (1991) Regulation of bacterial oxidative stress genes. *Annual review of genetics* 25:315-337.
163. Berlett BS & Stadtman ER (1997) Protein oxidation in aging, disease, and oxidative stress. *The Journal of biological chemistry* 272(33):20313-20316.
164. Gonzalez-Flecha B & Demple B (1995) Metabolic sources of hydrogen peroxide in aerobically growing *Escherichia coli*. *The Journal of biological chemistry* 270(23):13681-13687.
165. Hidalgo E, Ding H, & Demple B (1997) Redox signal transduction: mutations shifting [2Fe-2S] centers of the SoxR sensor-regulator to the oxidized form. *Cell* 88(1):121-129.
166. McCord JM & Fridovich I (1968) The reduction of cytochrome c by milk xanthine oxidase. *The Journal of biological chemistry* 243(21):5753-5760.
167. McCord JM & Fridovich I (1969) Superoxide dismutase. An enzymic function for erythrocuprein (hemocuprein). *The Journal of biological chemistry* 244(22):6049-6055.
168. Carlioz A, *et al.* (1988) Iron superoxide dismutase. Nucleotide sequence of the gene from *Escherichia col*i K12 and correlations with crystal structures. *The Journal of biological chemistry* 263(3):1555-1562.
169. Barondeau DP, Kassmann CJ, Bruns CK, Tainer JA, & Getzoff ED (2004) Nickel superoxide dismutase structure and mechanism. *Biochemistry* 43(25):8038-8047.
170. Chance B, Sies H, & Boveris A (1979) Hydroperoxide metabolism in mammalian organs. *Physiological reviews* 59(3):527-605.
171. Finn GJ & Condon S (1975) Regulation of catalase synthesis in *Salmonella typhimurium*. *Journal of bacteriology* 123(2):570-579.
172. von Ossowski I, Mulvey MR, Leco PA, Borys A, & Loewen PC (1991) Nucleotide sequence of *Escherichia coli* katE, which encodes catalase HPII. *Journal of bacteriology* 173(2):514-520.
173. Imlay JA (2006) Iron-sulphur clusters and the problem with oxygen. *Molecular microbiology* 59(4):1073-1082.

174. Blakley RL (1969) *The Biochemsitry of folic acid and related pteridines* (North-Holland Publishing Company, Amsterdam London).
175. Keltjens JT, Caerteling GC, Van Der Drift C, & Vogels GD (1986) Methanopterin and the intermediary steps of methanogenesis. *Systematic and Applied Microbiology* 7(2–3):370-375.
176. Sass H, Cypionka H, & Babenzien H-D (1997) Vertical distribution of sulfate-reducing bacteria at the oxic-anoxic interface in sediments of the oligotrophic Lake Stechlin. *FEMS Microbiology Ecology* 22(3):245-255.
177. Cypionka H, Widdel F, & Pfennig N (1985) Survival of sulfate-reducing bacteria after oxygen stress, and growth in sulfate-free oxygen-sulfide gradients. *FEMS microbiology letters* 31(1):39-45.
178. Brioukhanov AL & Netrusov AI (2007) Aerotolerance of strictly anaerobic microorganisms and factors of defense against oxidative stress: A review. *Appl Biochem Microbiol* 43(6):567-582.
179. Zhilina TN (1972) [Dying-off of *Methanosarcina* exposed to air]. *Mikrobiologiia* 41(6):1105-1106.
180. Fu R, Wall JD, & Voordouw G (1994) DcrA, a c-type heme-containing methyl-accepting protein from *Desulfovibrio vulgaris* Hildenborough, senses the oxygen concentration or redox potential of the environment. *Journal of bacteriology* 176(2):344-350.
181. Krekeler D, Teske A, & Cypionka H (1998) Strategies of sulfate-reducing bacteria to escape oxygen stress in a cyanobacterial mat. *FEMS Microbiology Ecology* 25(2):89-96.
182. Deckers HM & Voordouw G (1994) Identification of a large family of genes for putative chemoreceptor proteins in an ordered library of the *Desulfovibrio vulgaris* Hildenborough genome. *Journal of bacteriology* 176(2):351-358.
183. Brioukhanov AL, Netrusov AI, & Eggen RIL (2006) The catalase and superoxide dismutase genes are transcriptionally up-regulated upon oxidative stress in the strictly anaerobic archaeon *Methanosarcina barkeri*. *Microbiology* 152(6):1671-1677.
184. Jenney FE, Jr., Verhagen MF, Cui X, & Adams MW (1999) Anaerobic microbes: oxygen detoxification without superoxide dismutase. *Science* 286(5438):306-309.
185. Jenney FE, Verhagen MFJM, Cui X, & Adams MWW (1999) Anaerobic Microbes: Oxygen Detoxification Without Superoxide Dismutase. *Science* 286(5438):306-309.
186. Thorgersen MP, Stirrett K, Scott RA, & Adams MWW (2012) Mechanism of oxygen detoxification by the surprisingly oxygen-tolerant hyperthermophilic archaeon, *Pyrococcus furiosus*. *Proceedings of the National Academy of Sciences* 109(45):18547-18552.
187. Krätzer C, Welte C, Dörner K, Friedrich T, & Deppenmeier U (2011) Methanoferrodoxin represents a new class of superoxide reductase containing an iron–sulfur cluster. *FEBS Journal* 278(3):442-451.
188. Zehnder AJB & Wuhrmann K (1977) Physiology of a *Methanobacterium* strain AZ. *Archives of microbiology* 111(3):199-205.
189. Leadbetter JR & Breznak JA (1996) Physiological ecology of *Methanobrevibacter cuticularis* sp. nov. and *Methanobrevibacter curvatus* sp. nov., isolated from the hindgut of the termite *Reticulitermes flavipes*. *Applied and environmental microbiology* 62(10):3620-3631.
190. Seedorf H, Dreisbach A, Hedderich R, Shima S, & Thauer RK (2004) F420H2 oxidase (FprA) from *Methanobrevibacter arboriphilus*, a coenzyme F_{420}-dependent enzyme involved in O_2 detoxification. *Archives of microbiology* 182(2-3):126-137.
191. Kengen SWM, van der Oost J, & Vos WMd (2003) Molecular characterization of H_2O_2-forming NADH oxidases from *Archaeoglobus fulgidus*. *European Journal of Biochemistry* 270(13):2885-2894.
192. Ward DE, *et al.* (2001) The NADH oxidase from *Pyrococcus furiosus*. *European Journal of Biochemistry* 268(22):5816-5823.
193. Reed DW, Millstein J, & Hartzell PL (2001) H_2O_2-Forming NADH Oxidase with Diaphorase (Cytochrome) Activity from *Archaeoglobus fulgidus*. *Journal of bacteriology* 183(24):7007-7016.
194. Harris DR, *et al.* (2005) Discovery and characterization of a Coenzyme A disulfide reductase from *Pyrococcus horikoshii*. *FEBS Journal* 272(5):1189-1200.
195. Schut GJ, Bridger SL, & Adams MWW (2007) Insights into the Metabolism of Elemental Sulfur by the Hyperthermophilic Archaeon *Pyrococcus furiosus*: Characterization of a Coenzyme A- Dependent NAD(P)H Sulfur Oxidoreductase. *Journal of bacteriology* 189(12):4431-4441.

196. Case CL, Rodriguez JR, & Mukhopadhyay B (2009) Characterization of an NADH oxidase of the flavin-dependent disulfide reductase family from *Methanocaldococcus jannaschii*. *Microbiology* 155(Pt 1):69-79.
197. Adams MW & Kletzin A (1996) Oxidoreductase-type enzymes and redox proteins involved in fermentative metabolisms of hyperthermophilic Archaea. *Advances in protein chemistry* 48:101-180.
198. Pieulle L, *et al.* (1995) Isolation and characterization of the pyruvate-ferredoxin oxidoreductase from the sulfate-reducing bacterium *Desulfovibrio africanus*. *Biochimica et biophysica acta* 1250(1):49-59.
199. Pieulle L, Magro V, & Hatchikian EC (1997) Isolation and analysis of the gene encoding the pyruvate-ferredoxin oxidoreductase of *Desulfovibrio africanus*, production of the recombinant enzyme in *Escherichia coli*, and effect of carboxy-terminal deletions on its stability. *Journal of bacteriology* 179(18):5684-5692.
200. Pieulle L, *et al.* (2011) Study of the Thiol/Disulfide Redox Systems of the Anaerobe *Desulfovibrio vulgaris* Points Out Pyruvate:Ferredoxin Oxidoreductase as a New Target for Thioredoxin 1. *Journal of Biological Chemistry* 286(10):7812-7821.
201. Hausinger RP, Orme-Johnson WH, & Walsh C (1985) Factor 390 chromophores: phosphodiester between AMP or GMP and methanogenic factor 420. *Biochemistry* 24(7):1629-1633.
202. Vermeij P, Detmers FJ, Broers FJ, Keltjens JT, & Van der Drift C (1994) Purification and characterization of coenzyme F_{390} synthetase from *Methanobacterium thermoautotrophicum* (strain delta H). *European journal of biochemistry / FEBS* 226(1):185-191.
203. Vermeij P, Pennings JL, Maassen SM, Keltjens JT, & Vogels GD (1997) Cellular levels of factor 390 and methanogenic enzymes during growth of *Methanobacterium thermoautotrophicum* deltaH. *Journal of bacteriology* 179(21):6640-6648.
204. Gilbert HF (1990) Molecular and cellular aspects of thiol-disulfide exchange. *Adv Enzymol Relat Areas Mol Biol.* 63:69-172.
205. Messner KR & Imlay JA (1999) The Identification of Primary Sites of Superoxide and Hydrogen Peroxide Formation in the Aerobic Respiratory Chain and Sulfite Reductase Complex of *Escherichia coli*. *Journal of Biological Chemistry* 274(15):10119-10128.
206. Holmgren A (1989) Thioredoxin and glutaredoxin systems. *The Journal of biological chemistry* 264(24):13963-13966.
207. Montrichard F, *et al.* (2009) Thioredoxin targets in plants: the first 30 years. *Journal of proteomics* 72(3):452-474.
208. Saitoh M, *et al.* (1998) Mammalian thioredoxin is a direct inhibitor of apoptosis signal-regulating kinase (ASK) 1. *The EMBO journal* 17(9):2596-2606.
209. Stewart EJ, Aslund F, & Beckwith J (1998) Disulfide bond formation in the *Escherichia coli* cytoplasm: an in vivo role reversal for the thioredoxins. *The EMBO journal* 17(19):5543-5550.
210. Kang SW, *et al.* (1998) Mammalian peroxiredoxin isoforms can reduce hydrogen peroxide generated in response to growth factors and tumor necrosis factor-alpha. *The Journal of biological chemistry* 273(11):6297-6302.
211. Chae HZ, Kang SW, & Rhee SG (1999) Isoforms of mammalian peroxiredoxin that reduce peroxides in presence of thioredoxin. *Methods in enzymology* 300:219-226.
212. Asahi T, Bandurski RS, & Wilson LG (1961) Yeast sulfate-reducing system. II. Enzymatic reduction of protein disulfide. *The Journal of biological chemistry* 236:1830-1835.
213. Blacks S, Harte, E.M., Hudson, B., Wartofsky, L. (1960) A specific enzymatic reduction of L(-) methionine sulfoxide and a related non-specific reduction of disulfides. *J. Bio.Chem.* 235:2910-2916.
214. Laurent TC, Moore EC, & Reichard P (1964) Enzymatic Synthesis of Deoxyribonucleotides: IV. Isolation and Characterization of Thioredoxin, The Hydrogen Donor from *Escherichia coli* B. *Journal of Biological Chemistry* 239(10):3436-3444.
215. Buchanan BB, Holmgren A, Jacquot J-P, & Scheibe R (2012) Fifty years in the thioredoxin field and a bountiful harvest. *Biochimica et Biophysica Acta (BBA) - General Subjects* 1820(11):1822-1829.
216. Atkinson HJ & Babbitt PC (2009) An atlas of the thioredoxin fold class reveals the complexity of function-enabling adaptations. *PLoS computational biology* 5(10):e1000541.
217. Wilson LG, Asahi T, & Bandurski RS (1961) Yeast sulfate-reducing system. I. Reduction of sulfate to sulfite. *The Journal of biological chemistry* 236:1822-1829.

218. Moore EC, Reichard P, & Thelander L (1964) Enzymatic Synthesis of Deoxyribonucleotides: V. PURIFICATION AND PROPERTIES OF THIOREDOXIN REDUCTASE FROM ESCHERICHIA COLI B. *Journal of Biological Chemistry* 239(10):3445-3452.
219. Eklund H, Gleason FK, & Holmgren A (1991) Structural and functional relations among thioredoxins of different species. *Proteins* 11(1):13-28.
220. Stefankova P, Kollarova M, & Barak I (2005) Thioredoxin - structural and functional complexity. *General physiology and biophysics* 24(1):3-11.
221. Holmgren A, Söderberg BO, Eklund H, & Brändén CI (1975) Three-dimensional structure of *Escherichia coli* thioredoxin-S2 to 2.8 A resolution. *Proceedings of the National Academy of Sciences of the United States of America* 72(6):2305–2309.
222. Katti SK, LeMaster DM, & Eklund H (1990) Crystal structure of thioredoxin from *Escherichia coli* at 1.68 Å resolution. *Journal of molecular biology* 212(1):167-184.
223. Holmgren A (1968) Thioredoxin. 6. The amino acid sequence of the protein from *Escherichia coli* B. *European J. Biochem.* 6:475-484.
224. Holmgren A (1995) Thioredoxin structure and mechanism: conformational changes on oxidation of the active-site sulfhydryls to a disulfide. *Structure* 3(3):239-243.
225. Jeng M-F, *et al.* (1994) High-resolution solution structures of oxidized and reduced *Escherichia coli* thioredoxin. *Structure (London, England : 1993)* 2(9):853-868.
226. Eklund H, *et al.* (1984) Conformational and functional similarities between glutaredoxin and thioredoxins. *EMBO J.* 3(7):1443-1449.
227. Holmgren A (1979) Thioredoxin catalyzes the reduction of insulin disulfides by dithiothreitol and dihydrolipoamide. *The Journal of biological chemistry* 254(19):9627-9632.
228. Berndt C, Lillig CH, & Holmgren A (2008) Thioredoxins and glutaredoxins as facilitators of protein folding. *Biochimica et Biophysica Acta (BBA) - Molecular Cell Research* 1783(4):641-650.
229. Ferrari DM & Söling HD (1999) The protein disulphide-isomerase family: unravelling a string of folds. . *Biochem. J.* 339:1-10.
230. Martin JL (1995) Thioredoxin--a fold for all reasons. *Structure* 3(3):245-250.
231. Witte S, *et al.* (2000) Inhibition of the c-Jun N-terminal Kinase/AP-1 and NF-κB Pathways by PICOT, a Novel Protein Kinase C-interacting Protein with a Thioredoxin Homology Domain. *Journal of Biological Chemistry* 275(3):1902-1909.
232. Martin JL (1995) Thioredoxin —a fold for all reasons. *Structure* 3(3):245-250.
233. Fahey RC (Novel Thiols of Prokaryotes. *Annual Review of Microbiology* 55:333-356.
234. Holmgren A (1985) Thioredoxin. *Annual Review of Biochemistry* 54(1):237-271.
235. Xia TH, *et al.* (1992) NMR structure of oxidized *Escherichia coli* glutaredoxin: comparison with reduced *E. coli* glutaredoxin and functionally related proteins. *Protein science : a publication of the Protein Society* 1(3):310-321.
236. Fernandes AP & Holmgren A (2004) Glutaredoxins: glutathione-dependent redox enzymes with functions far beyond a simple thioredoxin backup system. *Antioxidants & redox signaling* 6(1):63-74.
237. Bardwell JC, McGovern K, & Beckwith J (1991) Identification of a protein required for disulfide bond formation in vivo. *Cell* 67(3):581-589.
238. Zapun A & Creighton TE (1994) Effects of DsbA on the disulfide folding of bovine pancreatic trypsin inhibitor and alpha-lactalbumin. *Biochemistry* 33(17):5202-5211.
239. Zapun A, Bardwell JC, & Creighton TE (1993) The reactive and destabilizing disulfide bond of DsbA, a protein required for protein disulfide bond formation in vivo. *Biochemistry* 32(19):5083-5092.
240. Zapun A, Cooper L, & Creighton TE (1994) Replacement of the Active-Site Cysteine Residues of DsbA, a Protein Required for Disulfide Bond Formation in vivo. *Biochemistry* 33(7):1907-1914.
241. Jacobi A, Huber-Wunderlich M, Hennecke J, & Glockshuber R (1997) Elimination of All Charged Residues in the Vicinity of the Active-site Helix of the Disulfide Oxidoreductase DsbA: Influence of electrostatic interactions on stability and redox properties. *Journal of Biological Chemistry* 272(35):21692-21699.
242. Huber-Wunderlich M & Glockshuber R (1998) A single dipeptide sequence modulates the redox properties of a whole enzyme family. *Folding & design* 3(3):161-171.

243. Wunderlich M & Glockshuber R (1993) Redox properties of protein disulfide isomerase (DsbA) from Escherichia coli. *Protein science : a publication of the Protein Society* 2(5):717-726.
244. Bardwell JCA, McGovern K, & Beckwith J (1991) Identification of a protein required for disulfide bond formation in vivo. *Cell* 67(3):581-589.
245. Joly JC & Swartz JR (1994) Protein folding activities of Escherichia coli protein disulfide isomerase. *Biochemistry* 33(14):4231-4236.
246. Joly JC & Swartz JR (1997) In vitro and in vivo redox states of the *Escherichia coli* periplasmic oxidoreductases DsbA and DsbC. *Biochemistry* 36(33):10067-10072.
247. Spehr V, Schlitt A, Scheide D, Guenebaut V, & Friedrich T (1999) Overexpression of the *Escherichia coli* nuo-operon and isolation of the overproduced NADH:ubiquinone oxidoreductase (complex I). *Biochemistry* 38(49):16261-16267.
248. Sone M, Akiyama Y, & Ito K (1997) Differential in vivo roles played by DsbA and DsbC in the formation of protein disulfide bonds. *The Journal of biological chemistry* 272(16):10349-10352.
249. Rybin V, *et al.* (1996) Crystallization of DsbC, the disulfide bond isomerase of *Escherichia coli*. *Acta crystallographica. Section D, Biological crystallography* 52(Pt 6):1219-1221.
250. Rietsch A, Belin D, Martin N, & Beckwith J (1996) An in vivo pathway for disulfide bond isomerization in *Escherichia coli*. *Proceedings of the National Academy of Sciences of the United States of America* 93(23):13048-13053.
251. Kobayashi T, *et al.* (1997) Respiratory chain is required to maintain oxidized states of the DsbA-DsbB disulfide bond formation system in aerobically growing *Escherichia coli* cells. *Proceedings of the National Academy of Sciences* 94(22):11857-11862.
252. Bader M, Muse W, Zander T, & Bardwell J (1998) Reconstitution of a Protein Disulfide Catalytic System. *Journal of Biological Chemistry* 273(17):10302-10307.
253. Bader M, Muse W, Ballou DP, Gassner C, & Bardwell JCA (1999) Oxidative Protein Folding Is Driven by the Electron Transport System. *Cell* 98(2):217-227.
254. Bader MW, Xie T, Yu CA, & Bardwell JC (2000) Disulfide bonds are generated by quinone reduction. *The Journal of biological chemistry* 275(34):26082-26088.
255. Chung J, Chen T, & Missiakas D (2000) Transfer of electrons across the cytoplasmic membrane by DsbD, a membrane protein involved in thiol-disulphide exchange and protein folding in the bacterial periplasm. *Molecular microbiology* 35(5):1099-1109.
256. Rietsch A, Bessette P, Georgiou G, & Beckwith J (1997) Reduction of the periplasmic disulfide bond isomerase, DsbC, occurs by passage of electrons from cytoplasmic thioredoxin. *Journal of bacteriology* 179(21):6602-6608.
257. Anfinsen CB & Scheraga HA (1975) Experimental and theoretical aspects of protein folding. *Advances in protein chemistry* 29:205-300.
258. Freedman RB, Bulleid NJ, Hawkins HC, & Paver JL (1989) Role of protein disulphide-isomerase in the expression of native proteins. *Biochemical Society symposium* 55:167-192.
259. Lambert N & Freedman RB (1985) The latency of rat liver microsomal protein disulphide-isomerase. *The Biochemical journal* 228(3):635-645.
260. Shorrosh BS, Subramaniam J, Schubert KR, & Dixon RA (1993) Expression and Localization of Plant Protein Disulfide Isomerase. *Plant Physiol.* 103(3):719-726.
261. Lundstrom J & Holmgren A (1993) Determination of the reduction-oxidation potential of the thioredoxin-like domains of protein disulfide-isomerase from the equilibrium with glutathione and thioredoxin. *Biochemistry* 32(26):6649-6655.
262. Li H, Hanson C, Fuchs JA, Woodward C, & Thomas GJ, Jr. (1993) Determination of the pKa values of active-center cysteines, cysteines-32 and -35, in Escherichia coli thioredoxin by Raman spectroscopy. *Biochemistry* 32(22):5800-5808.
263. Dillet V, Dyson HJ, & Bashford D (1998) Calculations of electrostatic interactions and pKas in the active site of Escherichia coli thioredoxin. *Biochemistry* 37(28):10298-10306.
264. Dyson HJ, Tennant LL, & Holmgren A (1991) Proton-transfer effects in the active-site region of Escherichia coli thioredoxin using two-dimensional 1H NMR. *Biochemistry* 30(17):4262-4268.

265. Forman-Kay JD, Clore GM, & Gronenborn AM (1992) Relationship between electrostatics and redox function in human thioredoxin: characterization of pH titration shifts using two-dimensional homo- and heteronuclear NMR. *Biochemistry* 31(13):3442-3452.
266. Jeng M-F, Holmgren A, & Dyson HJ (1995) Proton Sharing between Cysteine Thiols in Escherichia coli Thioredoxin: Implications for the Mechanism of Protein Disulfide Reduction. *Biochemistry* 34(32):10101-10105.
267. Kallis GB & Holmgren A (1980) Differential reactivity of the functional sulfhydryl groups of cysteine-32 and cysteine-35 present in the reduced form of thioredoxin from Escherichia coli. *The Journal of biological chemistry* 255(21):10261-10265.
268. Hoog JO, Jornvall H, Holmgren A, Carlquist M, & Persson M (1983) The primary structure of Escherichia coli glutaredoxin. Distant homology with thioredoxins in a superfamily of small proteins with a redox-active cystine disulfide/cysteine dithiol. *European journal of biochemistry / FEBS* 136(1):223-232.
269. Krause G, Lundstrom J, Barea JL, Pueyo de la Cuesta C, & Holmgren A (1991) Mimicking the active site of protein disulfide-isomerase by substitution of proline 34 in Escherichia coli thioredoxin. *The Journal of biological chemistry* 266(15):9494-9500.
270. Mössner E, Huber-Wunderlich M, & Glockshuber R (1998) Characterization of Escherichia coli thioredoxin variants mimicking the active-sites of other thiol/disulfide oxidoreductases. *Protein Science* 7(5):1233-1244.
271. Lundstrom J, Krause G, & Holmgren A (1992) A Pro to His mutation in active site of thioredoxin increases its disulfide-isomerase activity 10-fold. New refolding systems for reduced or randomly oxidized ribonuclease. *The Journal of biological chemistry* 267(13):9047-9052.
272. Quan S, Schneider I, Pan J, Von Hacht A, & Bardwell JC (2007) The CXXC motif is more than a redox rheostat. *The Journal of biological chemistry* 282(39):28823-28833.
273. Chivers PT, Prehoda KE, & Raines RT (1997) The CXXC motif: a rheostat in the active site. *Biochemistry* 36(14):4061-4066.
274. Sanger F (1949) Fractionation of oxidized insulin. *The Biochemical journal* 44(1):126-128.
275. Holmgren A (1976) Hydrogen donor system for *Escherichia coli* ribonucleoside-diphosphate reductase dependent upon glutathione. *Proceedings of the National Academy of Sciences* 73(7):2275-2279.
276. Laurent TC, Moore EC, & Reichard P (1964) Enzymatic Synthesis of Deoxyribonucleotides. Iv. Isolation and Characterization of Thioredoxin, the Hydrogen Donor from Escherichia Coli B. *The Journal of biological chemistry* 239:3436-3444.
277. Arner ES & Holmgren A (2000) Physiological functions of thioredoxin and thioredoxin reductase. *European journal of biochemistry / FEBS* 267(20):6102-6109.
278. Huber HE, Tabor S, & Richardson CC (1987) Escherichia coli thioredoxin stabilizes complexes of bacteriophage T7 DNA polymerase and primed templates. *The Journal of biological chemistry* 262(33):16224-16232.
279. Mark DF & Richardson CC (1976) Escherichia coli thioredoxin: a subunit of bacteriophage T7 DNA polymerase. *Proceedings of the National Academy of Sciences* 73(3):780-784.
280. Russel M & Model P (1986) The role of thioredoxin in filamentous phage assembly. Construction, isolation, and characterization of mutant thioredoxins. *The Journal of biological chemistry* 261(32):14997-15005.
281. Tabor S, Huber HE, & Richardson CC (1987) *Escherichia coli* thioredoxin confers processivity on the DNA polymerase activity of the gene 5 protein of bacteriophage T7. *The Journal of biological chemistry* 262(33):16212-16223.
282. Motohashi K, Kondoh A, Stumpp MT, & Hisabori T (2001) Comprehensive survey of proteins targeted by chloroplast thioredoxin. *Proceedings of the National Academy of Sciences* 98(20):11224-11229.
283. Wong JH, Yano H, Lee YM, Cho MJ, & Buchanan BB (2002) Identification of thioredoxin-linked proteins by fluorescence labeling combined with isoelectric focusing/sodium dodecyl sulfate-polyacrylamide gel electrophoresis. *Methods in enzymology* 347:339-349.

284. Wang P-F, Veine DM, Ahn SH, & Williams CH (1996) A Stable Mixed Disulfide between Thioredoxin Reductase and Its Substrate, Thioredoxin: Preparation and Characterization†. *Biochemistry* 35(15):4812-4819.
285. Yano H, Wong JH, Lee YM, Cho MJ, & Buchanan BB (2001) A strategy for the identification of proteins targeted by thioredoxin. *Proceedings of the National Academy of Sciences of the United States of America* 98(8):4794-4799.
286. Marx C, Wong JH, & Buchanan BB (2003) Thioredoxin and germinating barley: targets and protein redox changes. *Planta* 216(3):454-460.
287. Maeda K, Finnie C, & Svensson B (2004) Cy5 maleimide labelling for sensitive detection of free thiols in native protein extracts: identification of seed proteins targeted by barley thioredoxin h isoforms. *The Biochemical journal* 378(Pt 2):497-507.
288. Vignols F, Brehelin C, Surdin-Kerjan Y, Thomas D, & Meyer Y (2005) A yeast two-hybrid knockout strain to explore thioredoxin-interacting proteins in vivo. *Proceedings of the National Academy of Sciences of the United States of America* 102(46):16729-16734.
289. Verdoucq L, Vignols F, Jacquot J-P, Chartier Y, & Meyer Y (1999) In Vivo Characterization of a Thioredoxin h Target Protein Defines a New Peroxiredoxin Family. *Journal of Biological Chemistry* 274(28):19714-19722.
290. Hernandez HH, Jaquez OA, Hamill MJ, Elliott SJ, & Drennan CL (2008) Thioredoxin reductase from *Thermoplasma acidophilum*: a new twist on redox regulation. *Biochemistry* 47(37):9728-9737.
291. Jeon SJ & Ishikawa K (2002) Identification and characterization of thioredoxin and thioredoxin reductase from *Aeropyrum pernix* K1. *European journal of biochemistry / FEBS* 269(22):5423-5430.
292. Kashima Y & Ishikawa K (2003) A hyperthermostable novel protein-disulfide oxidoreductase is reduced by thioredoxin reductase from hyperthermophilic archaeon *Pyrococcus horikoshii*. *Archives of Biochemistry and Biophysics* 418(2):179-185.
293. Grimaldi P, *et al.* (2008) Characterisation of the components of the thioredoxin system in the archaeon *Sulfolobus solfataricus*. *Extremophiles : life under extreme conditions* 12(4):553-562.
294. Esposito L, *et al.* (2012) Crystallographic and spectroscopic characterizations of *Sulfolobus solfataricus* TrxA1 provide insights into the determinants of thioredoxin fold stability. *Journal of Structural Biology* 177(2):506-512.
295. Ruggiero A, *et al.* (2009) Crystallization and preliminary X-ray crystallographic analysis of two dimeric hyperthermostable thioredoxins isolated from *Sulfolobus solfataricus*. *Acta Crystallographica Section F* 65(6):604-607.
296. McFarlan SC, Terrell CA, & Hogenkamp HP (1992) The purification, characterization, and primary structure of a small redox protein from *Methanobacterium thermoautotrophicum*, an archaebacterium. *The Journal of biological chemistry* 267(15):10561-10569.
297. Amegbey GY, Monzavi H, Habibi-Nazhad B, Bhattacharyya S, & Wishart DS (2003) Structural and functional characterization of a thioredoxin-like protein (Mt0807) from *Methanobacterium thermoautotrophicum*. *Biochemistry* 42(26):8001-8010.
298. Bhattacharyya S, *et al.* (2002) Identification of a novel archaebacterial thioredoxin: determination of function through structure. *Biochemistry* 41(15):4760-4770.
299. Lee DY, Ahn B-Y, & Kim K-S (2000) A Thioredoxin from the Hyperthermophilic Archaeon *Methanococcus jannaschii* Has a Glutaredoxin-like Fold but Thioredoxin-like Activities. *Biochemistry* 39(22):6652-6659.
300. Cave JW, *et al.* (2001) Solution nuclear magnetic resonance structure of a protein disulfide oxidoreductase from *Methanococcus jannaschii*. *Protein science : a publication of the Protein Society* 10(2):384-396.
301. Miranda-Vizuete A, Damdimopoulos AE, Gustafsson J, & Spyrou G (1997) Cloning, expression, and characterization of a novel Escherichia coli thioredoxin. *The Journal of biological chemistry* 272(49):30841-30847.
302. Aslund F, Ehn B, Miranda-Vizuete A, Pueyo C, & Holmgren A (1994) Two additional glutaredoxins exist in Escherichia coli: glutaredoxin 3 is a hydrogen donor for ribonucleotide reductase in a thioredoxin/glutaredoxin 1 double mutant. *Proceedings of the National Academy of Sciences of the United States of America* 91(21):9813-9817.

303. Sodano P, *et al.* (1991) Sequence-specific 1H n.m.r. assignments and determination of the three-dimensional structure of reduced *Escherichia coli* glutaredoxin. *Journal of molecular biology* 221(4):1311-1324.
304. Gan ZR & Wells WW (1988) Immunological characterization of thioltransferase from pig liver. *The Journal of biological chemistry* 263(18):9050-9054.
305. Yang YF & Wells WW (1991) Catalytic mechanism of thioltransferase. *The Journal of biological chemistry* 266(19):12766-12771.
306. Buchanan BB, Schurmann P, Wolosiuk RA, & Jacquot JP (2002) The ferredoxin/thioredoxin system: from discovery to molecular structures and beyond. *Photosynth Res* 73(1-3):215-222.
307. Dai S, *et al.* (2000) How does light regulate chloroplast enzymes? Structure–function studies of the ferredoxin/thioredoxin system. *Quarterly reviews of biophysics* 33(01):67-108.
308. Schürmann P & Buchanan B (2004) The Structure and Function of the Ferredoxin/Thioredoxin System in Photosynthesis. *Regulation of Photosynthesis*, Advances in Photosynthesis and Respiration, eds Aro E-M & Andersson B (Springer Netherlands), Vol 11, pp 331-361.
309. Balsera M, *et al.* (2013) Ferredoxin:thioredoxin reductase (FTR) links the regulation of oxygenic photosynthesis to deeply rooted bacteria. *Planta* 237(2):619-635.
310. Luthman M & Holmgren A (1982) Rat liver thioredoxin and thioredoxin reductase: purification and characterization. *Biochemistry* 21(26):6628-6633.
311. Gladyshev VN, Jeang KT, & Stadtman TC (1996) Selenocysteine, identified as the penultimate C-terminal residue in human T-cell thioredoxin reductase, corresponds to TGA in the human placental gene. *Proceedings of the National Academy of Sciences of the United States of America* 93(12):6146-6151.
312. Russel M & Model P (1988) Sequence of thioredoxin reductase from Escherichia coli. Relationship to other flavoprotein disulfide oxidoreductases. *Journal of Biological Chemistry* 263(18):9015-9019.
313. Williams CH, Jr. (1995) Mechanism and structure of thioredoxin reductase from Escherichia coli. *FASEB journal : official publication of the Federation of American Societies for Experimental Biology* 9(13):1267-1276.
314. Veine DM, Mulrooney SB, Wang P-F, & Williams CH (1998) Formation and properties of mixed disulfides between thioredoxin reductase from *Escherichia coli* and thioredoxin: Evidence that cysteine-138 functions to initiate dithiol-disulfide interchange and to accept the reducing equivalent from reduced flavin. *Protein Science* 7(6):1441-1450.
315. Waksman G, Krishna TS, Williams CH, Jr., & Kuriyan J (1994) Crystal structure of *Escherichia coli* thioredoxin reductase refined at 2 A resolution. Implications for a large conformational change during catalysis. *Journal of molecular biology* 236(3):800-816.
316. Lennon BW & Williams CH, Jr. (1997) Reductive half-reaction of thioredoxin reductase from *Escherichia coli*. *Biochemistry* 36(31):9464-9477.
317. Lu J & Holmgren A (2009) Selenoproteins. *The Journal of biological chemistry* 284(2):723-727.
318. Zhong L & Holmgren A (2000) Essential role of selenium in the catalytic activities of mammalian thioredoxin reductase revealed by characterization of recombinant enzymes with selenocysteine mutations. *The Journal of biological chemistry* 275(24):18121-18128.
319. Gromer S, *et al.* (1998) A hypothesis on the catalytic mechanism of the selenoenzyme thioredoxin reductase. *The Biochemical journal* 332 (Pt 2):591-592.
320. Arnér ESJ, Nordberg J, & Holmgren A (1996) Efficient Reduction of Lipoamide and Lipoic Acid by Mammalian Thioredoxin Reductase. *Biochemical and biophysical research communications* 225(1):268-274.
321. Björnstedt M, Hamberg M, Kumar S, Xue J, & Holmgren A (1995) Human Thioredoxin Reductase Directly Reduces Lipid Hydroperoxides by NADPH and Selenocystine Strongly Stimulates the Reaction via Catalytically Generated Selenols. *Journal of Biological Chemistry* 270(20):11761-11764.
322. Andersson M, Holmgren A, & Spyrou G (1996) NK-lysin, a Disulfide-containing Effector Peptide of T-lymphocytes, Is Reduced and Inactivated by Human Thioredoxin Reductase: IMPLICATION FOR A PROTECTIVE MECHANISM AGAINST NK-LYSIN CYTOTOXICITY. *Journal of Biological Chemistry* 271(17):10116-10120.

323. Arscott LD, Gromer S, Schirmer RH, Becker K, & Williams CH, Jr. (1997) The mechanism of thioredoxin reductase from human placenta is similar to the mechanisms of lipoamide dehydrogenase and glutathione reductase and is distinct from the mechanism of thioredoxin reductase from Escherichia coli. *Proceedings of the National Academy of Sciences of the United States of America* 94(8):3621-3626.
324. Gasdaska PY, Gasdaska JR, Cochran S, & Powis G (1995) Cloning and sequencing of a human thioredoxin reductase. *FEBS Letters* 373(1):5-9.
325. Arscott LD, Gromer S, Schirmer RH, Becker K, & Williams CH (1997) The mechanism of thioredoxin reductase from human placenta is similar to the mechanisms of lipoamide dehydrogenase and glutathione reductase and is distinct from the mechanism of thioredoxin reductase from Escherichia coli. *Proceedings of the National Academy of Sciences* 94(8):3621-3626.
326. Sandalova T, Zhong L, Lindqvist Y, Holmgren A, & Schneider G (2001) Three-dimensional structure of a mammalian thioredoxin reductase: implications for mechanism and evolution of a selenocysteine-dependent enzyme. *Proceedings of the National Academy of Sciences of the United States of America* 98(17):9533-9538.
327. Ruepp A, *et al.* (2000) The genome sequence of the thermoacidophilic scavenger Thermoplasma acidophilum. *Nature* 407(6803):508-513.
328. Buchanan BB, Kalberer PP, & Arnon DI (1967) Ferredoxin-activated fructose diphosphatase in isolated chloroplasts. *Biochemical and biophysical research communications* 29(1):74-79.
329. Tagawa K & Arnon DI (1962) Ferredoxins as Electron Carriers in Photosynthesis and in the Biological Production and Consumption of Hydrogen Gas. *Nature* 195(4841):537-543.
330. Schurmann P & Buchanan BB (2008) The ferredoxin/thioredoxin system of oxygenic photosynthesis. *Antioxidants & redox signaling* 10(7):1235-1274.
331. Dai S, *et al.* (2007) Structural snapshots along the reaction pathway of ferredoxin-thioredoxin reductase. *Nature* 448(7149):92-96.
332. Hishiya S, *et al.* (2008) Binary Reducing Equivalent Pathways Using NADPH-Thioredoxin Reductase and Ferredoxin-Thioredoxin Reductase in the Cyanobacterium *Synechocystis* sp. Strain PCC 6803. *Plant and Cell Physiology* 49(1):11-18.
333. Dai S, Schwendtmayer C, Schürmann P, Ramaswamy S, & Eklund H (2000) Redox Signaling in Chloroplasts: Cleavage of Disulfides by an Iron-Sulfur Cluster. *Science* 287(5453):655-658.
334. Hammel KE, Cornwell KL, & Buchanan BB (1983) Ferredoxin/flavoprotein-linked pathway for the reduction of thioredoxin. *Proceedings of the National Academy of Sciences of the United States of America* 80(12):3681-3685.
335. Kumar AK, Yennawar NH, Yennawar HP, & Ferry JG (2011) Expression, purification, crystallization and preliminary X-ray crystallographic analysis of a novel plant-type ferredoxin/thioredoxin reductase-like protein from Methanosarcina acetivorans. *Acta crystallographica. Section F, Structural biology and crystallization communications* 67(Pt 7):775-778.

3 An Intertwined Evolutionary History of Methanogenic Archaea and Sulfate reduction

3.1 ABSTRACT

Hydrogenotrophic methanogenesis and dissimilatory sulfate reduction, two of the oldest energy conserving respiratory systems on Earth, apparently could not have evolved in the same host, as sulfite, an intermediate of sulfate reduction, inhibits methanogenesis. However, certain methanogenic archaea metabolize sulfite employing a deazaflavin cofactor (F_{420})-dependent sulfite reductase (Fsr) where N- and C-terminal halves (Fsr-N and Fsr-C) are homologs of $F_{420}H_2$ dehydrogenase and dissimilatory sulfite reductase (Dsr), respectively. From genome analysis we found that Fsr was likely assembled from freestanding Fsr-N homologs and Dsr-like proteins (Dsr-LP), both being abundant in methanogens. Dsr-LPs fell into two groups defined by the following sequence features: Group I (simplest), carrying a coupled siroheme-[Fe_4-S_4] cluster and sulfite-binding Arg/Lys residues; Group III (most complex), with group I features, a Dsr-type peripheral [Fe_4-S_4] cluster and an additional [Fe_4-S_4] cluster. Group II Dsr-LPs with group I features and a Dsr-type peripheral [Fe_4-S_4] cluster were proposed as evolutionary intermediates. Group III is the precursor of Fsr-C. The freestanding Fsr-N homologs serve as $F_{420}H_2$ dehydrogenase unit of a putative novel glutamate synthase, previously described membrane-bound electron transport system in methanogens and of assimilatory type sulfite reductases in certain haloarchaea. Among archaea, only methanogens carried Dsr-LPs. They also possessed homologs of sulfate activation and reduction enzymes. This suggested a shared evolutionary history for methanogenesis and sulfate reduction, and Dsr-LPs could have been the source of the oldest (3.47-Gyr ago) biologically produced sulfide deposit.

3.2 INTRODUCTION

Hydrogen-dependent dissimilatory sulfate reduction ($4H_2 + SO_4^{2-} + H^+ \rightarrow HS^- + 4H_2O$) is one of the oldest energy conserving respiratory systems on Earth that developed about 3.5 billion years ago (1-4). Sulfite is an obligate intermediate in this process ($SO_4^{2-} \rightarrow SO_3^{2-} \rightarrow HS^-$) and also highly toxic to all types of cells (5). Therefore, the first organism to develop dissimilatory sulfate reduction ability certainly had invented or acquired the $SO_3^{2-} \rightarrow HS^-$ conversion system and dissimilatory sulfite reductase gene (*dsr*) in advance. This would also be true for assimilatory sulfate reduction. Accordingly, primary structures of the sulfite reductases have been used to track the evolutionary history of biological sulfate reduction process. It is generally considered that the dissimilatory sulfate reduction system including *dsr* originated in the bacteria, and the sulfate reducing archaea acquired these through horizontal gene transfer (3, 6). However, the results from a genomic analysis of the methanogenic archaea as reported here puts this concept in doubt.

Hydrogenotrophic methanogenesis ($4H_2 + CO_2 \rightarrow CH_4 + 2H_2O$) is also one of the oldest energy conserving respiratory systems of Earth developing at least 2.7-3.2 billion years ago (2). In general, methanogenesis and sulfate reduction are incompatible with each other because sulfite inhibits methanogenesis (7). On the other hand, the geological data indicate that methanogens of early Earth had to be sulfite tolerant and this ability continues to be important in the deep-sea hydrothermal vent environment that mimics some aspects of early Earth. The development of a fully oxic atmosphere on Earth seemed to have been preceded by a protracted oxygenation period (8-10) where a small supply of oxygen was quickly and fully sequestered by a high level of sulfide. Such a reaction could lead to incomplete oxidation sulfide and produce sulfite. The vent fluid is rich in nutrients for methanogens, but its temperature, which is 300-350 °C (11), is not conducive for the survival of a living cell. However, a mixing of this hot fluid with cold seawater that permeates through the chimney wall provides more hospitable temperatures in some areas within the chimney where hyperthermophilic methanogens grow (12, 13). The small amount of oxygen brought into the vent by the seawater is neutralized through its reaction with sulfide, which is present in the vent fluid at high levels (5-7 mM) (11). This reaction helps to maintain anaerobic and low redox potential conditions that are required for the growth of a methanogen, but, as described above, it could generate sulfite. Therefore, one would expect the

methanogens of early Earth and extant methanogens of hydrothermal vents to be resistant to sulfite. Indeed certain thermophilic deeply rooted methanogens not only tolerate sulfite but can also use this oxyanion as the sole sulfur source (14-16). For *Methanocaldococcus jannaschii*, a hydrogenotrophic and autotrophic methanogen that lives in the deep-sea hydrothermal vents, this ability is due to a new type of sulfite reductase (Fsr) that utilizes coenzyme F_{420} as the electron carrier (15, 17) (Fig. 3.1). Coenzyme F_{420} is a deazaflavin derivative that is found in every methanogen (18). At the ground state it functions as a NAD(P) type two-electron (hydride) transfer coenzyme (18). Fsr homologs are present in sulfite resistant methanogens, and heterologous expression of this enzyme allows a sulfite-sensitive methanogen to tolerate sulfite and to use it as sulfur source (15, 17). With the discovery of Fsr we inquired how widely the sulfite reduction capabilities or sulfite reductase genes are present in the methanogens and found that ORFs with essential elements of siroheme sulfite reductases are wide spread in this group of euryarchaea. These ORFs show a logical path for the development of a variety of sulfite reductases, including Fsr. These data and additional corroborating evidences suggest an intertwined evolutionary history of methanogenesis and sulfate reduction and make sulfite reductase as a primordial enzyme of the methanogenic archaea. In fact, this conclusion now provides a support to a recent proposal that the first incident of vigorous biological sulfate reduction that occurred at about 2.7 billion years ago was preceded by much earlier occurrence of such an event of minor magnitude (19). The reported analyses also identified two more putative F_{420}-dependent enzymes, one of them being an assimilatory-type sulfite reductase in late evolving archaea.

3.3 RESULTS AND DISCUSSION

The synthesis presented below is based on the known structure-function relationships of Fsr, dissimilatory sulfite reductases and assimilatory sulfite reductases (Dsr and aSir) (20-23). The terms of Dsr and aSir traditionally refer to the determined physiological roles as well as distinct structural types (20). However, in some cases, such as in Fsr, Dsr type structures have been found to be associated with assimilatory functions. In this report the terms Dsr and aSir refer to the structural features and not necessarily the physiological functions.

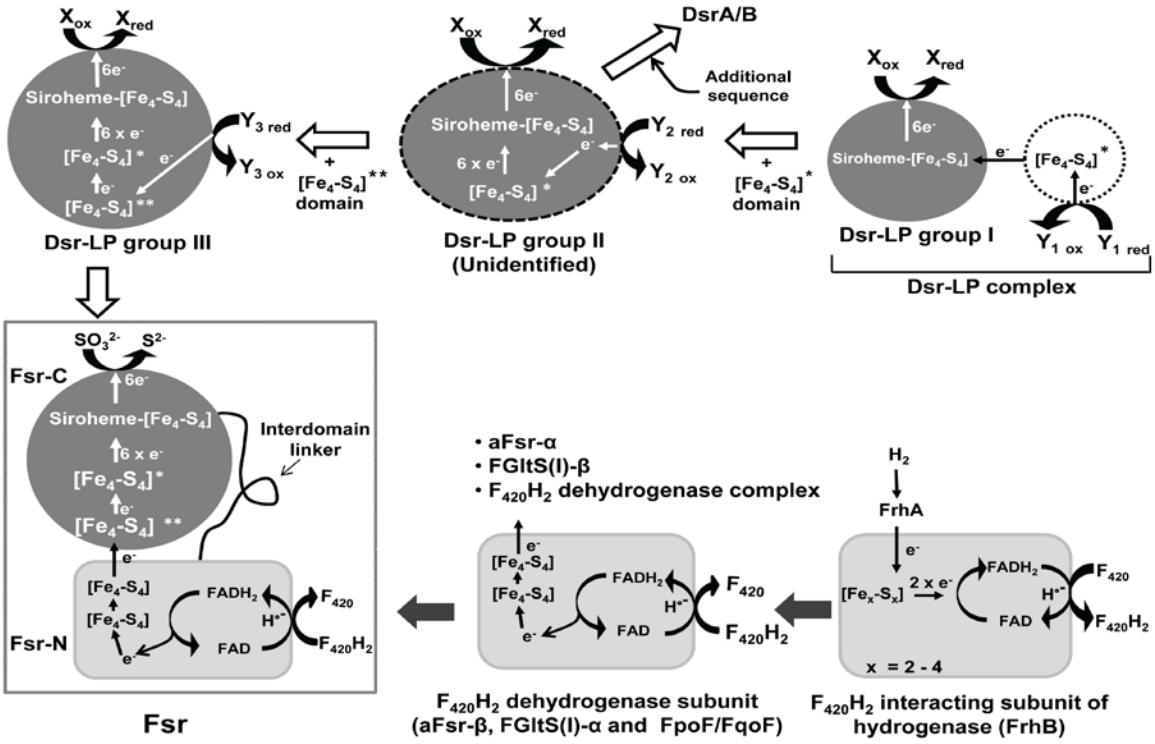

Figure 3.1 Development of dissimilatory sulfite reductase-like protein (Dsr-LP), $F_{420}H_2$-dependent sulfite reductase (Fsr) and dissimilatory sulfite reductase (Dsr).
Fsr-N and Fsr-C: N-terminal and C-terminal halves of Fsr, respectively. FGltS(I)-α and FGltS(I)-β: $F_{420}H_2$ dehydrogenase and glutamate synthase subunit of a putative $F_{420}H_2$-dependent glutamate synthase of methanogens; FpoF/FqoF: $F_{420}H_2$ dehydrogenase subunit of a membrane-bound proton pumping $F_{420}H_2$ dehydrogenase complexes of late evolving euryarchaea (24); aFsr-α and aFsr-β: aSir and $F_{420}H_2$ dehydrogenase subunits of a putative $F_{420}H_2$-dependent assimilatory type siroheme sulfite reductase found in haloarchaea. * and ** are peripheral and additional iron sulfur cluster [Fe_4-S_4], respectively. Filled and unfilled boxed arrows show the path for the development of Fsr-N and Fsr-C, respectively. Dashed oval or circle, unidentified protein. X and Y_{1-3}, unknown electron acceptors and donor, respectively.

3.3.1 Search for the origin of Fsr

Distribution of Fsr homologs in methanogens: The Fsr homologs had a significant presence within the methanogenic archaea and they could be considered a specialty of hyperthermophilic methanogens from the deep-sea hydrothermal vents and certain halophilic methanogens (Fig. 3. 2). Only exceptions are *Methanothermobacter thermoautotrophicus* and *Methanothermus fervidus* which are freshwater thermophiles from a municipal sewage digester and a hot spring, respectively (25, 26). However, *M. thermoautotrophicus* can grow at high salt concentrations (27). *M. fervidus* has not been tested for halotolerance. Every deep-sea hydrothermal vent

methanogen, including every *Methanocaldococcus* species, carried at least one Fsr homolog (Fig. 3.2); *Methanothermococcus thermolithotrophicus* (28) and *Methanohalobium evestigatum* Z-7303 (29), which are moderate thermophiles isolated from geothermally heated sea sediments, and salt lagoon respectively, and *Methanocaldococcus sp.* FS406-22 (30), a hydrothermal vent hyperthermophile, encode two Fsr homologs (Fig. 3.2). One of the two Fsr homologs of *M. thermolithotrophicus* is likely to be a nitrite reductase, because the organism can use nitrate as nitrogen source (31), a sulfite reductase often can reduce nitrite (20), and Fsr from *M. jannaschii* has been found to reduce nitrite with $F_{420}H_2$ (Eric F. Johnson and Biswarup Mukhopadhyay, unpublished observation).Three non-hydrothermal vent methanogens, *Methanohalobium evestigatum* (moderate thermophile) (32), *Methanococcus aeolicus* Nankai-3 (mesophile) (33), and *Methanococcoides burtonii* DSM 6242 (psychrophile) (34), that carried Fsr homologs (Fig. 3.2) live in marine environments. It is likely that they have acquired *fsr* via horizontal gene transfer from the vent methanogens. Cooler seawater is known to disperse vent organisms from one vent field to another and the strictly anaerobic vent methanogens can survive oxygen exposure at low temperatures (35). Therefore, vent methanogens could reach the habitats of mesophilic and psychrophilic marine methanogens. However, the genomic sequences at the immediate vicinity of *fsr* do not show conservation. This could indicate that the above-mentioned non-hydrothermal vent methanogens received *fsr* from vent methanogens early in their development or both groups arose from a common ancestor that carried *fsr* and continued genome evolution removed the context similarity. An Fsr homolog (GZ27A8_52) is present in ANME-1 (15), an uncultured archaeon that is a component of a consortium that performs anaerobic oxidation of methane (36). This observation raises the possibility of sulfite and even sulfate reduction coupled anaerobic oxidation of methane in this halophile from permanently cold methane rich marine sediment. This possibility is supported by the observation that *Methanococcoides burtonii*, a methanogen that is phylogenetically closely related to ANME-1 and lives in an environment that is similar to the habitat of ANME-1 (34), also carries an Fsr homolog (Fig. 3.2).

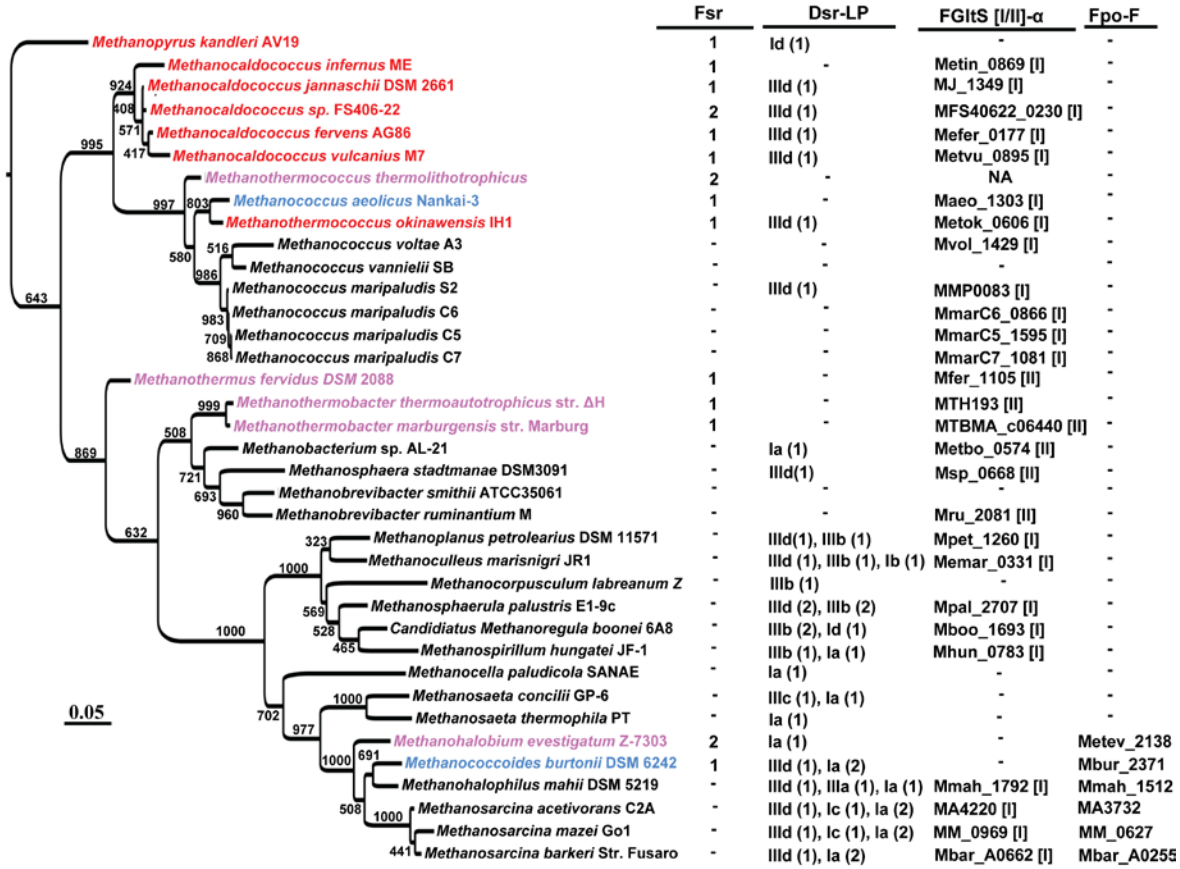

Figure 3.2 Distribution of Dsr-LP, Fsr, FGltS(I/II)-α and FpoF in methanogenic archaea. The information has been presented on a 16S rRNA sequence based phylogenetic tree of methanogens for which whole genome sequences are available. *Desulfurococcus fermentans* was used as an outgroup. The confidence values presented at the branches of the tree were estimated from 1000 bootstrap repetitions; the scale bar underneath the tree indicates the number of base substitutions per site. (1 or 2), number of each type of sulfite reductase homolog in a methanogen. Dsr-LP: dissimilatory sulfite reductase-like proteins; Fsr, FGltS(I/II)-α, and FpoF: same as in the legend of Fig. 3.1. The Dsr-LP group numbers (Ia-d and IIIa-d) are according to Fig. 3.3. Color representation of Fsr-containing methanogens (color, characteristic); red, hyperthermophilic vent methanogen (except *M. okinawensis* is a thermophile); lavender, thermophile; blue, mesophile and psycrophile. Classification of FGltS according to Fig. 3.7 is shown in square brackets.

A chimeric structure of Fsr likely developed through gene fusion: The N-terminal half of *M. jannaschii* Fsr (Fsr-N; residues 1-311 of ORF MJ_0870) is a homolog of a free-standing polypeptide called $F_{420}H_2$ dehydrogenase (FpoF/FqoF) that is found in late evolving methylotrophic and acetotrophic methanogens and *Archaeoglobus fulgidus*, a sulfate reducing

archaeon closely related to the methanogens (15, 17, 24) (Fig. 3.1). In these organisms FpoF/FqoF serves as the electron input subunit of a membrane-bound NADH-dehydrogenase type energy transduction system called $F_{420}H_2$ dehydrogenase complex (15, 17, 24**).** The C-terminal half of Fsr (Fsr-C; residues 325-620 of MJ_0870) is a homolog of Dsr (15, 17) **(**Figs. 3.1 and 3.4). Fsr functions both as a dissimilatory (detoxification) and an assimilatory (sulfide nutrition) enzyme (15, 17) and Fsr-C does not show significant sequence similarity to aSir (15). Two documented partial reactions of Fsr, namely dehydrogenation of $F_{420}H_2$ and reduction of sulfite (15) suggest that Fsr-N retrieves electrons from $F_{420}H_2$ and reduces FAD, and then via the Fe-S centers of Fsr-N and Fsr-C, the electrons from $FADH_2$ are transferred to siroheme of Fsr-C where sulfite is reduced to sulfide; FAD acts as 2-electron/1-electron switch connecting 2-electron-donating $F_{420}H_2$ and 1-electron-carrying Fe-S centers. Functionally Fsr reaction mimics NADH-dependent reduction of sulfite by *E. coli* aSir which is composed of a siroheme-containing protein subunit (Sir-HP) and a flavoprotein subunit (Sir-FP) (20); Sir-HP and Sir-FP are equivalent to Fsr-C and Fsr-N, respectively. However, as mentioned above Fsr-C and Sir-HP do not share a significant sequence homology, and Fsr-N and Sir-FP are also not homologous to each other (15).

Strategy for a search for the origin of Fsr: The chimeric nature of Fsr and the logic that simpler units would arrive first suggested that Fsr was built from pre-existing parts, Fsr-N and Fsr-C. These parts were either available in the methanogens or were transferred horizontally to these archaea from other organisms. The latter possibility seemed weak because Fsr homologs had a significant distribution within the methanogenic archaea and apparently absent in the eukaryotic and bacterial domain as well as in other members of the archaea. However, for Fsr to be a true invention of the methanogens, Fsr-N and Fsr-C homologs must be at least widespread if not fully restricted to these organisms. The results presented below show that this is indeed the case.

3.3.2 Search for Fsr-C homologs: discovery of Dsr-LP, a family of dissimilatory sulfite reductase like ORFs in methanogens

The homologs of Fsr-C as freestanding units were abundant in the methanogens and they were diverse in their contents of the characteristic sequence features (Figs. 3.3 and 3.4). About 67 %

of the fully closed methanogen genomes examined carried these homologs and their total number was 49 (Fig. 3.2). Since their catalytic and *in vivo* functions are not known, these ORFs with high sequence similarities with Dsr subunits (DsrA and DsrB) and low similarities with aSir were named Dsr-LP (dissimilatory sulfite reductase-like proteins). The Dsr-LP ORFs were compared with the DsrA/B sequences to locate their relevant structural features (Figs. 3.3 and 3.4). Dsr-LPs as a family were found to carry all of the following defining structural features of sulfite reductases: i. A coupled siroheme-iron sulfur cluster where sulfite or nitrite is reduced; ii. An iron-sulfur cluster (called peripheral [Fe_4-S_4] cluster) that shuttles electrons from a donor to the oxyanion reduction site; and iii. Arg/Lys residues that facilitate the binding of negatively charged sulfite (20-23, 37).

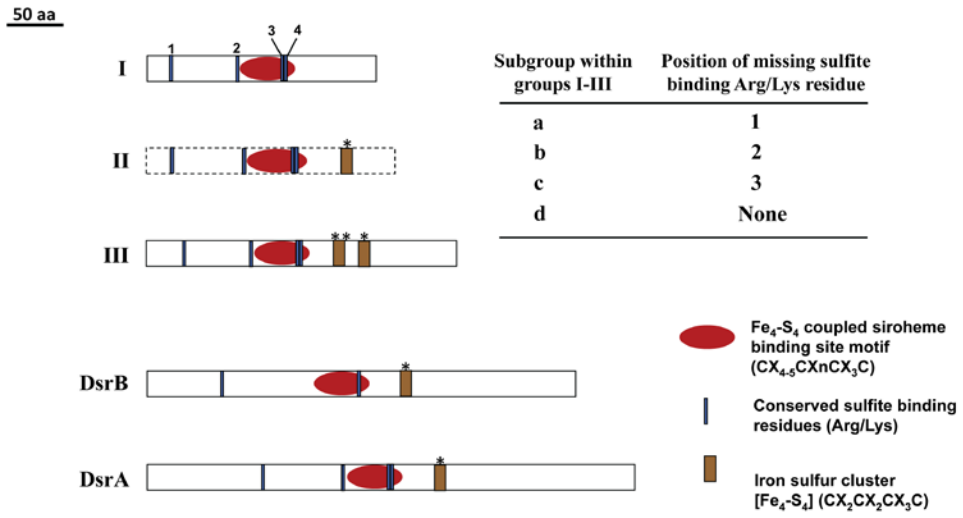

Figure 3.3 Groups of Dsr-LP and Dsr.

The Dsr-LP classification (groups Ia-d and IIIa-d) is based on the presence and absence of the following functionally important sequence signatures: [Fe_4-S_4]-coupled siroheme binding site; iron sulfur cluster sites (*, peripheral; ** additional); and sulfite binding amino acid residues (Arg or Lys). Numbers 1-4 indicates the positions (1st, 2nd, 3rd and 4th) of sulfite binding amino acid residues. The amino acid sequences representing these characteristics are shown in Fig. 3.4. Groups IIa-d, represented by dotted-line box are hypothetical and yet to be detected.

Fig. 3.4 shows the amino acid residues and sequence motifs representing these features in well-studied Dsr and their parallels in Dsr-LP and Fsr-C. In this comparison the Dsr-LPs fell into two broadly defined groups I and III (Fig. 3.3). As discussed below, the development of group III from group I had likely proceeded through an intermediate state and to represent this state we have proposed group II Dsr-LP (Figs. 3.1 and 3.3). We have not found a representative for group II thus far. Every Dsr-LP carried the sequence motif for the coupled siroheme-iron sulfur

cluster, the most defining feature of sulfite reductases. Group I had the simplest features as the members carried conserved signatures for siroheme-iron sulfur cluster but lacked ferredoxin domains (Figs. 3.3 and 3.4). The hypothesized group II would have the group I features and the peripheral [Fe_4-S_4] cluster (see * in Figs. 3.3 and 3.4). Group III was characterized by a siroheme-iron sulfur cluster, a peripheral Fe_4-S_4 cluster and an additional [Fe_4-S_4] cluster (Figs. 3.3 and 3.4). The members of each group carried either three or all of the four Arg/Lys residues that define sulfite-binding sites in Dsr (21-23, 37) and based on the positions of the missing Arg/Lys residue (1^{st}-4^{th}, counting from the NH_2-terminus of the polypeptide; Figs. 3.3 and 3.4) they were further classified in four sub-groups. Sub-groups a, b, and c lacked the 1^{st}, 2^{nd}, and 3^{rd} sulfite-binding Arg/Lys residue, respectively, and d, carried all four residues (Fig. 3.3). The 4^{th} sulfite-binding residue was fully conserved across all types of sulfite reductases and therefore could be critical to the binding of an anionic substrate, sulfite or nitrite. Group IIId could be considered the precursor of Fsr-C. DsrA/B lack the additional iron-sulfur cluster (See ** in Figs. 3.3 and 3.4) and the significance of the presence of this unit in groups III Dsr-LP is discussed below.

To gain better understanding on the evolutionary relationships between Dsr-LPs and Fsr-C homologs, we have performed phylogenetic analysis using two different approaches, namely Maximum likelihood (ML) (Fig. 3.5) and Bayesian Markov chain Monte Carlo (MCMC) phylogenetic inference (Fig. 3.6). Results from both approaches presented group I Dsr-LPs and Fsr-C as monophyletic (Figs. 3.5 and 3.6). Phylogenetically, group III was composed of more heterogeneous members, although individual sub-groups formed tighter clades. These observations allude to the following possibilities: i. Group I members are under strong selective pressures; ii. Group III members evolved from group I to provide functional diversity and the path of their development will be apparent when members of group II, the missing links, are identified.

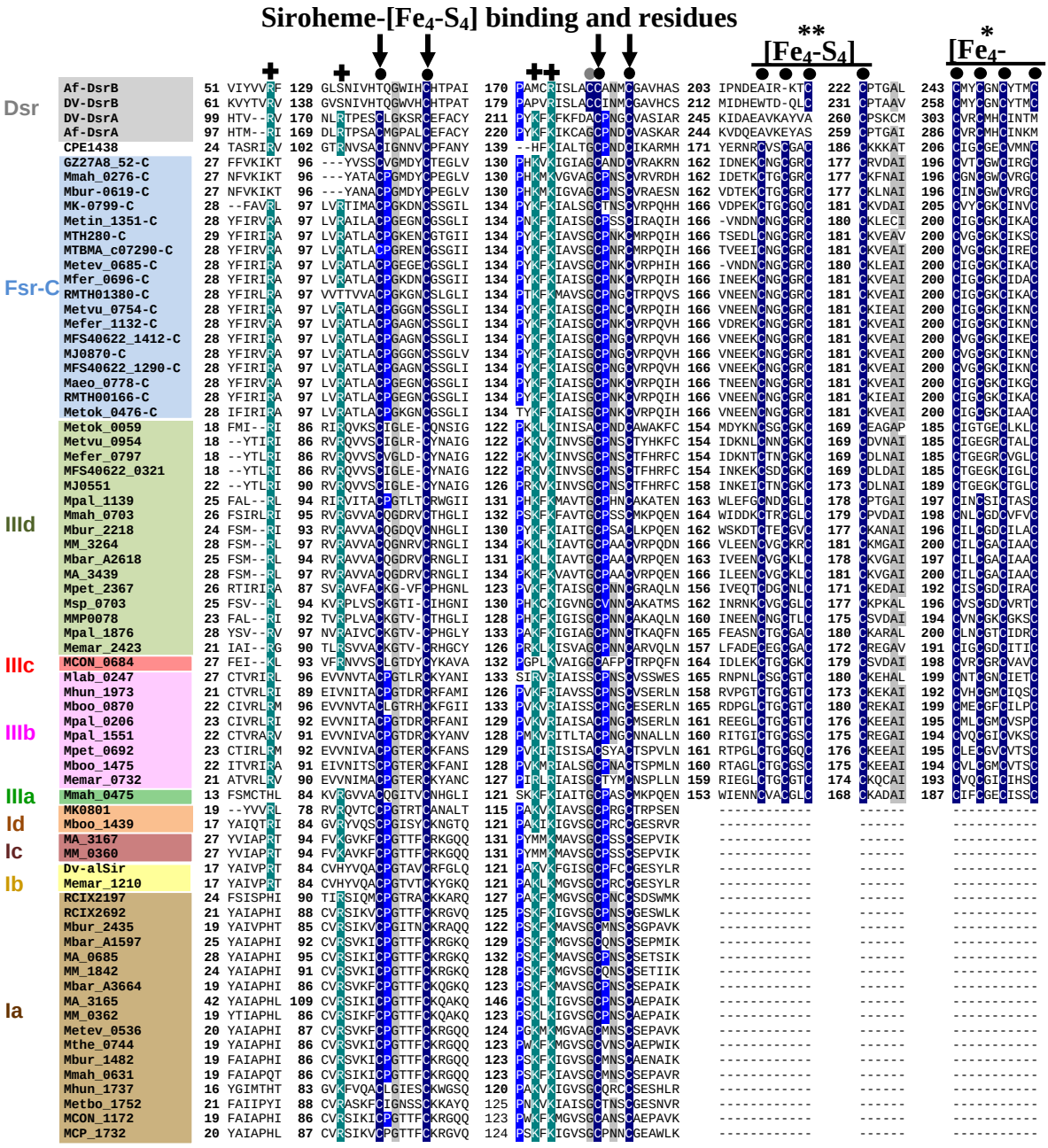

Figure 3.4 Primary structure comparison of Dsr-LPs of methanogenic archaea and archaeal and bacterial Dsr. Fsr-C, defined in Fig. 3.1. Structural type of Dsr-LP groups, as described in Fig. 3.3, shown as number Ia-d and IIIa-d left to the alignment (groups IIa-d, yet to be detected); "+", sulfite binding Arg or Lys residues; arrows, residues involved in assembling [Fe_4-S_4]-coupled siroheme; over-line, sequence motif involved in assembling [Fe_4-S_4] cluster; * and **, peripheral and additional [Fe_4-S_4] centers, respectively. Black bullets, conserved cysteine residues for [Fe_4-S_4] and siroheme sites. Red bullet, non-conserved cysteine residues coupling [Fe_4-S_4] center with siroheme in Dv-DsrB. The details of the abbreviations for organism names are in the legend of Fig. 3.5. The following color shadings have been used to represent conserved residues: teal, arginine or lysine; dark blue, cysteine; blue, prolin; grey, other residues. The color shadings in the left panel representing various sulfite reductases correspond to the same in Fig. 3.5.

Both ML and MCMC analyses divided group IIId into two sub-clades, A and B (Figs. 3.5 and 3.6), where IIId-A represented almost exclusively the hyperthermophilic methanogens from deep-sea hydrothermal vents and the members of the sub-clade IIId-B were mostly from evolutionarily late evolving mesophilic methanogens. ML tree presented group IIId-A as closely related to Fsr-C, whereas in MCMC tree group IIId-B was linked to Fsr-C. However, both Fsr and IIId-A exist in hyperthermophilic methanogens, and therefore, the relationship presented by ML analysis is more reliable.

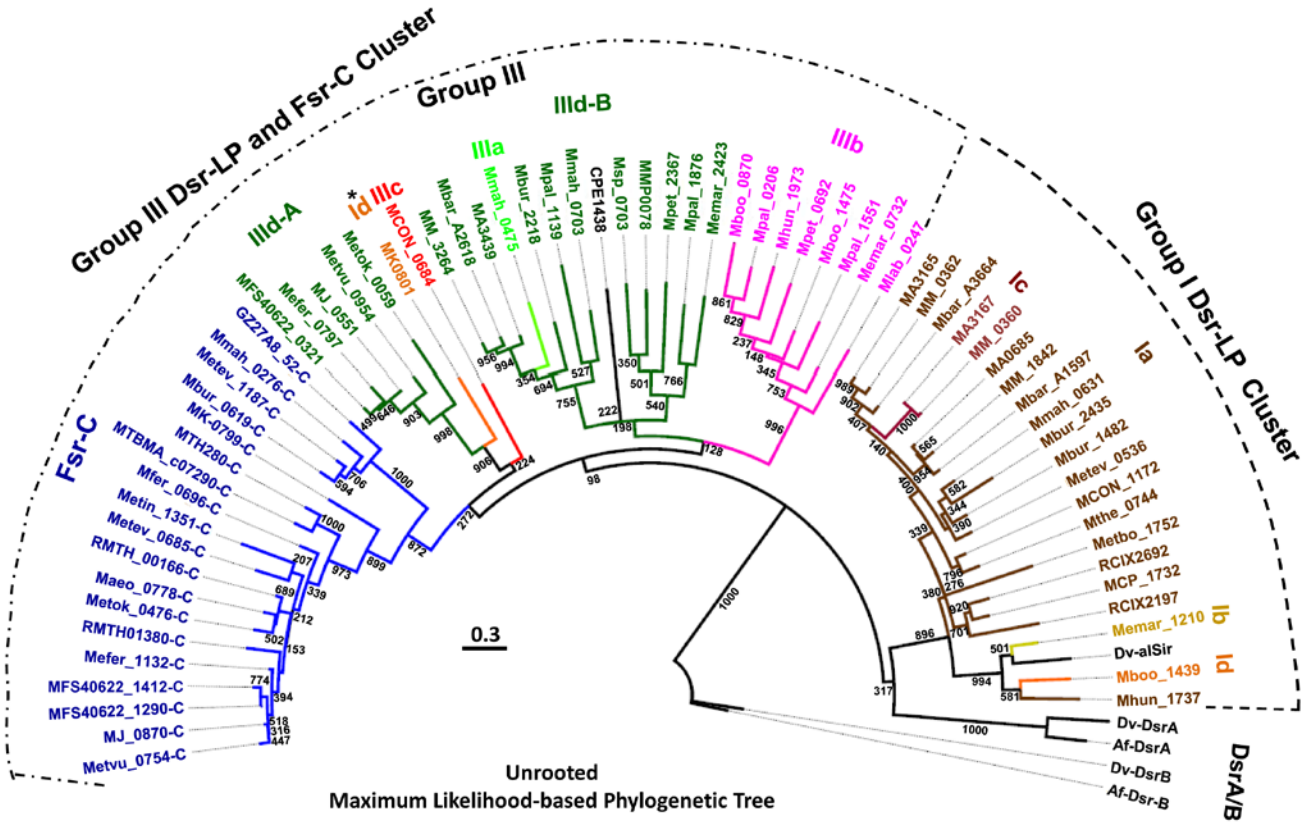

Figure 3.5 Phylogenetic tree of Dsr-LP and Dsr based on Maximum Likelihood method. Dsr-LP (Groups Ia-d and IIIa-d) and Dsr, defined in Fig. 3.3 and its legend. Dsr and Fsr-C, defined in the legend of Fig. 3.1. Dv-DsrA/B and Af-DsrA/B, Dsr subunits A and B of *Desulfovibrio vulgaris* strain Hildenborough (ORFs DVU0402 and DVU0403) and *Archaeoglobus fulgidus* DSM 4304 (ORFs AF0423 and AF0424), respectively (38, 39); Dv-alSir and CPE1438, anaerobic small sulfite reductase of *Desulfovibrio vulgaris* strain Hildenborough (ORF DVU_1597) and *Clostridium perfringens* strain 13, respectively (40); The ORF numbers followed by "-C", Fsr-C homologs. Abbreviation for organism names preceding the listed ORF numbers: MTBMA, *Methanothermobacter marburgensis* strain Marburg; MTH, *Methanothermobacter thermautotrophicus* ΔH; Metbo, *Mehanobacterium* sp. AL-21; RMTH, *Methanothermococcus thermolithotrophicus* (sequence obtained from Dr. William B. Whitman,

University of Georgia); Mfer, *Methanothermus fervidus* DSM 2088; Maeo, *Methanococcus aeolicu*s Nankai-3; Msp, *Methanosphaera stadtmanae* DSM 3091; MMP, *Methanococcus maripaludis* S2; Mpal, *Methanosphaerula palustris* E1-9c*;* Mpet, *Methanoplanus petrolearius* DSM 11571*;* Memar, *Methanoculleus marisnigri* JR1; MM, *Methanosarcina mazei* Gö1; MA, *Methanosarcina acetivorans* C2A; Mbar, *Methanosarcina barkeri* strain Fusaro*;* Mbur, *Methanococcoides burtonii* DSM 6242; Mmah, *Methanohalophilus mahii* DSM 5219; Metev, *Methanohalobium evestigatum* Z-7303; Mthe, *Methanosaeta thermophila* PT; MCON, *Methanosaeta concilii* GP-6; MCP, *Methanocella paludicola* SANAE; Mboo, *Candidiatus Methanoregula boonei* 6A8; Mlab, *Methanocorpusculum labreanum* Z; Mhun, *Methanospirillum hungatei* JF-1; Metbo, *Methanobacterium* sp. Al-21; Metok, *Methanothermococcus okinawensis* IH1; Metin, *Methanocaldococcus infernus* ME; MFS40622, *Methanocaldococcus sp.* FS406-22; MJ, *Methanocaldococcus jannaschii* DSM 2661; Mefer, *Methanocaldococcus fervens* AG86; Metvu, *Methanocaldococcus vulcanius* M7; MK, *Methanopyrus kandleri* AV19; GZ27A8_52, uncultured archaeon related to *Methanosarcina* and a member of an anaerobic methane oxidizing consortium; RCIX2692 and RCIX2197, uncultured methanogenic archaeon RC-1 and primary methane producer in rice rhizosphere. The bootstrap value shown at each branch is from 1000 replicates. Scale bar, number of amino acid substitutions per site. *, shows outliers. A and B, sub-clades of group IIId.

Among the structural sub-groups a-d (Figs. 3.5 and 3.6) only Ia, IIIb, and IIId were well represented and formed tight clades. Members of other sub-groups were rare and they showed a diversity of phylogenetic positions. In both ML and MCMC analysis MK0801 of *M. kandleri*, the sole member of group Id, was grouped with group IIId-A. Often *M. kandleri*, the most thermophilic methanogen (maximum growth temperature, 110 ^{o}C) and an inhabitant of deep-sea hydrothermal vents, is considered the most deeply-rooted methanogen (41-44). It is possible that MK0801 and group IIId-A Dsr-LPs arose from a common ancestor.

3.3.3 Distribution of Dsr-LP in the methanogens

The distribution of Dsr-LP in the methanogens exhibited a distinct pattern (Fig. 3.2). The deeply rooted organisms belonging to the classes of Methanopyri (*Methanopyrus kandleri*) and Methanococci (genera of *Methanocaldococcus, Methanotorris, Methanothermococcus,* and *Methanococcus*) carried limited numbers of sulfite reductase homologs. Each of the *Methanocaldococcus* species carried at least one Fsr homolog and a Dsr-LP, except *Methanocaldococcus infernus* lacked Dsr-LP. *Methanopyrus kandleri* possessed one Fsr and one Dsr-LP. With the exception of *Methanococcus maripaludis* strain S2, all *Methanococcus* species lacked Dsr-LP, and Fsr was absent in this genus. Of the two methanothermococci studied thus far, one carried two Fsr and lacked Dsr-LP and the other had one homolog for each of Fsr and

Dsr-LP (Fig. 3.2); these scenario might change as these two genomes have not yet been fully sequenced.

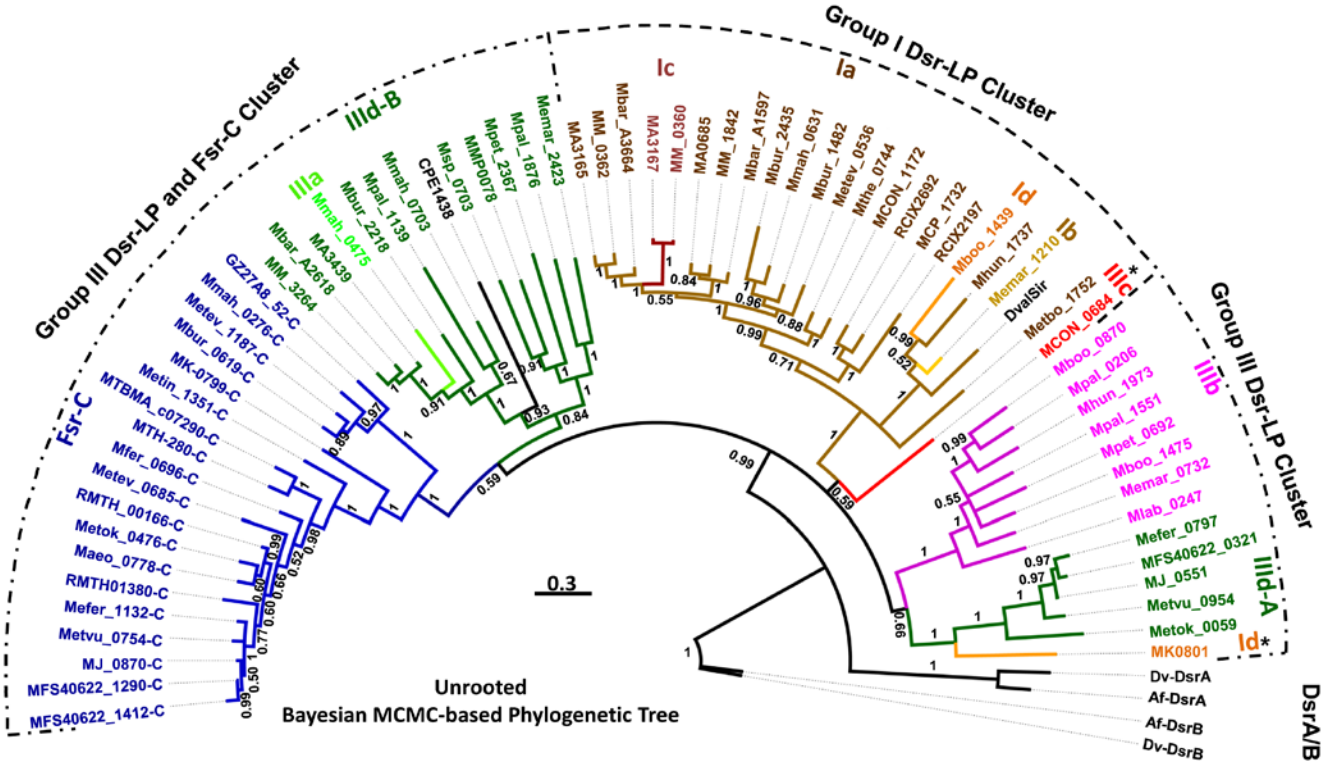

Figure 3.6 Phylogenetic tree of Dsr-LP homologs based on Bayesian Markov chain Monte Carlo (MCMC) analysis. ORF numbers and all abbreviations used are described in the legend of Fig. 3.5. For each branch a posterior probability value (0-1) is shown. Scale bar, number of amino acid substitutions per site.

Within the Methanobacteria class, each of *Methanothermobacter* and *Methanothermus* species carried an Fsr homolog and lacked Dsr-LP homolog. *Methanobrevibacter* genomes were devoid of sulfite reductase homologs (Fsr or Dsr-LP) whereas *Methanosphaera stadtmanae* carried one Dsr-LP and was devoid of Fsr. The Dsr-LP was highly prevalent in the class of Methanomicrobia, each member carrying 1-4 homologs of this protein; Fsr was only rarely found in this group. The genomes of *Methanosarcina and Methanosphaerula* species encoded the maximum number Dsr-LP proteins (four homologs) and lacked Fsr. Methanogens that contained more than two Dsr-LP homologs are mostly mesophilic and psycrophilic. It seems that in these late evolving organisms Dsr-LP underwent recruitment to multiple needs.

3.3.4 Fsr-N homologs: widespread in methanogens and being parts of two additional and novel enzymes, putative F_{420}-dependent glutamate synthase (FGltS) and assimilatory type Fsr (aFsr)

The identification of homologs of Fsr-N via automated similarity (BLAST) searches proved difficult because it is highly similar to the F_{420}-interacting subunits of F_{420}-dependent hydrogenases (FrhB) and formate dehydrogenases (FdhB) (15). In fact this factor has led to the misconception that FpoF/FqoF, the closest relative of Fsr-N (15), is absent in the strict hydrogenotrophic methanogens belonging to the orders of Methanobacteriales and Methanococcales and is a specialty of the methylotrophic methanogens of the Methanomicrobia class (45). We circumvented this problem by using the following primary sequence relationships: Fsr-N = FrhB + two additional ferredoxin-type [Fe_4-S_4] centers at the N-terminus; FdhB = FrhB + two additional [Fe_4-S_4] centers at the C-terminus (Fig. 3.7). This analysis showed that in the methanogens freestanding Fsr-N homologs were as abundant as Dsr-LPs (Figs. 3.2, 3.8 and 3.9).

Based on both Maximum Likelihood and Bayesian Markov chain Monte Carlo (MCMC) analyses, phylogenetically Fsr-N homologs fell into four distinct clades (FGltS(I)-α – aFsr-β – Fpo/FqoF; Fsr-N; FGltS(II)-α – FrhB; and FdhB) (Figs. 3.8 and 3.9), each of which was linked to a specific genomic context. From these clues the following two new putative F_{420}-dependent enzymes were located: an F_{420}-dependent glutamate synthase (FGltS(I)) in methanogens (L-glutamine + α-ketoglutarate + $F_{420}H_2$ → 2 L-glutamate + F_{420}), where FGltS(I)-α is the Frs-N homolog and FGltS(I)-β is the glutamate synthase subunit; an assimilatory Fsr (aFsr) of the halobacteria where the sulfite reductase subunit (aFsr-α) is aSir type and the electron retrieving subunit (aFsr-β) is a Fsr-N homolog. This is the first report for aFsr and FGltS(I); previously characterized glutamate synthases use NADH, NADPH or reduced ferredoxin as the reductant (46). Methanogen genomes encode another version of putative F_{420}-dependent glutamate synthase where F_{420}-interacting subunit is an FdhB homolog (Fig. 3.7) and here it has been named FGltS(II); a homolog of FGltS(II) has recently been found in *Methanothermobacter marburgensis* genome (47).

As shown in Figs. 3.7 and 3.10, among the Fsr-N homologs FrhB has the simplest structure. It also exists in every methanogen. Accordingly, we propose that from FrhB more complex Fsr-N

homologs evolved through recruitment of additional iron-sulfur centers, and therefore, FrhB is the ancestor of all Fsr-N homologs (Fig. 3.1).

3.3.5 The additional ferredoxin domain of group III Dsr-LPs: evolution of an inter-domain electron transfer conduit of Fsr

Group III Dsr-LPs showed the potential of assembling an additional [Fe_4-S_4] element (shown by ** in Figs. 3.1, 3.3 and 3.4) which has not been found in archaeal and bacterial DsrA and DsrB subunits. For Fsr-C this additional [Fe_4-S_4] cluster likely allows electron transfer between the Fsr-N and Fsr-C domains via the following path (Fig. 3.1): $F_{420}H_2$ → FAD (in Fsr-N) → *additional [Fe_4-S_4]* → peripheral [Fe_4-S_4] cluster → siroheme-coupled [Fe_4-S_4] → siroheme → sulfite. All of these steps except the first two operate in Dsr, which obtains electrons from iron-sulfur proteins (21-23).

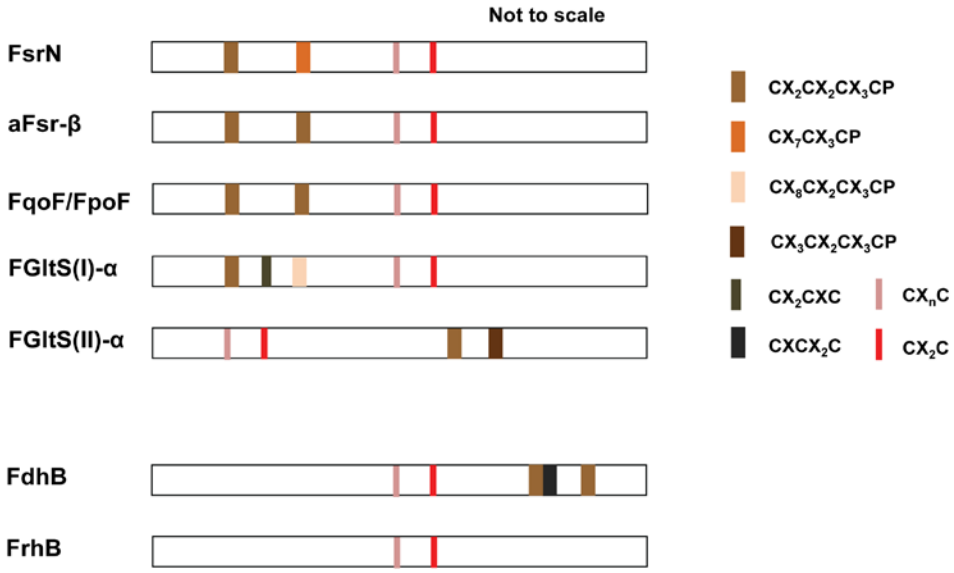

Figure 3.7 Groups of Fsr-N homologs. The sketches are based on respective amino acid sequence characteristics shown in Fig. 3.10. FGltS(I)-α and aFsr-β: $F_{420}H_2$-dehydrogenase subunit of a putative $F_{420}H_2$-dependent glutamate synthase of methanogens and a putative $F_{420}H_2$-dependent assimilatory type siroheme sulfite reductase found in haloarchaea; FpoF/FqoF: $F_{420}H_2$ dehydrogenase subunit of a membrane-bound proton pumping $F_{420}H_2$ dehydrogenase complex of late evolving euryarchaea (24). Note: FGltS(II)-α departs significantly from Fsr-N in primary sequence and it is not included in Fig. 3.10. F_{420}-interacting or β subunits of $F_{420}H_2$ reducing hydrogenase (FrhB) and formate dehydrogenase (FdhB) (48, 49) are shown for comparison.

3.3.6 Development of Fsr and aFsr

Based on the findings reported above, it is likely that Fsr is an invention of the methanogens and it was built in a methanogen from a group IIId Dsr-LP and a Fsr-N homolog that existed in these

archaea (Fig. 3.1); above described inter-domain electron transfer conduit was a key for this development. It is possible that the process involved an intermediate complex composed of Fsr-N and Fsr-C as individual subunits followed by a gene fusion event that generated the complete Fsr polypeptide; the discovery of a putative aFsr composed of Fsr-N and aSir subunits in the halobacteria provides further support to this hypothesis. Similar to Fsr, aFsr is also likely to be an archaeal invention, as an aSir homolog that is found in *Sulfolbus solfataricus*, a crenarchaeon, appears at the most basal position in a phylogenetic tree that covers archaeal, bacterial and eukaryotic aSirs (50).

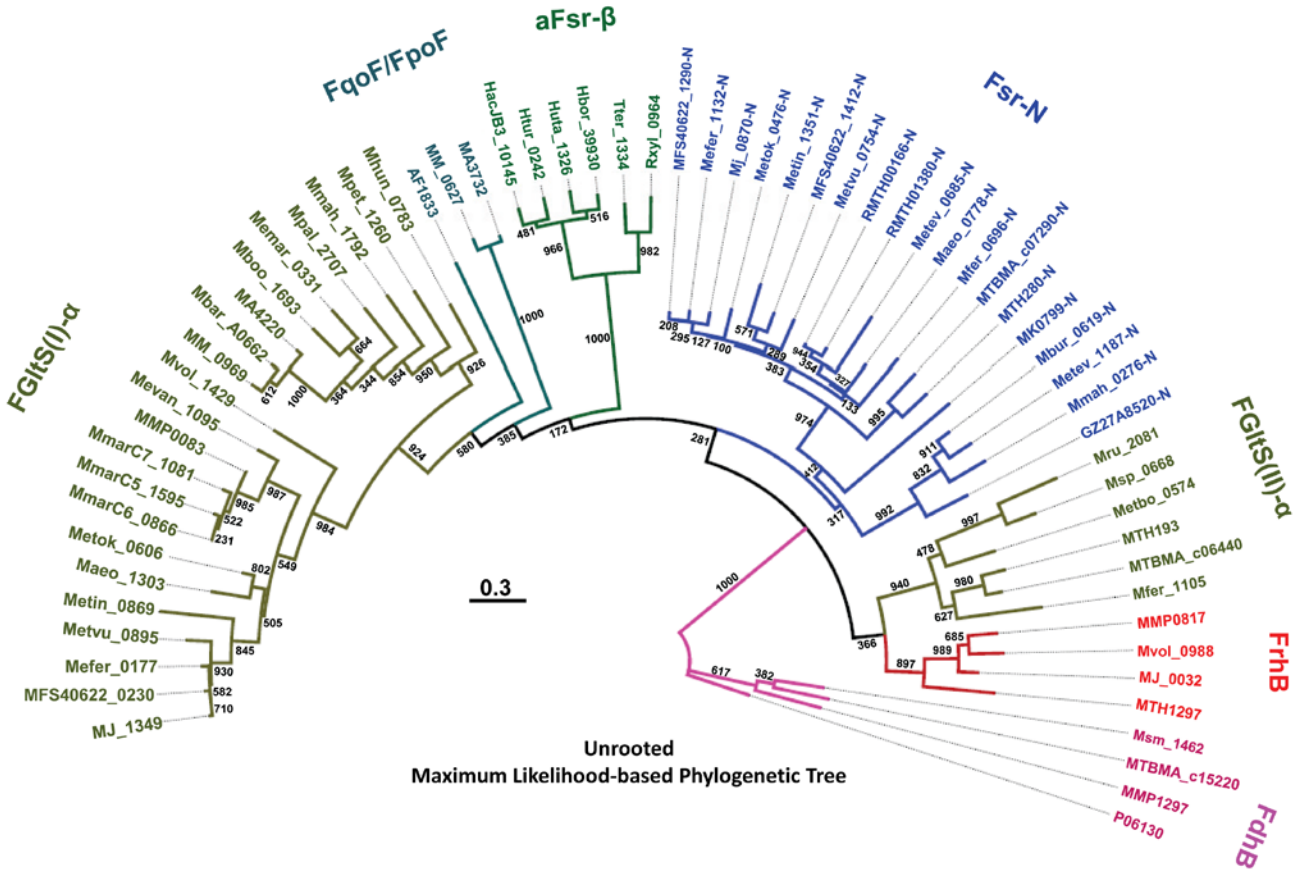

Figure 3.8 Phylogenetic tree of homologs of *M. jannaschii* Fsr-N according to Maximum Likelihood method. aFsr-β, FqoF, FpoF, and FGltS(I)-α are Fsr-N homologs. FrhB and FdhB are shown for comparison. See the legend of Fig. 3.1 for the full names of Fsr-N, aFsrβ, FqoF, FpoF and FGltS-α, and Fig. 3.7 for FrhB and FdhB. The ORF numbers followed by "-N", Fsr-N homologs. Abbreviations for organism names preceding the ORF numbers (in addition to those described in Fig. 3.5 legend): Hbor, *Halogeometricum borinquense* DSM 11551*;* Huta, *Halorhabdus utahensis* DSM 12940; HacJB3, *Halalkalicoccus jeotgali* B3; Htur, *Haloterrigena turkmenica* DSM 5511*;* Rxyl_0964, *Rubrobacter xylanophilus* DSM 9941; Tter, *Thermobaculum terrenum* ATCC BAA-798; GZ27A8_52, uncultured archaeon related to

Methanosarcina species; MmarC6, *Methanococcus maripaludis* C6; MmarC5, *Methanococcus maripaludis* C5; MmarC7, *Methanococcus maripaludis* C7; Mevan, *Methanococcus vannielii* SB; Mvol, *Methanococcus voltae* A3*;* AF, *Archaeoglobus fulgidus* DSM 4304, Msm, *Methanobrevibacter smithii* ATCC 35061*;* P06130, accession number for *Methanobacterium formicicum* FdhB. The bootstrap value shown at each branch is from 1000 replicates. Scale bar, number of amino acid substitutions per site.

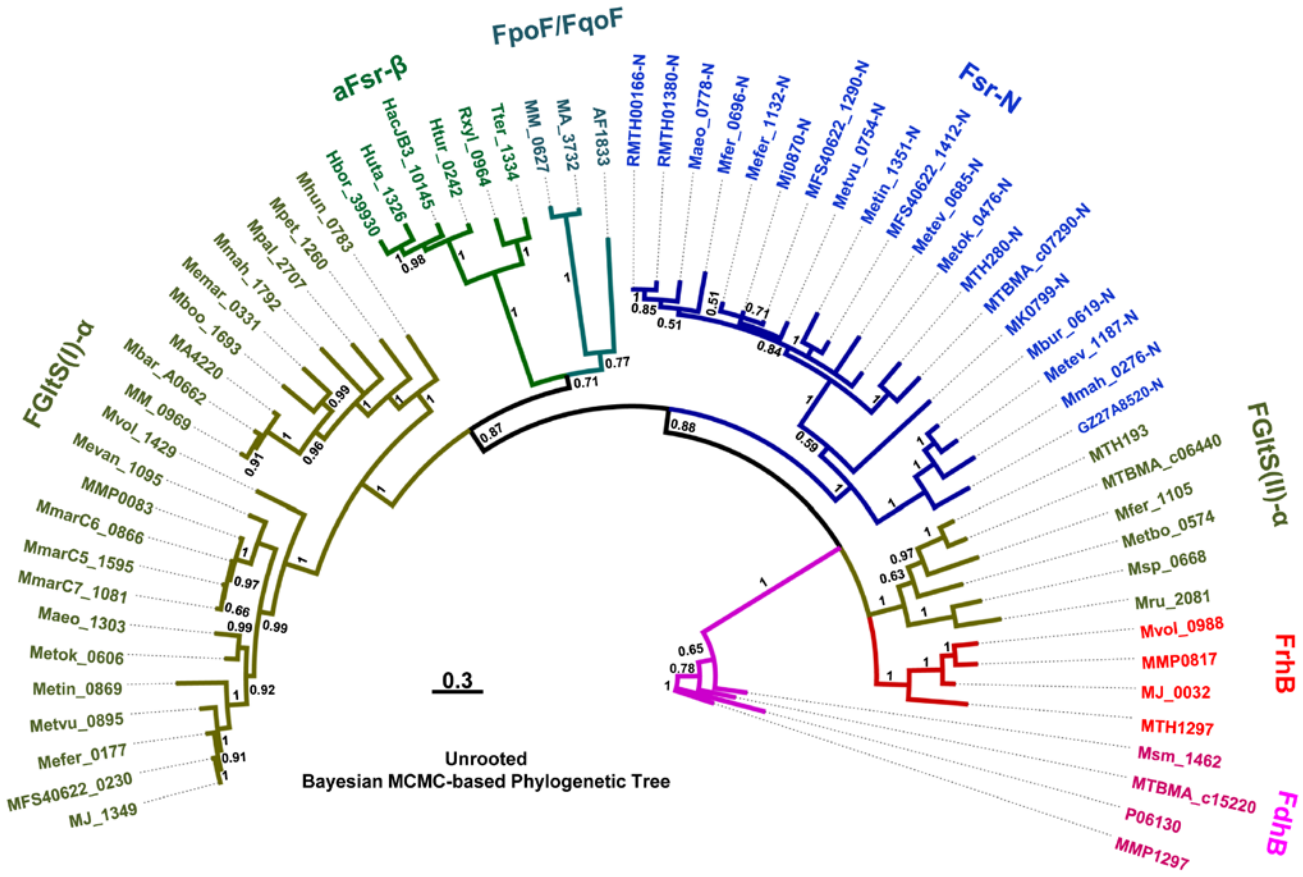

Figure 3.9 Phylogenetic tree of Fsr-N homologs based on Bayesian Markov chain Monte Carlo (MCMC) analysis. ORF numbers and all abbreviations used are described in the legend of Fig. 3.8. For each branch a posterior probability value (0-1) is shown. Scale bar, number of amino acid substitutions per site.

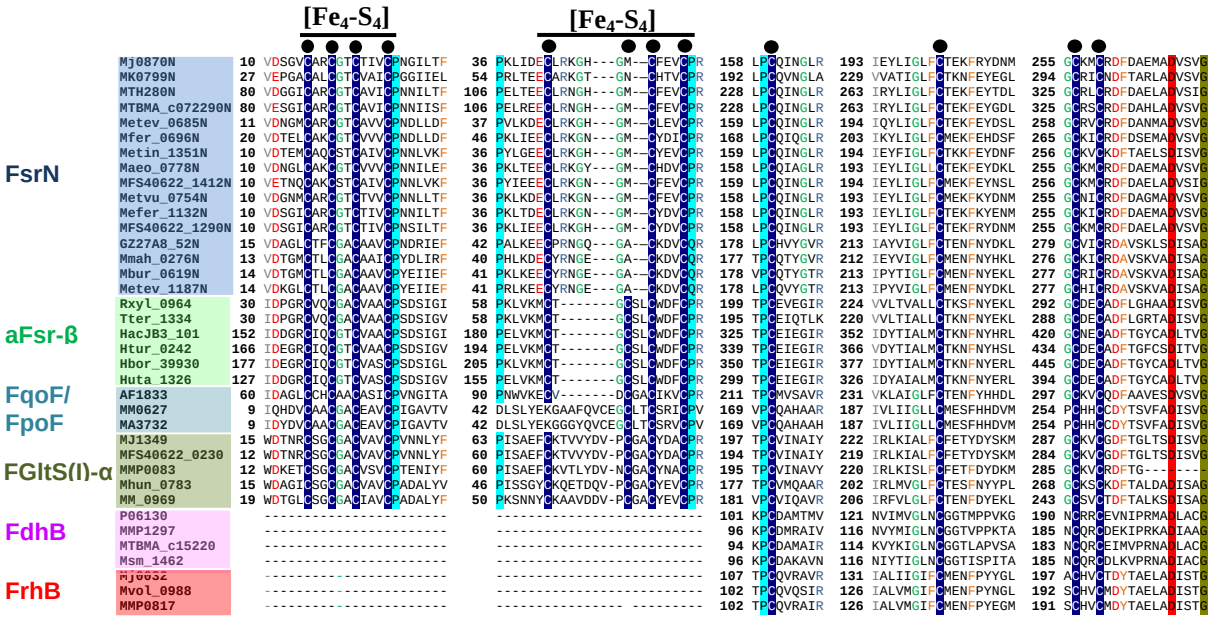

Figure 3.10 Primary structure comparison of homologs of *M. jannaschii* Fsr-N.
aFsr-β, FqoF, FpoF and FGltS(I)-α are Fsr-N homologs. FGltS(II)-α, FrhB and FdhB are shown for comparison. The details of the abbreviation for ORF numbers are in the legend of Figs. 3.5 and 3.8. The color shadings and colored letters represent conserved and partially conserved amino acid residues, respectively: dark blue, cysteine; turquoise, prolin; red, aspartate and glutamate; green, glycine; orange, phenylalanine or tyrosine; grey, valine or isoleucine. Black bullets, conserved cysteine residues for [Fe_4-S_4] sites; over-line, sequence motif involved in assembling [Fe_4-S_4] cluster. The color shadings in the left panel representing various proteins correspond to the same in Figs. 3.8 and 3.9.

3.3.7 Evolution of sulfite reductases: methanogens being the likely host for this development

The Dsr-LP ORFs were widely present in the methanogens (Fig. 3.2) and they represented from the very minimum to the most complex forms of Dsr proteins encountered in extant archaea and bacteria (Figs. 3.1, 3.3, and 3.4). Every functional unit of sulfite reductases, especially the Dsr, is represented by the Dsr-LPs (Figs. 3.3 and 3.4). Therefore, sulfite reductase type proteins have a long evolutionary history in methanogens and most likely one such ORF was present in their common ancestor or was acquired by this organism at a very early stage of evolution. This is consistent with the observation that the crenarchaeal DsrA and DsrB from *Pyrobaculum* species occupy the most basal position in a phylogenetic tree for archaeal and bacterial Dsr subunits (50). The group I Dsr-LPs with the simplest attributes (coupled siroheme-iron sulfur cluster and

sulfite binding Arg/Lys residues) could be considered as the recognizable earliest forms of sulfite reductases (Figs. 3.1, 3.3, and 3.4). Then through association and subsequent fusion with a ferredoxin (Fe_4-S_4) unit these forms gave rise to group II Dsr-LPs (Fig. 3.3), which remains unidentified (Figs. 3.1 and 3.3). Insertion of an additional ferredoxin (Fe_4-S_4) unit into group II Dsr-LPs resulted into III Dsr-LPs. Similarly, an expansion of the primary structure converted group II Dsr-LPs to DsrA/B (Figs. 3.1 and 3.3).

In a recent effort to locate the most ancestral sulfite reductase in the extant organisms the amino acid sequences at and around the coupled siroheme-iron sulfur clusters of several of these proteins were phylogenetiocally analyzed (50). In this analysis the small size monomeric assimilatory sulfite reductase of *Desulfovibrio vulgaris* (Dv-alSir) that carries a coupled [Fe_4-S_4]-siroheme center but lacks the peripheral [Fe_4-S_4] center was found to be the most deeply rooted in the aSir clade (50) and accordingly this simpler protein was considered as the recognizable earliest ancestor for all types of sulfite reductases. The anaerobic sulfite reductase (AsrC) which is expressed from the *asrABC* operon in *Salmonella typhimurium* and several *Clostridium* species was placed in a distinct clade. In our analysis we took a different approach. Since coupled [Fe_4-S_4]-siroheme center of sulfite reductases has not been altered significantly through about 3.5 billion years (19, 50), we considered full amino acid sequences of sulfite reductase proteins to obtain the clues to the evolutionary processes that have shaped the sulfite reductases of the methanogens and other organisms. In this analysis, alSir (DVU_1597 or Dv-alSir of *Desulfovibrio vulgaris*), AsrC (CPE1438 of *Clostridium perfringens*), Dsr-LP and Fsr-C were found to have Dsr type structural features (Figs. 3.3 and 3.4). Dv-alSir was similar to group I Dsr-LP, our proposed ancestral form, and AsrC was a group III Dsr-LP, possessing the more complex features. These observations are consistent with the previous report (50). In the bacterial domain Dsr-LP homologs were found only in anaerobic or facultative anaerobes belonging to the phyla of Firmicutes (such as *Clostridium*, *Desulfitobacterium*, *Desulfotomaculum*, and *Veillonella*) and Proteobacteria (such as *Geobacter*, *Desulfovibrio,* and *Syntrophus*). Most of the bacterial Dsr-LP homologs were AsrC or group III Dsr-LP type. All these bacteria are likely to associate with the methanogens in nature. In this context we note that within the archaeal domain Dsr-LPs are almost fully restricted to the methanogens (Phylum, Euryarchaeota) where they are widespread. Therefore, it is likely that the simplest form of

sulfite reductase was generated in a methanogen or was acquired by these archaea from anaerobic bacteria early in their evolution. The strict and apparently long association of Dsr-LPs with methanogens alludes to certain functions that are ecologically important to these organisms. *M. maripaludis* S2 does not carry an Fsr but possesses a group IIId Dsr-LP (ORF MMP0078) and it is sensitive to sulfite. When *M. jannaschii* Fsr is expressed in *M. maripaludis*, the recombinant tolerates sulfite and even uses this oxyanion as sulfur source (17). Hence, *M. maripaludis* not only folds Fsr properly but also assembles siroheme in the recombinant protein. Hence, it synthesizes a siroheme of the type that is recognized by the Dsr-LP domain of Fsr. It is likely that in wild-type *M. maripaludis* this cofactor is assembled in MMP0078, the only potential siroheme protein in this organism. By inference the same property could be expected for all Dsr-LP carrying methanogens (Fig. 3.2). Therefore, not only the sulfite reductase, but also siroheme, the most crucial part of this enzyme, is an ancient component of the methanogens. Most methanogens carry the homologs of two key enzymes for the reduction of sulfate to sulfite, sulfate adenylyltransferase (Sat) and adenosine 5'-phosphosulfate (APS) reductase (Apr) (15). The Apr homolog of *M. jannaschii* (MJ_0973) exhibits the relevant activity, albeit with a low V_{max} and k_{cat} values (51). Therefore, it is likely that the intertwined history of methanogens with sulfite reductase extends up to the full-scale sulfate reduction pathway. This hypothesis is consistent with a recent proposal about the first incident of sulfate reduction on Earth (19). Analysis of isotope records of sedimentary sulfides had identified a major microbial sulfate reduction event starting by 2.7 Gyr ago (52). However, 3.47-Gyr old barites from North Pole, Australia, have been found to carry biologically produced sulfide which has been taken as an indication of a more ancient but minor sulfate reduction process (19). From our results it could be hypothesized that this signature for ancient biogenic sulfide originated from minor sulfate reduction activities of the above-mentioned machineries of methanogens. Sulfite reduction had to develop before sulfate reduction for avoiding sulfite toxicity. Therefore, it is also possible that the ancient sulfide originated from reversible conversion of sulfite to sulfide catalyzed by an ancient Dsr-LP that led to an isotope signature (via fractionation (53)). If one or both of these hypotheses were proven to be true, the relationships of two of the most ancient respiratory metabolisms of earth, hydrogenotrophic methanogenesis and sulfate reduction, would be at least 3.47 Gyr old. Dsr-LPs have the essential features of Dsr and yet even their most complete

versions do not enable methanogens to reduce sulfite (17). A Dsr-LP type protein has been purified from *Methanosarcina barkeri* and it shows weak sulfite reductase activity with reduced methylviologen, an artificial electron carrier, as reductant (54). However, the physiological relevance of this observation is unclear as *M. barkeri* is sensitive to sulfite and cannot use this oxyanion as sulfur source (17). Since the synthesis of coenzyme M requires sulfite (55), it is possible that Dsr-LP is used to meet this need via the oxidation of sulfide. An example of the oxidation of sulfide to sulfite via a membrane-bound siroheme sulfite reductase complex has been found in *Allochromatium vinosum*, a phototrophic sulfur bacterium (56-62). However, certain methanogens do not carry either Dsr-LP or Fsr (Fig. 3.2) and this fact questions the role of Dsr-LP in the synthesis of coenzyme M which is essential for methanogenesis, the only source of energy for methanogens (63). It is conceivable that Dsr-LPs carry out certain heme-driven electron transport functions that relate someway to sulfite reduction.

3.4 METHODS

Multiple sequence alignment was performed using MUSCLE at the European Bioinformatics Institute web server (64). Regions with poor alignments were removed using Gblocks0.91b (65). Amino acid sequence for homologs of Mj-Fsr (MJ_0870), Dsr-LP and N-terminal half of Fsr (Fsr-N) were collected via Blastp and Psi-Blast searches into the non-redundant protein database of the National Center for Biotechnology Information (NCBI); MJ_0870 (amino acid residue 1–620 amino acids), C-terminal half of Mj-Fsr (amino acid residue 325–650), and N-terminal half of Mj-Fsr (amino acid residue 1–311), respectively were used as queries. Searches for the homologs of Dsr-LP in bacteria were performed by the use of Psi-Blast with MMP0078 and MK0801 as queries for group I and group III Dsr-LP, respectively.

Phylogenetic trees for Dsr-LPs, Fsr-N homologs, and 16S rRNAs of methanogens were constructed by Maximum Likelihood method using Phylip 3.69 (66) employing Proml and Dnaml with default parameters, respectively. The 16S ribosomal RNA of *Desulfurococcus fermentans*, a crenarchaeon (67), was used as an outgroup for building the 16S rRNA tree. Bootstrap values were estimated by Seqboot with 1000 replicates. Consensus trees were generated by Consense. Figtree v1.3.1, downloaded from http://tree.bio.ed.uk/software/Figtree, was used to view the phylogenetic trees.

For additional phylogenetic analysis, we employed Bayesian Markov chain Monte Carlo (MCMC) method that was implemented with MrBayes 3.2 (68). In brief, the WAG model, the best-fitting amino acid model priors with the highest posterior probability (1.0) was chosen for the amino acid replacement model in our analysis. Searching for the best amino acid model was performed by conducting preliminary runs on MrBayes 3.2 using the option of mixed amino acid model priors. Dsr-LP and Fsr-N sequence datasets were modeled with an independent gamma distribution of substitution rates and were simulated for 2,000,000 and 3,500,000 generations resulting in the "average standard deviation of split frequencies" (ASDSF) of 0.0055 and 0.0085, respectively. ASDSF was used for convergence assessment. A consensus tree was generated from two independent runs using a recommended "burn-in" value of 25%.

3.5 REFERENCES

1. Canfield DE, Habicht KS, & Thamdrup B (2000) The Archean sulfur cycle and the early history of atmospheric oxygen. *Science* 288(5466):658-661.
2. Leigh JA (2002) Evolution of energy metabolism. *Biodiversity of microbial life: foundation of earth biosphere*, eds Staley JT & Reysenbach AL (John Wiley & Sons, New York), pp 103-120.
3. Stahl DA, Fishbain S, Klein M, Baker BJ, & Wagner M (2002) Origins and diversification of sulfate-respiring microorganisms. *Antonie Van Leeuwenhoek* 81(1-4):189-195.
4. Teske A, Dhillon A, & Sogin ML (2003) Genomic markers of ancient anaerobic microbial pathways: sulfate reduction, methanogenesis, and methane oxidation. *Biol Bull* 204(2):186-191.
5. Wedzicha BL (1992) Chemistry of sulphiting agents in food. *Food additives and contaminants* 9(5):449-459.
6. Klein M, *et al.* (2001) Multiple lateral transfers of dissimilatory sulfite reductase genes between major lineages of sulfate-reducing prokaryotes. *J Bacteriol* 183(20):6028-6035.
7. Balderston WL & Payne WJ (1976) Inhibition of methanogenesis in salt marsh sediments and whole-cell suspensions of methanogenic bacteria by nitrogen oxides. *Applied and environmental microbiology* 32(2):264-269.
8. Kah LC, Lyons TW, & Frank TD (2004) Low marine sulphate and protracted oxygenation of the Proterozoic biosphere. *Nature* 431(7010):834-838.
9. Poulton SW, Fralick PW, & Canfield DE (2004) The transition to a sulphidic ocean approximately 1.84 billion years ago. *Nature* 431(7005):173-177.
10. Shen Y, Knoll AH, & Walter MR (2003) Evidence for low sulphate and anoxia in a mid-Proterozoic marine basin. *Nature* 423(6940):632-635.
11. Jannasch HW (1989) Chemosynthetically sustained ecosystems in the deep sea. *Autotrophic bacteria.*, eds Schlegel HG & Bowien B (Springer Verlag, N. Y.), pp 147-166.
12. Jones WJ, Leigh JA, Mayer F, Woese CR, & Wolfe RS (1983) *Methanococcus jannaschii* sp. nov., an extreme thermophilic methanogen from a submarine hydrothermal vent. *Archives of Microbiology* 136:254-261.
13. McCollom TM & Shock EL (1997) Geochemical constraints on chemolithoautotrophic metabolism by microorganisms in seafloor hydrothermal systems. *Geochim Cosmochim Acta* 61(20):4375-4391.

14. Daniels L, Belay N, & Rajagopal BS (1986) Assimilatory reduction of sulfate and sulfite by methanogenic bacteria. *Applied and environmental microbiology* 51(4):703-709.
15. Johnson EF & Mukhopadhyay B (2005) A new type of sulfite reductase, a novel coenzyme F_{420}-dependent enzyme, from the methanarchaeon *Methanocaldococcus jannaschii*. *The Journal of biological chemistry* 280(46):38776-38786.
16. Rothe O & Thomm M (2000) A simplified method for the cultivation of extreme anaerobic Archaea based on the use of sodium sulfite as reducing agent. *Extremophiles : life under extreme conditions* 4(4):247-252.
17. Johnson EF & Mukhopadhyay B (2008) Coenzyme F_{420}-dependent sulfite reductase-enabled sulfite detoxification and use of sulfite as a sole sulfur source by *Methanococcus maripaludis*. *Applied and environmental microbiology* 74(11):3591-3595.
18. DiMarco AA, Bobik TA, & Wolfe RS (1990) Unusual coenzymes of methanogenesis. *Annu Rev Biochem* 59:355-394.
19. Shen Y, Buick R, & Canfield DE (2001) Isotopic evidence for microbial sulphate reduction in the early Archaean era. *Nature* 410(6824):77-81.
20. Crane BR & Getzoff ED (1996) The relationship between structure and function for the sulfite reductases. *Current Opinion in Structural Biology* 6(6):744-756.
21. Parey K, Warkentin E, Kroneck PM, & Ermler U (2010) Reaction cycle of the dissimilatory sulfite reductase from *Archaeoglobus fulgidus*. *Biochemistry* 49(41):8912-8921.
22. Schiffer A, *et al.* (2008) Structure of the dissimilatory sulfite reductase from the hyperthermophilic archaeon *Archaeoglobus fulgidus*. *J Mol Biol* 379(5):1063-1074.
23. Oliveira TF, *et al.* (2008) Purification, crystallization and preliminary crystallographic analysis of a dissimilatory DsrAB sulfite reductase in complex with DsrC. *J Struct Biol* 164(2):236-239.
24. Deppenmeier U (2004) The membrane-bound electron transport system of *Methanosarcina* species. *J Bioenerg Biomembr* 36(1):55-64.
25. Zeikus JG & Wolfe RS (1972) Methanobacterium thermoautotrophicus sp. n., an anaerobic, autotrophic, extreme thermophile. *Journal of bacteriology* 109(2):707-715.
26. Stetter KO, *et al.* (1981) *Methanothermus fervidus*, sp. nov., a Novel extremely thermophilic methanogen isolated from an Icelandic Hot Spring. *Zentralbl. Mikrobiol. Parasitenkd. Infektionskr. Hyg. Abt. 1 Orig.* C2:166-178.
27. Ciulla R, *et al.* (1994) Halotolerance of Methanobacterium thermoautotrophicum delta H and Marburg. *J Bacteriol* 176(11):3177-3187.
28. Huber H, Thomm M, König H, Thies G, & Stetter KO (1982) *Methanococcus thermolithotrophicus*, a novel thermophilic lithotrophic methanogen. *Archives of Microbiology* 132:47-50.
29. Zhilina TN & Zavarzin GA (1987) *Methanohalobium evestigatus*, n. gen., n. sp. the extremely halophilic methanogenic archaebacterium. *Doklady Akademii Nauk SSSR* 293:464–468.
30. Mehta MP & Baross JA (2006) Nitrogen fixation at 92 degrees C by a hydrothermal vent archaeon. *Science* 314(5806):1783-1786.
31. Belay N, Jung K-Y, Rajagopal BS, Kremer JD, & Daniels L (1990) Nitrate as a Sole Nitrogen Source for *Methanococcus thermolithotrophicus* and Its Effect on Growth of Several Methanogenic Bacteria. *Current Microbiology* 21:193-198.
32. Zhilina TN, and Zavarzin, G.A. (1987) *Methanohalobium evestigatus*, n. gen., n. sp. The extremely halophilic methanogenic Archaebacterium. *Dokl. Akad. Nauk SSSR* 293:464-468.
33. Kendall MM, *et al.* (2006) *Methanococcus aeolicus* sp. nov., a mesophilic, methanogenic archaeon from shallow and deep marine sediments. *International journal of systematic and evolutionary microbiology* 56(Pt 7):1525-1529.
34. Franzmann PD, Springer N, Ludwig W, Conway de Macario E, & Rohde M (1992) A methanogenic archaeon from Ace Lake, Antarctica: *Methanococcoides burtonii* sp. nov *Systematic and Applies Microbiology* 15:573–581.

35. Jannasch HW, Wirsen CO, Molyneaux SJ, & Langworthy TA (1992) Comparative Physiological Studies on Hyperthermophilic Archaea Isolated from Deep-Sea Hot Vents with Emphasis on *Pyrococcus* Strain GB-D. *Appl Environ Microbiol* 58(11):3472-3481.
36. Orphan VJ, *et al.* (2001) Comparative analysis of methane-oxidizing archaea and sulfate-reducing bacteria in anoxic marine sediments. *Appl Environ Microbiol* 67(4):1922-1934.
37. Crane BR & Getzoff ED (1996) The relationship between structure and function for the sulfite reductases. *Curr Opin Struct Biol* 6(6):744-756.
38. Klenk HP, *et al.* (1997) The complete genome sequence of the hyperthermophilic, sulphate-reducing archaeon *Archaeoglobus fulgidus*. *Nature* 390(6658):364-370.
39. Heidelberg JF, *et al.* (2004) The genome sequence of the anaerobic, sulfate-reducing bacterium *Desulfovibrio vulgaris* Hildenborough. *Nat Biotech* 22(5):554-559.
40. Tan J, Helms LR, Swenson RP, & Cowan JA (1991) Primary structure of the assimilatory-type sulfite reductase from Desulfovibrio vulgaris (Hildenborough): cloning and nucleotide sequence of the reductase gene. *Biochemistry* 30(41):9900-9907.
41. Brochier C, Forterre P, & Gribaldo S (2004) Archaeal phylogeny based on proteins of the transcription and translation machineries: tackling the *Methanopyrus kandleri* paradox. *Genome Biology* 5(R17).
42. Brochier C, Forterre P, & Gribaldo S (2005) An emerging phylogenetic core of Archaea: phylogenies of transcription and translation machineries converge following addition of new genome sequences. *BMC Evol Biol* 5:36.
43. Branciamore S, Gallori E, & Di Giulio M (2008) The basal phylogenetic position of *Nanoarchaeum equitans* (*Nanoarchaeota*). *Frontiers in bioscience : a journal and virtual library* 13:6886-6892.
44. Slesarev AI, *et al.* (2002) The complete genome of hyperthermophile *Methanopyrus kandleri* AV19 and monophyly of archaeal methanogens. *Proceedings of the National Academy of Sciences* 99(7):4644-4649.
45. Baumer S, *et al.* (2000) The $F_{420}H_2$ dehydrogenase from *Methanosarcina mazei* is a Redox-driven proton pump closely related to NADH dehydrogenases. *J Biol Chem* 275(24):17968-17973.
46. van den Heuvel RH, Curti B, Vanoni MA, & Mattevi A (2004) Glutamate synthase: a fascinating pathway from L-glutamine to L-glutamate. *Cell Mol Life Sci* 61(6):669-681.
47. Kaster AK, *et al.* (2011) More Than 200 Genes Required for Methane Formation from H_2 and CO_2 and Energy Conservation Are Present in *Methanothermobacter marburgensis* and *Methanothermobacter thermautotrophicus*. *Archaea* 2011:973848.
48. Jacobson FS, Daniels L, Fox JA, Walsh CT, & Orme-Johnson WH (1982) Purification and properties of an 8-hydroxy-5-deazaflavin-reducing hydrogenase from Methanobacterium thermoautotrophicum. *Journal of Biological Chemistry* 257(7):3385-3388.
49. Shuber AP, *et al.* (1986) Cloning, expression, and nucleotide sequence of the formate dehydrogenase genes from *Methanobacterium formicicum*. *J Biol Chem* 261(28):12942-12947.
50. Dhillon A, Goswami S, Riley M, Teske A, & Sogin M (2005) Domain evolution and functional diversification of sulfite reductases. *Astrobiology* 5(1):18-29.
51. Lee J-S, *et al.* (2011) Discovery of a novel adenosine 5′-phosphosulfate (APS) reductase from the methanarcheon *Methanocaldococcus jannaschii*. *Process Biochemistry* 46:154-161.
52. Goodwin AM, Monster J, & Thode HG (1976) Carbon and sulfur isotope abundances in Archean iron-formations and early Precambrian life. *Economic Geology* 71:870-891.
53. Brunner B & Bernasconi SM (2005) A revised isotope fractionation model for dissimilatory sulfate reduction in sulfate reducing bacteria. *Geochimica et Cosmochimica Acta* 69(20):4759-4771.
54. Moura JJ, *et al.* (1982) Isolation of P590 from *Methanosarcina barkeri*: evidence for the presence of sulfite reductase activity. *Biochem Biophys Res Commun* 108(3):1002-1009.

55. Graham DE, Xu H, & White RH (2002) Identification of coenzyme M biosynthetic phosphosulfolactate synthase: a new family of sulfonate-biosynthesizing enzymes. *The Journal of biological chemistry* 277(16):13421-13429.
56. Grimm F, Franz B, & Dahl C (2011) Regulation of dissimilatory sulfur oxidation in the purple sulfur bacterium *Allochromatium vinosum*. *Front Microbiol* 2:51.
57. Grimm F, Cort JR, & Dahl C (2010) DsrR, a novel IscA-like protein lacking iron- and Fe-S-binding functions, involved in the regulation of sulfur oxidation in *Allochromatium vinosum*. *J Bacteriol* 192(6):1652-1661.
58. Sander J, Engels-Schwarzlose S, & Dahl C (2006) Importance of the DsrMKJOP complex for sulfur oxidation in *Allochromatium vinosum* and phylogenetic analysis of related complexes in other prokaryotes. *Arch Microbiol* 186(5):357-366.
59. Cort JR, *et al.* (2008) *Allochromatium vinosum* DsrC: solution-state NMR structure, redox properties, and interaction with DsrEFH, a protein essential for purple sulfur bacterial sulfur oxidation. *J Mol Biol* 382(3):692-707.
60. Grimm F, Dobler N, & Dahl C (2012) Regulation of *dsr* genes encoding proteins responsible for the oxidation of stored sulfur in *Allochromatium vinosum*. *Microbiology* 156(Pt 3):764-773.
61. Dahl C, *et al.* (2005) Novel genes of the dsr gene cluster and evidence for close interaction of Dsr proteins during sulfur oxidation in the phototrophic sulfur bacterium *Allochromatium vinosum*. *J Bacteriol* 187(4):1392-1404.
62. Lubbe YJ, Youn HS, Timkovich R, & Dahl C (2006) Siro(haem)amide in *Allochromatium vinosum* and relevance of DsrL and DsrN, a homolog of cobyrinic acid a,c-diamide synthase, for sulphur oxidation. *FEMS Microbiol Lett* 261(2):194-202.
63. Wolfe RS (1992) Biochemistry of methanogenesis. *Biochemical Society symposium* 58:41-49.
64. Edgar RC (2004) MUSCLE: multiple sequence alignment with high accuracy and high throughput. *Nucleic Acids Res* 32(5):1792-1797.
65. Castresana J (2000) Selection of conserved blocks from multiple alignments for their use in phylogenetic analysis. *Mol Biol Evol* 17(4):540-552.
66. Felsenstein J (2005) PHYLIP (Phylogeny Inference Package) version 3.67-1. *Department of Genome Sciences. University of Washington, Distributed by the author.*
67. Perevalova AA, *et al.* (2005) *Desulfurococcus fermentans* sp. nov., a novel hyperthermophilic archaeon from a Kamchatka hot spring, and emended description of the genus *Desulfurococcus*. *International journal of systematic and evolutionary microbiology* 55(Pt 3):995-999.
68. Ronquist F, *et al.* (2012) MrBayes 3.2: Efficient Bayesian Phylogenetic Inference and Model Choice across a Large Model Space. *Syst Biol*.

4 Thioredoxin-linked redox regulation in an evolutionarily deeply-rooted hyperthermophilic methane-producing archaeon, *Methanocaldococcus jannaschii*

4.1 ABSTRACT

Thioredoxin (Trx), a small redox protein, controls a spectrum of processes in eukaryotes and bacteria by changing the thiol redox status (SH/S-S) of selected proteins. Trx is also present in archaea, but its role in this diverse group is unknown. Consequently, we have conducted a study on a methanogen—an anaerobic archaeon that reduces CO_2 to methane with H_2 during respiration. Bioinformatic analyses suggest that Trx is nearly ubiquitous in methanogens. Moreover, its phylogenetic distribution parallels the evolutionary history of this group. Organisms primarily using H_2 to reduce CO_2 to methane carry two Trx homologs on average, whereas their more evolved, nutritionally versatile counterparts carry 4-8 Trx homologs. Due to the simplicity of its Trx system, we elected to study *Methanocaldococcus jannaschii*, a deeply-rooted hyperthermophilic methanogen inhabiting deep-sea hydrothermal vents. *M. jannaschii* carries two Trx homologs: Trx1 is a canonical Trx that reduces insulin and accepts electrons from *E. coli* NADP-thioredoxin reductase. Trx2 is atypical. Proteomic analyses identified 149 potential Trx1 targets in air-oxidized *M. jannaschii* extracts (74 detected in at least two independent experiments). The identity of these proteins suggests that Trx1 regulates a broad range of cellular processes including methanogenesis, the hallmark metabolism of methanogen, biosynthesis, transcription, translation and oxidative response. In enzyme assays, Trx1 activated F_{420}-dependent methylenetetrahydromethanopterin dehydrogenase, a methanogenesis enzyme, and sulfite detoxifying F_{420}-dependent sulfite reductase, validating proteomics observations. Our results suggest that Trx could play a role in the global carbon cycle.

4.2 INTRODUCTION

Thioredoxins (Trxs) are small (~12 kDa) redox proteins typically with a characteristic Cys-Gly-Pro-Cys motif that reduce specific disulfide bonds in diverse proteins (1). This reduction alters the biochemical properties of the proteins targeted, for example, by increasing their activity or solubility (1). Trxs are found in the three domains of life–bacteria, eukarya and archaea (2). In eukarya and bacteria, the regulatory role of Trx spans the major aspects of metabolism, including energy generation, biosynthesis and information processing such as replication, transcription, translation and stress response (3). In these organisms, Trx also functions as an electron donor for enzymes, notably ribonucleotide reductase, phosphoadenosinephosphosulfate (PAPS) reductase, methionine sulfoxide reductase, and peroxiredoxin (4-7). While our knowledge is extensive for Trxs from the eukarya and bacteria, our understanding of the archaeal counterpart is limited to its biochemical and structural properties (8-18). The function of Trx in this diverse domain of life is unknown.

To help fill this gap, we have investigated the role of Trx in a representative group of the archaea called methanogens—strictly anaerobic microorganisms that produce methane—a prominent greenhouse gas used globally as a fuel. More specifically, we have studied *Methanocaldococcus jannaschii*—a hyperthermophilic methanogen isolated from deep-sea hydrothermal vents (18). The environmental conditions prevailing in the habitat of *M. jannaschii* mimics some of those of early Earth. This phylogenetically deeply-rooted methanogen produces methane exclusively from H_2 and CO_2—a process believed to represent one of the most ancient types of respiration on Earth (19). In view of these features, *M. jannaschii* presents an opportunity to explore the role of Trx in an important largely unstudied group of organisms and at the same time gain insight into the evolutionary history of redox regulation. Our results suggest that Trx is fundamental to the regulation of biochemical processes in this group of anaerobes in response to changes in environmental redox potential. Its role both mimics and complements that established for aerobic forms of life.

4.3 RESULTS

4.3.1 *Thioredoxin Homologs of Methanogenic Archaea*

Iterative BLAST searches (20) using *E. coli* and *M. jannaschii* Trxs as queries showed that genes encoding Trx homologs exist in almost all methanogen genomes represented in the NCBI database (Fig. 4.1 and Table 4.1). *Methanopyrus kandleri* AV19, a hyperthermophilic methanogen (optimum growth temperature, 98°C) isolated from sediment sample from a hydrothermal vent in the Gulf of California (21, 22) was the only exception, lacking a Trx homolog.

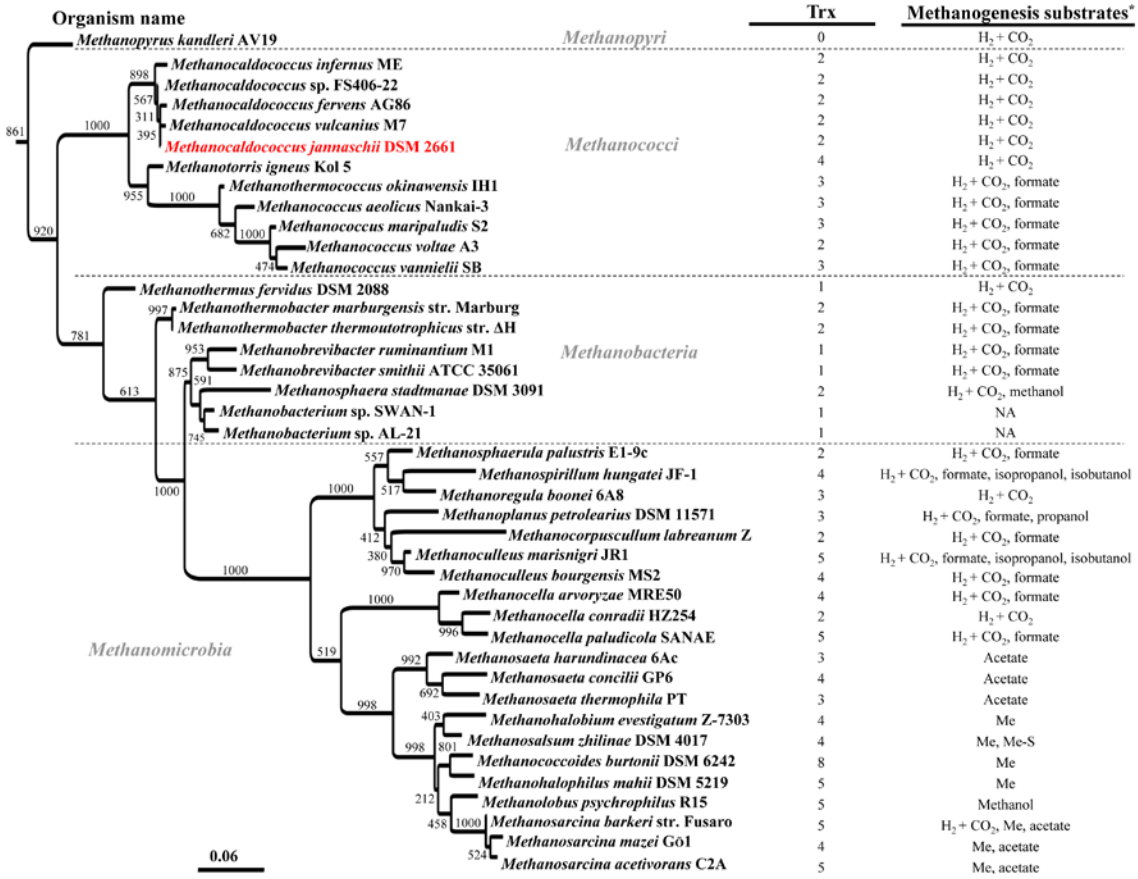

Figure 4.1. Distribution of thioredoxin homologs in methanogens. Trx homologs were identified via Psi-BLAST search in the methanogen genomes available in the NCBI database is shown. The details of the methods have been presented in the MATERIALS AND METHODS. The observed distribution has been presented using a 16S-ribosomal RNA gene-based maximum likelihood phylogenetic tree as the platform. Numbering presented at the branches of the tree are confidence values that were estimated from 1000 bootstrap replicates. The scale bar indicates number of base substitution per site. The 16S-rRNA gene of *Desulfurococcus fermentans*, not shown, was used as an outgroup. *Abbreviations for methanogenesis substrates; Me, methylated C1 compounds such as methanol, methyl-, dimethyl-, trimethylamine, methanol + H_2; Me-S, dimethylsulfide, and methanethiol.

Methanococci and *Methanobacteria* carried on the average of 2 Trx homologs, with their numbers ranging 1-4. On the other hand, methanogens belonging to the class of *Methanomicrobia* possessed 2-8 Trx homologs with an average number of four. For example, the genomes of *Methanosarcina barkeri* and *Methanocella paludicola* encode five Trx homologs. An exception in this class is *Methanocorpuscullum labreanum* which possessed only 2 Trx homologs.

4.3.2 *Trxs of M. jannaschii*

M. jannaschii carries two Trx homologs, Mj_0307 and Mj_0581 (17, 23), here called Trx1 and Trx2, respectively. Interestingly, the amino acid sequence of Trx1 bears a striking resemblance to counterparts of *E. coli* (Ec-Trx) (identity 30.9%, similarity 56.8%) and *Methanothermobacter thermoautotrophicus* ΔH (MTH807) (identity 53.7% similarity 84.1%) (15) compared to the second *M. jannaschii* Trx, Trx2 (identity 24%; similarity 65%). Trx2 has been recognized as a homolog of MTH895, the second Trx in *Methanothermobacter thermoautotrophicus* ΔH (identity 42%, similarity 75%) (16).

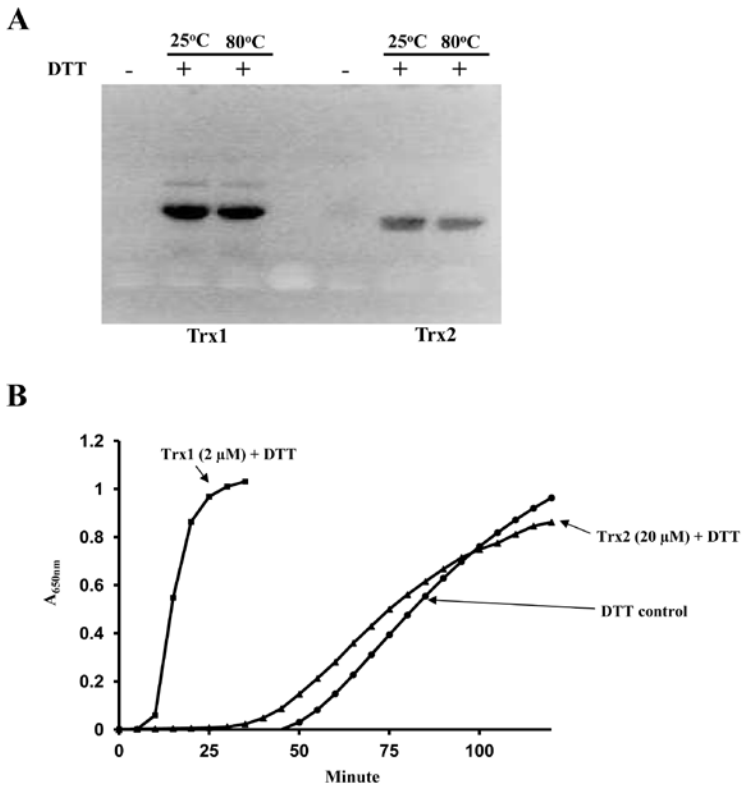

Figure 4.2. Characteristics of *Methanocaldococcus jannaschii* thioredoxins, Trx1 and Trx2. A. Reduction of Trx1 (Mj_0307) and Trx2 (Mj_0581) by dithiothreitol (DTT). These proteins were treated with 2 mM DTT either at 25°C or 80°C for 30 min and then their free sulfhydryl groups were alkylated with monobromobimane (mBBr). The next step was SDS-PAGE analysis where mBBr-labeled Trx bands were visualized under UV 365 nm. **B.** Reduction of insulin disulfides by Trx1 and Trx2. The rise in turbidity due to Trx-induced precipitation of insulin was followed at 650 nm. Other details are described in the MATERIALS AND METHODS. DTT was the primary electron donor.

Table 4.1 Thioredoxin homologs in methanogenic archaea

Order Species	Opt. Temp (^{o}C)	Natural habitat	Substrate for methanogenesis	Accession numbers of thioredoxin homologs (This study)	Refs
Methanopyrus					
Methanopyrus kandleri AV19	98	Hydrothermal vent	H_2 + CO_2	None	(21, 24)
Methanococcales					
Methanocaldococcus infernus ME	85	Hydrothermal vent	H_2 + CO_2	YP_003616341.1; YP_003616835.1	(25, 26)
Methanocaldococcus sp. FS406-22	90	Hydrothermal vent	H_2 + CO_2	YP_003458495.1; YP_003458967.1	(26, 27)
Methanocaldococcus fervens AG86	80	Hydrothermal vent	H_2 + CO_2	YP_003128641.1; YP_003128672.1	(26, 28)
Methanocaldococcus vulcanius M7	80	Hydrothermal vent	H_2 + CO_2	YP_003247556.1; YP_003247403.1	(26, 28)
Methanocaldococcus jannaschii DSM 2661	85	Hydrothermal vent	H_2 + CO_2, formate (some species)	NP_247280.1; NP_247560.1	(29, 30)
Methanotorris igneus Kol 5	88	Shallow submarine vent	H_2 + CO_2	YP_004484305.1; YP_004483931.1; YP_004484086.1; YP_004484049.1	(26, 31)
Methanothermococcus okinawensis IH1	60-65	Hydrothermal vent	H_2 + CO_2, formate	YP_004576182.1; YP_004577272.1; YP_004577341.1	(32, 33)
Methanococcus aeolicus Nankai-3	NR	Marine sediment	H_2 + CO_2, formate	YP_001324655.1; YP_001324701.1; YP_001324529.1	(26, 34)
Methanococcus maripaludis S2	35-39	Salt marsh sediment	H_2 + CO_2, formate	NP_988508.1; NP_987323.1; NP_988755.1	(35, 36)
Methanococcus voltae A3	35-40		H_2 + CO_2, formate	YP_003707881.1; YP_003707614.1	(26, 37, 38)
Methanococcus vannielii SB	35-40	Mud flat	H_2 + CO_2, formate	YP_001323456.1; YP_001323216.1; YP_001324188.1	(26, 39)

TABLE 4.1 (Continued)

Methanobacteriales					
Methanothermus fervidus DSM 2088	77-83	Sewage digester	H_2 + CO_2	YP_004004242.1	(40, 41)
Methanothermobacter marburgensis str. Marburg	55-70	Sewage digester	H_2 + CO_2, formate	YP_003850191.1; YP_003850106.1	(42, 43)
Methanothermobacter thermautotrophicus str. ΔH	55-70	Sewage digester	H_2 + CO_2, formate	NP_276032.1; NP_275946.1	(43, 44)
Methanobrevibacter ruminantium M1	37-39	Rumen	H_2 + CO_2, formate	YP_003424420.1	(45, 46)
Methanobrevibacter smithii ATCC 35061	37-39	Rumen	H_2 + CO_2, formate	YP_001273411.1	(47, 48)
Methanosphaera stadtmanae DSM 3091	37	Human intestine	H_2 , methanol	YP_447852.1; YP_447165.1	(49, 50)
Methanobacterium sp. SWAN-1	NA	NA	NA	YP_004519553.1	
Methanobacterium sp. AL-21	NA	NA	NA	YP_004291104.1	
Methanomicrobiales					
Methanosphaerula palustris E1-9c	28-30	Peatlands	H_2 + CO_2, formate	YP_002466095.1; YP_002467560.1	(26, 51)
Methanospirillum hungatei JF-1	35-40	Sewage sludge	H_2 + CO_2, formate, some species use isopropanol and isobutanol	YP_502331.1; YP_503912.1; YP_502981.1; YP_504576.1	(52, 53)
Methanoregula boonei 6A8	35	Acidic bog	H_2 + CO_2	YP_001403264.1; YP_001404957.1; YP_001403239.1	(26, 54)
Methanoplanus petrolearius DSM 11571	37	Offshore oil field	H_2 + CO_2, formate, propanol	YP_003894886.1; YP_003893564.1; YP_003895646.1	(55, 56)

TABLE 4.1 (Continued)

Methanocorpuscullum labreanum Z	37	Sediment of Tar Pits lake	H_2 + CO_2, formate	YP_001030253.1; YP_001029754.1	(52, 57)
Methanoculleus marisnigri JR1	40	Sediment of Black sea	H_2 + CO_2, formate, isopropanol and isobutanol	YP_001046143.1; YP_001047567.1; YP_001045935.1; YP_001045936.1; YP_001047892.1	(52, 58, 59)
Methanoculleus bourgensis MS2	37	Sewage sludge digester	H_2 + CO_2, formate	YP_006545581.1; YP_006543753.1; YP_006543653.1; YP_006543652.1	(60, 61)
Methanocella arvoryzae MRE50	45	Rice paddy soil	H_2 + CO_2, formate	YP_686211.1; YP_684546.1; YP_685724.1; YP_685723.1	(62, 63)
Methanocella conradii HZ254	55	Rice field soil	H_2 + CO_2	YP_005379709.1; YP_005380235.1	(64, 65)
Methanocella paludicola SANAE	35-37	Rice paddy soil	H_2 + CO_2, formate	YP_003355731.1; YP_003357232.1; YP_003355094.1; YP_003357453.1; YP_003356785.1	(66-68)
Methanosarcinales					
Methanosaeta harundinacea 6Ac	34-37	Anaerobic sludge reactor	Acetate	YP_005920527.1; YP_005920150.1; YP_005919905.1	(69, 70)
Methanosaeta concilii GP6	35-40	Anaerobic sludge reactor	Acetate	YP_004385149.1; YP_004383748.1; YP_004385304.1; YP_004382986.1	(71, 72)
Methanosaeta thermophila PT	55-60	Anaerobic digester	Acetate	YP_843556.1; YP_843121.1; YP_843141.1	(26, 71)
Methanohalobium evestigatum Z-7303	50	Geothermally heated sea sediment	Methanol, methyl-, dimethyl-, trimethylamine	YP_003725801.1; YP_003726675.1; YP_003726409.1; YP_003726719.1	(26, 73)
Methanosalsum zhilinae DSM 4017	45	Bosa lake	Methanol, methyl-, dimethyl-, trimethylamine, dimethylsulfide and methanethiol	YP_004615470.1; YP_004615797.1; YP_004616482.1; YP_004615169.1	(26, 74)

TABLE 4.1 (Continued)

Methanococcoides burtonii DSM 6242	23.4	Ace lake	Methanol, methyl-, dimethyl-, trimethylamine	YP_566484.1; YP_564870.1; YP_564987.1; YP_565635.1; YP_565021.1; YP_566957.1; YP_565881.1; YP_566314.1	(75, 76)
Methanohalophilus mahii DSM 5219	35	Great salt lake	Methanol, methyl-, dimethyl-, trimethylamine	YP_003542631.1; YP_003542351.1; YP_003541974.1; YP_003542119.1; YP_003543047.1	(77, 78)
Methanolobus psychrophilus R15	18	Wet sand soil	Methanol	YP_006921816.1; YP_006923638.1; YP_006922441.1; YP_006922879.1; YP_006921643.1	(79, 80)
Methanosarcina barkeri str. Fusaro	35-42	Freshwater lake	H_2 + CO_2, methanol, methyl-, dimethyl-, trimethylamine, acetate	YP_303720.1; YP_305814.1; YP_305788.1; YP_305232.1; YP_305379.1	(81, 82)
Methanosarcina mazei Go1	35-42	Sewage plant, animal rumen, human large intestine	Methanol, methyl-, dimethyl-, trimethylamine, acetate and H_2 + CO_2 (some species)	NP_632761.1; NP_632460.1; NP_634273.1; NP_634378.1	(83, 84)
Methanosarcina acetivorans C2A	35-40	Marine sediment	Methanol, methyl-, dimethyl-, trimethylamine, acetate	NP_616305.1; NP_618813.1; NP_619119.1; NP_618103.1; NP_618809.1	(85, 86)

Both Trx1 and Trx2 were expressed as soluble proteins in *E. coli* BL21 (DE3) and purified to homogeneity by Ni-NTA column chromatography. Western blots developed with antisera raised against *E.coli* Trx showed both preparations were free of *E. coli* Trx. Purified recombinant Trx1 and Trx2 were reduced by DTT (Fig. 4.2A) and both reduced insulin using DTT as reductant (Fig. 4.2B). However, the insulin reduction activity of Trx1 was 80-fold higher than that of Trx2 (Fig. 4.2B). Trx2 also showed a longer lag, 35 min vs. 10 min for Trx1. A lack of insulin reductase activity has been reported for Trx3 of *Desulfovibrio vulgaris* (87). The two Trxs also differed in the ability to be reduced by *E. coli* NADP-thioredoxin reductase (Ec-NTR) with NADPH: insulin reduction activity was observed with Trx1 but not with Trx2 (data not shown). It is noteworthy that the homolog of Trx2 in *M. thermoautotrophicus* ΔH (MTH895) accepts electrons from *E. coli* NTR (16).

4.3.3 *Identification of Trx1 targets*

The finding that *M. jannaschii* contains Trxs raised the question about the associated target proteins. A fluorescent gel/proteomics approach that proved successful with several plant investigations (88-91) was employed to identify the *M. jannaschii* proteins reduced by the more typical Trx in this organism, Trx1 (designated Trx1 targets). Briefly, in this procedure *M. jannaschii* cell extracts were oxidized by aerobic dialysis and the remaining free sulfhydryl groups of the air-exposed proteins were blocked by alkylation with iodoacetamide. The extract was then treated with Trx1 that had been reduced either by DTT or *E. coli* NTR and NADPH, anticipating that disulfide (S-S) groups generated during aerobic dialysis would be reduced by Trx. The newly formed free –SH groups were derivatized with monobromobimane (mBBr), a fluorescent probe, and the parent proteins were resolved in a 2-D gel, Fig. 4.3. The fluorescence spots observed were identified by mass spectrometry (92). The experiment with DTT as reducant was performed in triplicate and that with *E. coli* NTR + NAPDH was performed once.

From these experiments, we identified a total of 149 potential Trx1 targets (Table 4.2). Of those, 18 proteins were identified in all four experiments and 19, 37 and 75 targets were detected in three, two and one of the proteomics experiments, respectively. As shown in Tables 4.2, Trx1 reduced proteins participate in a spectrum of processes: methanogenesis, biosynthesis, information processing (transcription and translation), cell division, sulfite detoxification,

oxidative response and resistance to phages and invasion by foreign DNA. Structural proteins were also identified as Trx1 targets.

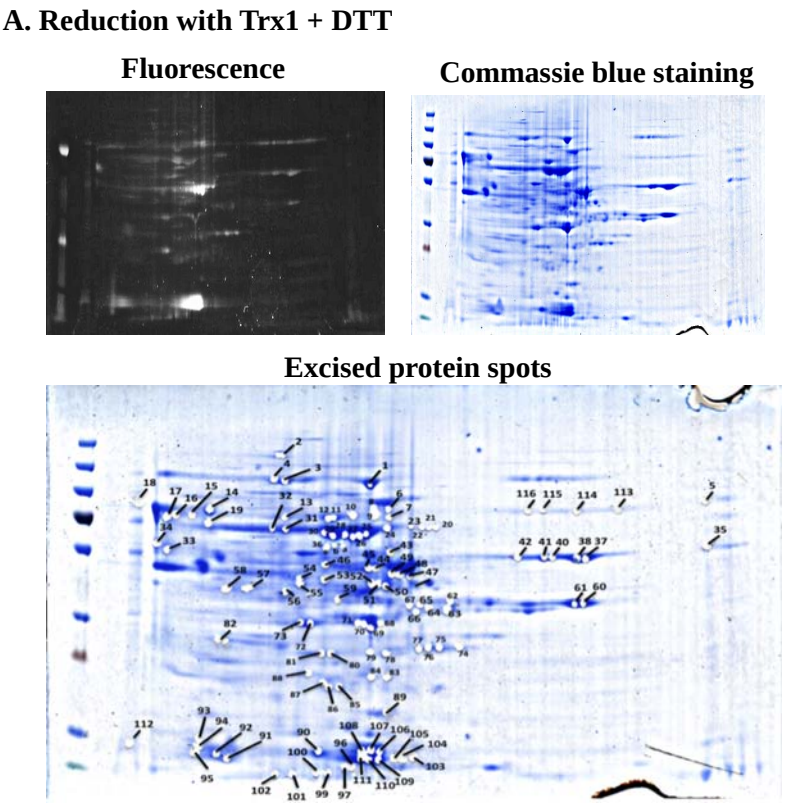

Figure 4.3. Two-dimensional gel analysis of *M. jannaschii* cell extract proteins after reduction with Trx 1. Reduction with DTT (A) and with *E. coli* NTR and NADPH (B). *M. jannaschii* cell extract proteins reduced by Trx1 with DTT or *E. coli* NTR and NADPH were labeled with fluorescent labeling mBBr through their free sulfhydryl groups and visualize under UV at 365 nm. These protein spots were excised from the gel for mass spectrometry. The identities of these proteins are presented in Table 4.2.

Table 4.2 List of potential *M. jannaschii* Trx1 targets

Function Protein	**ORF No. (No. of Cys residue)**	**Spot number in 2D-gel**			
		Reduction with Trx1 and DTT, first replicate (Fig. 4.3A)	**Reduction with Trx1 and DTT, second replicate (Gel picture not shown)**	**Reduction with Trx1 and DTT, third replicate (Gel picture not shown)**	**Reduction with Trx1 and *E. coli* NTR + NADPH (Fig. 4.3B)**
ATP synthesis					
V-type ATP synthase subunit A*	MJ_0217 (3)	10-13	26, 37	12, 13, 63	5, 6, 8, 38
V-type ATP synthase subunit B*	MJ_0216 (2)	-	29-30	27-32	11
Biosynthesis					
5-formaminoimidazole-4-carboxamide-1-β-D-ribofuranosyl 5'-monophosphate synthetase	MJ_0136 (5)	-	-	49	-
Adenylosuccinate synthetase*	MJ_0561 (6)	-	-	49-50	-
Bacteriochlorophyll synthase 43 kDa subunit ChlP	MJ_0532 (4)	-	-	41	-
Carbamoyl-phosphate synthase subunit CarB2	MJ_1381 (2)	13, 7	-	-	-
CTP synthetase	MJ_1174 (5)	-	-	26	-
GMP synthase I	MJ_1131 (5)	-	-	-	38, 40, 58
GMP synthase II	MJ_1575 (5)	-	-	78	58
Inosine-5'-monophosphate dehydrogenase GuaB I	MJ_0653 (5)	-	62	81, 82	6, 68
Inosine-5'-monophosphate dehydrogenase GuaB II	MJ_1616 (5)	-	-	-	6
Orotate phosphoribosyltransferase-like protein	MJ_1646 (2)	-	-	75-77	58, 64
Phosphoribosylamine--glycine ligase	MJ_0937 (3)	-	-	27-28	-
Phosphoribosylaminoimidazole synthetase	MJ_0203 (2)	-	-	-	35,36,38,40
Phosphoribosylaminoimidazole-succinocarboxamide synthase	MJ_1592 (1)	-	-	74	53, 54

Table 2S. (continued)

Phosphoribosylformylglycinamidine synthase I	MJ_1648 (7)	-	-	-	48, 49
Phosphoribosylformylglycinamidine synthase II	MJ_1264 (13)	-	21	10, 11, 23, 24	-
Phosphoribosylglycinamide formyltransferase 2	MJ_1486 (4)	-	-	44	-
Protoporphyrinogen oxidase HemK	MJ_0928 (1)	-	-	77	-
Pyridoxal biosynthesis lyase PdxS	MJ_0677 (2)	-	45, 46	-	40-41
Ribose-phosphate pyrophosphokinase	MJ_1366 (2)	-	-	59-62	43
Ribulose bisophosphate carboxylase	MJ_1235 (2)	-	-	44	43
Spermidine synthase*	MJ_0313 (6)	-	-	10, 61-64	42
Uridylate kinase*	MJ_1259 (1)	-	-	79	61, 63, 65, 67, 68
Bifunctional short chain isoprenyl diphosphate synthase IdsA	MJ_0860 (3)	-	-	-	36
Capsular polysaccharide biosynthesis protein	MJ_0924 (1)	78, 79	56, 57	71-73	49-51
Cellular Processes					
Methionine aminopeptidase	MJ_1329 (2)	-	-	-	38
Protein-L-isoaspartate O-methyltransferase	MJ_0172 (3)	-	-	-	63
Coenzyme A biosynthesis					
Phosphosulfolactate synthase	MJ_0255 (2)	80	58	74	53, 54
Defense against foreign DNA					
Csm5 family CRISPR-associated RAMP protein	MJ_1667 (3)	-	-	48	-
Csm3 family CRISPR-associated RAMP protein	MJ_1669 (4)	-	50-51	97	44, 45
Csm2 family CRISPR-associated RAMP protein	MJ_1670 (1)	-	-	-	81
Hypothetical protein					
Hypothetical protein MJ_0164	MJ_0164 (3)	-	-	51	26
Hypothetical protein MJ_0308	MJ_0308 (5)	75-77	52, 53	68, 69	46-48
Hypothetical protein MJ_0409	MJ_0409 (5)	-	-	11	-

Table 2S. (continued)

Hypothetical protein MJ_0513	MJ_0513 (1)	-	-	-	55
Hypothetical protein MJ_0919	MJ_0919 (1)	-	-	-	69
Hypothetical protein MJ_0948	MJ_0948 (1)	-	-	-	67
Hypothetical protein MJ_0989	MJ_0989 (3)	-	-	-	92
Hypothetical protein MJ_1099	MJ_1099 (4)	-	-	78, 79	63
Hypothetical protein MJ_1404	MJ_1404 (2)	-	-	44	-
Hypothetical protein MJ_1463	MJ_1463 (1)	-	-	34	-
Hypothetical protein MJ_1509	MJ_1509 (1)	-	-	-	87
Hypothetical protein MJ_1665	MJ_1665 (7)	-	-	8, 9	-
Metabolism					
Carboxymuconolactone decarboxylase	MJ_0742 (1)	-	-	-	100
Xylose isomerase	MJ_1455 (1)	-	-	49	-
2-oxoglutarate ferredoxin oxidoreductase subunit gamma	MJ_0536 (1)	-	60	80, 81	65, 66, 68
Acetyl-CoA decarbonylase/synthase complex subunit delta	MJ_0113 (6)	-	-	43	-
Acetyl-CoA decarbonylase/synthase complex subunit gamma	MJ_0112 (10)	-	-	20, 27-29	11
Adenylate kinase*	MJ_0479 (1)	-	-	-	58
Fructose-bisphosphate aldolase*	MJ_0400 (3)	-	-	67-70	46-48
Fructose-1,6-bisphosphatase*	MJ_0299 (8)	54-55	-	11, 47-48	25
Multifunctional 3-isopropylmalate dehydrogenase/D-malate dehydrogenase	MJ_0720 (5)	-	-	65	-
Phosphoenolpyruvate synthase	MJ_0542 (12)	-	4, 5	8-11	-
Phosphoglycerate kinase*	MJ_0641 (3)	-	-	-	22-24
Phosphopyruvate hydratase(enolase)*	MJ_0232 (1)	-	2	41-44, 46, 50	-

Table 2S. (continued)

Putative manganese-dependent inorganic pyrophosphatase*	MJ_0608 (1)	-	-	-	39
Putative transaldolase*	MJ_0960 (1)	83-84	59	78-79	59-61, 63, 68
Pyruvate carboxylase subunit B	MJ_1231 (7)	25, 26, 29	17, 18	18-20	7, 23
Pyruvate ferredoxin oxidoreductase subunit alpha PorA*	MJ_0267 (7)	53	-	46	24
Transketolase*	MJ_0679 (1)	-	-	-	36
Triosephosphate isomerase*	MJ_1528 (5)	-	-	77-78	-
UDP-glucose dehydrogenase*	MJ_1054 (9)	-	-	62, 65	42
Methanogenesis (Energy generation)					
F_{420}-dependent methylenetetrahydromethanopterin dehydrogenase	MJ_1035 (3)	-	5	11, 63	-
Formylmethanofuran dehydrogenase subunit C	MJ_1350 (1)	-	-	-	47
Formylmethanofuran dehydrogenase subunit FwdA	MJ_1169 (6)	24	-	-	-
Formylmethanofuran--tetrahydromethanopterin formyltransferase	MJ_0318 (6)	64	-	-	31, 32
H_2-dependent methylenetetrahydromethanopterin dehydrogenase	MJ_0784 (10)	50-52	26, 35, 37	-	18-24
H_2-dependent methylenetetrahydromethanopterin dehydrogenase-like protein I	MJ_0715 (2)	64	-	-	31-32
H^+-transporting ATP synthase subunit E AtpE	MJ_0220 (1)	-	-	79	60
Methyl coenzyme M reductase I subunit McrA	MJ_0846 (5)	10, 24-42, 3	14-23, 25	6-9, 16-27, 31, 37, 43	7-9, 66
Methyl coenzyme M reductase I subunit McrB	MJ_0842 (4)	43-49	26,32-35, 6	6, 16-17, 27, 30-31, 35-45,57-58, 69, 70, 76	6, 11, 14-15, 17-19, 34-35, 49

Table 2S. (continued)

Methyl coenzyme M reductase II protein MtrC	MJ_0094 (2)	-	-	-	30-31
Methylenetetrahydromethanopterin reductase	MJ_1534 (4)	63	42-45, 47	41-43, 47-53, 55, 57, 37-38, 62-65	35, 37,26, 28, 29, 38, 28
Methylviologen-reducing hydrogenase subunit alpha	MJ_1192 (4)	-	-	24-25, 58	41
N_5,N_{10}-methenyltetrahydromethanopterin cyclohydrolase	MJ_1636 (8)	2	-	24-25, 58	41
Tetrahydromethanopterin S-methyltransferase subunit H	MJ_0854 (3)	72-73	49	62-65	42
DsrE family protein	MJ_0760 (4)	-	-	-	49
Methanogenesis marker protein 17	MJ_0802 (2)	-	-	78-79	60, 63
AMMECR 1 domain protein	MJ_0810 (4)	-	63	82-83	-
Peptidase	MJ_0996 (5)	-	-	30	-
Methyltransferase	MJ_1273 (4)	-	-	10, 49, 50, 52	63
Iron-sulfur flavoprotein	MJ_1083 (5)	-	29-30	29-31, 44	57
Nitrogen and amino acid metabolism					
(R)-2-hydroxyglutaryl-CoA dehydratase activator	MJ_0800 (5)	45	-	42	-
2-hydroxyglutaryl-CoA dehydratase	MJ_0007 (10)	45	-	42	-
3-dehydroquinate synthase	MJ_1249 (3)	-	47	49, 62-65	42
3-isopropylmalate dehydratase large subunit*	MJ_0499 (10)	47-48	-	-	-
Acetolactate synthase catalytic subunit*	MJ_0277 (6)	7	-	12	-
Acetylornithine aminotransferase*	MJ_0721 (6)	-	-	48	-
Anthranilate synthase component II TrpD	MJ_0238 (1)	-	-	58	36
Argininosuccinate synthase*	MJ_0429 (5)	-	-	2, 39-42	-
Aspartate aminotransferase*	MJ_1391 (4)	-	21	24, 31	-
Aspartate aminotransferase AspC	MJ_0959 (4)	-	-	10, 47	-

Table 2S. (continued)

Aspartate-semialdehyde dehydrogenase*	MJ_0205 (4)	-	12	47, 49	25
Branched-chain amino acid aminotransferase	MJ_1008 (3)	-	-	4-5, 50, 60	43
D-3-phosphoglycerate dehydrogenase*	MJ_1018 (3)	-	-	16-17, 24, 25	6, 9
Dihydrodipicolinate reductase	MJ_0422 (2)	82	-	64, 5	45
Dihydrodipicolinate synthase	MJ_0244 (2)	-	47	62-65	45
Dihydroxy-acid dehydratase*	MJ_1276 (11)	20, 21	14	16-17	6
Glutamine synthetase*	MJ_1346 (6)	-	-	27-28	-
Histidinol dehydrogenase	MJ_1456 (4)	-	-	29	-
Hydroxylamine reductase	MJ_0765 (14)	-	-	20, 23-26	-
Ketol-acid reductoisomerase*	MJ_1543 (3)	62	-	56, 57	31
Phosphoribosylformimino-5-aminoimidazole carboxamide ribotide isomerase HisA1	MJ_1532 (2)	-	-	78-79	60
S-adenosylmethionine synthetase*	MJ_1208 (4)	44-45	-	37-43	20-21
Threonine synthase*	MJ_1465 (11)	-	-	37-41	-
Tryptophan synthase subunit beta*	MJ_1037 (7)	-	-	48	-
Oxidative stress response					
Flavoprotein FpaA	MJ_0748 (4)	44-45, 47-49	33-35, 39	4,6, 8, 17, 27, 35-38, 45	17-24, 34
NADH oxidase	MJ_0649 (8)	-	-	22-28, 38-39	18
Peroxiredoxin*	MJ_0736 (5)	85-86	61	44, 80-81	62-68
Protein Biosynthesis					
Leucyl-tRNA synthetase	MJ_0633 (14)	-	-	5	-
Phenylalanyl-tRNA synthetase subunit beta	MJ_1108 (4)	-	-	21-22	-
Valyl-tRNA synthetase*	MJ_1007 (16)	-	-	5	-

Table 2S. (continued)

Protein maturation					
Hydrogenase expression/formation protein HypE	MJ_0676 (4)	-	-	-	26
Replication, transcription and translation					
30S ribosomal protein S19e	MJ_0692 (1)	-	-	-	87
30S ribosomal protein S6e	MJ_1260 (1)	-	-	-	88-89
30S ribosomal protein S7	MJ_1047 (1)	-	-	82	63, 65, 67-68
30S ribosomal protein S8	MJ_0470 (2)	-	-	-	89
30S ribosomal protein S8e	MJ_0673 (1)	-	-	-	87
50S ribosomal protein L11	MJ_0373 (1)	-	-	-	76-77
50S ribosomal protein L30	MJ_0476 (1)	-	-	86	-
50S ribosomal protein L3P*	MJ_0176 (2)	-	-	-	26
50S ribosomal protein L6	MJ_0471 (1)	-	-	83	69-71
Acidic ribosomal protein P0	MJ_0509 (1)	57	-	51-52	26
Arginyl-tRNA synthetase	MJ_0237 (10)	24	15	17, 26	-
Aspartyl/glutamyl-tRNA amidotransferase subunit B	MJ_0160 (7)	-	-	27-28	-
Aspartyl-tRNA synthetase	MJ_1555 (3)	-	-	42	-
Cell division protein CDC48*	MJ_1156 (3)	1, 3, 4	1, 3	2-9, 18	-
Cell division protein FtsZ II*	MJ_0622 (5)	-	45	-	-
Cell division protein FtsZ I*	MJ_0370 (2)	50, 52	37	49-52	26, 41
DNA ligase	MJ_0171 (6)	-	-	25	-
DNA-directed RNA polymerase subunit beta*	MJ_1040 (7)	-	-	28	-
DNA-directed RNA polymerase subunit D	MJ_0192 (3)	-	-	-	63, 65, 67-68
Elongation factor 1-alpha*	MJ_0324 (3)	25, 37, 38, 40-42, 61, 62	26-28, 32, 40-44	11, 2, 4-8, 16-17, 34-36, 27, 28, 33, 37-41, 53, 57-58	6, 11, 14-19, 33

Table 2S. (continued)

Elongation factor EF-2	MJ_1048 (11)	8, 9	6	6-12, 17-20, 38-41	11
Prolyl-tRNA synthetase	MJ_1238 (2)	43	-	-	-
Seryl-tRNA synthetase*	MJ_0177 (7)	-	-	24	-
Thermosome	MJ_0999 (4)	27-28, 30-32, 36	19-23, 25	9-12, 3-5, 19-31, 43, 46, 47, 49, 50, 63-65	3, 7-11,
Transcription factor	MJ_0507 (2)	-	-	83	-
Transcriptional regulator	MJ_0300 (1)	-	-	-	42
Translation initiation factor aIF-2B subunit delta	MJ_0454 (5)	-	-	50	-
Translation initiation factor IF-2	MJ_0262 (7)	-	-	-	3
tRNA synthetase	MJ_0539 (8)	-	-	24	-
Structural proteins					
Flagella-like protein E	MJ_0896 (1)	-	83-84	88	82
S-layer protein	MJ_0822 (2)	14-18, 33-34	12, 13, 24, 25, 31, 38, 39	13-16, 32, 45, 46, 52	2, 5, 6, 13, 14
Sulfite detoxification					
F_{420}-dependent sulfite reductase	MJ_0870 (27)	7, 9, 10, 18,	-	-	5
Thiol-based redox regulation					
Thioredoxin	MJ_0307 (2)	-	72-74, 78-82	-	-
Transport proteins					
ABC transporter	MJ_0035 (5)	-	-	-	46-47
Transport proteins					
High-affinity branched-chain amino acid transport protein BraC	MJ_1266 (4)	-	-	36, 37	18

*Previously identified Trx target

4.3.4 *Effect of Reduction by Trx1 on the Activity of Selected M. jannaschii Enzymes*

F_{420}-dependent sulfite reductase (Fsr). A sulfite detoxifying enzyme**,** Fsr was partially purified from cell-free extracts by ammonium sulfate fractionation under strictly anaerobic conditions (93). The supernatant fraction containing ammonium sulfate at 65% saturation was highly enriched with Fsr. It was desalted to remove flavins that react with reduced F_{420} and thereby interfere with the Fsr assay (93, 94). This fraction was then dialyzed aerobically to generate S-S groups targeted by Trx1. This air-exposed Fsr preparation showed 66% lower specific activity compared to the corresponding anaerobic preparation, the respective values being 0.132 U/mg and 0.2 U/mg. When pre-incubated with DTT (10 mM), the former exhibited a 2.7-fold increase in Fsr activity, compared to a 2-fold enhancement observed with the anaerobic preparation. Therefore dialyzed Fsr was a potential substrate for Trx1. Indeed, a treatment of oxidized Fsr with 10-fold molar excess of Trx1 in the presence of 1 mM DTT at 65^{o}C increased the sulfite reductase activity of the enzyme by 2.9-fold (Fig. 4.4A). When twice as much Trx1 (20-fold excess) was added to the activation reaction, the specific activity increased 4.6-fold (data not shown). DTT alone at a level of 1 mM had no effect on Fsr activity. In the absence of DTT, Trx1 activated Fsr 1.5-fold, likely due to a crowding effect.

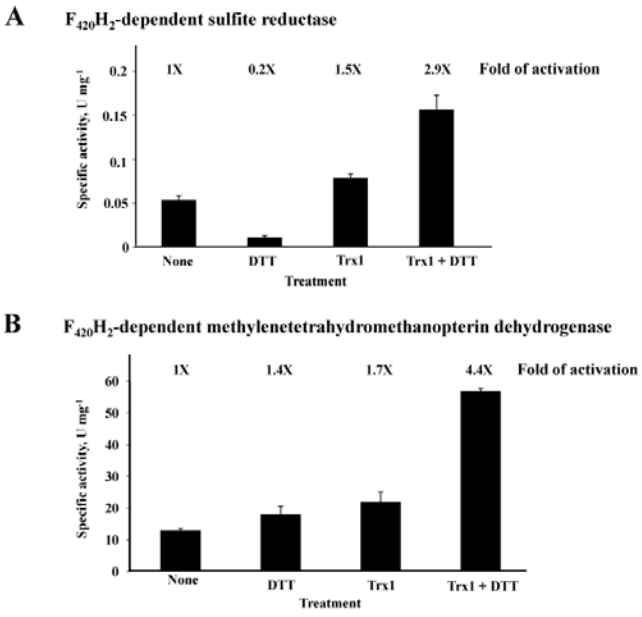

Figure 4.4. Activation of F_{420}-dependent sulfite reductase or Fsr (A) and F_{420} dependent methenyltetrahydromethano-pterin dehydrogenase or Mtd (B) by Trx1. Fsr and Mtd were incubated with Trx1, DTT or both at 65^{o}C for 5 min followed by an additional incubation at 25^{o}C for 20 min. Other details for these treatments appear in the MATERIALS AND METHODS. Enzyme without an exposure to DTT or Trx1 was used as the control. Each solid bar presents an average of the activity values from replicates (three independent experiments for Fsr and two for Mtd) and the respective standard deviation is shown as an error bar. The number shown on each solid bar represents the fold of activation of an enzyme and the reagents used for the respective treatment are indicated below the bar.

F_{420}-dependent methenyltetrahydromethanopterin dehydrogenase (Mtd). Recombinant His-tagged Mtd was expressed heterologously in *E.coli* BL21DE3. When expression was induced with 0.4 mM IPTG and the culture incubated at 37^{o}C for 3 hours, the recombinant enzyme was found almost exclusively in inclusion bodies. By contrast, with 0.1 mM IPTG and incubation overnight at 15^{o}C for overnight, 50% of the Mtd protein was expressed in soluble form. The enzyme was purified by Ni-NTA affinity chromatography. Since Mtd is stable in air, all purification steps were performed under aerobic conditions as described previously (95).

Non-reducing SDS-PAGE with an mBBr-treated preparation showed that recombinant Mtd was present mostly in a reduced form. To generate potential cystine disulfides, the preparation was treated with the following oxidizing agents (final concentration): H_2O_2 (100 µM), $CuCl_2$ (30 µM) and Aldrithiol-2 (100 µM). Based on mBBr fluorescence-based gel analysis, Aldrithiol-2 was most effective in oxidizing Mtd. Additionally, the oxidized enzyme could be reduced in the presence of Trx1 and DTT (data not shown). Thus, Aldrithiol-2 treatment provided an avenue for generating an Mtd preparation that would be a substrate of Trx1. Activation assays employing this strategy provided the following results.

Oxidation of Mtd with Aldrithiol-2 was accompanied by a 53% loss in activity. Incubation of the oxidized preparation with 5-fold molar excess Trx1 and 0.05 mM DTT at 65^{o}C yielded a 4.4-fold increase in activity *versus* the 1.4-fold enhancement seen with DTT alone (Fig. 4.4B).

4.4 DISCUSSION

Trx homologs appear to be nearly universal in methanogenic archaea and their number in a methanogen parallels their evolutionary history and metabolic diversity. The results from proteomics and enzyme activity studies with the phylogenetically deeply-rooted methanogen *Methanocaldococcus jannaschii* indicated that Trx could regulate a variety of cell functions, including methanogenesis—the hallmark of this group of organisms. We put these observations into perspective below.

Distribution of Trx homologs in methanogens. The distribution of Trx homologs in methanogens exhibited a pattern (Fig. 4.1 and Table 4.1). Almost all methanogens carried at least one Trx homolog. An exception was *Methanopyrus kandleri*, phylogenetically the most deeply-rooted and most thermophilic methanogen known (growth occurs at 84-110^{o}C) (21). This organism was devoid of a Trx homolog. Other phylogenetically deeply-rooted

methanogens belonging to the class of *Methanococci* and *Methanobacteria* carried a limited number of Trx homologs (2-4, 2 on average), whereas the late-evolving methanogens represented by the *Methanomicrobia* carried up to eight (on average, 4). *Methanococci* and *Methanobacteria* have relatively smaller genomes (1.24 – 2.94 Mbp) (41, 45) and include all of the hyperthermophilic and most thermophilic methanogens (18, 43, 96). Many of these organisms are restricted to H_2-dependent methanogenesis (96)—one of the most ancient respiratory metabolisms of earth (19). *Methanopyrus kandleri* is also solely dependent on H_2 and CO_2 for methanogenesis (21). Certain *Methanococci* and *Methanobacteria,* can utilize formate (96). By contrast, the *Methanomicrobia*, which have relatively large genomes (1.8 – 5.75 Mbp) (57, 86), use a range of methanogenesis substrates, including methanol, methylamine, dimethylamine, trimethylamine and acetate (96). In addition, some members of this class utilize isopropanol and isobutanol as electron sources for reducing CO_2 to methane (96). Most *Methanomicrobia* are mesophiles and are more tolerant to O_2 exposure (96, 97). It is possible that the Trx system came in to play in the deeply-rooted methanogenic archaea as these organisms faced hydrogen limitation and O_2 exposure, both of which raise cellular redox potential. Similarly, in the late-evolving methanogens, the number of Trx homologs likely increased to cater to their expanded metabolic versatility. Horizontal gene transfer from *Clostridia* and other anaerobes is thought to be the basis for the metabolic diversity of *Methanomicrobia* (83). It seems likely that the expansion of the Trx system followed the same path in this methanogen group.

***Methanocaldococcus jannaschii* thioredoxins.** The two Trxs identified in *M. jannashcii* were found to have defining characteristics, including amino acid sequence, reactivity toward insulin and activity with *E. coli* NTR. The latter two differences are possibly related to the nature of the variable amino acid residues (X's) in the putative redox active site C-X-X-C. In Trx1 and Trx2 this motif was C-P-H-C and C-P-K-C, respectively, both different from the classical C-G-P-C (98). It is known that the pKa's of the catalytic cysteine residues of a Trx are influenced by the two intervening variable amino acid residues (X's) which, in turn, define redox properties of the protein (99, 100). It is thus not surprising that Trx1 and Trx2 showed different specificities. Trx1 was a typical type—i.e., similar to its *E. coli* counterpart in primary structure, robust insulin reduction activity and reduction by *E. coli* NTR. Trx1 was, therefore, chosen for identifying Trx target proteins in *M. jannaschii*.

Targets of Trx1. Our proteomics study revealed a total of 149 *M. jannaschii* proteins as potential Trx1 targets (Table 4.2). Of these, 74 proteins were detected in at least two of four independent experiments and about 75 were observed only once (Table 4.2).

To confirm a link to Trx, we tested the effect of reduced Trx1 on the activity of two target enzymes in *in vitro* assays: F_{420}-dependent methylenetetrahydromethanopterin dehydrogenase (Mtd), a core enzyme of the methanogenesis pathway (93, 101, 102) and F_{420}-dependent sulfite reductase (Fsr), that allows certain methanogens to tolerate sulfite and to utilize this oxyanion as sulfur source (93, 102, 103). Oxidized forms of both Mtd and Fsr were activated by Trx1, giving further credence to the fluorescent/gel approach of target identification.

***Methanocaldococcus jannaschii* systems targeted by Trx1.** The Trx1 targets covered a range of proteins catering to a variety of cellular needs.

Methanogenesis – Many of the enzymes directly involved in the reduction of CO_2 to CH_4 were targeted by Trx1 (Fig. 4.5, Tables 4.2). Since Trx regulates the activity of target enzymes in response to changes in cellular redox balance (104, 105), it can be envisaged that Trx is invoked in response to change in their redox status resulting from either a drop in the partial pressure of H_2 or exposure to O_2. *M. jannaschii* is representative of a group of methanogens that use H_2 exclusively as an energy source (30, 106). In the natural habitats of these organisms, partial pressure of H_2 is subject to change, often in an extreme manner (107). These events can alter the redox status of the cells' environment markedly. As a resident of deep-sea hydrothermal vents, *M. jannaschii* is known to experience H_2 partial pressure fluctuations in the range of 4 Pa to 200 kPa (108). In such an environment, exposure to O_2-containing sea water is also a possibility. The temperature of the vent fluid, 300–350°C, is lowered to values more conducive to the survival of inhabitants by mixing with the cold seawater that permeates the chimney wall (18, 101, 109, 110). Although the O_2 introduced in this process is neutralized by reacting with sulfide, exposure to O_2 due to poor or slow mixing remains a possibility. Oxygen exposure is common for terrestrial methanogens (96).

The deductions in the preceding section suggest that the reductive activation of oxidized methanogenic enzymes via Trx-mediated disulfide exchange could be a normal physiological process for *M. jannaschii* and other methanogens. Trx could synchronize methanogenesis with the redox potential of the vent milieu by maintaining compatible activity of participating

enzymes. Previous transcriptomic and proteomic studies with *M. jannaschii* and two other hydrogen oxidizing methanogens, *Methanothermobacter thermautotrophicus* strain ΔH and *Methanococcus maripaludis*, have revealed that the expression of several methanogenesis-related genes is regulated by H_2 availability (111-114). Methylenetetrahydromethanopterin reductase (Mer), F_{420}-dependent metehylenetetrahydromethanopterin dehydrogenase (Mtd) and methyl coenzyme M reductase (Mcr) genes are subjected to this type of regulation (111-113). Significantly, each of these enzymes was identified as potential targets of Trx1 (Tables 4.2), and in the case of Mtd, the proteomic observations were confirmed by a direct activity assay (Fig 4.4B). The observation that Mtd is activated by Trx1 is consistent with previous reports that this enzyme (but not its alternate, the hydrogen-dependent methylenetetrahydromethanopterin dehydrogenase, Hmd) plays a major role in methanogenesis under low H_2 partial pressures (114-116). Regulation by Trx adds another level of control to the methanogenesis pathway and could allow methanogens to survive H_2 limitation and oxidative stress. Due to its link to redox, Trx could also regulate methanogenesis from substrates other than H_2, since these compounds provide reductant for cellular functions in addition to methanogenesis (117).

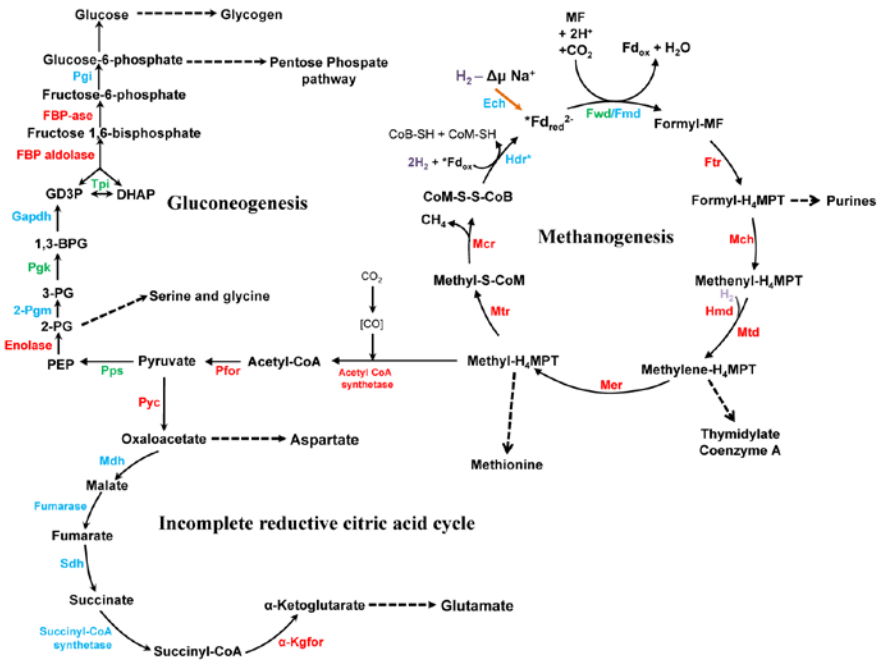

Figure 4.5. Select reactions and pathways of *M. jannaschii* targeted by Trx1 (Mj_0307). This presentation summarizes some of the finding documented in Tables 4.2. The methanogenesis pathway was redrawn from (118). Enzymes that were identified as Trx1 targets in at least three proteomic experiments are shown in red; those detected in one or two experiments are shown in green and blue show enzymes that were not Trx1 targets. **Abbreviations:** Pgi, phosphoglycerate isomerase; FBPase, Fructose bisphosphatase; FBP aldolase, fructose,1,6-bisphosphate aldolase; Tpi, triose phosphate isomerase; Gapdh, glyceraldehydes-3-phosphate dehydrogenase; Pgk, phosphoglycerate kinase; 2-Pgm, 2-phosphoglycerate mutase; Pps, phospoenolpyruvate synthase; Pyc, pyruvate carboxylase; Mdh, malate dehydrogenase; Frd, fumarate reductase; α-Kgfor, alpha ketoglutarate

ferredoxin oxidoreductase; Pfor, pyruvate ferredoxin oxidoreductase; Fwd, tungsten-dependent formylmethanofuran dehydrogenase; Fmd, molybdenum-dependent formylmethanofuran dehydrogenase; Ftr, formylmethanofuran-H_4MPT formyltransferase; Mch, methenyl-H_4MPT cyclohydrolase; Mtd, F_{420}-dependent methylene-H_4MPT dehydrogenase; Hmd, H_2-dependent methylene-H_4MPT dehydrogenase; Mer, methylene-H_4MPT reductase; Mtr, methyl-H_4MPT-coenzyme M methyltransferase; Mcr, methyl-coenzyme M reductase; Hdr-H_2ase, electron-bifurcating hydrogenase-heterodisulfidereductase complex; Ech, Energy converting hydrogenase; F_{420}, coenzyme F_{420}; *Fd, specific ferredoxin; H_4MPT, tetrahydromethanopterin; MF, methanofuran; CoB, coenzyme B; CoM, coenzyme M; [CO], enzyme-bound carbon monoxide (CO); ATP, adenosine triphosphate; NADH, nicotinamide adenine dinucleotide; GD3P, glyceraldehyde-3-phosphate; DHAP, dihydroxyacetone phosphate; 1,3-BPG, 1,3-bisphosphiglycerate; 3-PG, 3-posphoglycerate; 2-PG, 2-phosphoglycerate; PEP, phosphoenolpyruvate; HS-CoA, coenzyme A; $\Delta\mu Na^+$, electrochemical sodium ion potential. Dashed arrows show the extended biosynthetic routes for which details are not shown.

Sulfite detoxification – Identified as a target in proteomic studies (Table 4.2), F_{420}-dependent sulfite reductase (Fsr) was deactivated upon exposure to O_2 and the altered enzyme was reactivated by reduced Trx1 (Fig. 4.4A). These observations make physiological sense. Sulfite inhibits methyl-coenzyme M reductase and, thereby, impedes methanogenesis (119). In the habitat of *M. jannaschii*, sulfite is formed when O_2-containing cold sea-water permeates the vent chimney wall and mixes with the hot internal sulfide-rich vent fluid. Fsr detoxifies the newly formed sulfite by reducing it to sulfide—a metabolite used by *M. jannaschii* as a source of sulfur (93). Since sulfite is known to oxidize protein sulfhydryl (SH) to the disulfide (S-S) level (120), it is not surprising that oxidatively deactivated Fsr can be reductively activated by Trx1. It is possible that activation by Trx is a general feature of sulfite reductases. The enzyme in wheat starch endosperm has been identified as a Trx target (121).

Biosynthesis – Trx1 targets major biosynthetic processes in *M. jannaschii* (Fig. 4.5). For such an autotroph, the *de novo* synthesis of acetate and pyruvate are key initial anabolic steps. It is significant that the two key enzymes participating in CO_2 fixation, acetyl-CoA synthetase and pyruvate:ferredoxin oxidoreductase (PFOR), were identified as Trx1 targets (Table 4.2 and Fig. 4.5). This observation is reminiscent of recent findings with the sulfate-reducing bacterium *Desulfovibrio africanus* in which the deactivated form of PFOR was reactivated by Trx reduced with NADPH via NTR (87). The *M. jannaschii* counterparts of many other previously recognized bacterial and eukaryotic Trx targets were also reduced by Trx1. Examples include, enolase, phosphoglycerate kinase, triose phosphate isomerase, fructose bisphosphate aldolase and fructose 1,6-bisphosphatase (105). These enzymes are involved in gluconeogenesis, an

energy intensive process that also requires a reductant (117). Thus, the activities of these enzymes and associated pathways are expected to be regulated by the availability of low potential electrons and, consequently, by the redox status of the methanogen cell. Here, a role for Trx is appropriate. Additionally, amino acid biosynthesis enzymes, including glutamine synthetase, threonine synthase and aspartate semialdehyde dehydrogenase were reduced by Trx1. These enzymes have been previously reported as Trx targets in plants (105). Biosynthetic processes specific to methanogens also appeared to be regulated by Mj-Trx1—e.g., phosphosulfolactate synthase, an enzyme functional in the biosynthesis of coenzyme M—an requirement for methane production from all substrates (122). Thus, regulation of coenzyme M synthesis falls within the broader role of Trx in the regulation of methanogenesis.

Transcription, translation and cell division – Transcription and translation have previously been linked to Trx-based regulation in Bacteria and Eukarya (105, 123). Modification of the RNA polymerase ω subunit and elongation factors in *E. coli* (123) and several of chloroplast ribosomal proteins also fall into this category (105). Similar controls likely exist in *M. jannaschii* where TATA-box binding protein (Mj_0507), ribosomal protein S8 (Mj_0470) and several t-RNA synthethases were identified as Trx1 targets (Tables 4.2).

Following the precedence established with the chloroplast and *E. coli* models (123, 124), Trx1-reduced *M. jannaschii* FtsZ (125-127), a cytoskeletal protein similar to tubulin in eukaryotes (128). The associated GTPase activity is considered to promote the formation of a multimeric ring structure and thereby facilitate cell division. The three dimensional structure of *M. jannaschii* FtsZ shows that Cys45 and Cys129 have the potential to form a disulfide bond (127). It seems possible that these cysteine residues could regulate cell division in conjunction with Trx in *M. jannaschii* as well as other cells.

Structural proteins – S-layer protein was identified as potential Trx1 targets. These observations support and extend previously reported findings concerning their synthesis and structure. The S-layer constitutes the major component of the cell envelope in *M. jannaschii*, *M. maripaludis* and other methanogens (129). Moreover, in *M. maripaludis*, the level of S-layer protein decreases under limited H_2 supply (111). It is possible that both the generation and assembly of S-layer in *M. jannaschii* and perhaps other methanogens is redox controlled; Trx assists the latter via posttranslational modification.

Anti-oxidant and defense against foreign DNA – Similar to chloroplasts (124), a peroxiredoxin was identified as a Trx target in *M. jannaschii* (Table 4.2). Peroxiredoxins are anti-oxidant enzymes catalyzing the reduction of hydroperoxides and alkyl hydroperoxides to water and respective alcohols (130). Three CRISPR-associated proteins (Clustered Regularly Interspaced Short Palindromic Repeats) were also reduced by Trx1 (Table 4.2). CRISPR elements are common features of archaeal and bacterial genomes which, with their associated proteins, provide defense against invasion by external DNA materials such as plasmids and phage (131). A connection between phage infection and Trx was originally observed with the identification Trx as an essential subunit of phage T7 DNA polymerase and an essential element in filamentous phage assembly (132, 133). The results from our work suggest that archaea and bacteria employ a different Trx-based mechanism for defense external genetic materials.

4.5 CONCLUDING REMARKS

Findings reported here suggest that, while individual target proteins may differ, the pattern of Trx-based redox regulation established for bacteria and eukarya also applies to methanogenic archaea. The breadth of target proteins identified for *M. jannaschii* suggests that other archaea utilize Trx-based regulation. Moreover, many of the proteins identified as Trx targets in *M. jannaschii* have counterparts in plants where the oxidative type of regulation presently observed was first realized (134).

The current findings if true have far-reaching implications. Methanogens play a central role in global carbon balance through their ability to facilitate the mineralization (i.e., conversion to CO_2) of complex biopolymers in anaerobic niches of nature and produce methane—a greenhouse gas that is also a fuel. Since the redox state of their environment is subject to change due to variation in reductant supply and O_2 exposure, Trx control of methanogenesis now needs to be considered as a factor in the global carbon cycle and climate change. In addition to adding information to these critical areas, research on Trx in deeply-rooted members of the archaea such as *Methanocaldodoccus jannaschii* may give clues on how metabolism evolved and diversified.

4.6 MATERIALS AND METHODS

Materials. Insulin, monobromobimane (mBBr), aldrithiol-2 and NADPH were obtained from Sigma-Aldrich (Sigma, St. Louis, MO). Coenzyme F_{420} was purified from *Methanothermobacter marburgensis* as described previously (135). Coenzyme tetrahydrosarcinapterin (H_4SPT) was a gift from Dr. David A. Grahame of Uniformed Services University of the Health Sciences, Maryland. *E. coli* NTR and serum raised against *E. coli* Trx were kindly provided by Dr. Buchanan laboratory.

Growth of *Methanocaldococcus jannaschii*. The organism was grown in mineral salts medium at 85^{o}C under an atmosphere of H_2 and CO_2 (80:20 v/v; 3 x 10^5 Pa) in sealed 500 mL serum bottles with sulfide or sulfite as sole sulfur source (93, 136). Cells were harvested anaerobically by centrifugation for 10 min at 10,000 x g and 4^{o}C, under a mixture of N_2, CO_2 and H_2 (19:76:5 v/v).

Generation of Homogeneous Recombinant *M. jannaschii* Proteins. Coding sequences of Trx1 (*mj_0307*), Trx2 (*mj_0581*) and Mtd (*mj_1035*) were amplified by PCR from *M. jannaschii* chromosomal DNA using primers listed in Table 4.3. Amplicons were cloned into the *Nde*I and *BamH*I sites of the plasmid pTEV5 (137) generating the expression plasmids pUL204, pUL205 and pUL216, respectively. These plasmids were designed to generate the desired recombinant proteins with an NH_2-terminal His_6-tag. *E. coli* BL21(DE3)(pRIL) containing an appropriate expression plasmid was grown at 37^{o}C in LB medium containing 100 µg/mL ampicillin and 34 µg/mL chloramphenicol up to an OD_{600} of 0.6 measured with a DU800 spectrophotometer (Beckman Coulter, Brea, CA). Then the expression of the cloned gene was induced with IPTG: final concentration, 0.4 mM for pUL204 and pUL205 and 0.1 mM for pUL216. After IPTG addition, cultures were incubated for an additional 3 h at 37^{o}C except for pUL216 where incubation was at 15^{o}C overnight.

Purification of recombinant proteins was performed via Ni-NTA chromatography (138). Recombinant Trxs and Mtd were eluted with 150 mM and 350 mM imidazole, respectively.

Table 4.3 Oligonucleotide Primers

Gene product	Primer ID*	Oligo sequences
Mj-Trx1	Mj0307/F	5' - ATG CAT ATG TCA AAG GTA AAG ATA GAG C - 3'
	Mj0307/R	5' - AGA TCT TAT AGT CTT TTT TTG ATT GCC TC - 3'
Mj-Trx2	MJ0581/F	5' - ATG CAT ATG GTA GTG ATA AGG ATA TTC GG - 3'
	Mj0581/R	5'- AGA TCT TAT TTC CCC TCT AAG TAA CTT TTT AAC TCT TCC - 3'
Mj-Mtd	MJ1035/F	5' – AAA TCA TAT GGT CGT AAA AAT AGG AAT AAT AAA GTG - 3'
	MJ1035/R	5' – GAG AGG ATC CTT ATT CTG GTT TCT CCA TTA ATG C - 3'

* **F**, Forward primer; **R**, Reverse primer

Western Blot. Western blot experiments were performed as described previously (139). Antisera raised against *E. coli* Trx was used as primary antibodies at 1:1000 dilution.

Insulin Reduction Assay. Insulin reduction assay was performed at 25^{o}C as described previously (140). Briefly, *M. jannaschii* Trx1 (2 µM) or Trx2 (20 µM) was added to 100 mM potassium phosphate buffer pH 7.0, containing 2 mM EDTA and 0.83 mg/mL bovine insulin (Sigma, St. Louis, MO) (final vol, 0.6 ml). The assay was then initiated by addition of DTT (0.3 mM and 1 mM for Trx1 and Trx2, respectively). Insulin precipitation was followed spectrophotometrically at 650 nm using a Beckman DU800 spectrophotometer.

Preparation of *M. jannaschii* Cell Extracts for Proteomics Analysis. One gram *M. jannaschii* wet cell paste was resuspended in 4 mL of 25 mM potassium phosphate buffer pH 7.0. This low concentration buffer facilitated cell lysis via osmotic shock. Lysis was enhanced and viscosity was reduced by 10 subsequent passages through a 22 Gauge needle. The cell lysate was centrifuged for 30 min at 20,000 x g and 4^{o}C. All steps up to this stage were performed under anaerobic conditions. The resulting supernatant was subjected to overnight aerobic dialysis at 4^{o}C vs. 1 L of 25 mM potassium phosphate buffer, pH 7.0, containing 10% (w/v) of glycerol. To block free thiol groups in cell extract proteins, the dialyzed solution was incubated 20 min at 25°C with a mixture of iodoacetamide (IAA) and N-ethylmaleimide (NEM), each at a final concentration of 10 mM. 2-Mercaptoethanol was then added at a final concentration of 20 mM

to quench excess blocking reagents. Finally, the extract was dialyzed overnight at 4°C vs. 1 L of 50 mM potassium phosphate buffer, pH 7.5 with at least 3 buffer changes. All alkylation and dialysis steps were performed under air.

Reduction of *M. jannaschii* Trx Target Proteins. All reactions were performed under strictly anaerobic conditions using DTT or NADPH/*E. coli* NTR as reductant. **DTT**: 350 ug IAA-NEM-treated *M. jannaschii* extract proteins were incubated for 5 min at 80^{o}C in 20 mM potassium phosphate buffer, pH 7.2, containing 0.1 mM DTT and 2 μM recombinant Trx1. DTT was added last to start the reaction. **NADPH/*E. coli* NTR**: Details as the reduction with DTT except reaction was conducted at 37^{o}C for 30 min and *E. coli* NTR, NADPH and EDTA added at final concentrations of 1 μM, 10 μM and 1 mM, respectively, replaced DTT. In each case the fluorescence probe mBBr was added to a final concentration of 2 mM at the end of the incubation period, and the mixture was held at 25^{o}C for 15 min. 2-Mercaptoethanol was added to a final concentration of 20 mM to quench excess mBBr.

Isolation of *M. jannaschii* Trx1 Target Proteins. 2D gel electrophoresis was performed with 250 μg mBBr-labeled *M. jannaschii* cell extract proteins as described previously (91). In brief, prior to loading proteins were precipitated overnight at -20°C using 5 volumes of cold acetone. Protein pellets were washed three times in cold acetone and, after air drying for 5 min, were resuspended in rehydration buffer (8M urea, 4% CHAPS, 100 mM DTT, and 2% Servalyte, pH 3-10). Proteins (~250 μg) were loaded onto 11-cm IPG strips (pH 3-10) for rehydration and isoelectric focusing at 20°C using a Protean IEF Cell (Bio-Rad). Protein samples were actively rehydrated at 50V for 12 hr and then subjected to isoelectric focusing with the following parameters in rapid ramping mode: 0 to 250 V for 15 min; 250 to 8,000 V for 2.5 h; and 8,000 V until 35,000 V/h was reached. The strips were then sequentially equilibrated at room temperature with 375 mM Tris-HCl, pH 8.8, 6 M urea, 20% glycerol, 130 mM DTT and 2% SDS for 20 min and then for another 20 min with the same buffer in which DTT was replaced by 135 mM iodoacetamide. For separating proteins according to molecular mass in the second dimension, the equilibrated strips were placed on top of 12% Criterion XT Bis-Tris Gel and developed in 1X MOPS buffer, pH 7.7 at 150 V for 1 h and 20 min.

After electrophoresis, the gels were washed in 7% acetic acid for 30 min and fluorescent images of protein spots were captured with a Molecular Imager Gel Doc XR+ with Quantity One

program, version 4.6.9 (Bio-Rad, Hercules, CA) under long wavelength (365 nm) UV light. Gels were then stained for proteins with colloidal Coomassie Brilliant Blue overnight and destained with several changes of ddH_2O. The clarified protein gels were scanned on an Epson Perfection V700 PHOTO scanner.

Mass spectrophotometry analysis of target proteins

Protein spot preparation -- Stained spots of interest were excised from gels, and the pieces, approximately 1x1 mm, were placed in a 96-well perforated reaction plate (Intavis, Koeln, Germany). The loaded plate was then placed in an automated protein digester (DigestPro, Intavis, Koeln, Germany) that destained the gel, reduced the sample with dithiothreitol followed by alkylation with iodoacetamide. Next the gel pieces were rinsed with water and incubated with trypsin at 35°C (20 μg of trypsin per 96-well sample plate). The tryptic peptides generated were automatically eluted into a 96-well receiving plate that was subsequently inserted into an autosampler interfaced to the mass spectrometer.

LC/MS/MS of protein digests -- A QSTAR Pulsar *i* quadrupole time-of-flight (TOF) mass spectrometer (AB Sciex, Toronto, Canada) equipped with nano-electrospray source and nano-flow liquid chromatograph and autosampler was used to perform ESI-MS/MS of the tryptic digests (141).

Database construction and searches -- *Methanocaldococcus jannaschii* protein sequences were downloaded from the NCBI database, and a file of contaminant protein sequences was appended (cRAP or **c**ommon **R**epository of **A**dventitious **P**roteins from http://www.thegpm.org/crap/index.html) to create the target database. The use of a decoy database has become a routine procedure (142) and accordingly we created a reversed-sequence decoy database from the target database by using the "Edit FASTA database" function in Scaffold (http://www.proteomesoftware.com/). The decoy and target databases were then appended and the target-decoy database was used for MS/MS spectra queries. Analyst QS WIFF data files were first analyzed using Mascot (Matrix Science, London, UK; version 2.1) and the extracted spectral files (MGF) so generated were then analyzed using X!Tandem (http://www.thegpm.org/; Version: CYCLONE (2010.12.01.1). Variable modifications for both search engines were set as: +1 on asparagine and glutamine (deamidation), +16 on methionine (oxidation) and +57 on cysteine (carbamidomethyl). Following the initial database search by

Mascot and X! Tandem, the resulting .dat and .xml search results files were combined, analyzed, validated and visualized using Scaffold (http://www.proteomesoftware.com/). Scaffold was set to require a minimum of 5 peptides of 95% probability with a mass accuracy of 50 ppm or less and a protein probability of 99%. Using these settings 149 proteins having a calculated false discovery rate of 0 were detected. Since the information available on the NCBI database for *M. jannaschii* ORFs is not up to date, wherever possible we verified the annotated functions of the proteins detected in the mass spectrometric analysis through literature review. Functions were also assigned to several hypothetical proteins via homology searches using the non-redundant protein databases.

Partial Purification of *M. jannaschii* F_{420}-Dependent Sulfite Reductase (Fsr) and Preparation of Oxidized Enzyme. *M. jannaschii* was grown with 2 mM sulfite as sole sulfur source. Cells were harvested anaerobically under a mixture of N_2, CO_2, and H_2 (19:76:5 v/v). One gram *M. jannaschii* wet cell pellet was resuspended in 4 mL anaerobic 25 mM potassium phosphate buffer pH 7.0. Cells were lysed by osmotic shock and passage through a 22 Gauge needle inside an anaerobic chamber as described above and the lysate was centrifuged (4^{o}C, 20,000 x g, 20 min). Ammonium sulfate was added to 65% saturation to the supernatant. Precipitated proteins were removed by centrifugation (4^{o}C, 18,000 x g, 30 min) and the resulting anaerobic supernatant containing Fsr was oxidized by aerobic dialysis for 4 h vs. 1 L 25 mM potassium phosphate buffer, pH 7.0, containing 10% glycerol. The oxidized preparation was then put under a N_2 atmosphere by three alternate cycles of evacuation and pressurization with N_2 (95).

F_{420}-Dependent Sulfite Reductase (Fsr) Activation Assay. Partially purified Fsr, 28.7 μg, was incubated (5 min at 65^{o}C and then 20 min at 25^{o}C) in a solution containing 50 mM potassium phosphate buffer, pH 7.0; 100 mM KCl; 20 μM Trx1 and 1 mM DTT (final vol, 200 μL). One hundred microliter of this mixture was used to assay F_{420}-dependent sulfite reductase activity as previously (93) except that the assay mixture contained 100 mM KCl. KCl was found to enhance Fsr activity (D. Susanti and B. Mukhopadhyay, unpublished).

Oxidation of F_{420}-dependent Methylenetetrahydromethanopterin Dehydrogenase (Mtd)

Purified Mtd was incubated with Aldrithiol-2 (final concentration, 100 μM) at 25^{o}C for an hour. To remove the excess Aldrithiol-2 the solution (4 mL) was dialyzed vs. 1 L of a solution

containing 50 mM potassium phosphate buffer pH 7.0 and 10% (w/v) glycerol with three changes of dialysis solution. The oxidized enzyme preparation was then made anaerobic as described above.

Methylentetrahydromethanopterin Dehydrogenase (Mtd) Assay

Five microliter of 50 μM Mtd was incubated (5 min at 65^{o}C and then 20 min at 25^{o}C) in a solution containing 100 mM potassium phosphate buffer, pH 7.0; 0.5 M KCl; 5 μM Trx1 and 0.05 mM DTT (final volume, 0.15 ml). Twenty microliter of the mixture was used to assay Mtd activity as in (95), except for replacement of tetrahydromethanopterin with tetrahydrosarcinapterin and for changes in phosphate buffer and KCl concentrations (KCl has been found to enhance Mtd activity, D. Susanti and B. Mukhopadhyay, unpublished).

Search for Thioredoxin Homologs in Methanogenic Archaeal Genomes and Phylogenetic Tree Reconstructions. *M. jannaschii* Trx 1 (Mj_0307) and Trx of *E. coli* (Ec-TrxA) were used as queries for searching Trx homologs in the methanogen genome sequences that are available in the non-redundant database of the NCBI. Iterative BLAST searches (Psi-BLAST) were performed with 10 iterations using e-value threshold of 1e-4. From the resulting output, Trx homologs were identified manually by the existence of the C-X-X-C motif and the number of amino acid residues (Trxs typically fall in the 70 – 110 aa range (143)). Phylogenetic tree reconstructions for 16S rRNA gene sequences were performed as described previously (101).

4.7 REFERENCES

1. Holmgren A (1989) Thioredoxin and glutaredoxin systems. *The Journal of biological chemistry* 264(24):13963-13966.
2. Atkinson HJ & Babbitt PC (2009) An atlas of the thioredoxin fold class reveals the complexity of function-enabling adaptations. *PLoS computational biology* 5(10):e1000541.
3. Meyer Y, Buchanan BB, Vignols F, & Reichheld JP (2009) Thioredoxins and glutaredoxins: unifying elements in redox biology. *Annual review of genetics* 43:335-367.
4. Asahi T, Bandurski RS, & Wilson LG (1961) Yeast sulfate-reducing system. II. Enzymatic reduction of protein disulfide. *The Journal of biological chemistry* 236:1830-1835.
5. Blacks S, Harte, E.M., Hudson, B., Wartofsky, L. (1960) A specific enzymatic reduction of L(-) methionine sulfoxide and a related non-specific reduction of disulfides. *J. Bio.Chem.* 235:2910-2916.
6. Laurent TC, Moore EC, & Reichard P (1964) Enzymatic Synthesis of Deoxyribonucleotides: IV. Isolation and Characterization of Thioredoxin, The Hydrogen Donor from *Escherichia coli* B. *Journal of Biological Chemistry* 239(10):3436-3444.
7. Chae HZ, Chung SJ, & Rhee SG (1994) Thioredoxin-dependent peroxide reductase from yeast. *The Journal of biological chemistry* 269(44):27670-27678.
8. Hernandez HH, Jaquez OA, Hamill MJ, Elliott SJ, & Drennan CL (2008) Thioredoxin reductase from *Thermoplasma acidophilum*: a new twist on redox regulation. *Biochemistry* 47(37):9728-9737.
9. Jeon SJ & Ishikawa K (2002) Identification and characterization of thioredoxin and thioredoxin reductase from *Aeropyrum pernix* K1. *European journal of biochemistry / FEBS* 269(22):5423-5430.
10. Kashima Y & Ishikawa K (2003) A hyperthermostable novel protein-disulfide oxidoreductase is reduced by thioredoxin reductase from hyperthermophilic archaeon *Pyrococcus horikoshii*. *Archives of Biochemistry and Biophysics* 418(2):179-185.
11. Grimaldi P, *et al.* (2008) Characterisation of the components of the thioredoxin system in the archaeon *Sulfolobus solfataricus*. *Extremophiles : life under extreme conditions* 12(4):553-562.
12. Esposito L, *et al.* (2012) Crystallographic and spectroscopic characterizations of *Sulfolobus solfataricus* TrxA1 provide insights into the determinants of thioredoxin fold stability. *Journal of Structural Biology* 177(2):506-512.
13. Ruggiero A, *et al.* (2009) Crystallization and preliminary X-ray crystallographic analysis of two dimeric hyperthermostable thioredoxins isolated from *Sulfolobus solfataricus*. *Acta Crystallographica Section F* 65(6):604-607.
14. McFarlan SC, Terrell CA, & Hogenkamp HP (1992) The purification, characterization, and primary structure of a small redox protein from *Methanobacterium thermoautotrophicum*, an archaebacterium. *The Journal of biological chemistry* 267(15):10561-10569.
15. Amegbey GY, Monzavi H, Habibi-Nazhad B, Bhattacharyya S, & Wishart DS (2003) Structural and functional characterization of a thioredoxin-like protein (Mt0807) from *Methanobacterium thermoautotrophicum*. *Biochemistry* 42(26):8001-8010.
16. Bhattacharyya S, *et al.* (2002) Identification of a novel archaebacterial thioredoxin: determination of function through structure. *Biochemistry* 41(15):4760-4770.
17. Lee DY, Ahn B-Y, & Kim K-S (2000) A Thioredoxin from the Hyperthermophilic Archaeon *Methanococcus jannaschii* Has a Glutaredoxin-like Fold but Thioredoxin-like Activities. *Biochemistry* 39(22):6652-6659.
18. Jones WJ, Leigh JA, Mayer F, Woese CR, & RS W (1983) *Methanococcus jannaschii* sp. nov., an extreme thermophilic methanogen from a submarine hydrothermal vent. *Archives of microbiology* 136:254-261.
19. JA L (2002) Evolution of energy metabolism. *Biodiversity of microbial life: foundation of earth biosphere*, eds Staley J & Reysenbach A (John Wiley & Sons, New York), pp 103-120.

20. Altschul SF, *et al.* (1997) Gapped BLAST and PSI-BLAST: a new generation of protein database search programs. *Nucleic acids research* 25(17):3389-3402.
21. Kurr M, *et al.* (1991) *Methanopyrus kandleri*, gen. and sp. nov. represents a novel group of hyperthermophilic methanogens, growing at 110°C. *Archives of microbiology* 156(4):239-247.
22. Huber R, Kurr M, Jannasch HW, & Stetter KO (1989) A novel group of abyssal methanogenic archaebacteria (*Methanopyrus*) growing at 110^{o}C. *Nature* 342:833–836
23. Cave JW, *et al.* (2001) Solution nuclear magnetic resonance structure of a protein disulfide oxidoreductase from *Methanococcus jannaschii*. *Protein science : a publication of the Protein Society* 10(2):384-396.
24. Slesarev AI, *et al.* (2002) The complete genome of hyperthermophile *Methanopyrus kandleri* AV19 and monophyly of archaeal methanogens. *Proceedings of the National Academy of Sciences* 99(7):4644-4649.
25. Jeanthon C, *et al.* (1998) *Methanococcus infernus* sp. nov., a novel hyperthermophilic lithotrophic methanogen isolated from a deep-sea hydrothermal vent. *International Journal of Systematic Bacteriology* 48(3):913-919.
26. The Joint-Genome Institute UDoE (2009) (The Joint-Genome Institute, US Department of Energy).
27. Mehta MP & Baross JA (2006) Nitrogen fixation at 92 degrees C by a hydrothermal vent archaeon. *Science* 314(5806):1783-1786.
28. Jeanthon C, *et al.* (1999) *Methanococcus vulcanius* sp. nov., a novel hyperthermophilic methanogen isolated from East Pacific Rise, and identification of *Methanococcus* sp. DSM 4213Tas *Methanococcus fervens* sp. nov. *International Journal of Systematic Bacteriology* 49(2):583-589.
29. Bult CJ, *et al.* (1996) Complete genome sequence of the methanogenic archaeon, *Methanococcus jannaschii*. *Science* 273(5278):1058-1073.
30. Jones WJ, Leigh JA, Mayer F, Woese CR, & Wolfe RS (1983) *Methanococcus jannaschii* sp. nov., an extremely thermophilic methanogen from a submarine hydrothermal vent. *Archives of microbiology* 136(4):254-261.
31. Burggraf S, *et al.* (1990) *Methanococcus igneus* sp. nov., a novel hyperthermophilic methanogen from a shallow submarine hydrothermal system. *Syst Appl Microbiol.* 13:263-269.
32. Takai K, Inoue A, & Horikoshi K (2002) *Methanothermococcus okinawensis* sp. nov., a thermophilic, methane-producing archaeon isolated from a Western Pacific deep-sea hydrothermal vent system. *International journal of systematic and evolutionary microbiology* 52(4):1089-1095.
33. Health NCfBIotNIo ((National Center for Biotechnology Information of the National Institutes of Health).
34. Kendall MM, *et al.* (2006) *Methanococcus aeolicus* sp. nov., a mesophilic, methanogenic archaeon from shallow and deep marine sediments. *International journal of systematic and evolutionary microbiology* 56(Pt 7):1525-1529.
35. Hendrickson EL, *et al.* (2004) Complete Genome Sequence of the Genetically Tractable Hydrogenotrophic Methanogen Methanococcus maripaludis. *Journal of bacteriology* 186(20):6956-6969.
36. Jones WJ, Paynter MJB, & Gupta R (1983) Characterization of *Methanococcus maripaludis* sp. nov., a new methanogen isolated from salt marsh sediment. *Archives of microbiology* 135(2):91-97.
37. Whitman WB, Shieh J, Sohn S, Caras DS, & Premachandran U (1986) Isolation and characterization of 22 mesophilic *Methanococci*. *Systematic and Applied Microbiology* 7(2–3):235-240.
38. Ward JM (1970) Master (University of Florida, Gainesville, Florida).
39. Stadtman TC & Barker HA (1951) Studies on the methane fermentation X: A New Formate-Decomposing Bacterium, *Methanococcus vannielii*. *Journal of bacteriology* 62(3):269-280.

40. Stetter KO, *et al.* (1981) *Methanothermus fervidus*, sp. nov., a novel extremely thermophilic methanogen isolated from an Icelandic hot spring. *Zentralblatt für Bakteriologie Mikrobiologie und Hygiene: I. Abt. Originale C: Allgemeine, angewandte und ökologische Mikrobiologie* 2(2):166-178.
41. Anderson I, *et al.* (2010) Complete genome sequence of *Methanothermus fervidus* type strain (V24S). *Standards in genomic sciences* 3(3):315-324.
42. Liesegang H, *et al.* (2010) Complete Genome Sequence of *Methanothermobacter marburgensis*, a Methanoarchaeon Model Organism. *Journal of bacteriology* 192(21):5850-5851.
43. Zeikus JG & Wolee RS (1972) *Methanobacterium thermoautotrophicus* sp. n., an Anaerobic, Autotrophic, Extreme Thermophile. *Journal of bacteriology* 109(2):707-713.
44. Smith DR, *et al.* (1997) Complete genome sequence of *Methanobacterium thermoautotrophicum* deltaH: functional analysis and comparative genomics. *Journal of bacteriology* 179(22):7135-7155.
45. Leahy SC, *et al.* (2010) The Genome Sequence of the Rumen Methanogen *Methanobrevibacter ruminantium* Reveals New Possibilities for Controlling Ruminant Methane Emissions. *PLoS ONE* 5(1):e8926.
46. Smith PH & Hungate RE (1958) Isolation and characterization of *Methanobacterium ruminantium* n. sp. *Journal of bacteriology* 75(6):713-718.
47. Miller TL, Wolin MJ, de Macario EC, & Macario AJ (1982) Isolation of *Methanobrevibacter smithii* from human feces. *Applied and environmental microbiology* 43(1):227-232.
48. Samuel BS, *et al.* (2007) Genomic and metabolic adaptations of Methanobrevibacter smithii to the human gut. *Proceedings of the National Academy of Sciences* 104(25):10643-10648.
49. Fricke WF, *et al.* (2006) The Genome Sequence of *Methanosphaera stadtmanae* Reveals Why This Human Intestinal Archaeon Is Restricted to Methanol and H_2 for Methane Formation and ATP Synthesis. *Journal of bacteriology* 188(2):642-658.
50. Miller TL & Wolin MJ (1985) *Methanosphaera stadtmanae* gen. nov., sp. nov.-a species that forms methane by reducing methanol with hydrogen. *Arch. Microbiol.* 141:116-122.
51. Cadillo-Quiroz H, Yavitt JB, & Zinder SH (2009) Methanosphaerula palustris gen. nov., sp. nov., a hydrogenotrophic methanogen isolated from a minerotrophic fen peatland. *International journal of systematic and evolutionary microbiology* 59(5):928-935.
52. Anderson I, *et al.* (2009) Genomic Characterization of *Methanomicrobiales* Reveals Three Classes of Methanogens. *PLoS ONE* 4(6):e5797.
53. Qian Z & Zhu J (1987) Isolation and characterization of Methanospirillum hungatei JZ1. *Acta Microbiologica Sinica* 27(3):201-205.
54. Bräuer SL, Cadillo-Quiroz H, Ward RJ, Yavitt JB, & Zinder SH (2011) Methanoregula boonei gen. nov., sp. nov., an acidiphilic methanogen isolated from an acidic peat bog. *International journal of systematic and evolutionary microbiology* 61(1):45-52.
55. Brambilla E, *et al.* (2010) Complete genome sequence of Methanoplanus petrolearius type strain (SEBR 4847). *Standards in genomic sciences* 3(2):203-211.
56. Ollivier B, *et al.* (1997) *Methanoplanus petrolearius* sp. nov., a novel methanogenic bacterium from an oil-producing well. *FEMS microbiology letters* 147(1):51-56.
57. Anderson IJ, *et al.* (2009) *Complete genome sequence of Methanocorpusculum labreanum type strain Z*
58. Anderson IJ, *et al.* (2009) Complete genome sequence of Methanoculleus marisnigri Romesser et al. 1981 type strain JR1. *Standards in genomic sciences* 1(2):189-196.
59. Romesser JA, Wolfe RS, Mayer F, Spiess E, & Walther-Mauruschat A (1979) *Methanogenium*, a new genus of marine methanogenic bacteria, and characterization of *Methanogenium cariaci* sp. nov. and *Methanogenium marisnigri* sp. nov. *Archives of microbiology* 121(2):147-153.
60. Bernard M, Ollivier, Mah RA, Garcia JL, & Boonei DR (1986) Isolation and Characterization of *Methanogenium bourgense* sp.nov. . *International Journal of Systematic Bacteriology* 36(2):297-301.

61. Maus I, *et al.* (2012) Complete Genome Sequence of the Hydrogenotrophic, Methanogenic Archaeon *Methanoculleus bourgensis* Strain MS2T, Isolated from a Sewage Sludge Digester. *Journal of bacteriology* 194(19):5487-5488.
62. Sakai S, Conrad R, Liesack W, & Imachi H (2010) *Methanocella arvoryzae* sp. nov., a hydrogenotrophic methanogen isolated from rice field soil. *International journal of systematic and evolutionary microbiology* 60(12):2918-2923.
63. Erkel C, Kube M, Reinhardt R, & Liesack W (2006) Genome of Rice Cluster I Archaea—the Key Methane Producers in the Rice Rhizosphere. *Science* 313(5785):370-372.
64. Lü Z & Lu Y (2012) *Methanocella conradii* sp. nov., a Thermophilic, Obligate Hydrogenotrophic Methanogen, Isolated from Chinese Rice Field Soil. *PLoS ONE* 7(4):e35279.
65. Lü Z & Lu Y (2012) Complete Genome Sequence of a Thermophilic Methanogen, *Methanocella conradii* HZ254, Isolated from Chinese Rice Field Soil. *Journal of bacteriology* 194(9):2398-2399.
66. Sakai S, *et al.* (2008) *Methanocella paludicola* gen. nov., sp. nov., a methane-producing archaeon, the first isolate of the lineage 'Rice Cluster I', and proposal of the new archaeal order *Methanocellales* ord. nov. *International journal of systematic and evolutionary microbiology* 58(4):929-936.
67. Sakai S, *et al.* (2007) Isolation of Key Methanogens for Global Methane Emission from Rice Paddy Fields: a Novel Isolate Affiliated with the Clone Cluster Rice Cluster I. *Applied and environmental microbiology* 73(13):4326-4331.
68. Sakai S, *et al.* (2011) Genome Sequence of a Mesophilic Hydrogenotrophic Methanogen *Methanocella paludicola*, the First Cultivated Representative of the Order *Methanocellales. PLoS ONE* 6(7):e22898.
69. Zhu J, *et al.* (2012) The Genome Characteristics and Predicted Function of Methyl-Group Oxidation Pathway in the Obligate Aceticlastic Methanogens, *Methanosaeta* spp. *PLoS ONE* 7(5):e36756.
70. Ma K, Liu X, & Dong X (2006) *Methanosaeta harundinacea* sp. nov., a novel acetate-scavenging methanogen isolated from a UASB reactor. *International journal of systematic and evolutionary microbiology* 56(1):127-131.
71. Patel GB & Sprott GD (1990) *Methanosaeta concilii* gen. nov., sp. nov. ("*Methanothrix concilii*") and *Methanosaeta thermoacetophila* nom. rev., comb. nov. *International Journal of Systematic Bacteriology* 40(1):79-82.
72. Barber RD, *et al.* (2011) Complete Genome Sequence of *Methanosaeta concilii*, a Specialist in Aceticlastic Methanogenesis. *Journal of bacteriology* 193(14):3668-3669.
73. T.N. Z & G.A. Z (1987) *Methanohalobium evestigatus*, n. gen., n. sp. The extremely halophilic methanogenic Archaebacterium. *Dokl. Akad. Nauk SSSR* 293:464-468.
74. Mathrani I, Boone D, Mah R, Fox G, & Lau P (1988) *Methanohalophilus zhilinae* sp. nov., an alkaliphilic, halophilic, methylotrophic methanogen. *Int J Syst Bacteriol* 38(2):139-142.
75. Allen MA, *et al.* (2009) The genome sequence of the psychrophilic archaeon, Methanococcoides burtonii: the role of genome evolution in cold adaptation. *The ISME journal* 3(9):1012-1035.
76. Franzmann PD, Springer, N., Ludwig, W., Conway De Macario, E., Rohde, M. (1992) A Methanogenic Archaeon from Ace Lake, Antarctica: *Methanococcoides burtonii* sp. nov. *Systematic and Applied Microbiology* 15(4).
77. Paterek JR, Smith, P.H. (1988) *Methanohalophilus mahii* gen. nov. sp. nov. a Methylotrophic Halophilic Methanogen. *International Journal of Systematic Bacteriology* 38(1):122-123.
78. Spring S, *et al.* (2010) The genome sequence of *Methanohalophilus mahii* SLP(T) reveals differences in the energy metabolism among members of the *Methanosarcinaceae* inhabiting freshwater and saline environments. *Archaea* 2010:690737.
79. Chen Z, Yu H, Li L, Hu S, & Dong X (2012) The genome and transcriptome of a newly described psychrophilic archaeon, *Methanolobus psychrophilus* R15, reveal its cold adaptive characteristics. *Environmental Microbiology Reports* 4(6):633-641.

80. Zhang G, Jiang N, Liu X, & Dong X (2008) Methanogenesis from Methanol at Low Temperatures by a Novel Psychrophilic Methanogen, "*Methanolobus psychrophilus*" sp. nov., Prevalent in Zoige Wetland of the Tibetan Plateau. *Applied and environmental microbiology* 74(19):6114-6120.
81. Maeder DL, *et al.* (2006) The *Methanosarcina barkeri* Genome: Comparative Analysis with *Methanosarcina acetivorans* and *Methanosarcina mazei* Reveals Extensive Rearrangement within *Methanosarcinal* Genomes. *Journal of bacteriology* 188(22):7922-7931.
82. Kandler O & Hippe H (1977) Lack of peptidoglycan in the cell walls of *Methanosarcina barkeri*. *Archives of microbiology* 113(1-2):57-60.
83. U D, *et al.* (2002) The genome of *Methanosarcina mazei*: evidence for lateral gene transfer between bacteria and archaea. *J Mol Microbiol Biotechnol.* 4(4):453-461.
84. Deppenmeier U, Blaut M, Jussofie A, & Gottschalk G (1988) A methyl-CoM methylreductase system from methanogenic bacterium strain Go 1 not requiring ATP for activity. *FEBS letters* 241(1-2):60-64.
85. Sowers K, Baron S, & Ferry J (1984) *Methanosarcina acetivorans* sp. nov., an Acetotrophic Methane-Producing Bacterium Isolated from Marine Sediments. *Appl Environ Microbiol.* 47(5):971-978.
86. Galagan JE, *et al.* (2002) The genome of *M. acetivorans* reveals extensive metabolic and physiological diversity. *Genome research* 12(4):532-542.
87. Pieulle L, *et al.* (2011) Study of the Thiol/Disulfide Redox Systems of the Anaerobe *Desulfovibrio vulgaris* Points Out Pyruvate:Ferredoxin Oxidoreductase as a New Target for Thioredoxin 1. *Journal of Biological Chemistry* 286(10):7812-7821.
88. Yano H, Wong JH, Lee YM, Cho MJ, & Buchanan BB (2001) A strategy for the identification of proteins targeted by thioredoxin. *Proceedings of the National Academy of Sciences of the United States of America* 98(8):4794-4799.
89. Wong JH, *et al.* (2003) Unraveling thioredoxin-linked metabolic processes of cereal starchy endosperm using proteomics. *FEBS Letters* 547(1–3):151-156.
90. Balmer Y, Vensel WH, Hurkman WJ, & Buchanan BB (2006) Thioredoxin target proteins in chloroplast thylakoid membranes. *Antioxidants & redox signaling* 8(9-10):1829-1834.
91. Alkhalfioui F, *et al.* (2007) Thioredoxin-linked proteins are reduced during germination of Medicago truncatula seeds. *Plant physiology* 144(3):1559-1579.
92. Vensel WH, Dupont FM, Sloane S, & Altenbach SB (2011) Effect of cleavage enzyme, search algorithm and decoy database on mass spectrometric identification of wheat gluten proteins. *Phytochemistry* 72(10):1154-1161.
93. Johnson EF & Mukhopadhyay B (2005) A new type of sulfite reductase, a novel coenzyme F_{420}-dependent enzyme, from the methanarchaeon *Methanocaldococcus jannaschii*. *The Journal of biological chemistry* 280(46):38776-38786.
94. Spencer R, Fisher J, & Walsh C (1976) Preparation, characterization, and chemical properties of the flavin coenzyme analogues 5-deazariboflavin, 5-deazariboflavin 5'-phosphate, and 5-deazariboflavin 5'-diphosphate, 5'leads to5'-adenosine ester. *Biochemistry* 15(5):1043-1053.
95. Mukhopadhyay B & Daniels L (1989) Aerobic purification of N5,N10-methylenetetrahydromethanopterin dehydrogenase, separated from N5,N10-methylenetetrahydromethanopterin cyclohydrolase, from *Methanobacterium thermoautotrophicum* strain Marburg. *Canadian journal of microbiology* 35(4):499-507.
96. Boone DR, Whitman WB, & Rouviere P (1993) Diversity and taxonomy of methanogens. *Methanogenesis: ecology, physiology, biochemistry and genetics.*, ed Ferry JG (Chapman and Hall, New York, NY), pp 35-80.
97. Kiener A & Leisinger T (1983) Oxygen sensitivity of methanogenic bacteria. *Syst Appl Microbiol* 4(3):305-312.
98. Katti SK, LeMaster DM, & Eklund H (1990) Crystal structure of thioredoxin from *Escherichia coli* at 1.68 Å resolution. *Journal of molecular biology* 212(1):167-184.

99. Chivers PT, Prehoda KE, & Raines RT (1997) The CXXC motif: a rheostat in the active site. *Biochemistry* 36(14):4061-4066.
100. Quan S, Schneider I, Pan J, Von Hacht A, & Bardwell JC (2007) The CXXC motif is more than a redox rheostat. *The Journal of biological chemistry* 282(39):28823-28833.
101. Susanti D & Mukhopadhyay B (2012) An intertwined evolutionary history of methanogenic archaea and sulfate reduction. *PLoS One* 7(9):e45313.
102. Johnson EF & Mukhopadhyay B (2007) A novel coenzyme F_{420}-dependent sulfite reductase and a small size sulfite reductase in methanogenic archaea. *Proceedings of the International Symposium on Microbial Sulfur Metabolism*, eds Dahl C & Friedrich CG (Springer, New York, N.Y.).
103. Johnson EF & Mukhopadhyay B (2008) Coenzyme F_{420}-dependent sulfite reductase-enabled sulfite detoxification and use of sulfite as a sole sulfur source by *Methanococcus maripaludis*. *Applied and environmental microbiology* 74(11):3591-3595.
104. Buchanan BB, Holmgren A, Jacquot J-P, & Scheibe R (2012) Fifty years in the thioredoxin field and a bountiful harvest. *Biochimica et Biophysica Acta (BBA) - General Subjects* 1820(11):1822-1829.
105. Montrichard F, *et al.* (2009) Thioredoxin targets in plants: the first 30 years. *Journal of proteomics* 72(3):452-474.
106. Bult CJ, *et al.* (1996) Complete genome sequence of the methanogenic archaeon, *Methanococcus jannaschii*. *Science* 273(5278):1058-1073.
107. Zinder SH (1993) Physiological ecology of methanogens. *Methanogenesis: ecology, physiology, biochemistry, and genetics*, ed Ferry JG (Chapman and Hall, N.Y.), pp 128-206.
108. Jannasch HW & Mottl MJ (1985) Geomicrobiology of deep-sea hydrothermal vents. *Science* 229(4715):717-725.
109. Jannasch HW (1989) Chemosynthetically sustained ecosystems in the deep sea. *Autotrophic bacteria*, eds Schlegel HG & Bowien B (Springer Verlag, New York), pp 147-166.
110. McCollom TM & Shock EL (1997) Geochemical constraints on chemolithoautotrophic metabolism by microorganisms in seafloor hydrothermal systems. *Geochim Cosmochim Acta*:4375-4391.
111. Xia Q, *et al.* (2009) Quantitative proteomics of nutrient limitation in the hydrogenotrophic methanogen *Methanococcus maripaludis*. *BMC microbiology* 9:149.
112. Kato S, Kosaka T, & Watanabe K (2008) Comparative transcriptome analysis of responses of *Methanothermobacter thermautotrophicus* to different environmental stimuli. *Environmental Microbiology* 10(4):893-905.
113. Mukhopadhyay B, Johnson EF, & Wolfe RS (2000) A novel pH2 control on the expression of flagella in the hyperthermophilic strictly hydrogenotrophic methanarchaeaon Methanococcus jannaschii. *Proceedings of the National Academy of Sciences of the United States of America* 97(21):11522-11527.
114. Morgan RM, Pihl TD, Nolling J, & Reeve JN (1997) Hydrogen regulation of growth, growth yields, and methane gene transcription in *Methanobacterium thermoautotrophicum* deltaH. *Journal of bacteriology* 179(3):889-898.
115. Mukhopadhyay B, Johnson EF, & Wolfe RS (2000) A novel pH2 control on the expression of flagella in the hyperthermophilic strictly hydrogenotrophic methanarchaeaon *Methanococcus jannaschii*. *Proceedings of the National Academy of Sciences* 97(21):11522-11527.
116. Reeve JN, Nolling J, Morgan RM, & Smith DR (1997) Methanogenesis: genes, genomes, and who's on first? *Journal of bacteriology* 179(19):5975-5986.
117. Simpson PG & Whitman WB (1993) Anabolic pathways in methanogens. *Methanogenesis: ecology, physiology, biochemistry, and genetics*, ed Ferry JG (Chapman & Hall, New York), pp 445-472.
118. Thauer RK (2012) The Wolfe cycle comes full circle. *Proceedings of the National Academy of Sciences of the United States of America* 109(38):15084-15085.

119. Balderston WL & Payne WJ (1976) Inhibition of methanogenesis in salt marsh sediments and whole-cell suspensions of methanogenic bacteria by nitrogen oxides. *Applied and environmental microbiology* 32(2):264-269.
120. Wedzicha BL (1992) Chemistry of sulphiting agents in food. *Food additives and contaminants* 9(5):449-459.
121. Wong JH, *et al.* (2004) Thioredoxin targets of developing wheat seeds identified by complementary proteomic approaches. *Phytochemistry* 65(11):1629-1640.
122. Graham DE, Graupner M, Xu H, & White RH (2001) Identification of coenzyme M biosynthetic 2-phosphosulfolactate phosphatase. A member of a new class of Mg(2+)-dependent acid phosphatases. *European journal of biochemistry / FEBS* 268(19):5176-5188.
123. Kumar JK, Tabor S, & Richardson CC (2004) Proteomic analysis of thioredoxin-targeted proteins in *Escherichia coli*. *Proceedings of the National Academy of Sciences of the United States of America* 101(11):3759-3764.
124. Balmer Y, *et al.* (2003) Proteomics gives insight into the regulatory function of chloroplast thioredoxins. *Proceedings of the National Academy of Sciences of the United States of America* 100(1):370-375.
125. Lowe J (1998) Crystal structure determination of FtsZ from *Methanococcus jannaschii*. *J Struct Biol* 124(2-3):235-243.
126. Lowe J & Amos LA (2000) Helical tubes of FtsZ from *Methanococcus jannaschii*. *Biological chemistry* 381(9-10):993-999.
127. Lowe J & Amos LA (1998) Crystal structure of the bacterial cell-division protein FtsZ. *Nature* 391(6663):203-206.
128. Bi EF & Lutkenhaus J (1991) FtsZ ring structure associated with division in *Escherichia coli*. *Nature* 354(6349):161-164.
129. König H & Stetter KO (1986) Studies on archaebacterial S-layers. *Systematic and Applied Microbiology* 7(2–3):300-309.
130. Poole LB (2007) The catalytic mechanism of peroxiredoxins. *Sub-cellular biochemistry* 44:61-81.
131. Sorek R, Lawrence CM, & Wiedenheft B (2013) CRISPR-Mediated Adaptive Immune Systems in Bacteria and Archaea. *Annu Rev Biochem* 82:237-266.
132. Russel M & Model P (1986) The role of thioredoxin in filamentous phage assembly. Construction, isolation, and characterization of mutant thioredoxins. *The Journal of biological chemistry* 261(32):14997-15005.
133. Tabor S, Huber HE, & Richardson CC (1987) *Escherichia coli* thioredoxin confers processivity on the DNA polymerase activity of the gene 5 protein of bacteriophage T7. *The Journal of biological chemistry* 262(33):16212-16223.
134. Buchanan BB, Schurmann P, Wolosiuk RA, & Jacquot JP (2002) The ferredoxin/thioredoxin system: from discovery to molecular structures and beyond. *Photosynth Res* 73(1-3):215-222.
135. Purwantini E, Mukhopadhyay B, Spencer RW, & Daniels L (1992) Effect of temperature on the spectral properties of coenzyme F_{420} and related compounds. *Analytical biochemistry* 205(2):342-350.
136. Mukhopadhyay B, Johnson EF, & Wolfe RS (1999) Reactor-scale cultivation of the hyperthermophilic methanarchaeon *Methanococcus jannaschii* to high cell densities. *Applied and environmental microbiology* 65(11):5059-5065.
137. Rocco CR, Dennison KL, Klenchin VA, Rayment I, & Escalante-Semerena JC (2008) Construction and Use of New Cloning Vectors for the Rapid Isolation of Recombinant Proteins from *Escherichia coli*. *Plasmid* 59(3):231-237.
138. Case CL, Rodriguez JR, & Mukhopadhyay B (2009) Characterization of an NADH oxidase of the flavin-dependent disulfide reductase family from *Methanocaldococcus jannaschii*. *Microbiology* 155(Pt 1):69-79.
139. Mukhopadhyay B, Purwantini E, Pihl TD, Reeve JN, & Daniels L (1995) Cloning, sequencing, and transcriptional analysis of the coenzyme F_{420}-dependent methylene-5,6,7,8-

tetrahydromethanopterin dehydrogenase gene from *Methanobacterium thermoautotrophicum* strain Marburg and functional expression in *Escherichia coli*. *The Journal of biological chemistry* 270(6):2827-2832.

140. Holmgren A (1977) Bovine thioredoxin system. Purification of thioredoxin reductase from calf liver and thymus and studies of its function in disulfide reduction. *The Journal of biological chemistry* 252(13):4600-4606.
141. Vensel WH, *et al.* (2005) Developmental changes in the metabolic protein profiles of wheat endosperm. *Proteomics* 5(6):1594-1611.
142. Elias JE & Gygi SP (2007) Target-decoy search strategy for increased confidence in large-scale protein identifications by mass spectrometry. *Nature methods* 4(3):207-214.
143. Eklund H, Gleason FK, & Holmgren A (1991) Structural and functional relations among thioredoxins of different species. *Proteins* 11(1):13-28.

5 Ferredoxin:thioredoxin reductase (FTR) links the regulation of oxygenic photosynthesis to deeply-rooted bacteria

5.1 ABSTRACT

Ferredoxin-dependent thioredoxin reductase (FTR) is one of the major components of the ferredoxin:thioredoxin system (FTS). Function and mechanism of action of this enzyme have been studied extensively. However, little is known about its origin and evolution. To help fill this gap, we have taken advantage of available genome sequences to trace the origin of FTR. Our results suggested that (1) the catalytic subunit of FTR (FTRc) originated in deeply rooted microaerophilic, chemoauthotrophic bacteria where it appears to function in regulating CO_2 fixation by the reverse citric acid cycle; (2) FTRc was incorporated into oxygenic photosynthetic organisms without significant structural change except for the addition of a variable subunit (FTRv) to protect the Fe-S cluster against oxygen; (3) FTR is not universally present in oxygenic photosynthetic organisms, and in certain early representatives is seemingly functionally replaced by NADP-thioredoxin reductase (NTR); and (4) in a variety of bacteria and archaea, FTRc underwent structural diversification to meet the ecological needs.

5.2 INTRODUCTION

Discovered 35 years ago in studies on chloroplast enzymes, thioredoxin (Trx)-linked redox regulation is known to play a central role in a spectrum of processes in living cells (1-4). Events leading to the discovery and elucidation of the regulatory role of Trx have recently been recounted (5). It has become clear that despite an understanding of its mechanism, distribution and importance, little is known about how redox regulation originated and achieved its functional diversity.

To gain insight into this problem, we have initiated a study to analyze relevant genes in organisms whose genomes have been sequenced. Because it is best understood, we focused on oxygenic photosynthesis, specifically on the key enzyme

ferredoxin:thioredoxin reductase (FTR), which links light (via ferredoxin) to the regulation of target enzymes (via Trx) (6, 7). We have found that the catalytic subunit of FTR (FTRc), surprisingly, has deep phylogenetic roots and apparently originated in microaerophilic bacteria where it functions to link Trx to the regulation of CO_2 fixation—namely, by the reverse citric acid (RCA) cycle (8). When incorporated into certain oxygen-evolving bacteria, FTRc underwent little structural change, but it acquired a variable subunit (FTRv) for protecting the labile 4Fe-4S center from oxidative inactivation (9). In these organisms, FTR assumed a function in the regulation of the Calvin-Benson (CB) cycle, initially via the oxidative regulation of phosphoribulokinase (PRK) (2, 10). With time, the regulatory role of FTR and Trx expanded to include the classical light-dark regulation of the Calvin-Benson cycle via PRK and other Trx-linked enzymes (6). Redox regulation by Trx was also extended to additional processes in plants as well as to other types of cells (1, 5, 11).

5.3 RESULTS

5.3.1 Genomic dissection of FTRc

A thorough analysis of the occurrence of FTR in genomic sequences deposited at NCBI has extended and confirmed previous reports of its distribution (12-14). As originally described, cyanobacterial and plastid FTR is a heterodimer composed of a catalytic subunit (FTRc), with a Fe_4-S_4 cluster and a redox-active disulfide at the catalytic center, and a variable subunit (FTRv), which is believed to have a structural role and does not participate in the catalytic reaction (9). A protein resembling FTRc has been found in certain methanogenic archaea and closely related euryarchaea, such as *Archaeoglobus*, and in bacteria, including both mesophiles and thermophiles, anaerobic chemolithotrophic bacteria and in deeply rooted microaerophiles.

5.3.2 Sequence features divide FTRc into different groups

The catalytic motif in the FTRc subunit, $\underline{C}^{55}PC^{57}...\underline{C}^{74}P\underline{C}^{76}…\underline{C}^{85}HC^{87}$ (numbers according to *Synechocystis* sp PCC 6803 sequence), contains four Cys (underlined) that coordinate a Fe_4-S_4 center; two other Cys, Cys57 and Cys87, form the redox-active disulfide (15). Most homolog sequences detected in this study include the characteristic catalytic motif, with some variations (Figs. 5.1 and 5.2). The phylogenetic reconstruction (Figs. 5.3 and 5.4) together with the relative differences and similarities in primary structure served as a convenient means to classify the different forms of

FTRc homologs. Based on phylogenetic relationships and domain organization, the FTR superfamily separates into seven distinct groups (Figs. 5.1, 5.2, 5.3 and 5.4). The groups have been classified according to their protein sequence similarity with plant-type FTRc as group I. Note that due to its limited sequence, Group VII is not included in phylogenetic analyses.

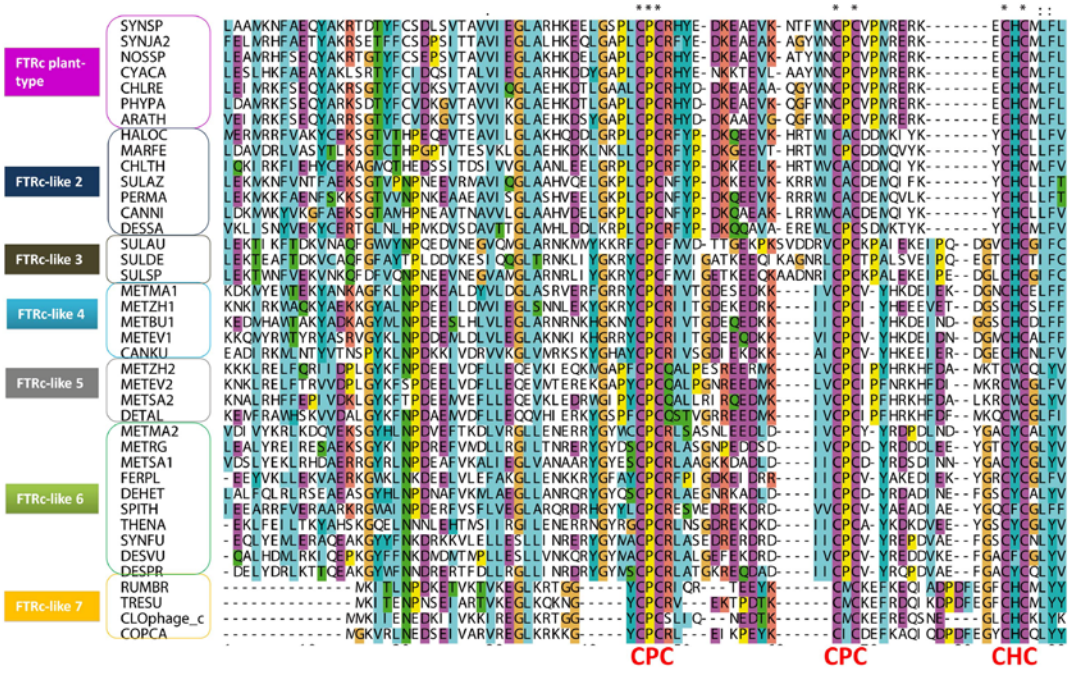

Figure 5.1 Multiple sequence alignment of the conserved core region of selected FTRc homologs. The alignment is displayed according to the default Clustal color scheme (16); asterisks indicate strictly conserved residues. The catalytic motif, CPC…CPC…CHC, is indicated. The different FTRc-homologs have been grouped according to sequence features (Fig. 2). Sequences are listed with abbreviations of the organism names. ARATH, *Arabidopsis thaliana*; CANKU, *Candidatus* Kuenenia stuttgartiensis; CANNI, *Candidatus* Nitrospira defluvii; CHLRE, *Chlamydomonas reinhardtii*; CHLTH, *Chloroherpeton thalassium*; CLOphage_C, *Clostridium* phage c-st; COPCA, *Coprococcus catus*; CYACA, *Cyanidium caldarium*; DEHET, *Dehalococcoides ethenogenes*; DESPR, *Desulfobulbus propionicus*; DESSA, *Desulfovibrio salexigens*; DESVU, *Desulfovibrio vulgaris*; DETAL, *Dethiobacter alkaliphilus*; FERPL, *Ferroglobus placidus*; HALOC, *Haliangium ochraceum*; MARFE, *Mariprofundus ferrooxydans*; METSA, *Methanocella paludicola SANAE*; METBU, *Methanococcoides burtonii*; METEV, *Methanohalobium evestigatum*; METMA, *Methanosarcina mazei*; METRG, *Methanothermobacter marburgensis*; METZH, *Methanosalsum zhilinae*; NOSSP, *Nostoc* sp PCC 7120; PERMA, *Persephonella marina*; PHYPA, *Physcomitrella patens*; RUMBR, *Ruminococcus bromii*; SPITH, *Spirochaeta thermophila*; SULAU, *Sulfurimonas autotrophica*; SULAZ, *Sulfurihydrogenibium azorense*; SULDN, *Sulfurimonas denitrificans*; SULDE,

Sulfurospirillum deleyianum; SULSP, *Sulfurovum* sp NBC37-1; SYNJA2, *Synechococcus* sp JA-2-3B'a(2-13); SYNSP, *Synechocystis* sp PCC 6803; SYNFU, *Syntrophobacter fumaroxidans*; THENA, *Thermodesulfobium narugense*; TRESU, *Treponema succinifaciens.*

Group I: FTRc-plant type

This group is composed exclusively of oxygenic phototrophs. It has the typical catalytic site signature $CPCX_{16}CPCX_8CHC$ (Figs. 5.1 and 5.2). Interestingly, not all oxygenic photosynthetic organisms possess FTR, e.g., *Gloeobacter violaceus*. This special cyanobacterium is considered the closest relative of the ancient cyanobacteria that gave rise to chloroplasts (17). FTR is also absent in *Prochlorococcus*, the so-called green oxyphotobacterium (18). FTRc homologs were, however, detected in eukaryotes with photosynthetic plastids acquired by secondary endosymbiosis, such as *Guillardia theta*, *Ectocarpus siliculosus* and *Bigelowiella natans* (19). However, other eukaryotes with non-photosynthetic plastids, such as apicomplexa (*Plasmodium falciparum*), lack FTRc like-sequences.

Group II: FTRc-like 2

Sequences from this group are characterized by the catalytic motif CPC $X_{16}CP/ACX_8CHC$ (Figs. 5.1 and 5.2). The group is restricted to a few phyla among eubacteria: *Aquificae*, two members of *Deltaproteobacteria*, single representatives of *Chloroflexi* and *Chlorobi*, and the sole member of the class *Zetaproteobacteria*. These are the best BLAST hits for FTRc plant type (e-values below 10^{-25}; alignment covered region over the whole sequence).

Group III: FTRc-like 3

The catalytic site signature of members of this group is similar to the Group I (plant-type): $CPCX_{11-18}CPCX_{13}CHC$, with some variation in the spacing among the motifs of the catalytic center (Figs. 5.1 and 5.2). This type of FTRc is found only in *Epsilonproteobacteria*. As a special feature, most members of group III contain a rhodanese domain fused at the C-terminus of the FTRc-like protein (Fig. 5.2). Exceptions are *Wolinella succinogenes* and *Nitratiruptor* sp. SB155-2. As typical rhodaneses, sequences of this group contain the conserved CxxGxR active-site loop (20).

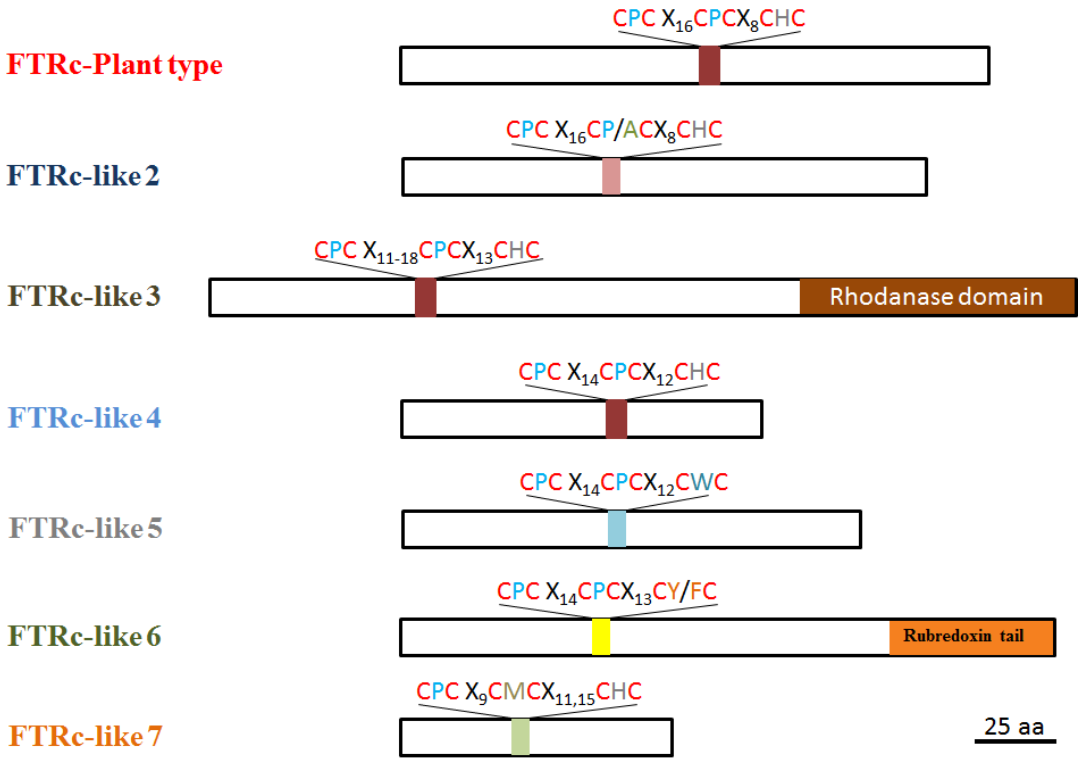

Figure 5.2 Bar diagram of different types of FTR. Bars shows primary sequence structures of various types of FTR and was drawn to scale. Colored-boxes indicate the active site of FTR that composed of two regulatory cys residues and Fe_4-S_4 center.

Group IV: FTRc-like 4

FTRc-like 4 sequences are found in some members of *Methanomicrobia* which are methanarchaea, two anaerobic ammonium-oxidizing (anammox) bacteria belonging to the phylum *Planctomycetes*, two representatives of *Firmicutes* and one *Proteobacterium*. Most representatives of this group have the conserved catalytic site $CPCX_{14}CPCX_{12}CHC$ (Figs. 5.1 and 5.2). Interestingly, the *Methanococcoides burtonii* gene (Mbur_0334) has an N-terminal extension that encodes a Trx-like protein with the catalytic motif CPPC. A closely related Trx gene forms an operon-like arrangement with the FTRc-like 4 gene in *Methanohalophilus mahii* and *Desulfotomaculum ruminis* genomes (Gene IDs: Mmah_0953/Mmah_0954; Desru_1975/Desru_1974, respectively).

Group V: FTRc-like 5

This group is present in only a few organisms, namely, four representatives of the *Methanomicrobia* class. When probing in the non-redundant NCBI protein database, including unfinished genomes, a member of this group was detected in *Dethiobacter*

alkaliphilus AHT1, a member of the order of *Clostridiales*. The sequences are characterized by the catalytic motif $CPCX_{14}CPCX_{12}CWC$ (Figs. 5.1 and 5.2). A block of genes including an FTRc-like FTR, a redoxin and Fdx-related Rieske type protein is found in the four *Methanomicrobia* genomes (21-24).

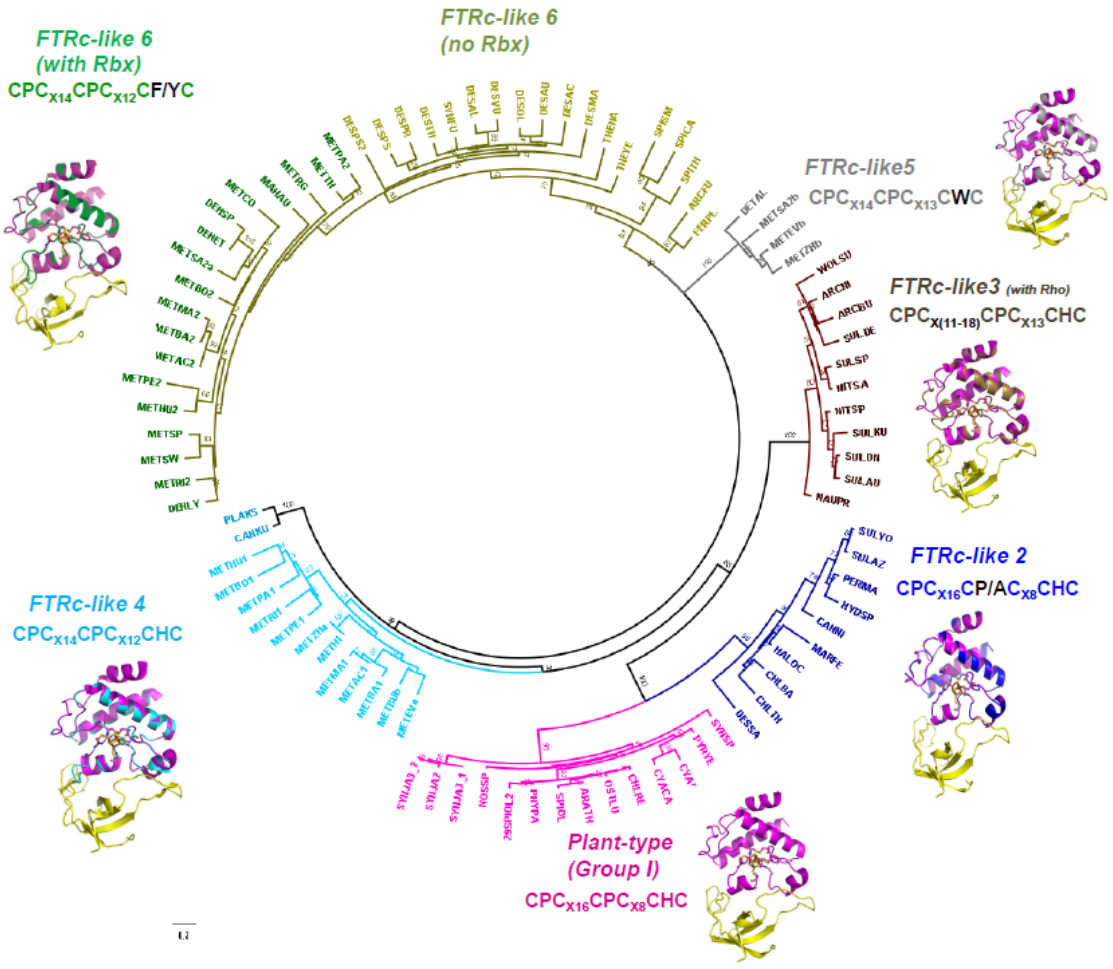

Figure 5.3 A maximum likelihood phylogenetic tree showing the evolutionary development of chloroplast FTR. The deduced tree provides a graphical representation of the different FTRc protein groups. The catalytic motif is indicated for each group together with the generated homology model. Boostrap values are shown in the nodes.

Group VI: FTRc-like 6

FTRc-like 6 sequences have the catalytic motif $CPCX_{14}CPCX_{12}CY/FC$ (Figs. 5.1 and 5.2). Representatives are present in several methanogenic archaea and a number of the eubacteria phyla. Some members of this group contain a rubredoxin (Rbx) domain fused at the C-terminus. These proteins are found in certain members of the methanoarchaeal classes of *Methanomicrobia* and *Methanobacteria*. *Chloroflexi* and

one member of *Firmicutes* are the bacteria that carry this version. Members of the *Archaeoglobi* class of archaea as well as certain bacteria, such as those belonging to the *Spirochaetes*, *Firmicutes* and *Nitrospirae*, and *Deltaproteobacteria*−showing the characteristic "PERRP" motif at the C-terminus of the FTRc-domain −lack the Rbx region. Notably, the FTRc-like gene is located next to an NrdH-redoxin gene in the genomes of all members of this group. This operon-like organization in the genome partly resembles the conserved FTRc-like and redoxin organization in Group V (see above). Indeed, the redoxin gene in this group is a homolog to that in Group IV. Significantly, in the sulfate reducing bacteria *Desulfotalea psychrophila* and *Desulfobulbus propionicus*, the FTRc-like and redoxin genes are fused in one gene resulting in a single polypeptide chain with the two functional domains (gene ID: DP2155, DP1729, Despr_2150). According to FSSP (families of structurally similar proteins) database (25), the NdrH-redoxin proteins from *M. mazei* (PDB code 3NZN) and *A. fulgidus* (PDB code 3IC4) are structurally related to small redox proteins in *E. coli* that contain a conserved CXXC motif, characterized by a glutaredoxin-like amino acid sequence and yet show a Trx-like activity (26).

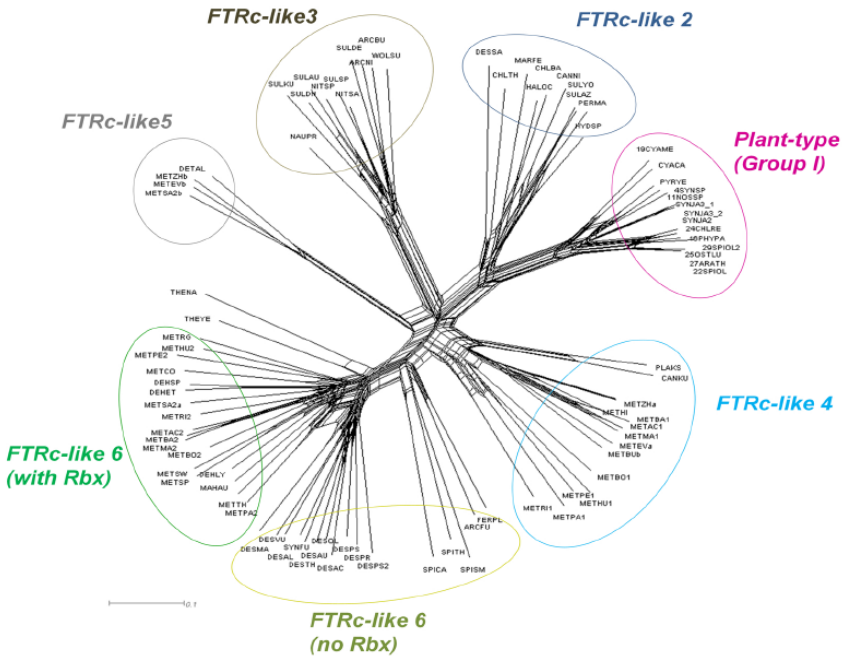

Figure 5.4 A phylogenetic network of FTR. The analysis was performed using the NeighborNet method implemented in the SplitsTree program (version 4.10) (27) as described in the Materials and Methods section.

Group VII: FTRc-like 7

Members of this group were detected in *Firmicutes* and one representative of the *Spirochaetes*. In addition, homologous genes were detected in two bacteriophages from *C. botulinum* strains, C-Stockholm and D-1873. It is of interest that the hosts of these viruses do not have an FTRc-like homologue. This type of FTRc, which is distantly related to the plant-type (Fig. 5.1), shows a $CPCX_9CMCX_{11,15}CHC$ catalytic motif. Due to the low sequence similarity this type has not been included in the phylogenetic analysis. The FTRc-like 7 protein sequences lack important secondary structure elements thus representing a minimal FTRc that might be unstable.

5.3.3 FTRc structural features

The high resolution X-ray structure of FTRc shows that the protein is mainly α-helical, with loops connecting the helices that contain redox-active Cys and residues involved in Fe-S coordination (9). The electron transfer capacity of FTRc is well explained by its structural features (9, 28). FTRc is a flat molecule with the Fe_4-S_4 cluster located in the center of the catalytic subunit. On one side of FTRc, the active disulfide covers the Fe-S cluster and forms part of the Trx-binding site. On the opposite side (the Fdx-binding site), the $C^{74}PC^{76}$ motif surrounds and coordinates the FeS cluster, likely facilitating electron transfer upon Fdx binding (28, 29).

5.4 DISCUSSION

5.4.1 FTRc evolutionary reconstruction

Using knowledge from complete genomes, we have investigated the path of the evolution of light/dark-regulation linked to the FTS in plants. Our results have shown that homologs of FTRc, the catalytic subunit of plant-type FTR, occur not only in oxygenic photosynthetic organisms, but also in archaea and evolutionarily deeply rooted bacteria such as the *Aquificales* (30, 31). In our analysis, we were unable to identify a protein with resemblance to the variable FTR subunit other than that associated with the plant-type enzyme. This finding suggests that the FTRv sequence is either very different and cannot be detected by direct sequence comparison, the subunit is substituted by a different form, or is not present at all. Although not directly implicated in catalysis, FTRv is essential for activity of the plant enzyme. The results suggest that FTRv was introduced in the cyanobacteria to protect the Fe-S cluster of the catalytic subunit from oxygen. The FTRv from cyanobacteria is smaller than the counterpart

from eukaryotic organisms due to the absence of N-terminal extensions and a ca. 10-amino acid insert close to the C-terminus (14). The N-terminal extensions in eukaryotic FTRv are quite variable and might have been introduced with the chloroplast transit peptides. The core of FTRv in cyanobacteria and Eukaryotes is less variable and contains a few strictly conserved residues. Whereas two FTRv genes have been found in *Arabidopsis* and spinach (14), no equivalents were observed in the oxy-photobacteria we have analyzed.

The FTRc-like 2 form (Group II) is the closest homolog to plant-type FTRc. In every phylogenetic reconstruction examined, plant-type FTR and FTRc-like 2 formed a coherent clade (Figs. 5.3 and 5.4). This tree topology suggests the clade originated in the *Aquificae* and was subsequently distributed to bacteria, eukaryotic algae and land plants. FTRc-like 2 is also closely related to FTRc-like 3, a bimodular enzyme with a fused Rhodanese domain at the C-terminus. In groups IV-VI, the presence of bacterial representatives in branches populated by archaeal proteins suggests the occurrence of horizontal gene transfer events in the acquisition of FTRc genes. Because all deeply rooted archaea (e.g., *Methanocaldococcus jannaschii*) lack FTR, an exchange of genetic material between the archaeal (e.g., *M. mazei*) and the bacterial domains appears to have taken place multiple times as has been discussed (32). In any case, no clear pattern of FTRc-type distribution within archaea and bacteria was observed. Typically, bacteria have one type of FTRc homolog while most archaea have two or more. In related analyses, we identified remote homologs in *Clostridium* phages. As the phage genome mainly encodes for proteins involved in DNA processing and nucleotide metabolism (33), it seems possible that the FTRc homologue is essential for the replication of the phage. This situation resembles the Trx produced by T4 bacteriophage in *E. coli* (34) or the core photosytem II genes carried by cyanophages (35) .

FTRc homologs have similar residues at positions where key conserved active-site residues of plant-type FTRc are found (Fig. 5.1). We anticipate conservation in the structure of the metal binding site, but the surrounding amino acids likely influence the fine-tuning of the redox activity to reflect unique redox chemistry. This point needs experimental investigation. We find that in certain species FTRc is immediately adjacent (in some cases fused) to a gene encoding a redoxin protein potentially capable

of Trx-like activity. Furthermore, in some organisms, a Fdx-Rieske type gene is organized in an operon-like fashion with FTRc-like and redoxin genes.

The presence of Rbx and rhodanese modules in certain FTRc homologs is intriguing. A Rbx tail is present only in the FTRc of anaerobes, where Rbx is reported to function in removing oxygen (36). Thus, similar to the proposed function of FTRv in plants, Rbx could stabilize the Fe-S in the presence of oxygen. Evidence for this conclusion comes from the observation that the recombinant FTRc-like protein from *Methanosarcina acetivorans* isolated and crystallized under aerobic conditions shows the color typical of a Fe-S protein (37). The rhodanese domain could also help to protect iron-sulfur clusters prone to oxidation (38).

Most organisms with an FTRc-like sequence have two alternate routes of Trx reduction: one linked to Fdx and the other to NADPH via NTR. However, some representatives of *Aquificae* do not have NTR, implicating a major role for FTR in reducing Trx. Considering that Fe-S clusters are thought to be among the oldest structures in biology (39), it seems plausible that Trx reductases were linked to Fdx early in evolution.

5.4.2 Functional implication: carbon fixation regulation

All organisms with Group I FTRc are oxygenic and use the Calvin-Benson (CB) for photosynthetic CO_2 fixation. The CB is known to be regulated by FTS (14, 89). It is noteworthy that organisms with FTRc-like genes of Groups II and III, the closest homologs to the plant-type, are present mainly in autotrophic bacteria (90, 91). Most organisms with FTRc-like 2 or 3 homologs use the Reverse Citric Acid (RCA) pathway for carbon fixation (Table 5.1). A surprising exception is *Mariprofundus ferrooxydans*, a *Zetaproteobacterium*, that appears to have a functional CB (65, 92). *Aquificales* and *Epsilonproteobacteria*, the organisms most represented in groups II and III, are microaerophiles and are found in similar environment such as deep-sea hydrothermal vents, terrestrial hot springs and adjoining areas with ample supplies of hydrogen and sulfur and low levels of oxygen. They fix CO_2 via RCA that has been shown to be regulated by Trx in certain bacteria (8). In view of this link to Trx, it seems possible that the catalytic subunit, FTRc, originated in deeply rooted microaerophilic, chemoauthotrophic bacteria (such as *Aquificales*) to regulate CO_2 fixation by the RCA.

Table 5.1 Distribution of FTRc and CO_2 fixation pathway

Organism	Phylogenetic lineage	FTRc type[a]	CO_2 fixation pathway[b]	Autotrophy (+) Heterotrophy (-) Phototrophy (P) Anaerobe (An) Aerobe (A) Microaerophile (M)	Refs
ARCHAEA					
Methanococcus aeolicus Nankai-3	Euryarchaeota	IV or VI	WL	+, An	(40)
Methanothermobacter thermoautootrophicus strain ΔH		VI	WL	+, An	(41)
Archaeoglobus fulgidus DSM 4304		VI	WL	+, An	(42)
Methanocorpusculum labreanum Z		IV	-	-, An	(43)
Methanocella paludicola SANAE		V, VI	WL	+, An	(23)
Methanosaeta thermophila		VI	WL	-, An	(44)
Methanohalophilus mahii DSM 5219		IV	WL	-, An	(45)
Methanococcoides burtonii str. DSM 6242		IV,VI	WL	-, An	(46)
Methanohalobium evestigatum Z-7303		IV,V	WL	-, An	(47)
Methanosalsum zhilinae		IV,V	WL	-, An	(48)
Methanosarcina mazei Go1		IV,VI	WL	+, An	(32)
Methanosarcina acetivorans C2A		IV,VI	WL	-, An	(49)
BACTERIA					
Persephonella marina EX-H1	Aquificae	II	RCA	+, M	(50)
Sulfurihydrogenibium azorense Az-Fu1		II	RCA	+, M	(51)
Dehalococcoides ethenogenes 195	Chloroflexi	VI	WL	-, An	(52)
Candidatus Kuenenia stuttgartiensis	Planctomycetes	IV	WL	+, A	(53)
Treponema succinifaciens DSM 2489	Spirochaetes	VII	RCA	+, An	(54)
Spirochaeta smaragdinae		VI	-	-, An	(55)
Spirochaeta caldaria DSM 7334		VI	-	-, An	(56)
Clostridium botulinum	Firmicutes	VII (Phage)	WL	-, An	(57)
Ruminococcus bromii		VII	-	-, An	(58)
Dethiobacter alkaliphilus		V	WL	+, An	(59)
Desulfotomaculum ruminis DSM 2154		IV	WL	-, An	(60)
Thermodesulfobium narugense DSM 14796		VI	WL	+, An	(61)
Chloroherpeton thalassium ATCC 35110	Chlorobi	II	RCA	P, An	(62)
Thermodesulfovibrio yellowstonii DSM 11347	Nitrospirae	VI	WL	-, An	(63)
Candidatus Nitrospira defluvii		II	RCA	+, M	(64)
Mariprofundus ferrooxydans PV-1	Zetaproteobacteria	II	CB	+, M	(65)
Sulfurospirillum deleyianum DSM 6946	Epsilonproteobacteria	III	WL	-, An	(66)
Wolinella succinogenes		III	RCA	-, An	(67)
Sulfurimonas autotrophica DSM 16294		III	RCA	+, A	(68)
Nautilia profundicola AmH		III	RCA	+, An	(69)
Nitratifractor salsuginis		III	RCA	+, An	(70)
Sulfurovum sp. NBC37-1		III, IV	RCA	+, A	(71)
Haliangium ochraceum DSM 14365	Deltaproteobacteria	II	WL	-, A	(72)

Table 5.1 continued

Organism	Phylogenetic lineage	FTRc type[a]	CO_2 fixation pathway[b]	Autotrophy (+) Heterotrophy (-) Phototrophy (P) Anaerobe (An) Aerobe (A) Microaerophile (M)	Refs
Desulfobulbus propionicus DSM 2032		VI	RCA	-, An	(73)
Desulfovibrio vulgaris str. Hildenborough		VI	WL	-, An	(74)
Desulfovibrio salexigens DSM 2638		II	WL	+, A	(75)
Gloeobacter violaceus	Cyanobacteria	-	CB	P, A	(76)
Synechococcus sp. JA-2-3B'a(2-13)		I	CB	P, A	(77)
Prochlorococcus marinus MIT9313		-	CB	P, A	(78)
Synechococcus elongatus PCC 6301		I	CB	P, A	(79)
Nostoc sp. PCC 7120		I	CB	P, A	(80)
Synechocystis sp. PCC 6803		I	CB	P, A	(81)
EUKARYA					
Cyanidioschyzon merolae	Chloroplast	I	CB	P, A	(82)
Chlamydomonas reinhardtii		I	CB	P, A	(83)
Physcomitrella patens		I	CB	P, A	(84)
Arabidopsis thaliana		I	CB	P, A	(85)
Spinacia oleracea		I	CB	P, A	(86)
Zea mays		I	CB	P, A	(87)
Oryza sativa		I	CB	P, A	(88)

[a] see Figs. 5.1 and 5.2 for the classification of FTRc; [b]abbreviations for CO_2 fixation pathway, WL, Wood-Ljungdahl pathway; RCA, Reverse citric acid cycle; CB, Calvin-Benson cycle

FTRc homologs of groups IV-VII are found in late-evolving methanogenic archaea and a variety of bacteria, where they may have arisen to meet ecological needs. Methanogenic euryarchaea belonging to the classes of *Methanobacteria* and *Methanomicrobia* and closely related sulfate-reducing *Archaeoglobi* use the reductive acetyl-CoA or Wood-Ljungdahl (WL) pathway for CO_2-fixation (90). Some of these archaea are capable of growing both heterotrophically and chemolithoautotrophically (with H_2 as the energy source). The rest are obligate heterotrophs (Table 5.1). Bacteria with FTRc homologs of group IV-VII are either autotrophs with the WL pathway (*e.g.*, *Candidatus* kuenenia stuttgartiensis) or heterotrophs, with or without the WL pathway (*e.g.*, *Dehalococcoides* species of the *Chloroflexaceae* family and *Mahella australiensis*, respectively). While the WL pathway is yet to be investigated for regulation by Trx, pyruvate:ferredoxin oxidoreductase (PFOR, also called "pyruvate synthase")—the closely associated enzyme that synthesizes pyruvate from autotrophically generated acetate (93)—is known to be regulated by Trx in *Desulfovibrio vulgaris*, a strictly anaerobic sulfate-reducing bacterium (94). As a Trx target, PFOR provides a link between Trx and the RCA in anaerobic and microaerophilic bacteria (95-99).

It is not yet clear whether the WL or RCA pathway is ancestral, but certainly the CB seems to be a relatively late development of the bacterial branch (91, 93). According to our compiled data, we visualize that FTS evolved as follows. The system likely arose in microaerophilic chemolithotrophic bacteria (such as the *Aquificae*) early in the evolution of autotrophy to regulate carbon assimilation by the RCA, possibly as a result of oxygen exposure (oxidative regulation) (100). The RCA could then have been adopted by anoxygenic photosynthetic bacteria, today represented by *Chlorobi* where it continues to be regulated by the ferredoxin/thioredoxin system (FTS) as well as the NADP/thioredoxin system (NTS). As the atmosphere became aerobic, the prevalence of the RCA would have been increasingly restricted, thus giving way to organisms with pathways more resistant to oxygen. At that time, the CB became the predominant pathway. In parallel, the FTS evolved to function under aerobic conditions through changes in the structure of Fdx and FTR (through the acquisition of FTRv). The FTR component of the FTS seems unique in being dedicated to regulation throughout this extended period of evolution. By contrast, Trx would have functioned in another capacity in addition to its regulatory role—i.e., as an electron donor in reactions such a ribonucleotide and methionine sulfoxide reduction. During this period, an oxidative type of regulation evolved to restore the activity of enzymes exposed to oxygen. While the FTS continued to act via oxidative regulation, classical light/dark regulation became increasingly important as photosynthetic eukaryotes assumed greater structural and functional complexity.

5.5 MATERIALS AND METHODS

5.5.1 Sequence retrieval and multiple sequence analysis

Homologs of FTRc were detected by combining recursive and reciprocal BLAST searches (101) at NCBI (http://www.ncbi.nlm.nih.gov) in combination with HMM searches (102). FTRc and FTRv sequences of *Synechocystis* sp. PCC 6803 (sll0554 and ssr0330) were used as initial template. The retrieved amino acid sequences were aligned with ClustalX (16), with manual adjustment. A similar approach was followed with PRK.

5.5.2 Phylogenetic analyses

For phylogenetic analyses, non-conserved regions of the alignment were manually removed and maximum likelihood (ML) phylogenetic analyses were performed by

PhyML 3.0 (103). The LG model was selected assuming an estimated proportion of invariant sites and a gamma correction (four categories). Bootstrap values were inferred from 100 replicates. The trees were displayed with FigTree (http://tree.bio.ed.ac.uk/software/figtree/). Phylogenetic network analysis was performed using the NeighborNet method implemented in the SplitsTree program (version 4.10) (27).

5.5.3 Homology modelling

Comparative modeling of FTRc-like domains was carried out using SwissModel (104). Project files were generated with the program DeepView (105), using the high-resolution structure of Synechocystis FTRc (PDB code 1dj7) as template (106). Figures were prepared with PyMOL (http://www.pymol.org).

5.6 REFERENCES

1. Arnér ESJ & Holmgren A (2000) Physiological functions of thioredoxin and thioredoxin reductase. *Eur. J. Biochem.* 267(20):6102-6109.
2. Buchanan BB & Balmer Y (2005) Redox regulation: A broadening horizon. *Annu. Rev. Plant Biol.* 56(1):187-220.
3. Ladenstein R & Ren B (2008) Reconsideration of an early dogma, saying "there is no evidence for disulfide bonds in proteins from archaea". *Extremophiles* 12(1):29-38.
4. Meyer Y, Buchanan BB, Vignols F, & Reichheld J-P (2009) Thioredoxins and glutaredoxins: Unifying elements in redox biology. *Annu. Rev. Genet.* 43(1):335-367.
5. Buchanan BB, Holmgren A, Jacquot JP, & Scheibe R (2012) Fifty years in the thioredoxin field and a bountiful harvest. *Biochim. Biophys. Acta* Epub 2012 Jul 27.
6. Schürmann P & Buchanan BB (2008) The ferredoxin/thioredoxin system of oxygenic photosynthesis. *Antioxid. Redox Signal.* 10(7):1235-1273.
7. Jacquot J-P, Eklund H, Rouhier N, & Schürmann P (2009) Structural and evolutionary aspects of thioredoxin reductases in photosynthetic organisms. *Trends Plant Sci.* 14(6):336-343.
8. Hosoya-Matsuda N, Inoue K, & Hisabori T (2009) Roles of thioredoxins in the obligate anaerobic green sulfur photosynthetic bacterium *Chlorobaculum tepidum*. *Molecular Plant* 2(2):336-343.
9. Dai S, Schwendtmayer C, Schürmann P, Ramaswamy S, & Eklund H (2000) Redox Signaling in Chloroplasts: Cleavage of Disulfides by an Iron-Sulfur Cluster. *Science* 287(5453):655-658.
10. Balmer Y, *et al.* (2003) Proteomics gives insight into the regulatory function of chloroplast thioredoxins. *Proc. Natl. Acad. Sci. U. S. A.* 100(1):370-375.
11. Montrichard F, *et al.* (2009) Thioredoxin targets in plants: The first 30 years. *J. Proteomics* 72(3):452-474.
12. Jacquot J-P, Eklund H, Rouhier N, & Schurmann P (2009) Structural and evolutionary aspects of thioredoxin reductases in photosynthetic organisms. *Trends Plant Sci.* 14(6):336-343.
13. Florencio FJ, Perez-Perez ME, Lopez-Maury L, Mata-Cabana A, & Lindahl M (2006) The diversity and complexity of the cyanobacterial thioredoxin systems. (Translated from English) *Photosynthesis Research* 89(2-3):157-171 (in English).
14. Schurmann P & Buchanan BB (2008) The ferredoxin/thioredoxin system of oxygenic photosynthesis. *Antioxid. Redox Signal.* 10(7):1235-1273.
15. Dai S, *et al.* (2007) Structural snapshots along the reaction pathway of ferredoxin-thioredoxin reductase. *Nature* 448(7149):92-96.

16. Thompson JD, Gibson TJ, Plewniak F, Jeanmougin F, & Higgins DG (1997) The CLUSTAL_X windows interface: flexible strategies for multiple sequence alignment aided by quality analysis tools. *Nucleic Acids Res.* 25(24):4876-4882.
17. Nakamura Y, *et al.* (2003) Complete genome structure of *Gloeobacter violaceus* PCC 7421, a cyanobacterium that lacks thylakoids. *DNA Res* 10(4):137-145.
18. Ting CS, Rocap G, King J, & Chisholm SW (2002) Cyanobacterial photosynthesis in the oceans: the origins and significance of divergent light-harvesting strategies. *Trends Microbiol.* 10(3):134-142.
19. Gould SB, Waller RF, & McFadden GI (2008) Plastid evolution. *Annual review of plant biology* 59:491-517.
20. Bordo D & Bork P (2002) The rhodanese/Cdc25 phosphatase superfamily - Sequence-structure-function relations. *EMBO Rep.* 3(8):741-746.
21. Mathrani I, Boone D, Mah R, Fox G, & Lau P (1988) *Methanohalophilus zhilinae* sp. nov., an alkaliphilic, halophilic, methylotrophic methanogen. *Int J Syst Bacteriol* 38(2):139-142.
22. T.N. Z & G.A. Z (1987) *Methanohalobium evestigatus*, n. gen., n. sp. The extremely halophilic methanogenic Archaebacterium. *Dokl. Akad. Nauk SSSR* 293:464-468.
23. Sakai S, *et al.* (2011) Genome Sequence of a Mesophilic Hydrogenotrophic Methanogen *Methanocella paludicola*, the First Cultivated Representative of the Order *Methanocellales*. *PLoS ONE* 6(7):e22898.
24. Sakai S, Conrad R, Liesack W, & Imachi H (2010) *Methanocella arvoryzae* sp. nov., a hydrogenotrophic methanogen isolated from rice field soil. *International journal of systematic and evolutionary microbiology* 60(12):2918-2923.
25. Holm L & Sander C (1996) The FSSP database: fold classification based on structure-structure alignment of proteins. *Nucleic Acids Res.* 24(1):206-209.
26. Stehr M, Schneider G, Åslund F, Holmgren A, & Lindqvist Y (2001) Structural basis for the thioredoxin-like activity profile of the glutaredoxin-like NrdH-redoxin from *Escherichia coli*. *J. Biol. Chem.* 276(38):35836-35841.
27. Kloepper T & Huson D (2008) Drawing explicit phylogenetic networks and their integration into SplitsTree. *BMC Evol. Biol.* 8(1):22.
28. Dai S, *et al.* (2007) Structural snapshots along the reaction pathway of ferredoxin-thioredoxin reductase. *Nature* 448(7149):92-96.
29. Xu XF, *et al.* (2009) Ternary protein complex of ferredoxin, ferredoxin:thioredoxin reductase, and thioredoxin studied by faramagnetic NMR Spectroscopy. (Translated from English) *J. Am. Chem. Soc.* 131(48):17576-17582 (in English).

30. Boussau B, Gueguen L, & Gouy M (2008) Accounting for horizontal gene transfers explains conflicting hypotheses regarding the position of aquificales in the phylogeny of Bacteria. *BMC Evol. Biol.* 8.
31. Oshima K, Chiba Y, Igarashi Y, Arai H, & Ishii M (2012) Phylogenetic position of aquificales based on the whole genome sequences of six aquificales species. *International journal of evolutionary biology* 2012:859264-859264.
32. Deppenmeier U, *et al.* (2002) The genome of Methanosarcina mazei: Evidence for lateral gene transfer between bacteria and archaea. *J. Mol. Microbiol. Biotechnol.* 4(4):453-461.
33. Sakaguchi Y, *et al.* (2005) The genome sequence of *Clostridium botulinum* type C neurotoxin-converting phage and the molecular mechanisms of unstable lysogeny. *Proc. Natl. Acad. Sci. U. S. A.* 102(48):17472-17477.
34. Holmgren A (1978) Glutathione-dependent enzyme reactions of the phage T4 ribonucleotide reductase system. *J. Biol. Chem.* 253(20):7424-7430.
35. Sullivan MB, *et al.* (2006) Prevalence and evolution of core Photosystem II genes in marine cyanobacterial viruses and their hosts. *PLoS Biol.* 4(8):e234.
36. Jenney FE, Verhagen M, Cui XY, & Adams MWW (1999) Anaerobic microbes: Oxygen detoxification without superoxide dismutase. *Science* 286(5438):306-309.
37. Kumar AK, Yennawar NH, Yennawar HP, & Ferry JG (2011) Expression, purification, crystallization and preliminary X-ray crystallographic analysis of a novel plant-type ferredoxin/thioredoxin reductase-like protein from *Methanosarcina acetivorans*. *Acta Crystallogr. F-Struct. Biol. Cryst. Commun.* 67:775-778.
38. Pagani S, Bonomi F, & Cerletti P (1984) Enzymic synthesis of the iron-sulfur cluster of spinach ferredoxin. *Eur. J. Biochem.* 142(2):361-366.
39. Beinert H, Holm RH, & Munck E (1997) Iron-Sulfur clusters: Nature's modular, multipurpose structures. *Science* 277(5326):653-659.
40. Kendall MM, *et al.* (2006) *Methanococcus aeolicus* sp. nov., a mesophilic, methanogenic archaeon from shallow and deep marine sediments. (Translated from eng) *International journal of systematic and evolutionary microbiology* 56(Pt 7):1525-1529 (in eng).
41. Smith DR, *et al.* (1997) Complete genome sequence of Methanobacterium thermoautotrophicum deltaH: functional analysis and comparative genomics. *Journal of bacteriology* 179(22):7135-7155.
42. Zellner G ES, Helmut Kneifel, Paul Messner, Uwe B. Sleytr, Everly Conway de Macario, Hans-Peter Zabel, Karl O. Stetter, Josef Winter (1987) Isolation and

Characterization of a Thermophilic, Sulfate Reducing Archaebacterium, *Archaeoglobus fulgidus* Strain Z. *Syst. Appl. Microbiol.* 11(2):151-160.

43. Zhao Y, BOONE DR, MAH RA, BOONE JE, & XUN L (1989) Isolation and Characterization of *Methanocorpusculum labreanum* sp. nov. from the LaBrea Tar Pits. *Int. J. Syst. Bacteriol.* 39(1):10-13.
44. Kamagata Y, *et al.* (1992) Characterization of three thermophilic strains of *Methanothrix ("Methanosaeta") thermophila* sp. nov. and rejection of Methanothrix ("Methanosaeta") thermoacetophila. (Translated from eng) *Int J Syst Bacteriol* 42(3):463-468 (in eng).
45. Paterek JR & Smith PH (1988) *Methanohalophilus mahii* gen. nov. sp. nov. a methylotrophic halophilic methanogen. *Int. J. Syst. Bacteriol.* 38(1):122-123.
46. Franzmann PD, Springer N, Ludwig W, Conway De Macario E, & Rohde M (1992) A methanogenic archaeon from cce lake, Antarctica: *Methanococcoides burtonii* sp. nov. *Syst. Appl. Microbiol.* 15(4).
47. Zhilina TN & Zavarzin GA (1987) *Methanohalobium evestigatus*, n. gen., n. sp. The extremely halophilic methanogenic Archaebacterium. *Dokl. Akad. Nauk SSSR* 293:464-468.
48. Mathrani IM, Boone DR, Mah RA, Fox GE, & Lau PP (1988) *Methanohalophilus zhilinae* sp. nov., an Alkaliphilic, Halophilic, Methylotrophic Methanogen. *International Journal of Systematic Bacteriology* 38(2):139-142.
49. Sowers KR, Baron SF, & Ferry JG (1984) *Methanosarcina acetivorans* sp. nov., an Acetotrophic Methane-Producing Bacterium Isolated from Marine Sediments. (Translated from eng) *Applied and environmental microbiology* 47(5):971-978 (in eng).
50. Gotz D, *et al.* (2002) *Persephonella marina* gen. nov., sp. nov. and *Persephonella guaymasensis* sp. nov., two novel, thermophilic, hydrogen-oxidizing microaerophiles from deep-sea hydrothermal vents. (Translated from eng) *International journal of systematic and evolutionary microbiology* 52(Pt 4):1349-1359 (in eng).
51. Aguiar P, Beveridge TJ, & Reysenbach AL (2004) *Sulfurihydrogenibium azorense*, sp. nov., a thermophilic hydrogen-oxidizing microaerophile from terrestrial hot springs in the Azores. (Translated from eng) *International journal of systematic and evolutionary microbiology* 54(Pt 1):33-39 (in eng).
52. Maymó-Gatell X, Chien Y-t, Gossett JM, & Zinder SH (1997) Isolation of a Bacterium That Reductively Dechlorinates Tetrachloroethene to Ethene. *Science* 276(5318):1568-1571.
53. Strous M, *et al.* (2006) Deciphering the evolution and metabolism of an anammox bacterium from a community genome. *Nature* 440(7085):790-794.

54. Cwyk WM C-PE (1979) *Treponema succinifaciens* sp. nov., an anaerobic spirochete from the swine intestine. *Arch Microbiol.* 122(3):231-239.
55. Magot M, *et al.* (1997) *Spirochaeta smaragdinae* sp. nov., a new mesophilic strictly anaerobic spirochete from an oil field. *FEMS microbiology letters* 155(2):185-191.
56. Pohlschroeder M, Leschine SB, & Canale-Parola E (1994) *Spirochaeta caldaria* sp. nov., a thermophilic bacterium that enhances cellulose degradation by *Clostridium thermocellum*. *Archives of microbiology* 161(1):17-24.
57. Eales CE & Gillespie JM (1947) The isolation of *Clostridium botulinum* type A from Victorian soils. *Aust. J. Sci.* 10(1):20.
58. Moore WEC, Cato, Elizabeth, P., Holdeman, Lillian V. (1972) *Ruminococcus bromii* sp. n. and Emendation of the Description of Ruminococcus Sijpestein. *International Journal of Systematic Bacteriology* 22(2):78-80.
59. Sorokin D, Tourova T, Mußmann M, & Muyzer G (2008) *Dethiobacter alkaliphilus* gen. nov. sp. nov., and *Desulfurivibrio alkaliphilus* gen. nov. sp. nov.: two novel representatives of reductive sulfur cycle from soda lakes. *Extremophiles : life under extreme conditions* 12(3):431-439.
60. Coleman GS (1960) A Sulphate-Reducing Bacterium from the Sheep Rumen. *J. gen. Microbiol.* 22:423-436.
61. Mori K, Kim H, Kakegawa T, & Hanada S (2003) A novel lineage of sulfate-reducing microorganisms: Thermodesulfobiaceae fam. nov.,*Thermodesulfobium narugense* gen. nov., sp. nov., a new thermophilic isolate from a hot spring. *Extremophiles : life under extreme conditions* 7(4):283-290.
62. Gibson J, Pfennig N, & Waterbury JB (1984) *Chloroherpeton thalassium* gen. nov. et spec. nov., a non-filamentous, flexing and gliding green sulfur bacterium. *Arch Microbiol.* 138(2):96-101.
63. Henry EA, *et al.* (1994) Characterization of a new thermophilic sulfate-reducing bacterium *Thermodesulfovibrio yellowstonii*, gen. nov. and sp. nov.: its phylogenetic relationship to Thermodesulfobacterium commune and their origins deep within the bacterial domain. (Translated from eng) *Archives of microbiology* 161(1):62-69 (in eng).
64. Lücker S, *et al.* (2010) A Nitrospira metagenome illuminates the physiology and evolution of globally important nitrite-oxidizing bacteria. *Proceedings of the National Academy of Sciences* 107(30):13479-13484.
65. Emerson D, *et al.* (2007) A Novel Lineage of Proteobacteria Involved in Formation of Marine Fe-Oxidizing Microbial Mat Communities. *PLoS ONE* 2(8):e667.

66. Schumacher W, Kroneck, PMH., Pfennig, N. (1992) Comparative systematic study on "Spirilum" 5175 Campylobacter and Wolinella species. Description of "Spirilum" 5175 as *Sulfurospirilum deleyianum* gen. nov., spec. nov. *Archives of microbiology* 158:287-293.
67. Wolin MJ, Wolin EA, & Jacobs NJ (1961) Cytochrome-producing Anaerobic Vibrio, *Vibrio succinogenes*, Sp. N. *Journal of bacteriology* 81(6):911-917.
68. Inagaki F, Takai K, Kobayashi H, Nealson KH, & Horikoshi K (2003) *Sulfurimonas autotrophica* gen. nov., sp. nov., a novel sulfur-oxidizing ε-proteobacterium isolated from hydrothermal sediments in the Mid-Okinawa Trough. *International journal of systematic and evolutionary microbiology* 53(6):1801-1805.
69. Smith JL, Campbell BJ, Hanson TE, Zhang CL, & Cary SC (2008) *Nautilia profundicola* sp. nov., a thermophilic, sulfur-reducing epsilonproteobacterium from deep-sea hydrothermal vents. *International journal of systematic and evolutionary microbiology* 58(7):1598-1602.
70. Nakagawa S, *et al.* (2005) Distribution, phylogenetic diversity and physiological characteristics of epsilon-Proteobacteria in a deep-sea hydrothermal field. *Environmental Microbiology* 7(10):1619-1632.
71. Nakagawa S, *et al.* (2007) Deep-sea vent epsilon-proteobacterial genomes provide insights into emergence of pathogens. *Proceedings of the National Academy of Sciences of the United States of America* 104(29):12146-12150.
72. Fudou F, Jojima, Y., Iizuka, T., Yamanaka, S. (2002) *Haliangium ochraceum* gen. nov., sp. nov. and *Haliangium tepidum* sp. nov.: Novel moderately halophilic myxobacteria isolated from coastal saline environments. *J. Gen. Appl. Microbiol.* 48(2):109-115.
73. Widdel F & Pfennig N (1982) Studies on dissimilatory sulfate-reducing bacteria that decompose fatty acids II. Incomplete oxidation of propionate by *Desulfobulbus propionicus*; gen. nov., sp. nov. *Archives of microbiology* 131(4):360-365.
74. Heidelberg JF, *et al.* (2004) The genome sequence of the anaerobic, sulfate-reducing bacterium *Desulfovibrio vulgaris* Hildenborough. *Nat Biotech* 22(5):554-559.
75. Postgate JR & Campbell LL (1966) Classification of Desulfovibrio species, the nonsporulating sulfate-reducing bacteria. *Bacteriol Rev* 30(4):732-738.
76. Rippka R, Waterbury J, & Cohen-Bazire G (1974) A cyanobacterium which lacks thylakoids. *Archives of microbiology* 100(1):419-436.
77. Bhaya D, *et al.* (2007) Population level functional diversity in a microbial community revealed by comparative genomic and metagenomic analyses. *The ISME journal* 1(8):703-713.

78. Kettler GC, *et al.* (2007) Patterns and Implications of Gene Gain and Loss in the Evolution of *Prochlorococcus*. *PLoS Genet* 3(12):e231.
79. Sugita C, *et al.* (2007) Complete nucleotide sequence of the freshwater unicellular cyanobacterium *Synechococcus elongatus* PCC 6301 chromosome: gene content and organization. *Photosynthesis Research* 93(1):55-67.
80. Kaneko T, *et al.* (2001) Complete genomic sequence of the filamentous nitrogen-fixing *Cyanobacterium Anabaena* sp. strain PCC 7120. *DNA Research* 8(5):205-213.
81. Kaneko T, Tabata, S. (1997) Complete Genome Structure of the Unicellular Cyanobacterium *Synechocystis* sp. PCC6803. *Plant Cell Physiol.* 38(11):1171-1176.
82. Misumi O, *et al.* (2005) *Cyanidioschyzon merolae* genome. A tool for facilitating comparable studies on organelle biogenesis in photosynthetic eukaryotes. (Translated from eng) *Plant physiology* 137(2):567-585 (in eng).
83. Merchant SS, *et al.* (2007) The Chlamydomonas genome reveals the evolution of key animal and plant functions. (Translated from eng) *Science* 318(5848):245-250 (in eng).
84. Rensing SA, *et al.* (2008) The Physcomitrella genome reveals evolutionary insights into the conquest of land by plants. (Translated from eng) *Science* 319(5859):64-69 (in eng).
85. Cao J, *et al.* (2011) Whole-genome sequencing of multiple *Arabidopsis thaliana* populations. (Translated from eng) *Nat Genet* 43(10):956-963 (in eng).
86. Schmitz-Linneweber C, *et al.* (2001) The plastid chromosome of spinach (*Spinacia oleracea*): complete nucleotide sequence and gene organization. (Translated from eng) *Plant molecular biology* 45(3):307-315 (in eng).
87. Maier RM, Neckermann K, Igloi GL, & Kossel H (1995) Complete sequence of the maize chloroplast genome: gene content, hotspots of divergence and fine tuning of genetic information by transcript editing. (Translated from eng) *Journal of molecular biology* 251(5):614-628 (in eng).
88. Yu J, *et al.* (2005) The genomes of *Oryza sativa*: a history of duplications. (Translated from eng) *PLoS Biol.* 3(2):e38 (in eng).
89. Buchanan BB (1980) Role of light in the regulation of chloroplast enzymes. *Annual review of plant physiology* 31(1):341-374.
90. Berg IA, *et al.* (2010) Autotrophic carbon fixation in archaea. *Nat. Rev. Microbiol.* 8(6):447-460.
91. Hügler M & Sievert SM (2011) Beyond the Calvin Cycle: Autotrophic Carbon fixation in the ocean. *Annual Review of Marine Science* 3(1):261-289.
92. Singer E, *et al.* (2011) *Mariprofundus ferrooxydans* PV-1 the first fenome of a marine Fe(II) oxidizing *Zetaproteobacterium*. *PLoS ONE* 6(9):e25386.

93. Fuchs G (2011) Alternative pathways of carbon dioxide fixation: Insights into the early evolution of life? *Annu. Rev. Microbiol.* 65(1):631-658.
94. Pieulle L, *et al.* (2011) Study of the Thiol/Disulfide Redox Systems of the Anaerobe *Desulfovibrio vulgaris* Points Out Pyruvate:Ferredoxin Oxidoreductase as a New Target for Thioredoxin 1. *Journal of Biological Chemistry* 286(10):7812-7821.
95. Deckert G, *et al.* (1998) The complete genome of the hyperthermophilic bacterium *Aquifex aeolicus*. *Nature* 392(6674):353-358.
96. Yoon K-S, Hille R, Hemann C, & Tabita FR (1999) Rubredoxin from the green sulfur bacterium *Chlorobium tepidum* functions as an electron acceptor for Pyruvate Ferredoxin Oxidoreductase. *J. Biol. Chem.* 274(42):29772-29778.
97. Tang K-H & Blankenship RE (2010) Both forward and reverse TCA cycles operate in green sulfur bacteria. *J. Biol. Chem.* 285(46):35848-35854.
98. Hügler M, Wirsen CO, Fuchs G, Taylor CD, & Sievert SM (2005) Evidence for autotrophic CO2 fixation via the reductive tricarboxylic acid cycle by members of the ε subdivision of proteobacteria. *J. Bacteriol.* 187(9):3020-3027.
99. Evans MC, Buchanan BB, & Arnon DI (1966) A new ferredoxin-dependent carbon reduction cycle in a photosynthetic bacterium. *Proc. Natl. Acad. Sci. U. S. A.* 55(4):928-934.
100. Balmer Y, *et al.* (2003) Proteomics gives insight into the regulatory function of chloroplast thioredoxins. *Proc. Natl. Acad. Sci. U. S. A.* 100(1):370-375.
101. Altschul SF, *et al.* (1997) Gapped BLAST and PSI-BLAST: a new generation of protein database search programs. *Nucleic Acids Res.* 25(17):3389-3402.
102. Finn RD, Clements J, & Eddy SR (2011) HMMER web server: interactive sequence similarity searching. *Nucleic Acids Res.* 39(suppl 2):W29-W37.
103. Guindon S, *et al.* (2010) New Algorithms and Methods to Estimate Maximum-Likelihood Phylogenies: Assessing the Performance of PhyML 3.0. *Syst. Biol.* 59(3):307-321.
104. Bordoli L, *et al.* (2008) Protein structure homology modeling using SWISS-MODEL workspace. *Nat. Protocols* 4(1):1-13.
105. Guex N & Peitsch M (1997) SWISS-MODEL and the Swiss-Pdb Viewer: an environment for comparative protein modeling. *Electrophoresis* 15:2714-2723.
106. Dai S, Schwendtmayer C, Schurmann P, Ramaswamy S, & Eklund H (2000) Redox signaling in chloroplasts: cleavage of disulfides by an iron-sulfur cluster. *Science* 287(5453):655-658.

6 Concluding Remarks

Results presented in this thesis have significant implications. Methanogens utilize simple compounds such as H_2+CO_2, acetate and methanol for production of methane. Methane is a potent green-house gas, a valuable fuel and a feedstock for chemical industry. Thus, methanogens have both economic and ecological importance. Methanogen habitats are not always anoxic due to occasional O_2 exposure or experience changes in reductants supply (1-5). Studies on responses of methanogens towards oxidative stress or redox shock could enrich our knowledge about physiology of methanogens and provide us valuable information for mitigation methane emission from paddy fields and rumen of ruminants and for increasing methane yield from biomass conversion to methane including methane production in anaerobic waste digesters. In addition, methanogens also have a major role in global carbon cycle. In biomass degradation in anaerobic environment, anaerobic bacteria, protozoa and fungi convert biomass into monomers and further to simple compounds such as CO_2, H_2 and acetate. Accumulation of H_2 exerts a thermodynamic block on biomass degradation and acetate lowers pH. Thus, consumption of H_2 as well as acetate by methanogens helps to pull the degradation reactions forward.

Our discoveries about a group of heme proteins, named dissimilatory sulfite reductase-like protein (Dsr-LP), could open up new area of research, namely heme-based mechanisms of oxidative responses. The presence of Dsr-LP in almost all methanogens, often in multiple copies, is intriguing. This suggests the importance of Dsr-LP in methanogens. Yet very limited biochemical data is available for these proteins. Further biochemical and protein-structure function relationship studies are needed to unravel the function of these proteins in methanogens.

Our findings in *Methanocaldococcus jannaschii* that Trx targets cover a wide range of cellular processes from methanogenesis to defense against foreign DNA suggest that Trx-based regulation exists in methanogens and most likely also in other archaea. From this point, Trx-based regulation needs to be considered as an important component while studying the physiology of methanogens. In addition, the finding of a unique type of thioredoxin reductase in several phylogenetically-deeply rooted methanogens suggests that novel mechanism of Trx reduction might be present in methanogens (Dwi Susanti, Biswarup Mukhopahdyay, unpublished data). We are currently performing biochemical and structural characterization of these Trx reductases.

Our studies on the genome of *Desulfurococcus fermentans*, the first known cellulolytic crenarchaeaon, could be extended further leading to the discovery of novel thermophilic cellulose degrading systems. Our work on the *in-vivo* tagging of a gene in *Methanococcus maripaludis* opened up an area of methanogen research that involves large biochemical complexes.

Reference:

1. Liu C-T, Miyaki T, Aono T, & Oyaizu H (2008) Evaluation of Methanogenic Strains and Their Ability to Endure Aeration and Water Stress. *Current microbiology* 56(3):214-218.
2. Morozova D & Wagner D (2007) Stress response of methanogenic archaea from Siberian permafrost compared with methanogens from nonpermafrost habitats. *FEMS Microbiol Ecol* 61(1):16-25.
3. Kato MT, Field JA, & Lettinga G (1993) High tolerance of methanogens in granular sludge to oxygen. *Biotechnology and bioengineering* 42(11):1360-1366.
4. Peters V & Conrad R (1995) Methanogenic and other strictly anaerobic bacteria in desert soil and other oxic soils. *Applied and environmental microbiology* 61(4):1673-1676.
5. Peter Mayer H & Conrad R (1990) Factors influencing the population of methanogenic bacteria and the initiation of methane production upon flooding of paddy soil. *FEMS microbiology letters* 73(2):103-111.

Appendix A

Genome sequence of *Desulfurococcus fermentans*, the first reported cellulolytic crenarchaeota isolated from a hot spring in Kamchatka Peninsula Russia

A.1 ABSTRACT

Desulfurococcus fermentans is the first known cellulolytic archaeon. This hyperthermophilic and strictly anaerobic crenarchaeon produces hydrogen from fermentation of various carbohydrates and peptides without an inhibition by accumulating hydrogen. The complete genome sequence reported here suggested that *D. fermentans* employs membrane-bound hydrogenases and novel glycohydrolases for hydrogen production from cellulose.

A.2 INTRODUCTION

Desulfurococcus fermentans, a hyperthermophilic crenarchaeon belonging to the *Desulfurococcaceae* family, is the first reported celluloytic archaeon (1). It was isolated from a freshwater hot spring of the Uzon caldera on the Kamchatka peninsula, Russia. This obligate anaerobe grows optimally at temperatures of 80-82^{o}C. It ferments cellulose, various other carbohydrates (fructose, lactose, maltose, ribose and starch), and peptides in peptone and casein hydrolysate for growth, and produces hydrogen in the process (1); hydrogen production is not impeded by hydrogen accumulation (1). In contrast, other *Desulfurococcus* species do not utilize cellulose, are inhibited by hydrogen, and require elemental sulfur for growth (1-5); reduction of sulfur to H_2S removes inhibition by hydrogen. *D. fermentans* neither requires nor is stimulated

by elemental sulfur (1). To gain insights into the underpinnings for the cellulose degradation and uninhibited hydrogen production abilities in *D. fermentans*, we have sequenced the genome of this crenarchaeon.

A.3 RESULTS AND DISCUSSIONS

The *D. fermentans* genome consists of 1,384,116 bp with a 44.8% GC content. It contains 49 tRNA genes (including three with non-canonical introns), 5 structural RNA genes (one each of 5S rRNA, 16S rRNA, 23S rRNA, archaeal type A RNase P RNA, one SRP RNA), 1 CRISPR array, and 1,475 putative protein-coding genes of which 1,075 have predicted functions. *D. fermentans* possesses membrane-bound hydrogenases but lacks soluble hydrogenases. As expected, the *D. fermentans* genome does not carry genes encoding known sulfur-reducing enzymes. Interestingly, homologs of known cellulases are also missing in this archaeon, suggesting that it might employ new cellulose degradation systems.

Nucleotide sequence accession number

This Whole Genome Shotgun project has been deposited at DDBJ/EMBL/GenBank under the accession CP003321.1.

A.4 MATERIALS AND METHODS

Whole genome sequencing was performed using a combination of Illumina and 454 sequencing platforms. An Illumina GAII shotgun library, a 454 Titanium draft library, and a paired end 454 library with average insert size of 6.0 kb were generated. Illumina sequencing data were assembled with Velvet (6), and the consensus sequences were shredded into 1.5-kb overlapped fake reads, then assembled together with the 454 data using Newbler. The Newbler assembly contained two contigs in one scaffold. The Newbler assembly was converted into a Phrap assembly by making fake reads from the consensus, collecting the read pairs in the 454-paired end library. The Phred/Phrap/Consed software package (http://www.phrap.com) was used for sequence assembly and quality assessment in the finishing process as follows. Illumina data were used to correct potential base errors and increase consensus quality using Polisher (A. Lapidus, unpublished). Possible misassemblies were corrected with gapResolution (C. Han, unpublished), Dupfinisher (7) or sequencing of cloned bridging-PCR fragments. Gaps between contigs were closed by editing in Consed, by PCR, and by Bubble PCR primer walks. Open reading frames were identified using Prodigal (8) as part of the Oak Ridge National Laboratory

genome annotation pipeline, followed by a round of manual curation using GenePRIMP (9). Putative protein functions were inferred by searches in the National Center for Biotechnology Information (NCBI) non-redundant, UniProt, TIGR-Fam, Pfam, PRIAM, KEGG, COG and InterPro databases.

A.5 REFERENCES

1. Perevalova AA, *et al.* (2005) *Desulfurococcus fermentans* sp. nov., a novel hyperthermophilic archaeon from a Kamchatka hot spring, and emended description of the genus Desulfurococcus. *Int J Syst Evol Microbiol* 55(Pt 3):995-999.
2. Zillig W, *et al.* (1982) *Desulfurococcaceae*, the 2nd Family of the Extremely Thermophilic, Anaerobic, Sulfur-Respiring *Thermoproteales*. *Zbl Bakt Mik Hyg I C* 3(2):304-317.
3. Slobodkin AI, and E. A. Bonchosmolovskaya (1994) Growth and Formation of Metabolic Products by Extremely Thermophilic Archaea of the Genus *Desulfurococcus* in the Presence and Absence of Elemental Sulfur. *Microbiology* 63:552-554.
4. Bonch-Osmolovskaya EA, Slesarev, A.I., Mirosh-nichenko, M.L., Svetlichnaya, T.P., Alekseev, V.A. (1988) Characteristics of *Desulfurococcus amylolyticus* n. spec. a new extremely thermophilic archaebacterium isolated from thermal springs of Kamchatka and Kunashir Island. *Mikrobiologiya* 57:94-101.
5. Kublanov IV, Bidjieva S, Mardanov AV, & Bonch-Osmolovskaya EA (2009) Desulfurococcus kamchatkensis sp. nov., a novel hyperthermophilic protein-degrading archaeon isolated from a Kamchatka hot spring. *Int J Syst Evol Microbiol* 59(Pt 7):1743-1747.
6. Zerbino DR & Birney E (2008) Velvet: algorithms for de novo short read assembly using de Bruijn graphs. *Genome Res* 18(5):821-829.
7. Han CS, Chain. P. (2006) Finishing repeat regions automatically with Dupfinisher. *Proceedings of the 2006 International Conference on Bioinformatics and Computational Biology CSREA Press, Las Vegas, NV.*:141-146.
8. Hyatt D, *et al.* (2010) Prodigal: prokaryotic gene recognition and translation initiation site identification. *BMC Bioinformatics* 11:119.
9. Pati A, *et al.* (2010) GenePRIMP: a gene prediction improvement pipeline for prokaryotic genomes. *Nat Methods* 7(6):455-457.

Appendix B

In vivo 5'-$(His)_6$-HA tagging of *rpp30*, encoding a subunit of RNAseP, in *Methanococcus maripaludis*

B.1 ABSTRACT

RNase P is a ribonucleoprotein (RNP) that catalyzes′5 -maturation of precursor tRNAs (pre-tRNAs). In bacteria, RNase P is composed of one RNAse P RNA (RPR) and one RNase P Protein (RPP). Bacterial RPPs which are not homologous to eukaryal and archaeal RPPs increase pre-tRNA cleavage efficiency of RPR and its affinity to substrate and Mg^{2+}. In comparison to the bacterial system, RNase P in eukarya and archaea are more complex as they are built from one RPR and 9 to 10 RPPs and one RPR and 4 RPPs, respectively. The archaeal RPPs resemble those in eukarya. However, the function of each archaeal and eukaryal RPP is unknown. Due to its simpler properties and similarities to eukaryal system, archaeal RNase P is often used as a surrogate for studying the functions of the components of the eukaryal counterparts. Here, we studied the role of the archaeal ribosomal protein L7Ae, a homolog of one of the eukaryal RPPs, in RNase P activity. Our contribution to this study was in the construction of a $(His)_6$-HA-*rpp30* strain of *Methanococcus maripaludis* which expresses RPP30 with a His_6-HA tandem tag at the N-terminus. Metal affinity chromatographic fractionation showed that L7Ae is a part of the RNase P complex and follow up studies established the role of L7Ae in RNase P catalysis, increasing its optimal temperature activity as well as catalytic efficiency.

B.2 INTRODUCTION

RNase P is a Mg^{2+}-dependent endoribonuclease that is primarily responsible for catalyzing the removal of the ′5leaders of precursor-tRNAs (pre-tRNAs) (1-3). Except for some unique organellar variants, RNase P functions in all three domains of life as a ribonucleoprotein (RNP) (1, 2). Although catalysis rests with the essential RNase P RNA (RPR) in all three domains of life (4-6), the RNase P protein (RPP) cofactors play essential roles. In the simple one RPR-one RPP bacterial RNase P, the RPP aids RPR catalysis by enhancing cleavage efficiency and affinity for substrate and Mg^{2+} (7-9). The bacterial RPP has not been found in any archaeal or eukaryal genome (10). Eukaryal (nuclear) RNase P, which comprises an RPR and 9 or 10 RPPs (11, 12), has not been reconstituted from recombinant subunits, thus thwarting efforts to uncover the individual functions of eukaryal RPPs. Archaeal RNase P, with an RPR and four RPPs (all homologous to eukaryal RPPs), has therefore been explored as an experimental surrogate for its so-far-intractable eukaryal cousin (13-16). Although native archaeal RNase P has not been characterized, Western analysis and immunoprecipitation validated that these four RPPs (POP5, RPP21, RPP29, and RPP30) as being associated with partially purified *Methanothermobacter thermautotrophicus* (*Mth*) RNase P activity (14). Subsequent structural and biochemical reconstitution studies using recombinant subunits have proven the utility of archaeal RNase P as a model system to dissect the role of multiple protein cofactors in facilitating RNA catalysis (16). Besides POP5, RPP21, RPP29, and RPP30, weak homologies are evident in the archaeal genomes with three other eukaryal RPPs. The first candidate is Alba, an archaeal chromatin protein, whose family members include human RPP20 and RPP25 (17-19). However, despite weak binding of the *Pyrococcus horikoshii* (*Pho*) Alba to its cognate RPR, it neither affects the cleavage rate nor the temperature optimum of the in vitro reconstituted *Pho* RNase P activity (19). Also, Alba did not copurify with *Mth* RNase P and polyclonal antisera against it failed to immunoprecipitate *Mth* RNase P activity (18).

The second candidate is the archaeal ribosomal protein L7Ae (12 kDa) that displays ~25% identity to human RPP38 (~35 kDa); the latter has additional sequences that probably facilitate subcellular localization and protein- or RNA-protein interactions in the eukaryotic context (10, 20, 21). To test if this homology is a coincidence, Fukuhara et al. (20) added *Pho* L7Ae to an in vitro reconstituted *Pho* RNase P (RPR + 4 RPPs). They found that *Pho* L7Ae increased (*i*) the maximal activity temperature from 54 to 72°C, a temperature similar to that of partially purified

native *Pho* RNase P assayed in vitro, and (*ii*) the V_{max} for pre-tRNA cleavage by 5-fold (activities compared at 55 and 65°C in the absence and p resence of L7Ae, respectively) (20). Although they concluded that *Pho* RPR lacked kink-turns (K-turns) (22, 23), the typical binding sites of L7Ae, Fukuhara et al. (20) used gel-shift assays to examine the binding of L7Ae to a series of *Pho* RPR deletion mutants and showed that L7Ae binds with unequal affinities to two different stem-loops in the RPR (20). However, there was no evidence for archaeal L7Ae being associated with RNase P in vivo or for the molecular mechanism underlying its recognition of the RPR.

Because we expected studies on a mesophilic variant to yield results that are also applicable to eukaryal RNase P, we decided to focus on RNase P from *Methanococcus maripaludis* (*Mm*); this choice was also inspired in part by the fact that transformation and homologous recombination are possible for *Mma* (24, 25). By characterizing native *Mm* RNase P tagged with $(His)_6$-HA in the N-terminus, we have now established that L7Ae is indeed a bona fide subunit of RNase P.

B.3 RESULTS AND DISCUSSIONS

B.3.1 Construction of the 5'-affinity tagged-*rpp30* strain, BM100

DNA sequences encoding six histidine residues followed by that of Hemagglutinin A were introduced at the 5' end of *mmp0430* open reading frame by means of in vivo homology recombination as shown in Figure B.1. The presence of the $(His)_6$-HA affinity tag in the chromosomal DNA of *Methanococcus maripaludis* BM100 was confirmed by PCR amplification of the region at which affinity tag was inserted and DNA hybridization using chromosomal DNA isolated from the strain with affinity tag (Figs B.1 and B.2). To check the effect of additional sequences at the N-terminal of RPP30 on the growth of BM100, we performed growth studies of BM100 in comparison with the wild type strain, Mm 900. As shown in Fig. B.3, there was no significant difference on the growth of the affinity tag strain BM100 compared to the wild type Mm 900. It suggested that the affinity tag did not perturb the overall growth of BM100. Though, it is not surprising to find that that the RNase P activity of the affinity tag strain was slightly lower than that of the wild type strain (data not shown). This might be due to the effect of affinity tag on the formation of RNase P complex between RPP30 with other RPPs.

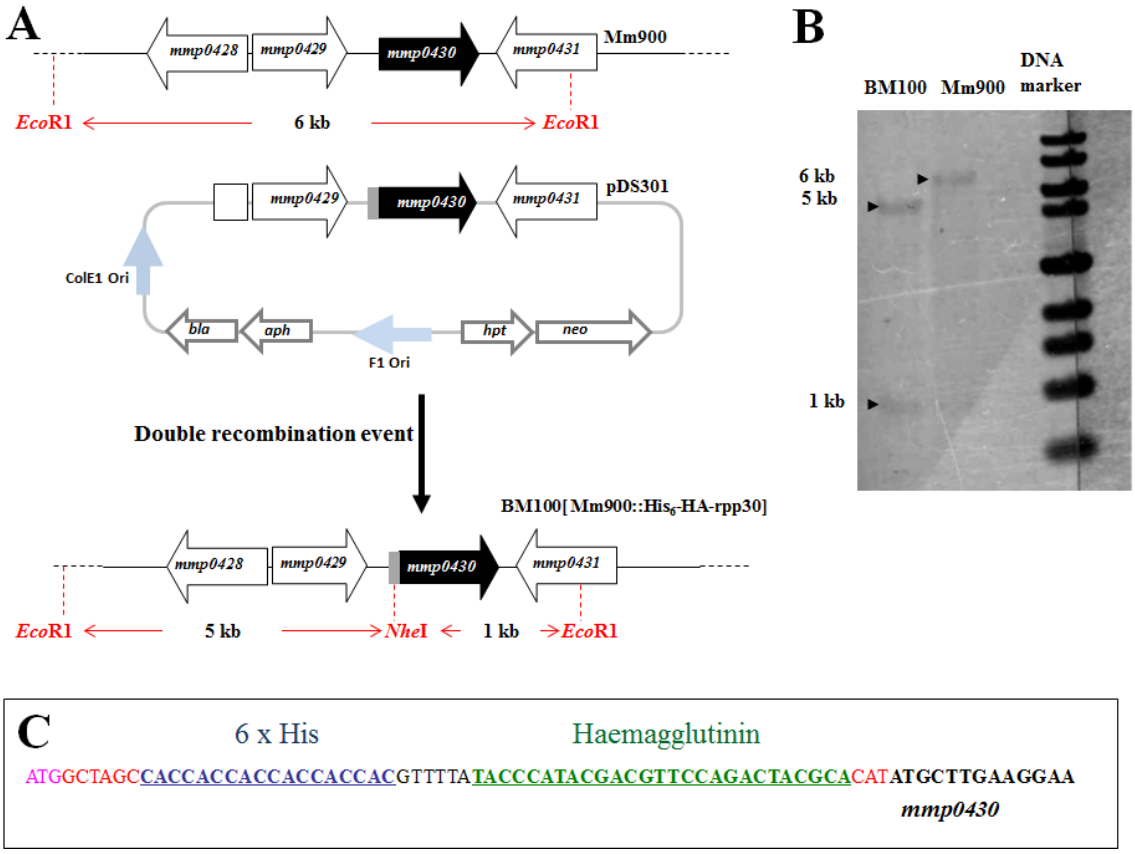

Figure B.1 Construction of *M. maripaludis* strain BM100 [Mm 900::$(His)_6$-HA-*rpp30*]. (A) Diagrams showing *mmp0430*, a gene enconding RPP30, with its neighboring regions in the chromosome of wild type strain Mm 900, in the plasmid pCRPrtNeo-$(His)_6$-HA-*rpp30*+UD and in chromosome of the affinity-tagged strain BM100 [Mm 900:: $(His)_6$-HA-*rpp30*]. Genomic DNA of both Mm 900 and BM100 were digested with *Eco*R1 and *Nhe*I. The relevant *Eco*R1 and *Nhe*I restriction sites in the chromosomes of wildtype Mm 900 and affinity-tagged strain BM100 are shown as red dashed-lines and the expected digestion products are illustrated with red arrows. OriC1, origin of replication of *E. coli*; Ori F1, F1 origin of relication; *bla*, *neo* and *aph*, genes for ampicillin, neomycine and kanamycine resistances; *hpt*, hypoxanthine (guanine) phosphoribosyltransferase, to confer sensitivity to the base analog 8-azahypoxanthine. **(B)** Southern hybridization of *Nhe*I+*Eco*R1-digested BM100 genomic DNA (lane 1) and Mm 900 chromosomal DNA (lane 2). Arrow heads point to the expected hybridized bands in each lane. DNA marker sizes (top to bottom); 10, 8, 6, 4, 3, 2, 1.5, 1 and 0.5 kb. **(C)** DNA sequence of the affinity tag $(His)_6$-HA. Sequence code; Pink, 5' start codon; red, additional sequences introduced; blue, sequence encoding six histidine residues; green, sequence encoding hemagglutinin A; and black, *mmp0340*.

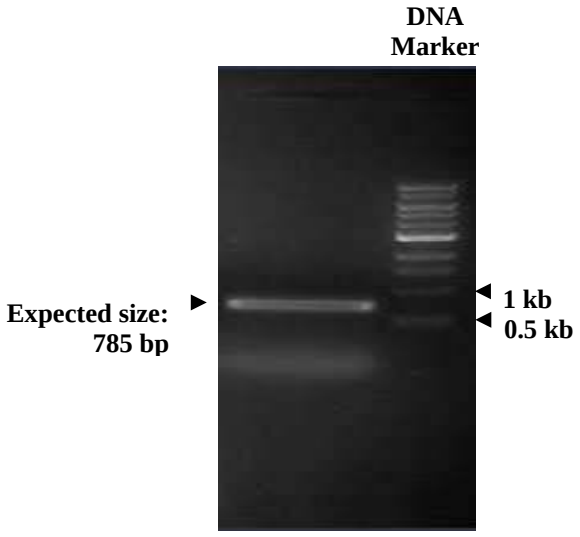

Figure B.2 PCR confirmation of 5' $(His)_6$-HA tagged *rpp30* in the chromosome of BM100 strain. Chromosomal DNA of BM100 was used as the template. PCR amplification reaction was performed using primers Ver/1F and Ver/2R listed in Table B.1. Amplicons showed the expected size as shown in arrow (lane1).

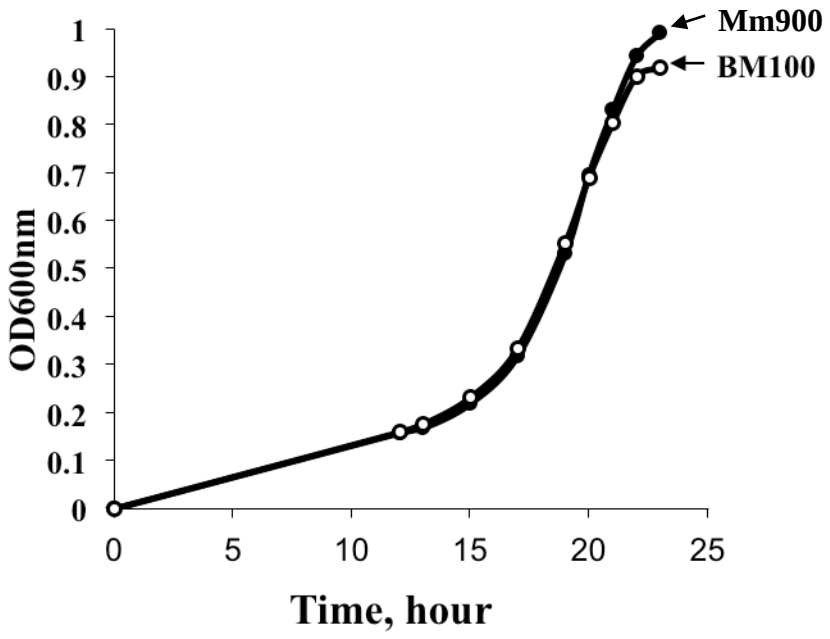

Figure B.3 Growth of *M. maripaludis* strains Mm 900 (solid circle) and BM100 [Mm 900:: $(His)_6$-HA-*rpp30*] (open circle). Growth was observed by measuring the optical density at 600 nm. Optical density was an average of two independent cultures using the conditions as described in the Materials and Methods section.

B.3.2 L7Ae is an archaeal RPP

To examine whether L7Ae is an archaeal RPP, we first investigated if L7Ae coelutes with *Mm* RNase P activity. Because L7Ae is also a subunit of the large ribosome, we first separated the ribosomes from RNase P by subjecting clarified *Mm* cell extracts to ultracentrifugation at 100,000 × *g*. Although RNase P was expected in S100 (the supernatant), some activity did appear in P100 (the ribosomal pellet). Therefore, we used a 500-mM NaCl wash to dissociate RNase P from this ribosomal pellet and repeated the ultracentrifugation to obtain the S100* and P100* fractions. Whether we used S100 alone or a pool of S100 + S100* as the starting material for the subsequent purification, similar results for L7Ae coelution were obtained.

RNase P was partially purified from S100 + S100* by ion-exchange chromatography using heparin- and Q-Sepharose sequentially. The Q-Sepharose fractions constituting the peak of RNase P activity are shown in Fig. B.4(A). Proteins from these fractions were precipitated with trichloroacetic acid and then subjected to Western blot analysis using a rabbit polyclonal antiserum raised against recombinant *Mma* L7Ae (Fig. B.4 (B)). The results clearly demonstrate the correspondence of L7Ae in the peak of *Mm* RNase P activity.

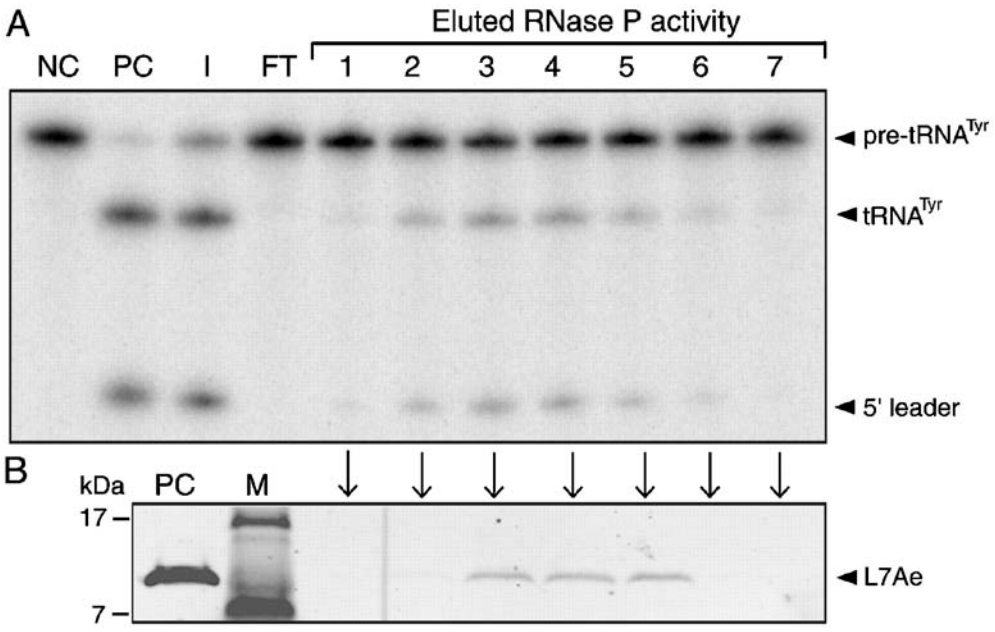

Figure B.4 Coelution of *Mm* RNase P activity and L7Ae. (A) Partially purified native Mm RNase P was assayed for pre-tRNA^{tyr}-processing activity at 37^{o}C. PC, positive control, generated from processing of pre-tRNA^{tyr} by in vitro reconstituted *Eco*RNase P. NC, negative control, pre-tRNA^{tyr} substrate; I and FT, input and flow-through, respectively. (B) Western blot analysis of L7Ae from Q-Sepharose fractions of peak activity (A) using rabbit polyclonal antiserum raised against *Mma* L7Ae. PC, positive control, refers to recombinant Mm L7Ae. M, size markers. The figure was adapted from ( ) with permission.

As an additional confirmation, the ribosome-free extract from the affinity tag strain BM100 was subjected to partial purification of RNase P using sequential heparin-Sepharose and immobilized metal (Ni^{2+}) affinity chromatography (IMAC), which exploited the presence of $(His)_6$-HA-RPP30 in RNase P. Analysis of the IMAC fractions corresponding to the peak of RNase P activity confirmed the coelution of L7Ae with RNase P activity (Fig. B.5).

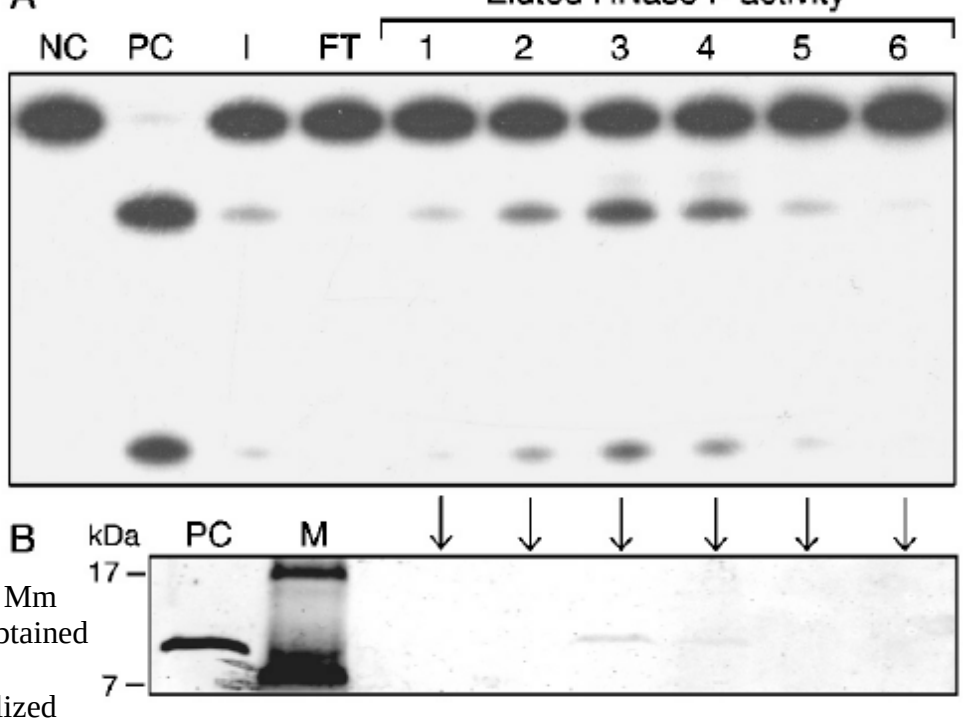

Figure B.5 Coelution of *Mm* RNase P and L7Ae activity from BM100. (A) Partially purified native Mm RNase P (obtained after immobilized metal affinity chromatography) was assayed for pre-$tRNA^{tyr}$-processing activity at 37°C. PC, positive control, generated from processing of pre-$tRNA^{tyr}$ by in vitro reconstituted *Eco*RNase P. NC, negative control, pre-$tRNA^{tyr}$ substrate only. I and FT, input and flow-through, respectively. (B) Western blot analysis of L7Ae from IMAC fractions of peak activity (A) using rabbit polyclonal antiserum raised against *Mm* L7Ae. PC, positive control, refers to recombinant Mm L7Ae. M, size markers. The figure was adapted from (39) with permission.

B.3.3 Validating L7Ae as a Subunit of Archaeal RNase P

L7Ae coelutes with partially purified native *Mm* RNase P activity (wild-type and affinity-tagged versions; Figs. B.4 and B.5). It also enhances by ~360-fold the k_{cat}/Km of the RNP complex reconstituted from the *Mm* RPR and four previously established RPPs (Fig. B.6). Notably, the in vitro reconstituted *Mm* RNase P holoenzyme with L7Ae exhibits a k_{cat}/Km of 2.4×10^7 M^{-1} s^{-1}, a value similar to those reported for native RNase P partially purified from *Mth* (type A)

and *Mja* (type M) (26). The presence of L7Ae also increases by ~12 °C the maximal temperature for realizing robust pre-tRNA processing activity of in vitro reconstituted *Mm* RNase P, as reported earlier for*Pho* RNase P (20). Additionally, we have evidence from a heterologous reconstitution assay that *Mm* L7Ae could activate an RNase P holoenzyme assembled from the *Mj* RPR and four RPPs (data not shown). Collectively, these findings establish L7Ae as a bona fide subunit of archaeal RNase P.

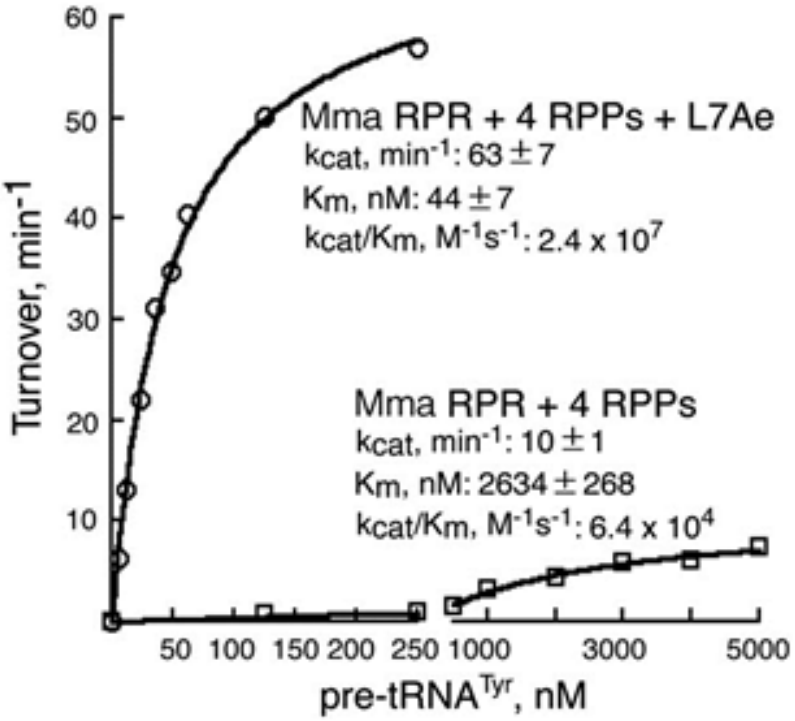

Figure B.6 Activity of in vitro reconstituted Mm Rnase P. Michaelis-Menten analysis of reconstituted Mm Rnase P holoenzyme with or without L7Ae, while representative plots are depicted, the K_{cat} and K_m values reported are the mean and standard deviation from three independent experiments. The curve-fit errors did not exceed 13% (K_{cat}) and 26% (K_m) in individual trials. The figure was adapted from (39) with permission.

B.3.4 Evolutionary Perspectives

L7Ae, a subunit of the large ribosome, plays multiple roles in archaea. It is part of the H/ACA and the C/D box snoRNPs, which catalyze rRNA pseudouridylation and ′2 -O-methylation,

respectively (27-30). Through biochemical characterization, we have now confirmed an earlier suggestion that archaeal RNase P should be added to the list of RNPs that contain L7Ae. Specifically, our mutagenesis data permit us to conclude that L7Ae recognizes a K-turn to promote RNase P function (data not shown), as demonstrated earlier with snoRNPs. L7Ae's multifunctionality may partly be attributable to its using the same RNA-recognition surface to bind similar structures in different RNA ligands and suggests coevolution of these roles. The ribosome, snoRNPs, and RNase P, all of which contain L7Ae in archaea, are linked by their biological function in some aspect of translation. L7Ae's ability to influence the architecture and activity of these distinct RNPs raises the prospect of it playing a role in coordinate regulation, a premise supported by the recent observation that the chaperone Hsp90 might serve as a master control for cell signaling and growth by aiding the biogenesis of human and yeast RNPs containing L7Ae homologs (31).

There is a variable requirement of L7Ae members to nucleate assembly of their resident RNPs. For example, L7Ae binding drives the specificity and affinity for proteins that are subsequently assembled into the C/D box snoRNP (30). In contrast, because a fairly active *Mm* RNase P holoenzyme (made up of the RPR and four RPPs) can be reconstituted even in the absence of L7Ae (Fig. B.6), L7Ae is not critical for initiating RNase P assembly, akin to the scenario with H/ACA snoRNP (29). In *Mm* RNase P (Fig. B.6), L7Ae's ability to increase the maximal temperature for activity and decrease the *Km* for pre-$tRNA^{Tyr}$ argues that it is a key structural subunit and not merely an accessory chaperone that increases the number of functional holoenzyme molecules assembled. Nevertheless, the possibility remains that L7Ae binding remodels the RPR structure and facilitates high-affinity binding of the other RPPs to the RPR. Consistent with this claim, L7Ae-mediated stabilization of the sharply bent K-turn has been proposed to promote shape/surface features (e.g., exposed base planes) and a strong local electronegative density in the cognate RNA, thereby creating context-dependent platforms for recruitment of other RNA-binding proteins (32, 33). We are attempting to elucidate how L7Ae promotes RPR conformational changes that affect archaeal RNase P assembly and function.

Although eukaryal RNase P does not have L7Ae, it has RPP38, an L7Ae homolog. Replacement of L7Ae with a homolog has also occurred in eukaryal snoRNPs, exemplifying the idea that the emergence of new functions is in part dictated by gene duplication and divergence. There has been a shift from L7Ae, which plays multiple roles in archaea, to diverse and distinctive eukaryal

L7Ae homologs, each of which play specific biological roles as part of RNase P, snoRNPs, and snRNPs (27, 34). The driving force for these changes might be the finer regulation and stringent recognition specificity demanded by the complexity of the eukaryotic cell (27, 34, 35).

B.4 METHODS

B.4.1 Growth conditions

Methanococcus maripaludis Mm 900 (Δ*hpt*), a strain lacking hypoxanthine phosphoribosyltransferase (*hpt*) gene, was kindly provided by Dr. John A. Leigh, University of Washington. This strain and its derivatives were cultivated in either sealed 5-mL serum tubes or 500-mL serum bottles, as described previously (24), except incubation was at 37°C and McC medium (a complex medium containing yeast extract, vitamins, and minerals) or McCas medium (McC without yeast extract but with casamino acids) was used instead of a mineral salts medium (24). Hydrogen (H_2+CO_2, 80:20 vol/vol, 3×10^5 Pa) or 100 mM formate (under a gas atmosphere of N_2+CO_2, 80:20 vol/vol, 3×10^5 Pa) was used as the electron source for methanogenesis.

B.4.2 Construction of BM100 [Mm 900::$(His)_6$-HA-*rpp30* strain]

We employed homologous recombination to generate an Mm 900 derivative carrying a sequence encoding a tandem $(His)_6$-HA tag at the 5′ end of the RPP30 gene in the chromosome. The underlying principle is to use markerless mutagenesis (24) to replace the native ORF with this affinity tagged ORF, which was first subcloned into a vector containing both neomycin phosphotransferase (Neo^r , for positive selection) and hypoxanthine phosphotransferase (Hpt, for negative selection with 8-aza-hypoxanthine) genes, and then introduced into Mm 900 (Δ*hpt*).

The gene encoding Mm RPP30 (*mmp0430*), together with 1 kb of upstream and downstream genomic sequences, was amplified by PCR from Mm genomic DNA using appropriate primers (MmRPP30HR-F and MmRPP30HR-R; Table B.1). The PCR product was digested with BamHI and KpnI and cloned into these sites in pBT7 (36) to yield pBT7-Mm *rpp30*+UD. Subsequently, insertional mutagenesis was used to insert sequences encoding the tags into pBT7-Mm *rpp30*+UD. Briefly, T4 polynucleotide kinase was used to phosphorylate the primers HH-RPP30-F and HH-RPP30-R (Table B.1), whose sequences are juxtaposed in the template but oriented outward. These primers were then used to amplify by PCR the entire pBT7-Mma RPP30+UD sequence and thereby incorporate the $(His)_6$ and HA tags upstream of RPP30 coding

sequence. The resulting PCR product was circularized by ligation to generate pBT7-$(His)_6$-HA-*rpp30*+UD. The $(His)_6$-HA-*rpp30*+UD construct was subcloned from this plasmid into pCRPrtNeo via the KpnI and BamHI sites generating pCRPrtNeo-$(His)_6$–HA-*rpp30*+UD.

Table B.1 Oligonucleotide primers

Primers	Sequences
MmaRPP30-HR-F	5'- ATGGTACCTGCACCAACTGTGTTATCAAC -3'
MmaRPP30-HR-R	5'- ATGGATCCCCAGGTACAATCATCCAAAAGAT -3'
HH-Mma30-F	5'- TTATACCCATACGACGTTCCAGACTACGCACAT ATGCTTGAAGGAATTTT -3'
HH-Mma30-R	5'- AACGTGGTGGTGGTGGTGGTGGCTAGCCATTA AATCCCCTGAAATTAAAT -3'
Ver-1F	5'- AGGGGATTTAATGGCTAGCC -3'
Ver-2R	5'- TCAGAAAAAAAGATTATTCTTCGAC -3'

Mm 900 (Δhpt) was transformed with 1 μg of pCRPrtNeo-$(His)_6$-HA-*rpp30*+UD using the polyethylene glycol (PEG) method (25). The transformants were grown overnight in McC liquid medium under H_2+CO_2 without shaking (25). One hundred μL of this culture were then transferred to 5-mL McC medium containing 1 mg/mL neomycin sulfate. After overnight growth, 100 μL of this culture were plated onto a McC agar plate containing 0.5 mg/mL neomycin sulfate and incubated in an anaerobic jar pressurized with H_2+CO_2+H_2S (79.9∶20∶0.1 vol/vol) to 2×10^5Pa. Colonies of merodiploid strains formed after 4–7 days of incubation. To allow accumulation of segregants arising from recombinations between upstream or downstream elements, merodiploid cells from one colony were transferred to neomycin-free McCas medium, and the culture was grown overnight under H_2+CO_2. One hundred μl of this culture were plated onto a McCas plate containing 250 μg/mL of 8-aza-hypoxanthine as a counterselective agent to obtain colonies of segregants (tagged and wild-type strains); the gas atmosphere was H_2+CO_2 (80∶20, vol/vol) with H_2S (1,000 ppm). Using the primers Ver- 1F and Ver-2R (Table B.1),

modification of the *rpp30* chromosomal locus was confirmed by PCR-based amplification and DNA sequencing of the expected 785-bp product in a segregant representing the tagged strain, which we call BM100 [Δhpt$(His)_6$ -HA-*rpp30*].

B.4.3 Southern blot hybridization

DNA hybridization was performed as described previously (37). Briefly, chromosomal DNA of BM100 was digested with *Nhe*I and *Eco*RI and analyzed by Southern blotting using pCRPrtNeo-$(His)_6$-HA-*rpp30*+UD as the probe. In this analysis, while a single 6-kb band was detected for Mma 900 consistent with the wild-type locus, two bands (5 and 1 kb) were observed with Mma BM100 as expected for the tagged *rpp30* locus.

B.4.4 Growth studies of *M. maripaludis*

A hundred microliter of *M. maripaludis* inoculum with the optical density of 0.5, measured by DU800-spectrophotometer (Beckman Coulter, Brea, CA), was transferred into 150 mL sealed serum bottles containing anaerobic McC media pressured with H_2+CO_2 (80∶20 vol/vol, 3×10^5 Pa). The cells were incubated overnight at 37°C without shaking. The culture was then shaken in the gyratory shaker (model 3527X Orbit Environ-Shaker; Lab-Line Instruments, Inc., Melrose Park, IL) and incubated at the same temperature with shaking at 240 rpm. As the H_2 and CO_2 were consumed and CH_4 was produced, the gas atmosphere was vented and re-pressured with H_2+CO_2 (80∶20 vol/vol, 3×10^5 Pa) every 30 minutes. The optical density of the culture was measured at an hour interval.

B.4.5 Purification of native Mma RNase P (wild-type and affinity-tagged variants)

Approximately 1 gram of Mm 900 cells was resuspended in 10 mL extraction buffer [EB, 20 mM Tris-HCl (pH 8), 5 mM $MgCl_2$, 2 mM DTT, 0.1 mM PMSF, and 10% (vol/vol) glycerol] supplemented with 50 mM NaCl, sonicated, and centrifuged at 30,000 ×g for 30 min at 4 °C. The supernatant was subjected to ultracentrifugation 100,000 ×g for 2 h at 4 °C, resulting in S100, the supernatant expected to have free RNase P, and P100, the ribosomal pellet. Activity assays revealed that P100 also contained RNase P activity. Therefore, to recover the ribosome-associated RNase P, P100 was resuspended in EB500 (EB supplemented with 500 mM NaCl) by gentle agitation for 2 h at 4 °C; a similar approach was used for isolating the bacterial RPP (38).

Mm RNase P, dissociated from the ribosome, was recovered by ultracentrifugation at 100,000×g. This new supernatant, which we termed S100*, was combined with S100, and the pool was subjected to sequential purification with ion-exchange chromatography columns (5-mL HiTrap heparin- and Q-Sepharose, GE Healthcare). All the inputs were dialyzed in EB50 before loading on columns and a linear NaCl gradient (50–2,000 mM) was used to elute RNase P. Typically, Mm RNase P eluted between ~600 and 800 mM NaCl from these matrices. In addition, BM100 was also used for purification of $(His)_6$-HA-RPP30-associated native Mm RNase P. We followed the same purification scheme as the untagged, native Mm RNase P except that the Q-Sepharose step was replaced by immobilized metal affinity chromatography (IMAC) using a 1-mL HiTrap chelating column precharged with Ni^{2+}. When this affinity column is subjected to a linear 0- to 500 mM imidazole gradient, $(His)_6$-HA-RPP30-associated Mm RNase P typically elutes around 150 mM imidazole.

B.4.6 Assays for Native and Reconstituted *Mma* RNase P

RNase P was assayed at 37°C in 50 mM Tris-HCl (pH 7.5), 500 mM NH_4OAc, and 7.5 mM $MgCl_2$ (assay buffer) using *Eco* pre-$tRNA^{Tyr}$ substrate, a trace amount of which was α-^{32}P labeled. For in vitro reconstitutions, *Mm* RPR was first folded in water by incubating for 50 min at 50°C, 10 min at 37°C, and then 30 min at 37°C in assay buffer. Assembly was initiated by preincubating folded *Mm* RPR, 4 RPPs (POP5, RPP30, RPP21, and RPP29), with or without L7Ae in assay buffer for 5 min at 37°C, prior to addition of *Eco* pre-$tRNA^{Tyr}$. (*Note*: In the experiment to establish the optimal temperature for maximum activity, an additional 5-min preincubation at the specified temperatures was performed after the preincubation at 37°C (Assay pH was maintained at the specified temperatures). Because of the large change in k_{cat} and *Km* values upon addition of L7Ae, the reconstituted enzyme with RPR + 4 RPPs + L7Ae (0.625 nM RPR + 31.25 nM of each protein) was assayed with 250 nM of *Eco* pre-$tRNA^{Tyr}$, whereas the RPR + 4 RPPs (50 nM RPR + 500 nM of RPPs) was assayed with 2,500 nM pre-$tRNA^{Tyr}$. The optimal RPR:RPP ratios for each combination were empirically determined. The pre-$tRNA^{Tyr}$ concentration ranges used for measuring the *Km* were 6–250 nM for RPR + 4 RPPs + L7Ae, and 62.5–5,000 nM for RPR + 4 RPPs. Turnover numbers were calculated assuming that all of the RPR is assembled into holoenzyme.

All RNase P reactions were quenched after defined incubation periods with urea-phenol dye [8 M urea, 0.04% (wt/vol) bromophenol blue, 0.04% (wt/vol) xylene cyanol, 0.8 mM EDTA, 20% (vol/vol) phenol] and separated on an 8% (wt/vol) polyacrylamide gel containing 8 M urea. The reaction products were visualized by phosphorimaging on the Typhoon (GE Healthcare). The resulting bands were quantitated by ImageQuant (GE Healthcare) to assess the extent of pre-$tRNA^{Tyr}$ cleavage. The initial velocity data were converted to turnover numbers and then subjected to Michaelis-Menten analysis using Kaleidagraph (Synergy Software).

B.6 REFERENCES

1. Lai LB, Vioque A, Kirsebom LA, & Gopalan V (2010) Unexpected diversity of RNase P, an ancient tRNA processing enzyme: challenges and prospects. *FEBS Lett* 584(2):287-296.
2. Liu F & Altman S (2010) *Ribonuclease P* (Springer, New York).
3. Walker SC & Engelke DR (2006) Ribonuclease P: the evolution of an ancient RNA enzyme. *Critical reviews in biochemistry and molecular biology* 41(2):77-102.
4. Guerrier-Takada C, Gardiner K, Marsh T, Pace N, & Altman S (1983) The RNA moiety of ribonuclease P is the catalytic subunit of the enzyme. *Cell* 35(3, Part 2):849-857.
5. Kikovska E, Svärd SG, & Kirsebom LA (2007) Eukaryotic RNase P RNA mediates cleavage in the absence of protein. *Proceedings of the National Academy of Sciences* 104(7):2062-2067.
6. Pannucci JA, Haas ES, Hall TA, Harris JK, & Brown JW (1999) RNase P RNAs from some Archaea are catalytically active. *Proceedings of the National Academy of Sciences* 96(14):7803-7808.
7. Crary SM, Niranjanakumari S, & Fierke CA (1998) The Protein Component of Bacillus subtilis Ribonuclease P Increases Catalytic Efficiency by Enhancing Interactions with the 5‘ Leader Sequence of Pre-tRNAAsp†. *Biochemistry* 37(26):9409-9416.
8. Sun L, Campbell FE, Zahler NH, & Harris ME (2006) Evidence that substrate-specific effects of C5 protein lead to uniformity in binding and catalysis by RNase P. *The EMBO journal* 25(17).
9. Sun L & Harris ME (2007) Evidence that binding of C5 protein to P RNA enhances ribozyme catalysis by influencing active site metal ion affinity. *RNA* 13:1505-1515.
10. Rosenblad MA, López MD, Piccinelli P, & Samuelsson T (2006) Inventory and analysis of the protein subunits of the ribonucleases P and MRP provides further evidence of homology between the yeast and human enzymes. *Nucleic acids research* 34(18):5145-5156.
11. Chamberlain JR, Lee Y, Lane WS, & Engelke DR (1998) Purification and characterization of the nuclear RNase P holoenzyme complex reveals extensive subunit overlap with RNase *MRP*. *Genes Dev* 12:1678-1690.
12. Jarrous N (2002) Human ribonuclease P: subunits, function, and intranuclear localization. *RNA* 8(1):1-7.
13. Boomershine WP, *et al.* (2003) Structure of Mth11/Mth Rpp29, an essential protein subunit of archaeal and eukaryotic RNase P. *Proceedings of the National Academy of Sciences of the United States of America* 100(26):15398-15403.
14. Hall TA & Brown JW (2002) Archaeal RNase P has multiple protein subunits homologous to eukaryotic nuclear RNase P proteins. *RNA* 8:296–306.
15. Kouzuma Y, *et al.* (2003) Reconstitution of archaeal ribonuclease P from RNA and four protein components. *Biochemical and biophysical research communications* 306(3):666-673.

16. Lai L, Cho IM, Chen W-Y, & Gopalan V (2010) Archaeal RNase P: A Mosaic of Its Bacterial and Eukaryal Relatives. *Ribonuclease P*, Protein Reviews, eds Liu F & Altman S (Springer New York), Vol 10, pp 153-172.
17. Aravind L, Iyer LM, & Anantharaman V (2003) The two faces of Alba: the evolutionary connection between proteins participating in chromatin structure and RNA metabolism. *Genome Biology* 4:R64.
18. Ellis JC, Barnes J, & Brown JW (2007) Is Alba an RNase P subunit? *RNA Biol.* 4:169-172.
19. Hada K, *et al.* (2008) Crystal structure and functional analysis of an archaeal chromatin protein Alba from the hyperthermophilic archaeon Pyrococcus horikoshii OT3. *Bioscience, biotechnology, and biochemistry* 72(3):749-758.
20. Fukuhara H, *et al.* (2006) A fifth protein subunit Ph1496p elevates the optimum temperature for the ribonuclease P activity from Pyrococcus horikoshii OT3. *Biochemical and biophysical research communications* 343(3):956-964.
21. Jarrous N, Wolenski JS, Wesolowski D, Lee C, & Altman S (1999) Localization in the nucleolus and coiled bodies of protein subunits of the ribonucleoprotein ribonuclease P. *The Journal of cell biology* 146(3):559-572.
22. Klein DJ, Schmeing TM, Moore PB, & Steitz TA (2001) The kink-turn: a new RNA secondary structure motif. *The EMBO journal* 20(15):4214-4221.
23. Vidovic I, Nottrott S, Hartmuth K, Lührmann R, & Ficner R (2000) Crystal Structure of the Spliceosomal 15.5kD Protein Bound to a U4 snRNA Fragment. *Molecular cell* 6(6):1331-1342.
24. Moore BC & Leigh JA (2005) Markerless Mutagenesis in *Methanococcus maripaludis* Demonstrates Roles for Alanine Dehydrogenase, Alanine Racemase, and Alanine Permease. *J. Bacteriol.* 187 (3): 972-979.
25. Tumbula DL, Makula RA, & Whitman WB (1994) Transformation of *Methanococcus maripaludis* and identification of a Pst I-like restriction system. *FEMS microbiology letters* 121(3):309-314.
26. Andrews Andrew J, Hall Thomas A, & Brown James W (2001) Characterization of RNase P Holoenzymes from Methanococcus jannaschii and Methanothermobacter thermoautotrophicus. in *Biological chemistry*, p 1171.
27. Kuhn JF, Tran EJ, & Maxwell ES (2002) Archaeal ribosomal protein L7 is a functional homolog of the eukaryotic 15.5kD/Snu13p snoRNP core protein. *Nucleic acids research* 30(4):931-941.
28. Rozhdestvensky TS, *et al.* (2003) Binding of L7Ae protein to the K-turn of archaeal snoRNAs: a shared RNA binding motif for C/D and H/ACA box snoRNAs in Archaea. *Nucleic acids research* 31(3):869-877.
29. Charpentier B, Muller S, & Branlant C (2005) Reconstitution of archaeal H/ACA small ribonucleoprotein complexes active in pseudouridylation. *Nucleic acids research* 33(10):3133-3144.
30. Omer AD, Ziesche S, Ebhardt H, & Dennis PP (2002) In vitro reconstitution and activity of a C/D box methylation guide ribonucleoprotein complex. *Proceedings of the National Academy of Sciences* 99(8):5289-5294.
31. Boulon S, *et al.* (2008) The Hsp90 chaperone controls the biogenesis of L7Ae RNPs through conserved machinery. *JCB* 180(3):579-595.
32. Klein DJ, Schmeing TM, Moore PB, & Steitz TA (2001) The kink-turn: a new RNA secondary structure motif. *The EMBO journal* 20(15): 4214-4221.
33. Moore T, Zhang Y, Fenley MO, & Li H (2004) Molecular Basis of Box C/D RNA-Protein Interactions: Cocrystal Structure of Archaeal L7Ae and a Box C/D RNA. *Structure* 12(5):807-818.
34. Watkins NJ, *et al.* (2000) A Common Core RNP Structure Shared between the Small Nucleoar Box C/D RNPs and the Spliceosomal U4 snRNP. *Cell* 103(3):457-466.

35. Charron C, *et al.* (2004) The Archaeal sRNA Binding Protein L7Ae has a 3D Structure Very Similar to that of its Eukaryal Counterpart While Having a Broader RNA-binding Specificity. *Journal of molecular biology* 342(3):757-773.
36. Tsai Y-H, Lai LB, & Gopalan V (2002) A Modified pBluescript-Based Vector for Facile Cloning and Transcription of RNAs. *Analytical biochemistry* 303(2):214-217.
37. Lai H, Kraszewski JL, Purwantini E, & Mukhopadhyay B (2006) Identification of Pyruvate Carboxylase Genes in *Pseudomonas aeruginosa* PAO1 and Development of a *P. aeruginosa*-Based Overexpression System for α4- and α4β4-Type Pyruvate Carboxylases. *Appl Environ Microbiol.* 72(12):7785–7792.
38. Vioque A, Arnez J, & Altman S (1988) Protein-RNA interactions in the RNase P holoenzyme from Escherichia coli. *Journal of molecular biology* 202(4):835-848.
39. Cho I-M, Lai LB, Susanti D, Mukhopadhyay B, & Gopalan V (2010) Ribosomal protein L7Ae is a subunit of archaeal RNase P. *Proceedings of the National Academy of Sciences* 107(33):14573-14578.

Chapter 3:

An Intertwined Evolutionary History of Methanogenic Archaea and Sulfate Reduction

Copyright from PLOS ONE

Chapter 5:

Ferredoxin:thioredoxin reductase (FTR) links the regulation of oxygenic photosynthesis to deeply rooted bacteria

Volume number

237

Issue number

2

Type of Use

Thesis/Dissertation

Portion

Full text

Number of copies

1

Author of this Springer article

Yes and you are a contributor of the new work

Order reference number

Title of your thesis / dissertation

Evolution of sulfite reductase and thioredoxin systems in methanogenic archaea

Expected completion date

May 2013

Estimated size(pages)

150

Total

0.00 USD

Terms and Conditions

Limited License
With reference to your request to reprint in your thesis material on which Springer Science and Business Media control the copyright, permission is granted, free of charge, for the use indicated in your enquiry.

Licenses are for one-time use only with a maximum distribution equal to the number that you identified in the licensing process.

This License includes use in an electronic form, provided its password protected or on the university's intranet or repository, including UMI (according to the definition at the Sherpa website: http://www.sherpa.ac.uk/romeo/). For any other electronic use, please contact Springer at (permissions.dordrecht@springer.com or permissions.heidelberg@springer.com).

The material can only be used for the purpose of defending your thesis, and with a maximum of 100 extra copies in paper.

Although Springer holds copyright to the material and is entitled to negotiate on rights, this license is only valid, subject to a courtesy information to the author (address is given with the article/chapter) and provided it concerns original material which does not carry references to other sources (if material in question appears with credit to another source, authorization from that source is required as well).

Permission free of charge on this occasion does not prejudice any rights we might have to charge for reproduction of our copyrighted material in the future.

Altering/Modifying Material: Not Permitted
You may not alter or modify the material in any manner. Abbreviations, additions, deletions and/or any other alterations shall be made only with prior written authorization of the author(s) and/or Springer Science + Business Media. (Please contact Springer at (permissions.dordrecht@springer.com or permissions.heidelberg@springer.com)

Reservation of Rights
Springer Science + Business Media reserves all rights not specifically granted in the combination of (i) the license details provided by you and accepted in the course of this licensing transaction, (ii) these terms and conditions and (iii) CCC's Billing and Payment terms and conditions.

Copyright Notice:Disclaimer
You must include the following copyright and permission notice in connection with any reproduction of the licensed material: "Springer and the original publisher /journal title, volume, year of publication, page, chapter/article title, name(s) of author(s), figure number(s), original copyright notice) is given to the publication in which the material was originally published, by adding; with kind permission from Springer Science and Business Media"

Warranties: None

Example 1: Springer Science + Business Media makes no representations or warranties with respect to the licensed material.

Example 2: Springer Science + Business Media makes no representations or warranties with respect to the licensed material and adopts on its own behalf the limitations and disclaimers established by CCC on its behalf in its Billing and Payment terms and conditions for this licensing transaction.

Indemnity
You hereby indemnify and agree to hold harmless Springer Science + Business Media and CCC, and their respective officers, directors, employees and agents, from and against any and all claims arising out of your use of the licensed material other than as specifically authorized pursuant to this license.

No Transfer of License
This license is personal to you and may not be sublicensed, assigned, or transferred by you to any other person without Springer Science + Business Media's written permission.

No Amendment Except in Writing
This license may not be amended except in a writing signed by both parties (or, in the case of Springer Science + Business Media, by CCC on Springer Science + Business Media's behalf).

Objection to Contrary Terms
Springer Science + Business Media hereby objects to any terms contained in any purchase order, acknowledgment, check endorsement or other writing prepared by you, which terms are inconsistent with these terms and conditions or CCC's Billing and Payment terms and conditions. These terms and conditions, together with CCC's Billing and Payment terms and conditions (which are incorporated herein), comprise the entire agreement between you and Springer Science + Business Media (and CCC) concerning this licensing transaction. In the event of any conflict between your obligations established by these terms and conditions and those established by CCC's Billing and Payment terms and conditions, these terms and conditions shall control.

Jurisdiction
All disputes that may arise in connection with this present License, or the breach thereof, shall be settled exclusively by arbitration, to be held in The Netherlands, in accordance with Dutch law, and to be conducted under the Rules of the 'Netherlands Arbitrage Instituut' (Netherlands Institute of Arbitration).***OR:***

All disputes that may arise in connection with this present License, or the breach thereof, shall be settled exclusively by arbitration, to be held in the Federal Republic of Germany, in accordance with German law.

Other terms and conditions:

v1.3

If you would like to pay for this license now, please remit this license along with your payment made payable to "COPYRIGHT CLEARANCE CENTER" otherwise you will be invoiced within 48 hours of the license date. Payment should be in the form of a check or money order referencing your account number and this invoice number RLNK500990673.
Once you receive your invoice for this order, you may pay your invoice by credit card. Please follow instructions provided at that time.

Make Payment To:
Copyright Clearance Center
Dept 001
P.O. Box 843006
Boston, MA 02284-3006

For suggestions or comments regarding this order, contact RightsLink Customer Support:customercare@copyright.com or +1-877-622-5543 (toll free in the US) or +1-978-646-2777.

Gratis licenses (referencing $0 in the Total field) are free. Please retain this printable license for your reference. No payment is required.

Appendix A:

Genome Sequence of *Desulfurococcus fermentans*, the First Reported Cellulolytic Crenarchaeota isolated from a Hot Spring in Kamchatka Peninsula Russia

Copyright Clearance Center RightsLink®

Home | Account Info | Help

AMERICAN SOCIETY FOR MICROBIOLOGY

Title: Complete Genome Sequence of Desulfurococcus fermentans, a Hyperthermophilic Cellulolytic Crenarchaeon Isolated from a Freshwater Hot Spring in Kamchatka, Russia

Author: Dwi Susanti, Eric F. Johnson, Jason R. Rodriguez et al.

Publication: Journal of Bacteriology

Publisher: American Society for Microbiology

Date: Oct 15, 2012

Copyright © 2012, American Society for Microbiology

Logged in as:
Dwi Susanti
Account #:
3000641521

LOGOUT

Permissions Request

Authors in ASM journals retain the right to republish discrete portions of his/her article in any other publication (including print, CD-ROM, and other electronic formats) of which he or she is author or editor, provided that proper credit is given to the original ASM publication. ASM authors also retain the right to reuse the full article in his/her dissertation or thesis. For a full list of author rights, please see: http://journals.asm.org/site/misc/ASM_Author_Statement.xhtml

BACK | CLOSE WINDOW

Copyright © 2013 Copyright Clearance Center, Inc. All Rights Reserved. Privacy statement.
Comments? We would like to hear from you. E-mail us at customercare@copyright.com

LAST UPDATED: November 5, 2009

ASM Journals Statement of Authors' Rights

Authors may post their articles to their institutional repositories

ASM grants authors the right to post their accepted manuscripts in publicly accessible electronic repositories maintained by funding agencies, as well as appropriate institutional or subject-based open repositories established by a government or non-commercial entity. Since ASM makes the final, typeset articles from its primary-research journals available free of charge on the ASM Journals and PMC websites 6 months after final publication, ASM recommends that when submitting the accepted manuscript to PMC or institutional repositories, the author specify that the posting release date for the manuscript be no earlier than 6 months after the final publication of the typeset article by ASM.

Authors may post their articles in full on personal or employer websites

ASM grants the author the right to post his/her article (after publication by ASM) on the author's personal or university-hosted website, but not on any corporate, government, or similar website, without ASM's prior permission, provided that proper credit is given to the original ASM publication.

Authors may make copies of their articles in full

Corresponding authors are entitled to 10 free downloads of their papers. Additionally, all authors may make up to 99 copies of his/her own work for personal or professional use (including teaching packs that are distributed free of charge within your own institution). For orders of 100 or more copies, you should seek ASM's permission or purchase access through Highwire's Pay-Per-View option, available on the ASM online journal sites.

Authors may republish/adapt portions of their articles

ASM also grants the authors the right to republish discrete portions of his/her article in any other publication (including print, CD-ROM, and other electronic formats) of which he or she is author or editor, provided that proper credit is given to the original ASM publication. "Proper credit" means either the copyright lines shown on the top of the first page of the PDF version, or "Copyright © American Society for Microbiology, [insert journal name, volume number, year, page numbers and DOI]" of the HTML version. For technical questions about using Rightslink, please contact Customer Support via phone at (877) 622-5543 (toll free) or (978) 777-9929, or e-mail Rightslink customer care at **customercare@copyright.com.**

Please note that the ASM is in full **compliance with NIH Policy.**

Back to **Top^**

About ASM
Inquiries from the Press
Permissions & Commercial Reprints
ASM Journals Public Access Policy

Subscribe to our RSS content feed.
Journals.ASM.org
Microbiology Buyer's Guide
find what you need GO
Join the ASM Conversation:
HighWire

Appendix B:

In-vivo Tagging of *rpp30*, encoding a subunit of RNAse-P in *Methanococcus maripaludis*

Copyright and License to Publish

4. Retail price of work
5. Number of copies of work to be produced
6. Intended audience
7. Whether work is for nonprofit or commercial use

PNAS authors need not obtain permission for the following cases: (1) to use their original figures or tables in their future works; (2) to make copies of their papers for their own personal use, including classroom use, or for the personal use of colleagues, provided those copies are not for sale and are not distributed in a systematic way; **(3) to include their papers as part of their dissertations**; or (4) to use all or part of their articles in printed compilations of their own works. Citation of the original source must be included and copies must include the applicable copyright notice of the original report.

Authors whose work will be reused should be notified. PNAS cannot supply original artwork. Use of PNAS material must not imply any endorsement by PNAS or the National Academy of Sciences. The full journal reference must be cited and, for articles published in Volumes 90–105 (1993–2008), "Copyright (copyright year) National Academy of Sciences, USA."

Requests for Permission to Photocopy

For permission to photocopy beyond that permitted by Section 107 or 108 of the US Copyright Law, contact:

Copyright Clearance Center
222 Rosewood Drive
Danvers, MA 01923 USA
Phone: 1-978-750-8400
Fax: 1-978-750-4770
E-mail: info@copyright.com

Authorization to photocopy items for the internal or personal use of specific clients is granted by The National Academy of Sciences provided that the proper fee is paid directly to CCC.

[11/12]